# Regulation of gametophyte-to-sporophyte transitions during the file cycle of Ectocarpus

Haiqin Yao

Sorbonne Université

Ecole Doctorale 515 Complexité du Vivant

*UMR 8227 CNRS – Sorbonne Université*

*Laboratoire de Biologie Intégrative des Modèles Marins*

*Equipe Génétique des Algues*

# Régulation des transitions de gamétophyte à sporophyte pendant le cycle de vie *d'Ectocarpus*

*Regulation of gametophyte-to-sporophyte transitions during the life cycle of* Ectocarpus

Par Haiqin YAO

Thèse de doctorat de Biologie du développement

Dirigée par J. Mark Cock et Susana M. Coelho

Présentée et soutenue publiquement le 9 Décembre 2019

Devant un jury composé de :

| | |
|---|---|
| **Dr Akira F. Peters, Rapporteur** | Chercheur Indépendant |
| **Dr Azeddine Driouich, Rapportrice** | Université de Rouen Normandie |
| **Dr Bernard Kloareg, Président du Jury** | Sorbonne Université - CNRS |
| **Dr Kenny Bogaert, Examinateur** | Ghent University, Beligum |
| **Dr J. Mark Cock, Co-directeur de thèse** | Sorbonne Université – CNRS |
| **Dr Susana M. Coelho, Co-directrice de thèse** | Sorbonne Université – CNRS |

# Acknowledgements

I am grateful to everyone who helped me complete this work. I am grateful to my supervisors, Dr. Mark Cock and Dr. Susana Coelho, for providing me with the chance to do a PhD in their laboratory, Biologie Integrative des Modèles Marins, and helping me embark on a memorable journey of science in the most romantic country France. They have been the best mentors and have brought constructive suggestions, deep trust, constant encouragement and great patience to me throughout all three years of my PhD. I owe my sincere respect and gratitude to them.

I am also thankful to my committee thesis members Dr. Philippe Potin, Dr. Cécile Hervé and Dr. Gorge Pohnert for their critical input and advice which helped me to carry out and improve my research during this thesis. I also thank the director of our unit (UMR 8227) Stéphane Egee and the director of Station Biologique de Roscoff Catherine Boyen.

I am extremely thankful to Dr. Murielle Jam, Dr. Delphine Scornet, Dr. Sébastien Colin, Dr. Diane Jouanneau and Qikun Xing. They helped me a lot and gave me guidance in experiment techniques. Without their help I would not have been able to complete my experiments on time. Also, a very special word of thanks goes out to Dr. Akira Peters whose scientific spirit and kindness encouraged me a lot, together with his cake made of algae. Moreover, I have to thank Lydie Correia for her help with peptide sequencing, Sylvie Rousvoal for organising training courses, Elodie Rolland, Laurence Dartevelle and other colleagues, also those wonderful teachers or trainers who have taught me and generously supported me during these three years.

I was very fortunate that during my academic life because I received guidance and support from Professor Feijiu Wang, who was my master supervisor. I am very grateful to him for bringing me to the feild of algal research. I would also like to acknowledge here the constant encouragement and motivation given to me by Dr. Fuli Liu. Without his recommendation, I would never have the chance to meet my supervisor Mark Cock, I appreciate him very much.

I would like to thank all the team members: present and past, Aga Lipinska, Yacine Badis, Olivier Godfroy, Zofia Nehr, Laurent Peres, Marie-Mathilde Perrineau, Svenja Heesch, Céline Caillard, Nick Toda, Komlan Avia and as well as the doctors, Simon Bourdareau, Laure Mignerot, Josselin Guéno.

I would like to express my thanks to all people with whom I made friends in this friendly country. Especially thanks to Maria Matard-Man, Eugénie Grigorian and my Landlords Mrs Marie Helene Pors and Mr Louis Pors. Goulou, they provided a lot of help during my life in France.

I would like to acknowledge the scholarship provided by the China Scholarship Council (CSC). Also, I would like to thank the CNRS for providing me with funding during the final phase of my PhD.

Finally, I want to thank my parents, my sisters and brothers, they have been with me forever despite the distance. A special thanks to Zaihui Zhou, my fiance. Without their understanding, encouragement and support, it would have been impossible for me to stay alone in France.

Last but not least, I am thanks to the peaceful and picturesque town, Roscoff, where make me fall in love with nature and the country of France for giving me the experience of a lifetime. Merci beaucoup!

# Contents

# Chapter I

# General Introduction

# 1. Eukaryotic life cycles

## 1.1 Eukaryotic life cycle structure

The eukaryotic tree of life has been divided into seven major lineages (Fig. 1) (Parfrey et al., 2011): the excavates (Simpson et al., 2005), the haptophytes and the cryptophytes (Burki et al., 2016), the archaeplastids (Umen, 2014), the SAR lineage (consisting of stramenopiles, alveolates and rhizarians) (Burki et al., 2007), the amoebozoans and the group that includes the most complex multicellular organisms, the opisthokonts (Cavalier-Smith et al., 2015). These diverse organisms share several basic biological features, despite the many differences between lineages and the long evolutionary times that separate them. For example, most of these organisms reproduce sexually (Fig. 2A) and have life cycles that involve an alternation between haploid and diploid phases (Fig. 2B) due to two fundamental processes: meiotic cell division (which results in the production of haploid cells from diploid cells) and gamete fusion or syngamy (which results in a doubling of the ploidy level). This alternation between ploidy phases was first recognised by Hofmeister (1851) and has been called Hofmeister alternation. The term “alternation of generations” was proposed several years later by Roe (1975). In the following sections, we will describe the life cycle diversity across the eukaryotes and discuss the relationship between life cycle structure and multicellular complexity.

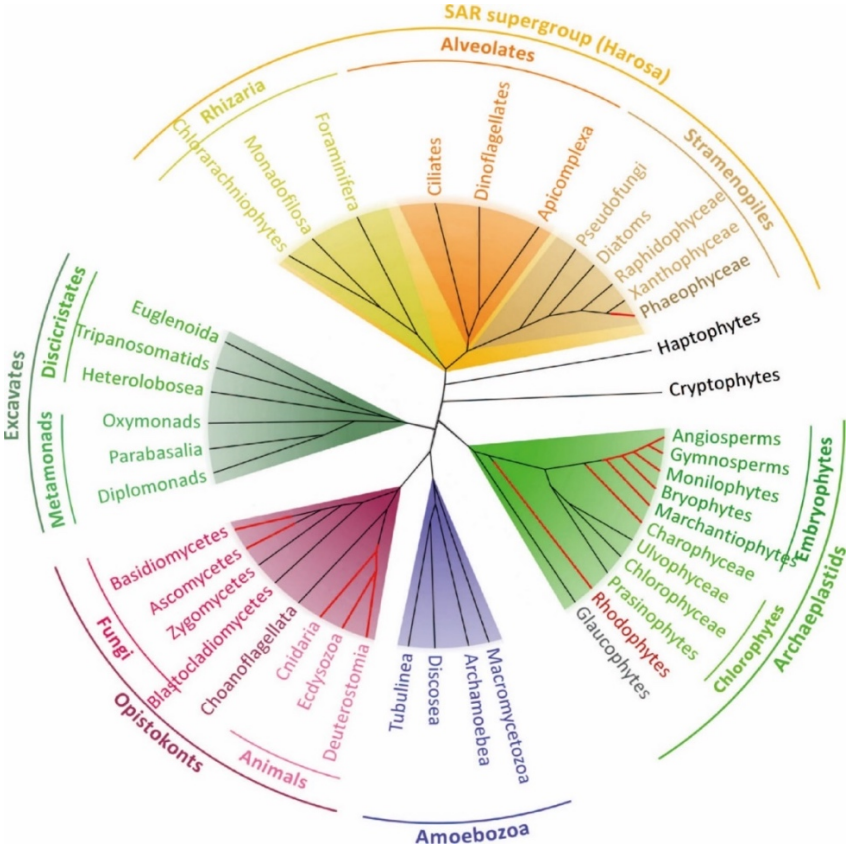


**Figure 1. Phylogenetic tree of the eukaryotes.** There are seven main lineages in the eukaryotic tree of life: the excavates (gray-green background), the haptophytes and the cryptophytes, the archaeplastids (green background), the SAR lineage (consisted by stramenopiles, alveolates and rhizarians; orange background), the amoebozoans (blue background) and the opisthokonts (red background). Only a few of these lineages have evolved complex multicellular organisms (branches in red). (Bourdareau, 2018)

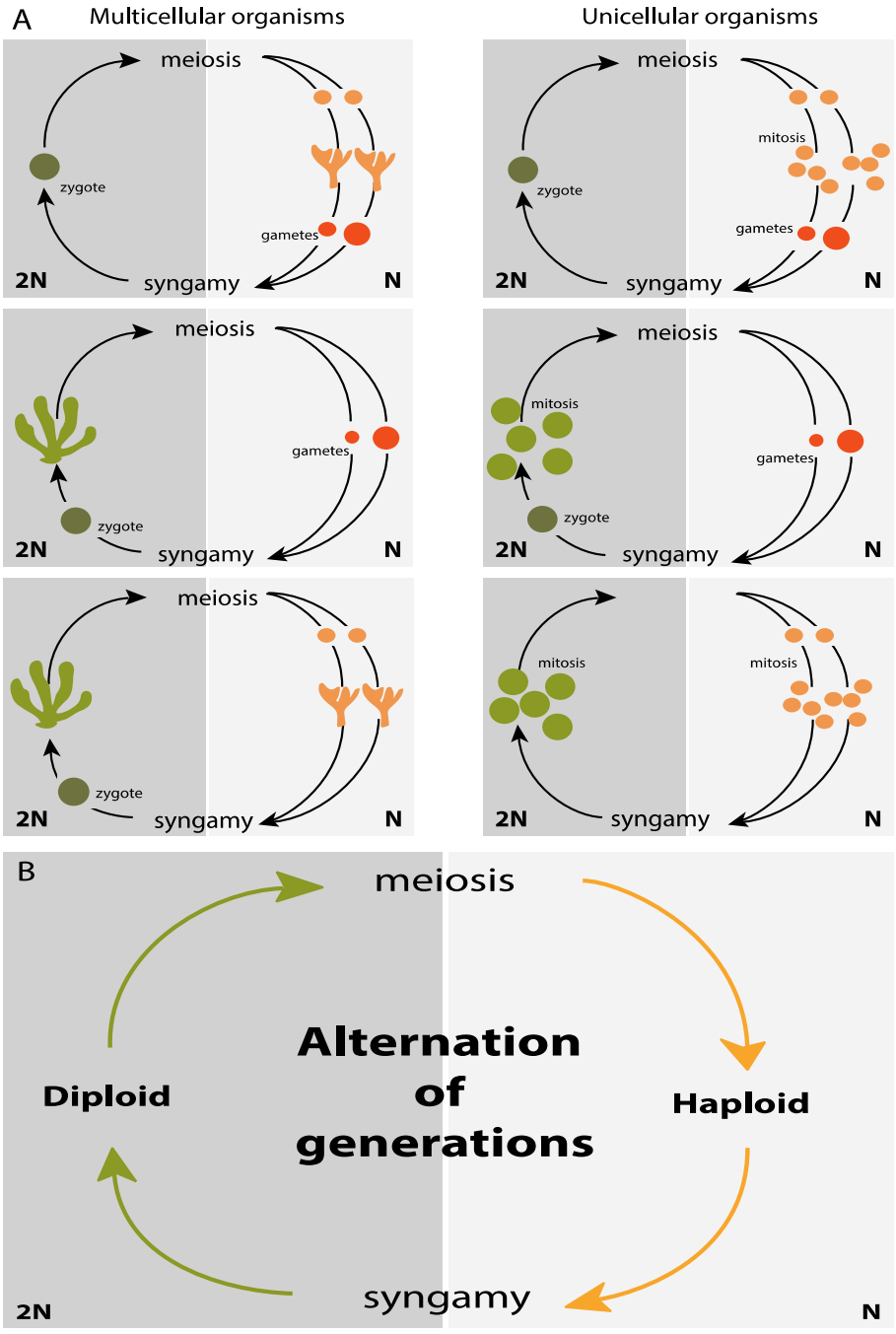


**Figure 2. Sexual life cycles of eukaryotic organisms.** Both multicellular (left) and unicellular (right) organisms produce offspring via sexual reproduction (A). Multicellular development (indicated by branched structures) can occur during only the haploid phase, during only the diploid phase or during both phases. These sexual life cycles share a common feature, the alternation between haploid and diploid phases (B), due to two fundamental processes: meiotic cell division, which results in the production of haploid cells from diploid cells and gamete fusion or syngamy, which results in a doubling of the ploidy level.

## 1.2 Life cycle diversity in eukaryotic lineages

Three main types of sexual life cycle (Fig.3) can be defined, based on whether mitotic divisions occur during the haploid phase, the diploid phase or during both phases of the life cycle (Arun, 2012; Coelho et al., 2007; Perrot et al., 1991; Richerd et al., 1993; Valero et al., 1992).

Diploid (or diplontic) life cycles: in this type of life cycle, fertilization directly follows meiosis, so that mitotic cell divisions (and development in multicellular organisms) occur only in the diploid generation (e.g. *Fucus*). Gametes are therefore the only haploid cells. This type of life cycle is commonly observed in animals (including humans) (Mable and Otto, 1998; Trivers and Hare, 1976).

Haploid life cycles (also called haplontic life cycles or haplobiontic-haploid life cycles): in this type of cycle meiosis directly follows fertilization, so that mitotic divisions (and somatic development in multicellular organisms) only occur during the haploid generation and the zygote is the only diploid cell. This kind of life cycle is observed in a variety of green algae, such as *Volvox*.

Haploid-diploid (or haplo-diplontic) life cycles: in this type of life cycle, mitosis (and somatic development in multicellular organisms) occurs during both the haploid and diploid generations so that meiosis and fertilization are temporally separated in the life cycle. The land plants, including all mosses (such as the model moss *Physcomitrella patens*) and ferns, some fungi (such as the model yeast *Saccharomyces cerevisiae*), red algae (Destombe et al., 1992), many green algae (*Ulva*, for example) and most brown algae have this kind of life cycle. One important consequence of this type of life cycle for multicellular organisms is that it implies the deployment of two multicellular bodyplans during the life cycle, one during the haploid phase and the other during the diploid phase. In plants and algae, these haploid and diploid phases correspond to the gametophyte and sporophyte generations, respectively, and these can occur separately or be dependent, with one generation growing on the other. The relative lengths of the haploid and diploid phases of a haploid-diploid life cycle are highly variable among multicellular eukaryotes, especially among the algae and protists, which exhibit life cycles that together correspond to the

complete range from complete haploid development to complete diploid development (Mable and Otto, 1998).

The following sections will discuss the life cycles of members of the major eukaryotic lineages that have evolved complex multicellularity, describing life cycle diversity and the relationship between life cycle and development.

In the green lineage (Viridiplantae), life cycles are highly variable but the majority of green algae have a haploid life cycle (e.g. *Spirogyra* and *Zygnema*) (Lewis and McCourt, 2004). The red algae (Rhodophyceae), which are an ancient sister group of the green lineage (Baldauf, 2008), exhibit both asexual and sexual life cycles. Sexual reproduction has not been reported for unicellular species (Charles, 1985; Yoon et al., 2006) but multicellular red algae have a range of different sexual life cycles. For example, the edible seaweed *Porphyra* has two morphologically distinct generations with different levels of ploidy (Hawkes, 1990). Some red algae of the Florideophyceae, including algae of economic interest (*Gracilaria, Gelidium*) and carragheenophytes (*Chondrus, Eucheuma*) have life cycles that involve either alternation between haploid and diploid phases, or transitions between a haploid (gametophyte) phase and two diploid (carposporophyte and tetrasporophyte) phases, the latter being referred as a "triphasic" (Graham and Wilcox, 2000) or "*Polysiphonia*-type" life cycle (e.g. *Polysiphonia*; Fig. 4) (Hoek et al., 1995). This latter class of life cycle involves two types of transition: a Steenstrupt alternation (Steenstrup, 1845) between two diploid phases (represented by the diploid carposporophyte and the diploid tetrasporophyte) and a Hofmeister alternation between haploid and diploid phases (represented by the gametophyte to carposporophyte transition) (Bell, 1994). Most animals (metazoans) have diploid life cycles, in which the haploid phase consists only of the single-celled gametes. However, some groups of metazoans have asexual life cycles.

In the fungi, somatic development does not usually occur during the diploid phase except in some groups such as certain chytrids, which exhibit an alternation between simple, filamentous haploid and diploid generations. However, syngamy and karyogamy are often delayed in the fungi resulting in an additional phase, the dikaryon, during which there is a proliferation of cells with

two unfused, haploid nuclei. This phenomenon only exists in the fungi and increases the complexity of life cycles in this group (Raper and Flexer, 1970).

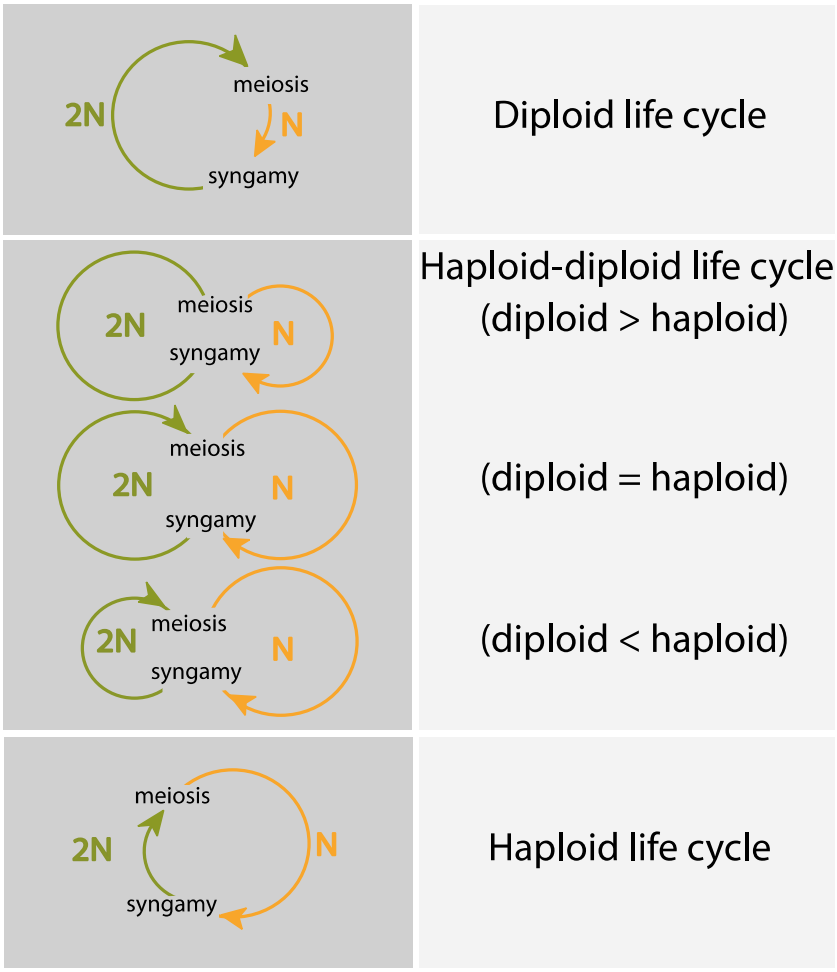


**Figure 3. Diversity of eukaryotic life cycles.** Life cycles involve two major events of meiosis and syngamy. The relative time spent in the haploid and diploid phase determines the organisms belong to which type of life cycle. Three main types of life cycles can be defined depending on the phase or phases that exhibit mitotic growth, they are diploid, haploid-diploid and haploid life cycles. Reproduced from Cock et al. (2014).

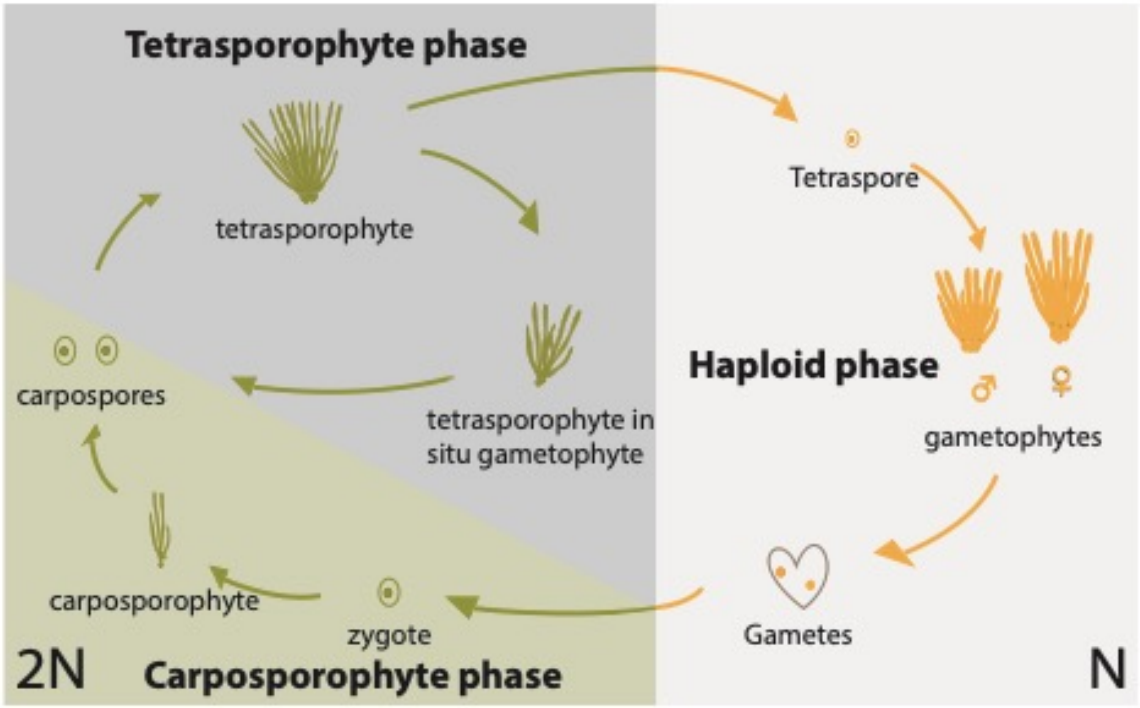


**Figure 4. The tri-phasic life cycle of the red alga *Polysiphonia*.** The diploid and haploid phases of the life cycle are shown on the left and on the right, respectively. Note that the diploid phase includes two generations, the carposporophyte (green shading) and the tetrasporophyte generation (grey shading). Reproduced from Arun (2012).

### 1.3 The relationship between life cycle structure and multicellularity

The life cycles of multicellular eukaryotic organisms are complex and multiple kinds of life cycles are found in different multicellular lineages in the tree of life. However, when the distribution of the three main types of the sexual life cycle (diploid, haploid and haploid-diploid) is evaluated across the eukaryotes, a clear trend can be discerned: the organisms with the highest levels of developmental complexity tend to have diploid or diploid-dominant life cycles. Nonetheless, haploid and haploid-diploid life cycles are also distributed across multiple eukaryotic lineages and have not displayed a tendency to disappear during the process of evolution (Mable and Otto, 1998). Based on these distributions, we can conclude that all three types of the life cycle are evolutionarily stable, presumably because each has an evolutionary advantage under particular environmental conditions.

### 1.4 Life cycle diversity in the brown algae

The brown algal lineage is placed within the stramenopiles of the eukaryotic supergroup SAR (Hackett et al., 2007). The brown algae are multicellular, photosynthetic organisms and are one of only a few eukaryotic lineages that are considered to have evolved complex multicellularity (Fig. 5) (Cock et al., 2014; Cock et al., 2010; Knoll, 2011; Niklas and Newman, 2013). The brown algae diverged from other well-studied multicellular lineages such as land plants and animals more than a billion years ago (Bourdareau, 2018) and multicellularity then evolved independently in each lineage. Brown algae are interesting models for the study of life cycles both due to this large evolutionary distance from other eukaryotic lineages and because they exhibit a broad range of different types of life cycle ranging from haploid-dominant haploid-diploid life cycles to diploid life cycles (Fig. 6) (Cock et al., 2014; Woelkerling, 2004). Molecular phylogenetic analysis has established a robust phylogeny for the brown algae (Fig. 7). Based on this phylogeny, the ancestral life cycle of this group is thought to have consisted of two multicellular generations (gametophyte and sporophyte) (Coelho et al., 2007; Kawai et al., 2007).

The order Ectocarpales, which consists principally of small, ephemeral brown algae, exhibits a remarkably wide range of different haploid-diploid life cycles. Across the different life cycles of organisms of this order, the two generations can be isomorphic (family Acinetosporaceae), slightly heteromorphic (Ectocarpaceae) or strongly heteromorphic with either a microscopic gametophyte or a microscopic sporophyte (Peters and Ramírez, 2001). Moreover, both generations may be capable of asexual reproduction, providing additional means to produce new offspring (de Reviers, 2006). The pathways of asexual reproduction include parthenogenetic development of unfertilised gametes, which can develop into either partheno-gametophytes (e.g. *Myriotrichia*) or partheno-sporophytes (e.g. *Ectocarpus*) depending on the species, the mito-spores produced in the plurilocular sporangia of sporophytes (Peters et al., 2008), and fragmentation of the sporophyte (e.g. Naples strain) (Müller, 1964).

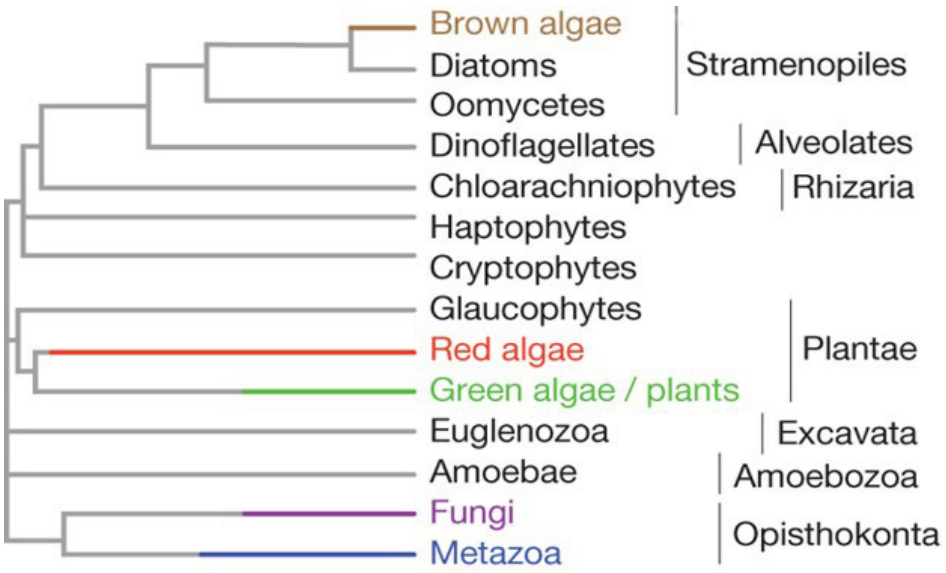


**Figure 5. Simplified representation of the evolutionary tree of complex multicellular organisms (highlighted in colour).** Five groups show complex multicellularity, i.e. they include macroscopic organisms with defined, recognisable morphologies that are composed of multiple cell types. Colour bars indicate the approximate, relative time when complex multicellularity emerged in each lineage (Cock et al., 2010).

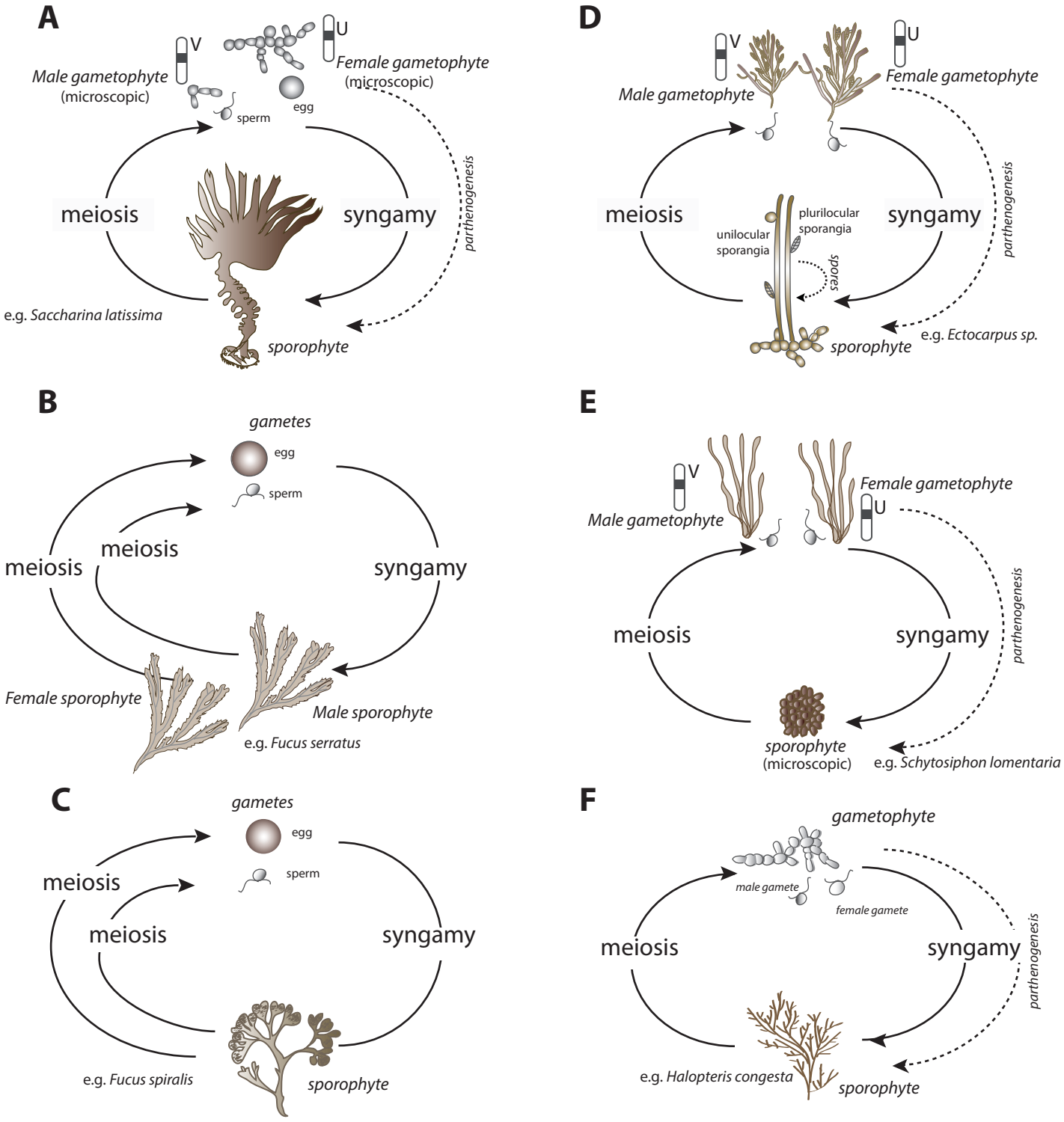


**Figure 6. Life cycles of brown algae.** The brown algae exhibit a wide range of life cycles, including haploid-diploid (haploid < diploid, A and F; haploid = diploid, D; haploid > diploid, E) and diploid life cycles (B and C). Meiosis results in the formation of haploid meio-spores, these develop into either male or female gametophytes in some species (e.g. A, D, E) depending on which sex chromosome (U or V) they inherited from the parent sporophyte.

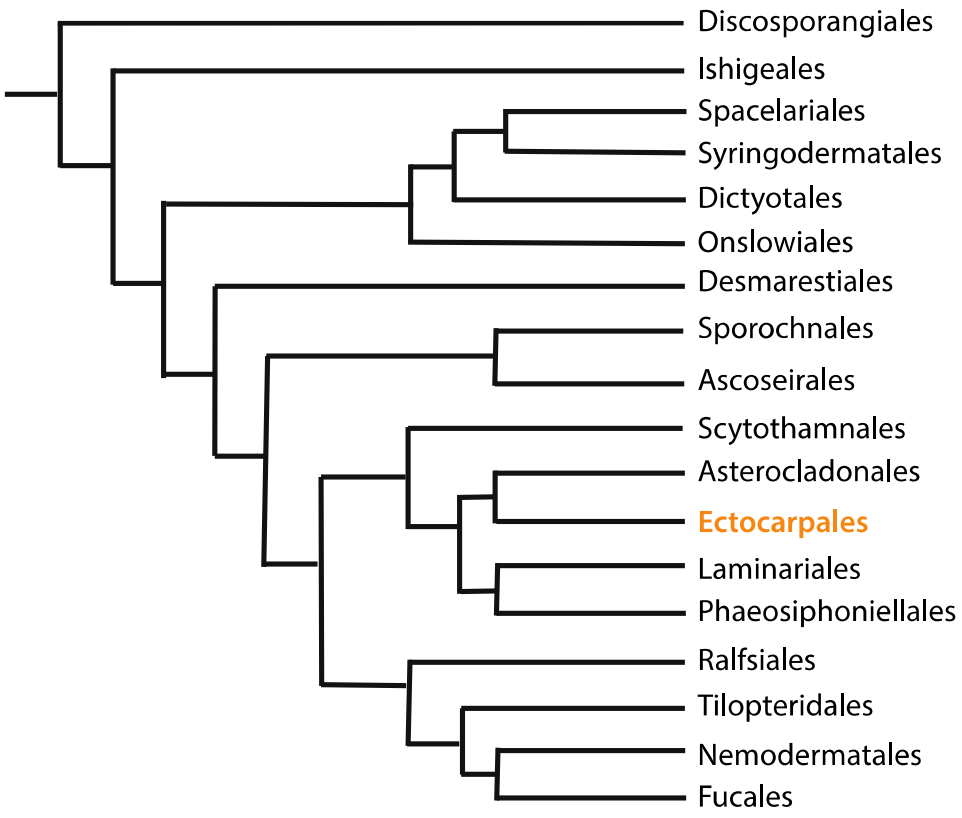


**Figure 7. Phylogenetic tree of the major brown algal orders.** The filamentous *Ectocarpus* (highlight in yellow) emerged as a model organism and provides a series of genetic tools to investigate the brown algae. The length of each branch is not proportional to the relative evolutionary time. Adapted from Silberfeld et al. (2014).

### 1.5 Model systems to study life cycle regulation

Evidence of genetic control of the alternation between generations was first reported in the unicellular fungus *Saccharomyces cerevisiae,* where the mating-type factors α2 and a1 were shown to bind to haploid-specific genes and repress them (Goutte and Johnson, 1988). Among photosynthetic organisms, the flowering plant *Arabidopsis* is a major model system for the study of various phenomenon associating life cycle progression with development. This phenomena does, however, pose some limitations for life cycle analysis because the gametophyte is highly dependent on the sporophyte generation and develops surrounded by sporophyte tissues. Despite this limitation, several studies have used *Arabidopsis* to study the alternation of generations (e.g. Yadegari and Drews, 2004). The moss *Physcomitrella patens* is also being used to study life cycle regulation. Moss life cycles involve two generations that both exhibit considerable developmental complexity but in *Physcomitrella patens* the sporophyte grows on the macroscopic gametophyte and depends on the latter for nutrients, again making it difficult to separate the two generations and study them individually (Bowman et al., 2007). The fern *Ceratopteris* (pteridophytes) has independent, multicellular gametophyte and sporophyte generations and is considered to be a suitable system to investigate haploid-diploid life cycles, but no mutant affected in the alternation of the two generations has yet been described in this system (Banks, 1999).

Marine algae are found in most lineages of the eukaryotic tree of life and have played an important role in the evolution of life. Consequently, these organisms offer the opportunity to tackle diverse questions regarding the origin and evolution of general eukaryotic traits. As far as life cycles are concerned, as discussed above, the existence of a broad range of the life cycles in the brown algae makes them good candidates to study life cycle evolution. This is particularly the case for brown algae where, in addition, a powerful model organism has become available in recent years. *Ectocarpus* was the first brown alga (also the first macroalga) to be sequenced (Cock et al., 2010) and has since emerged as a genetic model for the brown algae (Peters et al., 2004b). Many genetic and genomic tools are available for *Ectocarpus* including a high-quality genome annotation (Cock et al., 2010; Cormier et al., 2017), transcriptomic data based on

microarrays (Dittami et al., 2009) and RNA-seq technologies (Ahmed et al., 2014; Luthringer et al., 2015; Macaisne et al., 2017), genetic maps based both on microsatellite (Heesch et al., 2010) and restriction-site-associated DNA sequencing (RAD-seq) markers (Avia et al., 2017) and forward genetics methodologies (Godfroy et al., 2017; Macaisne et al., 2017). These features have made *Ectocarpus* a good choice as a model organism providing a novel system to shed light onto developmental processes such as the regulatory mechanisms that control the life cycle at the molecular level (Mignerot and Coelho, 2016; Peters et al., 2004a).

*Ectocarpus* is a small filamentous alga, which can be easily grown and induced to become fertile under laboratory conditions. Wild strains can grow up to 30 cm in length but individuals in culture can become fertile when they are less than 2 cm in length. *Ectocarpus* species are distributed worldwide in temperate coastal areas of both hemispheres but are absent from tropical seas. This seaweed usually grows in the intertidal zone on rocks or other substrates, often as an epiphyte on other brown and red algae (Coelho et al., 2012a). *Ectocarpus* has a haploid-diploid sexual life cycle (Fig. 8), which involves an alternation between a diploid sporophyte and dioicous, haploid gametophytes. Sporophytes produce meio-spores, following meiotic division in unilocular sporangia. The meio-spores are released into the surrounding seawater and develop as gametophytes, which produce gametes in plurilocular gametangia. Zygotes, produced by the fusion of male and female gametes, develop as diploid sporophytes, completing the sexual cycle. Unfertilized gametes can enter an asexual, parthenogenetic cycle by germinating to produce partheno-sporophytes, which can also produce both unilocular and plurilocular sporangia. As with diploid sporophytes, meio-spores produced in the unilocular sporangia of partheno-sporophytes develop into gametophytes to complete the asexual parthenogenetic cycle.

The sexual life cycle of *Ectocarpus* involves an alternation between two morphologically similar but independent sporophyte and gametophyte generations. There are several indications that the developmental programs of these two generations are not absolutely linked to ploidy. For example, ploidy and life cycle generation have been shown to be uncoupled during variant life cycles (Arun et al., 2013; Bothwell et al., 2010; Coelho et al., 2011). These features, together with the technical resources described above, make *Ectocarpus* a good choice among eukaryotic

organisms to carry out experiments to investigate the mechanisms of life cycle regulation at the molecular level.

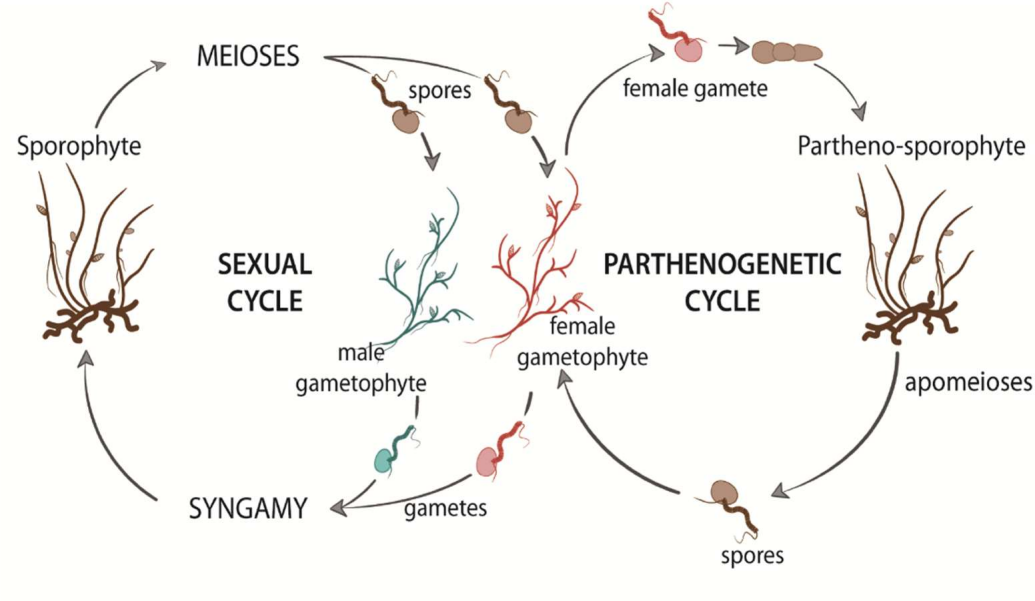


**Figure 8. The life cycle of the brown alga *Ectocarpus* sp.** The haploid-diploid life cycle of *Ectocarpus* is very complex. It consists of both sexual and asexual cycles (see text for details). Reproduced from Arun et al. (2019).

## 2. Alternation between gametophyte and sporophyte generations during the life cycle

### 2.1 The gametophyte and sporophyte generations during life cycle progression

The life cycles of multicellular photosynthetic organisms with haploid-diploid life cycles include two distinct multicellular organisms, the gametophyte and the sporophyte. In multicellular organisms, developmental processes need to be very precisely coordinated with life cycle progression and this is particularly important in organisms with haploid-diploid life cycles because the appropriate processes also need to be deployed during the appropriate generation of the life cycle (Arun et al., 2019). In this context, work carried out on both land plants and brown algae has aimed at addressing several specific questions: 1) what is the extent of differential gene expression between the two generations of the life cycle? 2) Which genes and genetic pathways are involved in generation-specific gene expression? 3) what are the common patterns in

generation-specific gene expression in different lineages of eukaryotes? 4) What general conclusions can be drawn from analyses of the evolution of life cycles across eukaryotic organisms (Szövényi et al., 2010). In the following section, we will discuss work on genes that exhibit generation-biased expression during the gametophyte and sporophyte generations.

## 2.2 Gene expression during the gametophyte and sporophyte generations of haploid-diploid life cycles

Differential gene expression during the life cycle results in a significant number of gametophyte- and sporophyte-biased genes (Dolan, 2009; Langdale, 2008; Mosquna et al., 2009; Okano et al., 2009). For example, in brown algal genomes (i.e. *Ectocarpus* sp., *Scytosiphon lomentaria*, *Macrocystis pyrifera*, *Saccharina japonica*) more than 30% of genes exhibit generation-biased expression patterns (Lipinska et al., 2019). The proportion of generation-biased genes is also high in land plants such as the moss *Funaria hygrometrica* (24%) or the seed plant *Arabidopsis thaliana* (23%-27%) (Szövényi et al., 2010; Szövényi et al., 2013). In the Ectocarples species *Ectocarpus* sp. and *Scytosiphon lomentaria*, gametophyte-biased genes (20-23% of the genome) are more numerous than sporophyte-biased genes (12-13% of the genome), whereas gametophyte-based genes are less numerous than sporophyte-based genes in the Laminariales (14-17% and 16-19% of the genome, respectively, in *Macrocystis pyrifera* and *Saccharina japonica*), *Funaria hygrometrica* (2.5% for the gametophyte and 5% for the sporophyte) and *A. thaliana* (5% for the gametophyte and 25% for the sporophyte) (Haerizadeh et al., 2009; Honys and Twell, 2003; Ma et al., 2008; Pina et al., 2005). Differential gene expression during haploid-diploid life cycles (Fig. 9) is often associated with marked differences in the morphology and functions of the gametophyte and sporophyte generations and there has been considerable interest in the roles of generation-biased genes in mediating these morphological and functional differences (Shaw et al., 2011; Szövényi et al., 2010).

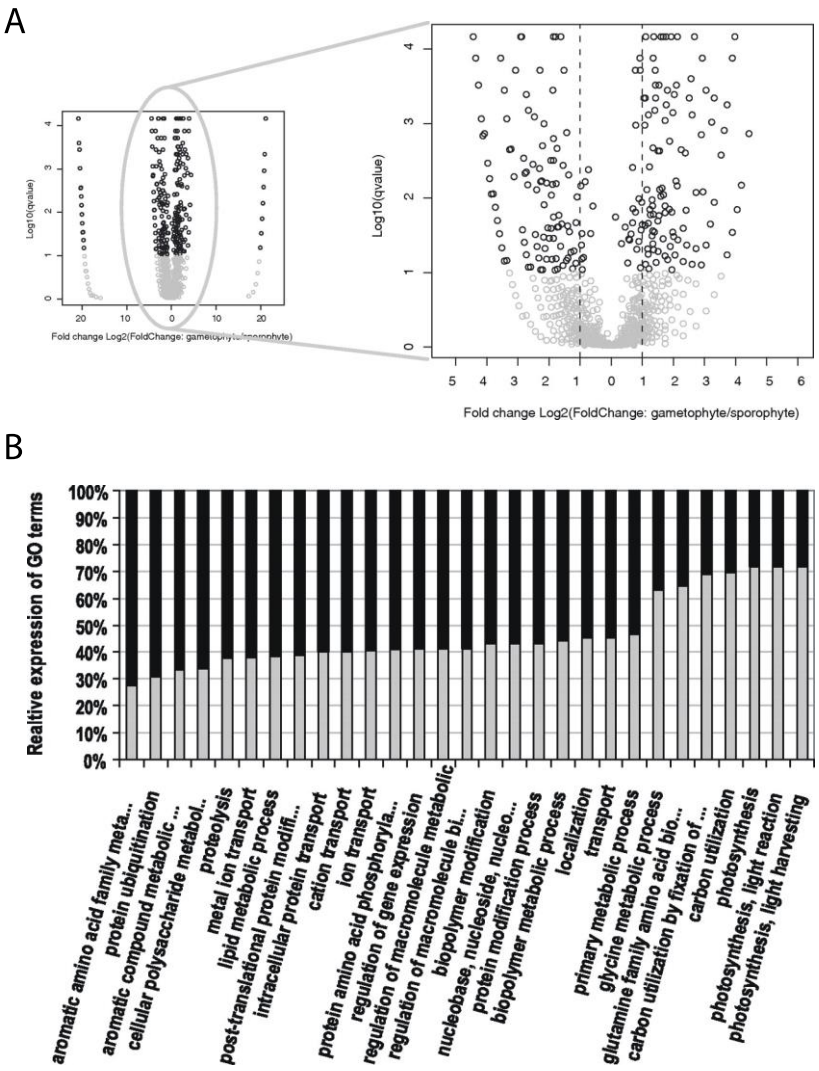


**Figure 9. Differential gene expression during the sporophyte and gametophyte generations of the moss *Funaria hygrometrica*.** (A). Volcano plot showing the significance and fold change of differential expression of genes between isogenic gametophyte and sporophyte generations. Non-differentially expressed transcripts ($q$ value > 0.1) are in grey, whereas significant genes are in black. (B). Most specific significant ($q$ value ≤ 0.1) GO terms (biological process ontology) and their relative expression level during the sporophyte and gametophyte generations of *Funaria hygrometrica.* Relative expression levels refer to the relative proportion of reads mapped to gene models with a particular GO term (black: sporophyte, gray: gametophyte). Reproduced from Szövényi et al. (2010).

## 2.3 Evolution of gametophyte and sporophyte developmental programs

As discussed above, various types of life cycles exist stably in nature, indicating that each type provides a unique advantage in a particular environment. Interpretation of the stability of haploid-diploid life cycles is difficult because both gametophyte and sporophyte generation possess their unique advantages and this is expected to lead to the dominance of one of the two generations under a wide range of conditions (Mable and Otto, 1998). However, it has been proposed that if the two generations are adapted to different ecological niches, a haploid-diploid life cycle could be stabilised over evolutionary time (Hughes and Otto, 1999; Stebbins and Hill, 1980; Willson, 1981).

Analysis of generation-biased gene expression can provide insights into the evolution of life cycles (Szövényi et al., 2010). In particular, such analyses can provide information about whether developmental pathways evolved independently in each generation or whether there has been the recruitment of developmental pathways from one generation to the other. For example, analysis of land plant developmental networks indicates that genetic components that played a role during the gametophyte generation, which was the dominant generation in ancestors of the land plants, were recruited to create the sporophyte generation developmental program (Dolan, 2009; Niklas and Kutschera, 2010). In addition, some aspects of the sporophyte generation program represent specific innovations associated with that generation (Sano et al., 2005; Szövényi et al., 2010).

In *Ectocarpus*, the gametophyte and sporophyte generations exhibit several morphological differences, with a particularly marked difference during the initial cell division of each generation. Early development of the gametophyte involves an asymmetric division of the initial cell, which is immediately followed by differentiation to form an erect thallus and a basal rhizoid (formation of an apical/basal axis) (Fritsch, 1935; Godfroy et al., 2017). In contrast, early development of the sporophyte involves symmetric division of initial cell that leads to the formation of a prostrate basal structure before the development of the erect thallus. The sporophyte of the *immediate upright (imm)* mutant exhibits several characteristics typical of the gametophyte. The initial cell of the *imm* mutant sporophyte undergoes asymmetric division and the sporophyte fails to form an extensive basal system, which is replaced by a rhizoid (Peters et

al., 2008). Therefore, analysis of the genetic mutant *imm* has shown that, in principle, both symmetric (wild type) and asymmetric (mutant) initial cell divisions can be at the origin of sporophyte development. Based on this, it has been proposed that the ancestral sporophyte developmental program may have more closely resembled that of the gametophyte (Macaisne et al., 2017). In other words, the sporophyte generation probably evolved from an ancestor that resembled the gametophyte generation with an asymmetrical initial cell division that gave rise directly to apical and basal organs (Macaisne et al., 2017). In the *distag* (*dis*) mutant, the gametophyte generation lacks a rhizoid and in the sporophyte generation prostrate filaments (i.e. the basal system) fail to develop (Godfroy et al., 2017). The phenotype of this mutant, therefore, supports the hypothesis that gametophyte rhizoids and sporophyte prostrate filaments are actually developmentally equivalent, despite marked differences in terms of morphological features such as cell form and size. In summary, the basal structures of both generations seem to be homologous but only in the sporophyte has the rhizoid been modified to produce an extensive system of prostrate filaments. *IMM* encodes the IMM protein, which does not have any known biochemical function (Macaisne et al., 2017). The developmental program associated with the *IMM* gene appears to be a specific innovation in the sporophyte generation because the *imm* mutation has no phenotype in the gametophyte. In contrast, the *DIS* gene, which encodes the TBCCd1 protein in *Ectocarpus*, is required for the formation of basal structures during both the gametophyte and the sporophyte generations (Godfroy et al., 2017). This suggests that the genetic system that includes the *DIS* gene was shared by both gametophyte and sporophyte generations during the process of evolution.

### 2.4 Evolution of patterns of gametophyte and sporophyte gene expression

In nearly all metazoan taxa, multicellular development only occurs during the diploid phase of the life cycle (Couceiro et al., 2015). Diploid dominance is also observed in land plants in the sense that this lineage is thought to be derived from a haplontic ancestor, with an expansion of the sporophyte generation and a shortening of the gametophyte generation (d'Amato, 1977). There is also evidence for a tendency towards diploid dominance in the brown algae, particularly in recently evolved lineages such as the Laminariales and the Fucales. However, haploid-diploid

life cycles can, nonetheless, be stable over evolutionary time. This is the case for red algae, most brown algae, many green algae, some fungi, foraminiferans, mosses and ferns (Richerd et al., 1993). In these latter examples, independent gametophyte and sporophyte generations have been stably maintained over long periods of evolutionary time (Mable and Otto, 1998).

Brown algae are thought to be derived from a last common ancestor whose life cycle involved alternation between gametophyte and sporophyte generations without a clearly dominant generation. However, during evolution, there has been a tendency for most brown algae to evolve towards increased complexity of either the gametophyte or the sporophyte generation (Silberfeld et al., 2010). As mentioned above, there is a general tendency in the brown algae towards diploid dominance but, in some species, the gametophyte generation can be considered to be dominant, either because it is more complex morphologically or because the species has more gametophyte-biased than sporophyte-biased genes. This is the case, for example, in the Ectocarpales species *Ectocarpus* sp. and *Scytosiphon lomentaria* (Lipinska et al., 2019). Note that, when considering gene expression, it is important to take into account both generation-biased gene expression and the proportions of the total gene set expressed in each generation. For example, in *Arabidopsis*, 69% of the genes are expressed in the male gametophyte, but only 7.9% of these genes are gametophyte-specific. In most species with haploid-diploid life cycles, the majority of genes are expressed in both the gametophyte and sporophyte generation (Honys and Twell, 2004; Lipinska et al., 2019).

It is currently thought that the majority of the genetic and regulatory networks that operate during the sporophyte generation in land plants originated from equivalent components that originally functioned during the gametophyte generation (Menand et al., 2007; Nishiyama et al., 2003). However, this idea of unidirectional recruitment from gametophyte to sporophyte may be a simplification, as analysis of the evolution of generation-biased gene sets in the brown algae indicates a dynamic process with a proportion of the genes frequently changing their pattern of expression, often leading to expression during the opposite generation (Lipinska et al., 2019). Nonetheless, analysis of the extensive generation-specific gene expression across different species indicates that the genetic programs that underlie each generation evolved relatively

independently and developmental innovations were selected under natural selection for each generation (Szövényi et al., 2013). One consequence of these differences in selection is that genes associated with different generations may evolve at different rates (Orr and Otto, 1994; Otto and Gerstein, 2008). For example, in *F. hygrometrica* and *A. thaliana*, gametophyte-specific genes evolve faster than sporophyte-specific genes (Anderson et al., 2004; Orr and Otto, 1994; Otto and Gerstein, 2008; Zeyl et al., 2003). Similarly, gametophyte-biased genes are evolving rapidly compared with unbiased genes in some brown algae, e.g. Ectocarpales and Laminariales (Lipinska et al., 2019).

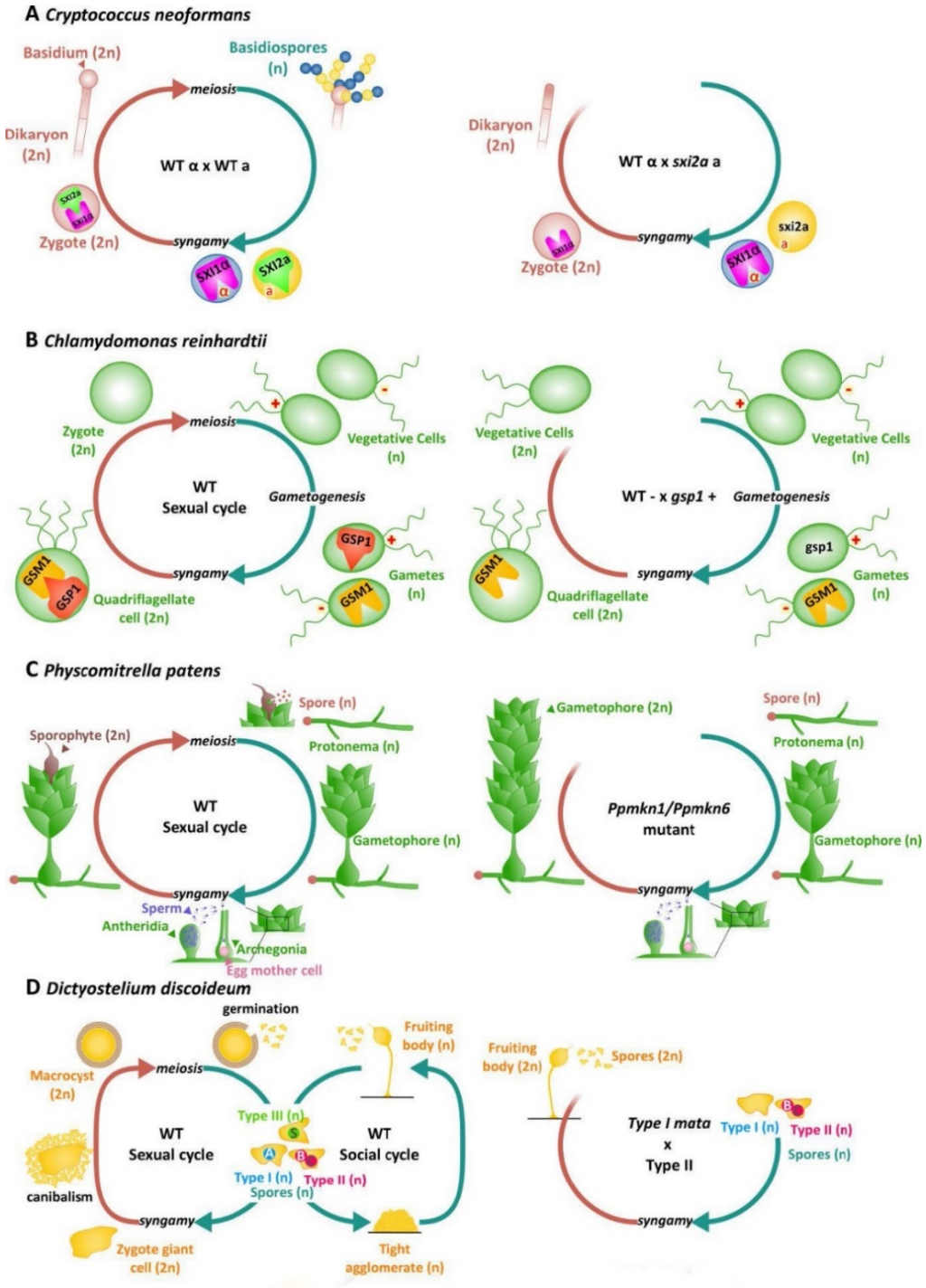


**Figure 10. Homeodomains, homeodomain-like transcription factors and life cycle regulation.** Reproduced from Bourdareau (2018).

A: Life cycle of *Cryptococcus neoformans*. Haploid a (yellow, expressing the homeodomain transcription factor SIX2a) and α (blue, expressing the homeodomain transcription factor SIX1α) gametes fuse to form a diploid zygote. SIX1α and SIX2a interact after syngamy to initiate sexual development (Left). Zygotes that originate from a cross between a wild-type α gamete and a *six2a* gamete cannot initiate sexual development (right). For detailed information see Hull et al. (2005).

B: Life cycle of the green alga *Chlamydomonas reinhardtii*. The homeodomain transcription factors GSP1 (in plus gametes) and GSM (in minus gametes) form a heterodimer and move to the nucleus after plus and minus gametes fuse and initiate the zygote program (left). A zygote derived from a cross between a minus gamete (wild-type) and a *gsp1* gamete fails to implement the zygote program (right). For details see Lee et al. (2008b).

C: Life cycle of the moss *Physcomitrella patens*. Haploid spores develop to produce protonema filaments on which grow the gametophores. Male gametes swim to the archegonia from the neighbouring antheridia and fuse with egg cells to produce diploid sporophytes (left). A functional diploid gametophyte develops instead of the sporophyte in the *Ppmkn1-Ppmkn6* double mutant (right). For details see (Sakakibara et al., 2013).

D: Life cycle of the amoeba *Dictyostelium discoidem*. Three types of haploid spores (Type I, Type II and Type III) produce three different homeodomain-like transcription factors MatA, MatB and MatC respectively. Zygotes, which are formed when each type of spore fuses with either of the other two spore mating types, form a macrocyst by attracting and engulfing nearby haploid cells. Mature macroysts produce haploid spores to complete the life cycle (Left). Zygote derived from a cross between a wild-type Type II spore and a *mata* Type I spore develop to produce a fruiting body with diploid spores similar to haploid cells. For details see Hedgethorne et al. (2017).

## 3. Genetic control of transitions between the gametophyte and the sporophyte generation

### 3.1 Genetic regulators of life cycle transitions

As both the gametophyte and sporophyte generations are constructed using information from a shared genome, it follows that epigenetic regulatory processes must operate both during meiosis (at the diploid-to-haploid transition) and during syngamy (at the haploid-to-diploid transition) to trigger the initiation of the appropriate developmental program associated with each generation (Bourdareau, 2018). As discussed before, in many organisms the gametophyte and sporophyte generations are morphologically and functionally different, so the developmental switches must be precisely controlled to avoid the production of chimeric organisms.

Genetic studies have improved our understanding of the molecular basis of life cycle progression, particular the haploid-to-diploid transition (Fig. 10). The first evidence for genetic control of a transition between generations of a life cycle was reported for a unicellular fungus, the yeast *Saccharomyces cerevisiae*. The mating-type genes *MATα2* and *MATa1* produce the α2 and a1 proteins that bind to haploid-specific genes and repress them (Goutte and Johnson, 1988). α2 shares homology with homeodomain proteins in *Drosophila* (Shepherd et al., 1984), and similar systems, also involving homeodomain regulators, have been described in other fungi such as *Ustilago maydis* (Gillissen et al., 1992), *Coprinus cinereus* and the human pathogen *Cryptococcus neoformans* (Kües et al., 1992). The mating system of *Crytococcus neoformans* has been particularly well described. Zygotes form by fusion of a and α gametes (Hull et al., 2005), which express a and α mating-type-specific factors, respectively. After gamete fusion, these two proteins interact to form a heterodimer, which initiates zygote development. The a and α factors are encoded by genes localized at the mating-type locus (*SEX INDUCER α2* or *SEX INDUCER a1*) and both proteins are homeodomain transcription factors (HD TFs). In the amoebozoan *Dictyostelium discoideum* the mating-type locus encodes two pairs of gametologs that suffice to specify sexual compatibility: *matA* for type I, *matS* for type III, *matB* and *matC* for type II (Hedgethorne et al., 2017). During the sexual cycle, each mating-type can fuse with either of the two other types to initiate the diploid phase. This mating-type system involves genetic

interactions between mating-type loci suggesting that heterodimerization (in this case of homeodomain-like mating-type proteins (i.e. genes that do not have a recognisable, conserved homeodomain motif but which possess a domain that resembles the homeodomain in terms of its three dimensional structure) may also play a role in inducing the diploid program in slime mould (Bourdareau, 2018; Hedgethorne et al., 2017).

A similar system, involving homeodomain transcription factors, has been described for the haploid life cycle of the unicellular, green alga *Chlamydomonas* (Fig. 10B). Homeodomain transcription factor-encoding genes have been classed into two major groups, the TALE (three-amino acid loop extension) and the non-TALE homeodomain transcription factor, because the later have no the characteristic of three amino acid loop extension of the 60 amino acid homeodomains (Nam and Nei, 2005; Nasmyth and Shore, 1987). Both classes of homeodomain transcription factor are very ancient and both are widely distributed across all the major eukaryotic lineages (Cock et al., 2014; Derelle et al., 2007). Initiation of the diploid program in *Chlamydomonas* is controlled by a heterodimeric homeodomain transcription factor composed of two TALE homeodomain proteins: Gsm1 (gamete-specific *minus*1), which is a knotted-like homeobox (KNOX) gene, and Gsp1 (gamete-specific *plus*1), which is a BEL-like (BELL) TALE homeodomain transcription factor. The major function of this system appears to be to act as a detector of the transition from haploid to diploid (when gametes fuse to form a zygote).

Recent work indicates that the multicellular streptophyte moss *Physcomitrella patens* may possess a similar system (Fig. 10C). Mutation of two KNOX class genes *PpMKN1* and *PpMKN6* results in the sporophyte generation being replaced by a fully functional diploid gametophyte (Sakakibara et al., 2013). In addition, the *P. patens* genome is predicted to encode four BEL-class proteins, similar to Gsp1. Several lines of evidence indicate a role for these BEL genes in controlling the life cycle. First, *PpBELL1* and *PpBELL2* are expressed in eggs and embryos. Second, loss or overexpression of *PpBELL1* leads to a failure to build sporophytic structures or, conversely, to the production of apogamous sporophyte-like bodies on haploid caulonemal cells, respectively (Horst et al., 2016). To summarise, in the green lineage both KNOX and the BELL class TALE homeodomain transcription factors are necessary for the deployment of the

sporophyte generation. Together they act as master regulators of the gametophyte-to-sporophyte transition because loss of these genes leads to a block of the sporophyte developmental program leading to conversion of this generation of the life cycle into a diploid gametophyte.

Modification of chromatin by the Polycomb Repressive Complex 2 (PRC2), which regulates gene expression by tri-methylation of lysine 27 of histone H3, also appears to be involved in regulating the gametophyte-to-sporophyte transition in the green lineage. *Arabidopsis* mutants affected in PRC2 components such as *MEDEA* (*MEA*), *MULTICOPY SUPPRESSOR OF IRA I* (*MSI1*) and *FERTILISATION INDEPENDENT SEED 2* (*FIS2*) exhibit switching from gametophyte cell fate to endosperm or embryo-like structures (Chaudhury et al., 1997; Ebel et al., 2004; Guitton and Berger, 2004; Köhler et al., 2003; Ohad et al., 1996; Ohad et al., 1999). Similar phenotypes have been observed in the moss *P. patens*. Two PRC2 genes *PHYSCOMITRELLA PATENS FERTILIZATION INDEPENDENT ENDOSPERM* (*PpFIE*) and *PHYSCOMITRELLA PATENS CURLY LEAF* (*PpCLF*) induce the growth of sporophyte-like bodies on the side branches of the gametophyte (Mosquna et al., 2009; Okano et al., 2009). Ectopic expression of other genes such as *SERK*, *BABY BOOM (BBM)*, and *LEC* (*LEC1* and *LEC2)* has also been shown to affect the initiation of the sporophyte developmental program in flowering plants. These genes may act downstream of the regulator that controls the switch from gametophyte to sporophyte (Schiefthaler et al., 1999).

Evidence that TALE homeodomain transcription factors also control life cycle transitions in brown algae has come from recent work on two *Ectocarpus* mutants, *ouroboros* (*oro)* and *samsara (sam)*. These two mutations have been shown to cause the sporophyte generation to be converted into a fully functional gametophyte generation. The two genes therefore appear to act as master regulators of the gametophyte to sporophyte transition. The corresponding genes, *ORO* and *SAM*, both encode TALE homeodomain transcription factors and these two proteins appear to act as a heterodimer to initiate the sporophyte developmental program (Arun et al., 2019; Coelho et al., 2011). Although chromatin remodelling is probably also involved in the control of life cycle transitions in brown algae, this is unlikely to require PRC2 because genes encoding PRC2 components appear to be absent from the *Ectocarpus* genome (Bourdareau, 2018).

### 3.2 Non-cell autonomous regulation of life cycle generation identity

Genetic analysis has proved to be an important tool for understanding the molecular mechanisms underlying the life cycle but alternative, physiological approaches have also provided important insights in the model brown alga *Ectocarpus*. These analyses have shown that the alternation of generations in *Ectocarpus* is not only under the control of the TALE homeodomain transcription factors ORO and SAM (Arun et al., 2019) but is also influenced by a non-cell-autonomous factor designated the sporophyte-inducing factor that is secreted into the surrounding seawater medium by *Ectocarpus* sporophytes in culture (Arun et al., 2013). During the sexual life cycle of *Ectocarpus*, meiotic divisions in unilocular sporangia produce haploid meio-spores that normally develop to produce gametophytes. Occasionally, a small proportion of meio-spores develop into sporophytes instead of gametophytes, a phenomenon called heteroblasty (Müller, 1967). Arun et al. (2013) showed that the proportion of heteroblastic meio-spores was significantly increased if the spores were allowed to develop in sporophyte-conditioned medium (SCM, i.e. cell-free medium in which sporophytes had previously been cultured). Gametophyte-condition medium (GCM) did not have the same effect indicating that heteroblasty is induced by a molecule specifically produced by the sporophyte. The sporophyte identity of the heteroblastic individuals was confirmed by staining with Congo red (a water-soluble, carbohydrate-binding dye which binds to xylan fibres in algal cell walls and specifically stains *Ectocarpus* gametophytes but not sporophytes) (Coelho et al., 2011; Yadegari and Drews, 2004). Moreover, these individuals produced reproductive structures typical of the sporophyte generation, i.e., unilocular sporangia (a structure that is only observed during the sporophyte generation).

These experiments demonstrated that there is some plasticity with respect to the deployment of the sporophyte or gametophyte pathways, even in the absence of genetic mutations, and support the idea that life cycle generation is not strictly correlated with ploidy (Cock et al., 2014). Interestingly, additional variations of the *Ectocarpus* life cycle have been observed that support this idea of independent life cycle generation and ploidy. For example, unfused gametes of wild type strains can develop autonomously to produce haploid partheno-sporophytes (Müller, 1967; Mignerot et al., 2019). Therefore, the sporophyte generation can be haploid under some

conditions. Similarly, it is possible to construct diploid gametophytes by crossing two strains carrying the *oro* mutation (Coelho et al., 2011).

Meio-spores carrying either the *oro* or the *sam* mutation are resistant to the action of the diffusible sporophyte-inducing factor (Arun et al., 2019), indicating that the *ORO* and *SAM* genes are necessary for developmental reprogramming to occur and, therefore, that *ORO* and *SAM* may be part of the regulatory network triggered by the sporophyte-inducing factor (Fig. 11).

Developmental reprogramming was not observed when meio-spores were treated with SCM 48 hours after their release from the unilocular sporangium. This corresponds with the time required for the meio-spores to synthesise a cell wall, suggesting that the diffusible factor is unable to act on a cell that is surrounded by a cell wall (although it is also possible that other cellular events occur at this stage to render the developing meio-spore insensitive to the factor). The role of the cell wall was further investigated using protoplasts. Gametophyte-derived protoplasts obtained by digesting the cell walls of gametophyte filament cells normally develop as gametophytes, but a proportion regenerates into sporophytes if they are incubated with SCM (Arun et al., 2013). This experiment supported the idea that cells must lack a cell wall to respond to the diffusible factor but other processes may be involved, as the protoplast process presumably also induces some dedifferentiation of the filament cells. Note that there is evidence that the cell wall influences other developmental processes. For example, in the brown alga *Fucus spiralis*, the cell wall influences cell fate by inducing switching from thallus to rhizoid identity (Berger et al., 1994; Bouget et al., 1998). Similarly, the cell wall plays an important role in terrestrial plant morphogenesis (Hamant et al., 2010).

Based on this potential link between the presence or absence of the cell wall and the capacity to switch between life cycle generations and on the likely hypothesis that the sporophyte-inducing diffusible factor originates from or corresponds to a cell wall component, the following section will look more closely at the composition of brown algal cell walls.

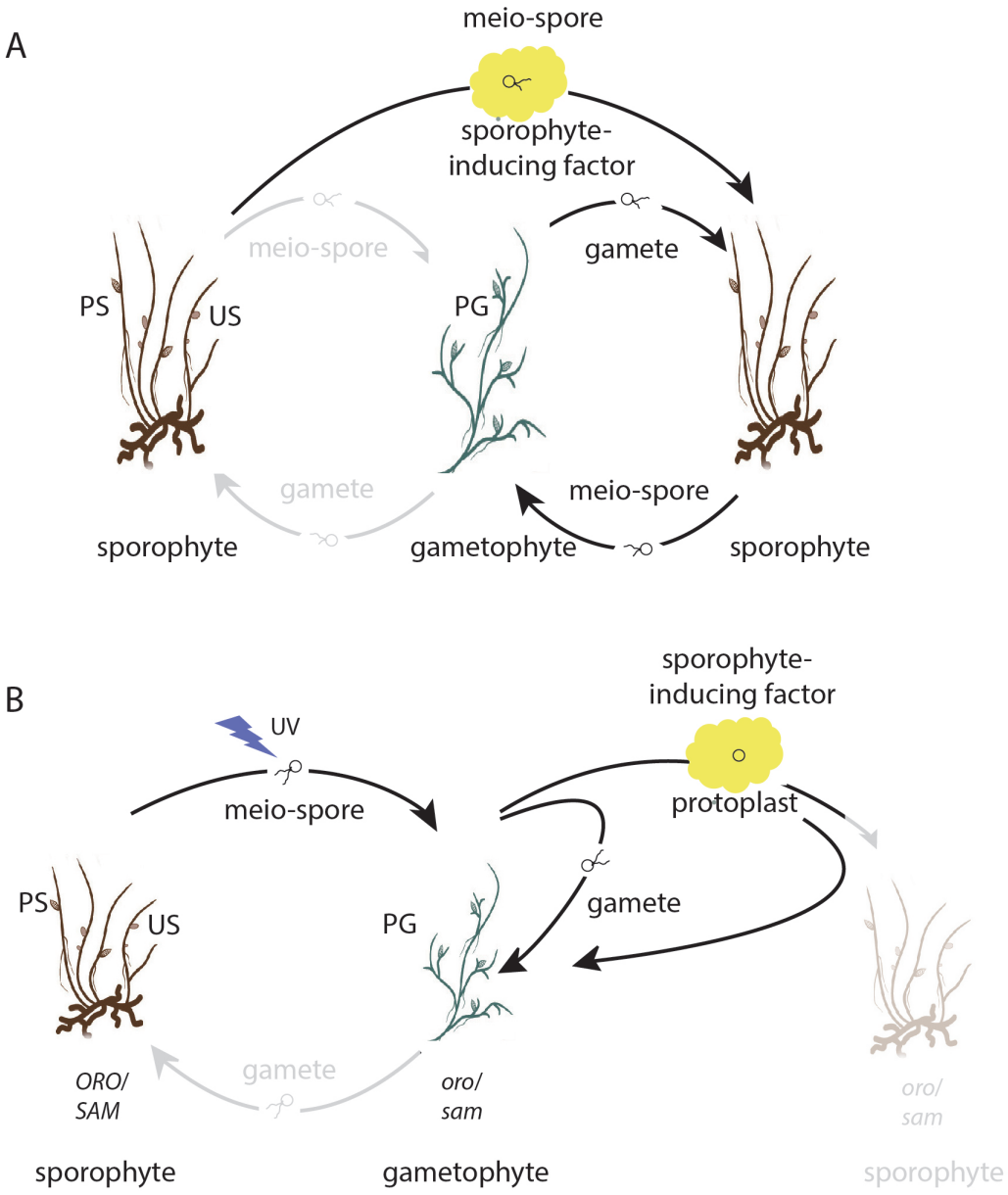


**Figure 11. The life cycle of *Ectocarpus* is regulated by the diffusible sporophyte-inducing factor and by the genetic factors, *ORO* and *SAM*.** (A). The wild sporophyte produces meio-spores, via a meiotic division in the unilocular sporangia, which develop as gametophytes and produce gametes in plurilocular gametangia. However, a proportion of meio-spores develop as full functional sporophytes when incubated with sporophyte-inducing factor (heteroblasty). In strains carrying mutations in either *ORO* or *SAM*, the sporophyte is converted into a fully functional gametophyte. (B). *oro* and *sam* mutants are insensitive to the sporophyte-inducing factor. PS: plurilocular sporangia; US: unilocular sporangia; PG: plurilocular gametangia. Reproduced from Arun et al. (2019).

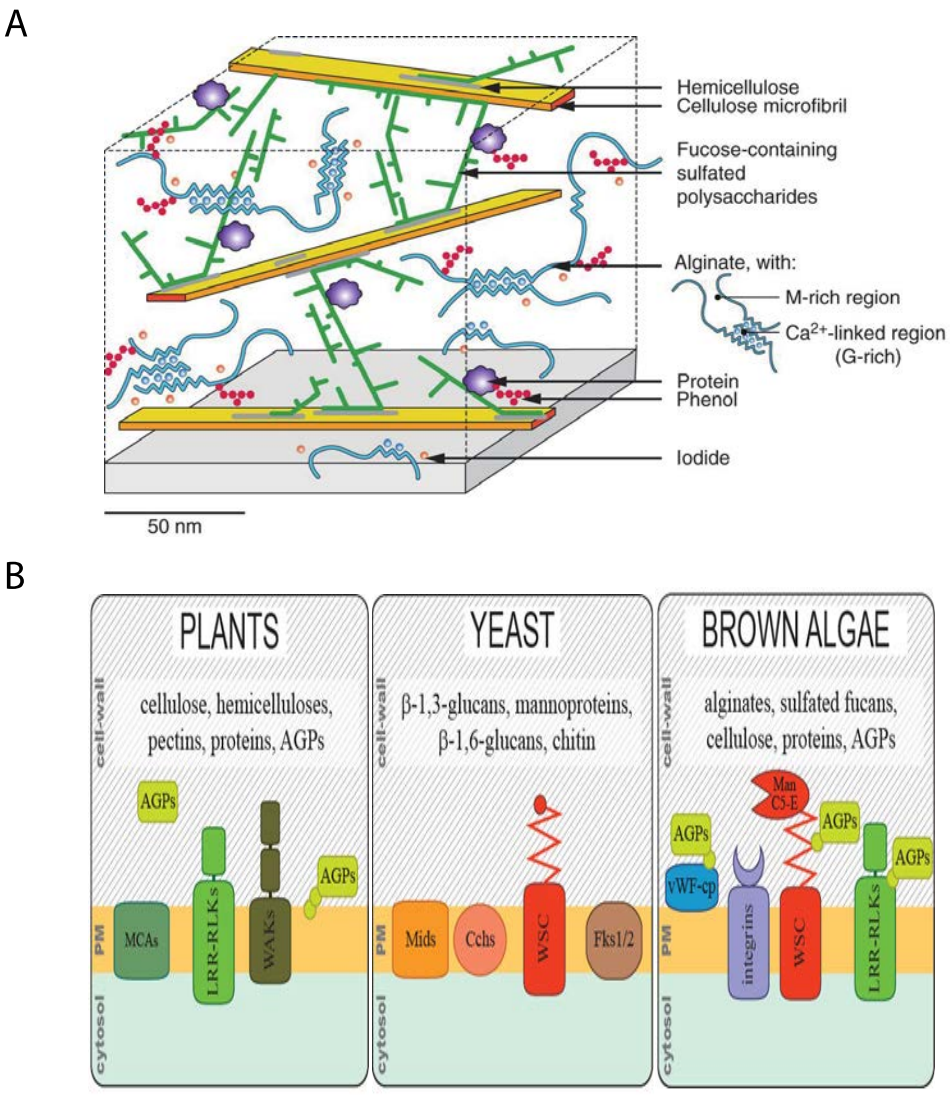


**Figure 12. Cell wall model for brown algae from the order Fucales and comparison with plants and fungi.** A: The main components of brown algal cell walls are alginates and sulphated fucans. Alginates and fucose-containing sulfated polysaccharides form the greater part of cell wall polymers, the latter acting as cross-linkers between cellulose microfibrils. See details in Deniaud-Bouët et al. (2014). B: Putative cell wall sensing proteins in brown, compared with equivalent molecules found in other kingdoms. AGPs, arabinogalactan proteins; WSC, wall sensing component; ManC5-E, mannuronan C5-epimerase. Reproduced from Hervé et al. (2016).

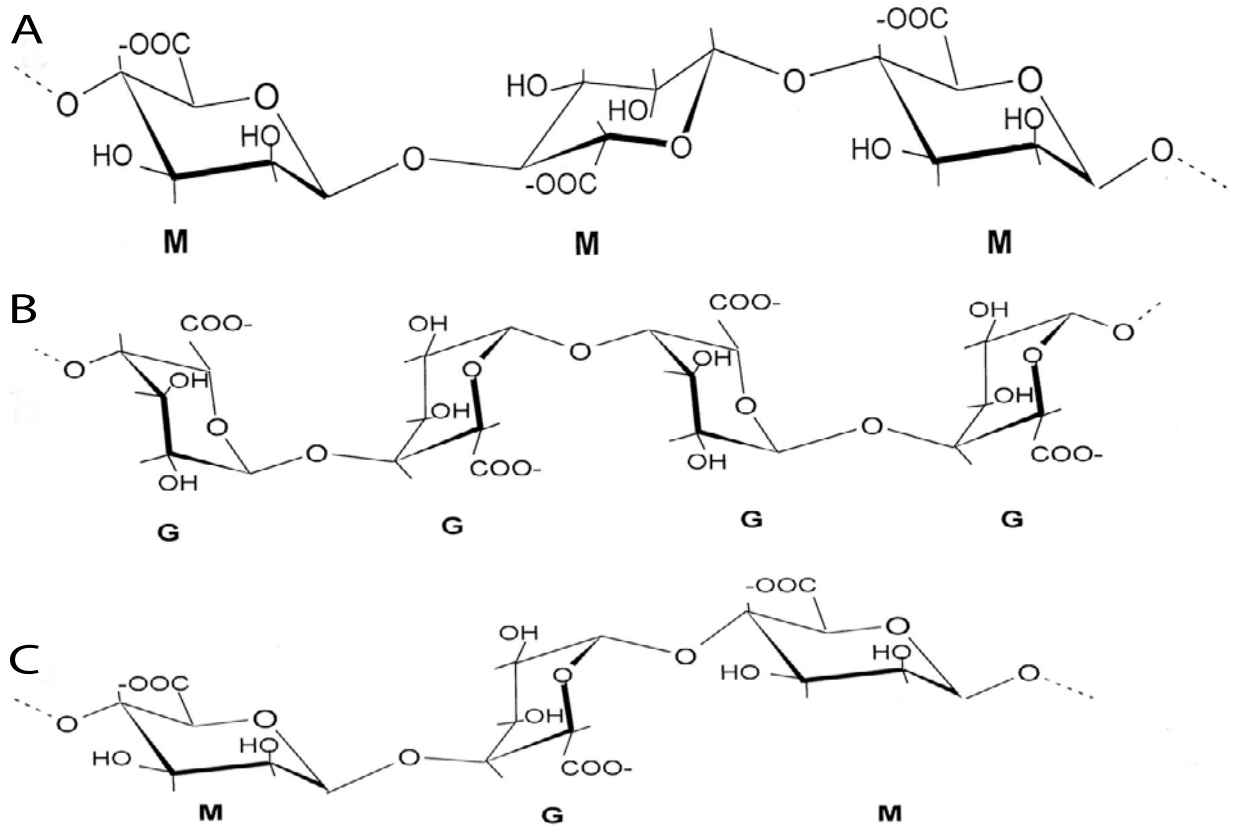


**Figure 13. Chemical structures of alginates from brown algae.** Alginates are linear anionic copolymers of β-1,4-d-mannuronic acid and of its C5 epimer, α-1,4-l-guluronic acid. They consist of an alternation of homopolymeric blocks of poly-β-1,4-d-mannuronic acid, referred to here as MM blocks (A), of homopolymeric blocks of poly-α-1,4-l-guluronic acid (GG blocks; B), and of heteropolymeric blocks with random arrangements of both monomers (MG blocks; C). (Küpper et al., 2001)

### 3.3 Composition of brown algal cell walls

The cells of all photosynthetic, multicellular, eukaryotic organisms, including terrestrial plants and brown algae, are surrounded by a dynamic, complex, carbohydrate-rich cell wall (Popper et al., 2011b). In the tree of life, complex multicellular organisms evolved in only a small number of eukaryotic groups including notably the plants and the brown algae. Interestingly, in both the plants and the brown algae, this process was associated with the evolution of complex cell walls which play important roles in cell-to-cell recognition, adhesion and communication.

The brown algae (Phaeophyceae) are a group of multicellular algae that arose within the stramenopile lineage and which therefore obtained their plastids through a secondary endosymbiosis with a red alga (Berney and Pawlowski, 2006; Michel et al., 2010; Reyes-Prieto et al., 2007). This endosymbiosis event explains why brown algae share many features of their photosynthetic system and cell wall components with land plants because photosynthesis and carbohydrate synthesis genes were acquired during this event. Brown algal cell walls (Fig. 12A) share features with both plant and fungus cell walls, but also posses some unique characteristics (Fig. 12B). The cell walls of brown algae, like those of other marine algae and plants, can be understood as a two-phase system: a crystalline phase (the skeleton) embedded in a more amorphous phase (the matrix) (Kloareg and Quatrano, 1988). In brown algae, the skeletal phase is made up of natural, linear polymers, while in other algae the skeletal phase contains chitin-like polymers built with N-acetyl-glucosamine (Herth and Schnepf, 1982) or highly crystalline glycoproteins based with hydroxyproline (in the Volvocales) (Roberts et al., 1974).

Anionic polysaccharides, namely alginates (which also occur in some bacteria) and fucoidans (which also occur in animals), are the main components of brown algal cell walls (up to 45% of algal dry weight, e.g. alginates constitute about 60% of *L. digitata* cell walls) (Kloareg and Quatrano, 1988; Mabeau and Kloareg, 1987). In contrast, cellulose (which also occurs in plants) only accounts for a relatively low proportion of the cell wall (1-8% of dry weight) (Cronshaw et al., 1958). In intertidal brown algae, the average weight ratios of alginate, fucoidans and cellulose are about 3:1:1 (Mabeau and Kloareg, 1987; Kloareg and Quatrano, 1988). Alginate consists of two uronic acids (Fig. 13): β-1-4-D-mannuronate and α-1-4-L-guluronate, which initially polymerise as mannuronan. The guluronate residues are made at the polymer level by mannuronate C5-epimerases (MC5Es), which convert mannuronan to guluronate. Fucoidans are sulfated polysaccharides containing α-L fucose residues. Echinoderm fucans have regular structures composed of liner and repetitive polysaccharides (Pereira et al., 1999). Sulfated fucans may be present as either homofucans or heterofucans. These polysaccharides are referred to as fucose-containing sulfated polysaccharides (FCSPs) (Ale et al., 2011; Sakai et al., 2003). In addition, brown algal cell walls contain phlorotannins (Schmidt-Nielsen, 1997), which are composed of halogenated or sulfated phenolic compounds and about 5% protein (Quatrano and

Stevens, 1976). In general, brown algal cell walls differ markedly from those of land plants (Hervé et al., 2016).

In brown algae the alginates, sulfated fucans and phlorotannins are synthesized in the Golgi, transported in vesicles to the plasma membrane and secreted into the expanding cell wall (Callow et al., 1978; Schoenwaelder and Wiencke, 2000). In contrast, cellulose microfibrils are produced and deposited *in situ* by cellulose synthase complexes localized in the plasma membrane (Peng and Jaffe, 1976). Microchemical imaging analyses have indicated that apoplastic, vanadate-dependent iodoperoxidase (Colin et al., 2005) binds to large amounts of iodine in Laminariales cell walls (Verhaeghe et al., 2008). In the presence of halides, vanadate-dependent iodoperoxidase also catalyses the cross-linking of alginates with phlorotannins (Berglin et al., 2004), implying that halogenated and phenolic compounds have an important role in cell wall cohesion.

The composition of the cell wall or extracellular matrix of brown algae is variable depending on the developmental stage and season. Brown algal cell walls are thought to play an important role in innate immunity (Küpper et al., 2001), resistance to mechanical stress and protection from predators (Popper et al., 2011a). They also play crucial roles in controlling cell differentiation (development), as in land plants, and developmental processes such as growth, differentiation and morphogenesis are intimately associated with alternations in cell wall metabolism (Quatrano and Stevens, 1976). The link between cell morphogenesis and the deposition of the cell wall has been studied in Fucales zygotes, which have long served as models to study cell polarization and asymmetrical cell division in relation to the cell wall (Belanger and Quatrano, 2000; Brownlee, 2002; Deniaud-Bouët et al., 2014; Paciorek and Bergmann, 2010). During germination, tip growth is initiated at a pre-determined site on the surface of the zygote and a rhizoid emerges (Fowler and Quatrano, 1997; Kropf et al., 1988). The apical cell of the rhizoid will then elongate, whereas the thallus cell will proliferate by diffuse growth (Bisgrove and Kropf, 2001). Cell wall components (e.g. transmembrane proteins with potential roles in cell-cell communication) are thought to control cell differentiation during the sporophyte generation of *Ectocarpus* sp. (Le Bail et al., 2011). The important function of the major cell wall constituent, alginate, is reflected in

brown algal genomes, which encode a large number of MC5E enzymes (28 in *Ectocarpus* sp.) and many WSC (cell wall sensing components) domain proteins. The latter may be involved in interactions between alginate and proteins. Both of these large multigenic families, together with brown algae-specific receptor kinases and an expanded complement of cell wall-related genes, were described in detail as part of the analysis of the genome of the model brown alga *Ectocarpus* sp. (Michel et al., 2010). Structural genomic evidence showed that MC5E genes were associated with both WSC domains (Oide et al., 2019; Wawra et al., 2019) and arabinogalactan protein (AGP) protein core motifs (Hervé et al., 2016).

**Objectives**

The main objective of this study was to characterize the diffusible factor produced by sporophytes that modifies the cell fate of initial cells of the gametophyte generation, switching them to sporophyte identity. The work focused on optimizing production, storage and bioassay of this sporophyte-inducing factor to increase our understanding of its biochemical nature. The study also investigated the relationship between the sporophyte-inducing factor and two genetic regulators, *ORO* and *SAM,* to understand the developmental pathway triggered by the sporophyte-inducing factor. In addition to this work on life cycle generation identity, the thesis has also involved characterisation of the *Ectocarpus baseless* mutant, which exhibits a similar phenotype to the *distag* mutant (Godfroy et al., 2017) and is affected in developmental patterning during both the gametophyte and sporophyte generations. The specific objectives of the thesis were:

1. To set up a standardised protocol for the production and bio-assay of the diffusible factor (Chapter II).
2. To characterise the sporophyte-inducing factor that induces gametophyte-to-sporophyte developmental reprogramming in Ectocarpus (Chapter III). The work principally included the optimization of production, bioanalysis of the factor and preliminary biochemical characterisation.

3. To investigate relationships between life cycle regulators: i.e. between the sporophyte-inducing factor and two genetic regulators, ORO and SAM (Chapter IV), as part of a broader study aimed at characterising the latter two genetic regulators.
4. To characterise the *baseless* mutant, which is affected in developmental patterning during both generations (Chapter V).

# Chapter II

# Protocol for the production and bioassay of a diffusible factor that induces gametophyte-to-sporophyte developmental reprogramming in *Ectocarpus*

Previous studies demonstrated that alternation of generations in *Ectocarpus* is not determined by ploidy but is under genetic control, and can be influenced by a non-cell-autonomous factor produced by the sporophyte (Arun et al., 2013; Bothwell et al., 2010). Genetic control is mediated by two TALE HD transcription factors, ORO and SAM, which are required for the induction of the sporophyte developmental program in *Ectocarpus* (Arun et al., 2019; Coelho et al., 2011). The non-cell-autonomous factor produced by the sporophyte acts on gametophyte initial cells inducing a switch to the sporophyte developmental program (Arun et al., 2013; Bothwell et al., 2010). However, the exact biochemical nature of this diffusible factor is still not known. The main task of this Ph.D project was to characterise the sporophyte-inducing diffusible factor. To this end, the establishment of a standardised procedure for the production and bioassay of the diffusible factor was a key objective for the project and this protocol represents an important resource for future study of the diffusible factor. This chapter will present the optimised protocol, which has been prepared in the form of a manuscript and will be submitted for publication.

# Protocol for the production and bioassay of a diffusible factor that induces gametophyte-to-sporophyte developmental reprogramming in *Ectocarpus*

**Haiqin Yao[1], Delphine Scornet[1], Akira F. Peters[2], Murielle Jam[1], Cecile Hervé[1], Philippe Potin[1], Susana M. Coelho[1,*], J. Mark Cock[1,*]**

[1]CNRS, Sorbonne Université, UPMC University Paris 06, UMR 8227, Integrative Biology of Marine Models, Station Biologique de Roscoff, CS 90074, F-29688, Roscoff, France; [2]Bewhin Rosko, Santec, France

[*]Authors for correspondence (cock@sb-roscoff.fr, coelho@sb-roscoff.fr), joint last authors.

Keywords: sporophyte-inducing factor; *Ectocarpus*; life cycle; sporophyte

## Introduction

The brown algae, which are one of only a small number of eukaryotic lineages that have evolved complex multicellularity, exhibit a broad range of life cycles (Cock et al., 2010). *Ectocarpus* is a small, filamentous brown alga that has been adopted as a genetic model organism for the brown algae (Cock et al., 2010; Coelho et al., 2007; Peters et al., 2004a). This alga has a haploid-diploid life cycle that involves an alternation between two multicellular generations, the gametophyte and the sporophyte (Bothwell et al., 2010; Müller, 1967). These two generations are free-living and exhibit distinct morphologies and functions. Mature diploid sporophytes can produce two kinds of reproductive structure, unilocular sporangia and plurilocular sporangia. Meio-spores, which are produced by meiotic cell divisions in unilocular sporangia, are released into the surrounding

environment and germinate to produce separate male and female (dioecy), haploid gametophytes. Mature female and male gametophytes produce only one type of reproductive structure, plurilocular gametangia, where gametes are formed through mitotic cell divisions. Female and male gametes fuse to produce zygotes that develop to produce diploid sporophytes, completing the life cycle (Fig. 1). It is known that the life cycle generation (i.e. sporophyte or gametophyte identity) is not determined by ploidy because single gametes are able to develop parthenogenetically, without fusing to produce a zygote, leading to the production of haploid patheno-sporophytes that are phenotypically indistinguishable from diploid sporophytes derived from a zygote (Bothwell et al., 2010; Müller, 1967). These partheno-sporophytes can produce unilocular sporangia and release meio-spores to complete this asexual, parthenogenetic cycle. The gametophyte and sporophyte generations of *Ectocarpus*, therefore, show spatio-temporal independence, facilitating the study of the developmental program of each generation and their relationship with the life cycle.

Alternation of generations in *Ectocarpus* has been shown to be controlled by two homeodomain transcription factors (HD TFs) of the three amino acid loop extension (TALE) class, OUROBOROS (ORO) and SAMSARA (SAM), which are necessary for the initiation of the sporophyte program (Arun et al., 2019; Arun et al., 2013). In addition, the sporophyte has been shown to secrete a non-cell-autonomous, diffusible factor that can cause receptive cells to switch from the gametophyte to the sporophyte developmental program (Arun et al., 2019; Arun et al., 2013). This diffusible factor is only effective at the single-cell stage and Arun et al. (2013) showed that developing meio-spores became resistant to the factor at the same point in time as they synthesise a cell wall, about 24-48h after release from unilocular sporangia. This suggests that the cell wall may play a role in locking the individual into the developmental program that has been initiated.

The protocol provided below describes both how to produce the diffusible factor and how to assay its activity using a meio-spore-based bioassay.

**Production of sporophyte-conditioned medium**

**Culture of *Ectocarpus* tissues**

Culture sporophytes and gametophytes of *Ectocarpus* male strain Ec32 separately in 55-mm diameter Petri dishes in 10 ml of Provasoli-enriched seawater (PES, i.e. natural seawater enriched with Provasoli supplement; Starr and Zeikus, 1993) or in 150-mm diameter Petri dishes with 100 ml PES. Cultures are grown under standard conditions: 13°C, 12h:12h (light:dark) and 20 µM photons/$m^2$/s (Coelho et al., 2012b).

**SCM production**

Grow cultures of *Ectocarpus* strain Ec32 gametophytes in 150 mm Petri dishes for 2 weeks (about 0.13 grams per Petri dish) under low light (2-3 µM photons/$m^2$/s, 12h:12h light: dark) in PES at 13°C. Induce the release of gametes by grouping 20-30 gametophytes together in a small volume of medium (to simulate low tide conditions) and incubation in the dark for four hours. Then add 300 µl PES and under light to induce gametes release. Use each batch of released gametes to inoculate two 150 mm Petri dishes (about $10^6$ gametes per petri dish) and cultivate the resulting partheno-sporophyte germlings under low light conditions for 14 days. Inoculate a 10 L bottle of PES with 0.5 g partheno-sporophyte thalli and grow for between four and eleven weeks at 13°C under low light conditions. The bottle culture should be aerated by pumping air through a 0.2 µm filter.

**Collection and storage of the SCM**

Use a large size cell strainer to remove the partheno-sporophyte tissue from the culture and then filter the SCM through a Falcon 40 µm cell strainer and a 0.22 µm filter to remove any remaining cells. The SCM is then stored in bottles (prepared beforehand by cleaning with 70% ethanol) in a cold room at 4°C.

**Bioassay to detect the diffusible sporophyte-inducing factor**

**Production of meio-spores**

The bioassay of the diffusible sporophyte-inducing factor is carried out using meio-spores produced by fertile sporophytes. Depending on the strain of *Ectocarpus*, meio-spores can exhibit different levels of heteroblasty, i.e. spontaneous initiation of the sporophyte program instead of the gametophyte program (Müller, 1967). To assay the activity of the diffusible factor, it is therefore important to use a strain that exhibits a low level of spontaneous heteroblasty, such as the strain Ec32.

The culture conditions used to grow fertile partheno-sporophytes have been described in (Coelho et al., 2012b). Gametes released from 45 to 60 mature gametophytes are cultured in 150-mm Petri dishes under standard culture conditions (with a light intensity of 20 µM photons/$m^2$/s, 12h:12h light: dark at 13°C). When upright filaments are produced, remove individual partheno-sporophytes and culture separately. Cultures grown at high density will not produce unilocular sporangia. Change the culture medium regularly (once every 2 weeks) until the partheno-sporophyte filaments produce upright filaments. Plurilocular sporangia should develop after about 1 to 2 weeks and the unilocular sporangia appear about one week later.

Alternatively, unilocular sporangia can be produced on cultured upright filaments, for example by transferring dissected upright filaments with unilocular sporangia that have released meio-spores back into culture. These filaments will adhere to the bottom of a 55-mm petri dish and produce new upright filaments in few days under the standard culture condition. These new upright filaments will produce many unilocular sporangia, which appear after about one week in general, and they produce fewer or no plurilocular sporangia. This method of producing unilocular sporangia is more rapid than culturing whole partheno-sporophytes.

**Bioassay of the diffusible factor**

Dissect a piece of sporophyte upright filament that bears one or more unilocular sporangia using a sterilized glass pipette under a binocular microscope. Wash the fragment twice in PES by

transferring sequentially to two 55-mm Petri dishes, each containing 10 ml of PES (to ensure that there is no carry-over of possible contaminating mito-spores), then transfer into a drop of 300 µl of SCM (Fig. 2) on a coverslip. The coverslip should be fixed to the bottom of the Petri dish by placing it on a drop of 10 µl of PES. In parallel, test similarly isolated unilocular sporangia in PES as a negative control. Note that the SCM can be replaced by any other seawater-based sample that you would like to test for diffusible factor activity. The unilocular sporangia, which are cultured under strong light conditions (30 µM photons/$m^2$/s) overnight, are then allowed to release their meio-spores (100-200 per unilocular sporangium) directly into the 300 µl drop of the test solution (Coelho et al., 2012b). This should take less than 48 hours. Discard any plates where the release has not occurred within this time frame. After releasement of the meio-spores, remove the piece of sporophyte upright filament. At 72 hours, gently add 10 ml of PES to the Petri dish. The meio-spore-derived germling is (weakly) attached to the coverslip at this stage and the added medium assures that they grow under optimal conditions. After an additional three or four days examine the Petri dish under an inverted microscope to score the numbers of gametophyte and sporophyte individuals (Fig. 3). Note that, if meio-spores are released within 48 hours but then germinate slowly, the germination process can be accelerated by adding an additional 300 µl of the test medium to the 300 µl drop. This will allow the germlings to grow and attach to the coverslip before the plate is flooded with the 10 ml of PES.

When working with active preparations of SCM, expect between 2% and 30% of the meio-spores to be switched from gametophyte to sporophyte identity but note that the percentage of switching can be highly variable between assays. It is therefore preferable to carry out at least three assays for each test to obtain statistically robust estimations of diffusible factor activity.

## References


Ahmed S, Cock JM, Pessia E*, et al.*, 2014. A haploid system of sex determination in the brown alga *Ectocarpus* sp. *Current biology* **24**, 1945-57.

Arun A, Coelho SM, Peters AF*, et al.*, 2019. Convergent recruitment of TALE homeodomain life cycle regulators to direct sporophyte development in land plants and brown algae. *Elife* **8**.

Arun A, Peters NT, Scornet D, Peters AF, Mark Cock J, Coelho SM, 2013. Non-cell autonomous regulation of life cycle transitions in the model brown alga *Ectocarpus*. *New Phytol* **197**, 503-10.

Bothwell JH, Marie D, Peters AF, Cock JM, Coelho SM, 2010. Role of endoreduplication and apomeiosis during parthenogenetic reproduction in the model brown alga *Ectocarpus*. *New Phytologist* **188**, 111-21.

Cock JM, Sterck L, Rouze P*, et al.*, 2010. The *Ectocarpus* genome and the independent evolution of multicellularity in brown algae. *Nature* **465**, 617-21.

Coelho SM, Godfroy O, Arun A, Le Corguillé G, Peters AF, Cock JM, 2011. *OUROBOROS* is a master regulator of the gametophyte to sporophyte life cycle transition in the brown alga *Ectocarpus*. *Proceedings of the National Academy of Sciences* **108**, 11518-23.

Coelho SM, Peters AF, Charrier B*, et al.*, 2007. Complex life cycles of multicellular eukaryotes: New approaches based on the use of model organisms. *Gene* **406**, 152-70.

Coelho SM, Scornet D, Rousvoal S*, et al.*, 2012. How to cultivate *Ectocarpus*. *Cold Spring Harbor Protocols* **2012**, pdb. prot067934.

Gane AM, Craik D, Munro SL, Howlett GJ, Clarke AE, Bacic A, 1995. Structural analysis of the carbohydrate moiety of arabinogalactan-proteins from stigmas and styles of *Nicotiana alata*. *Carbohydrate Research* **277**, 67-85.

Hervé C, Simeon A, Jam M*, et al.*, 2016. Arabinogalactan proteins have deep roots in eukaryotes: identification of genes and epitopes in brown algae and their role in *Fucus serratus* embryo development. *New Phytol* **209**, 1428-41.

Laemmli UK, 1970. Cleavage of structural proteins during the assembly of the head of bacteriophage T4. *Nature* **227**, 680.

Müller DG, 1967. Generationswechsel, kernphasenwechsel und sexualität der braunalge *Ectocarpus siliculosus* im kulturversuch. *Planta* **75**, 39-54.

Moller I, Sørensen I, Bernal AJ*, et al.*, 2007. High ‐ throughput mapping of cell ‐ wall polymers within and between plants using novel microarrays. *The Plant Journal* **50**, 1118-28.

Niklas KJ, Newman SA, 2013. The origins of multicellular organisms. *Evolution & development* **15**, 41-52.

Paulsen BS, Craik DJ, Dunstan DE, Stone BA, Bacic A, 2014. The Yariv reagent: behaviour in different solvents and interaction with a gum arabic arabinogalactan-protein. *Carbohydr Polym* **106**, 460-8.

Peters AF, Marie D, Scornet D, Kloareg B, Mark Cock J, 2004. Proposal of *Ectocarpus siliculosus* (Ectocarpales, Phaeophyceae) as a model organism for brown algal genetics and genomics 1, 2. Journal of Phycology 40, 1079-1088.

Van Holst G-J, Clarke AE, 1985. Quantification of arabinogalactan-protein in plant extracts by single radial gel diffusion. *Analytical biochemistry* **148**, 446-50.

Zsebo KM, Wypych J, Mcniece IK*, et al.*, 1990. Identification, purification, and biological characterization of hematopoietic stem cell factor from buffalo rat liver-conditioned medium. *Cell* **63**, 195-201.

## Figures

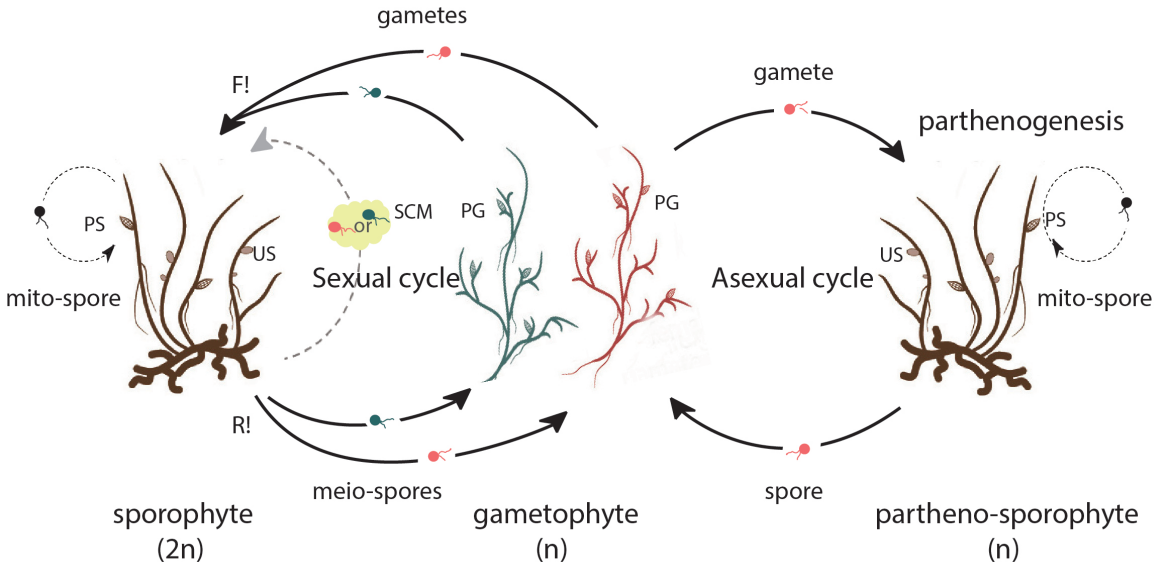


**Figure 1. The *Ectocarpus* life cycle.** The diploid sporophyte produces meio-spores via a meiotic division, in the unilocular sporangia. These meio-spores are released and develop as gametophytes, which produce male and female gametes in plurilocular gametangia. Male and female gametes fuse to form zygotes, that develop as diploid sporophytes and complete the sexual cycle (left). Unfertilized gametes can enter an asexual cycle via parthenogenesis and germinate as partheno-sporophytes. Partheno-sporophyte produce spores in unilocular sporangia which develop as gametophytes and complete the asexual cycle (right). Two additional pathways of asexual reproduction are possible, one is sporophyte produces mito-spores in plurilocular sporangia, that germinate to the sporophytes (dotted line). The other one is a proportion of meio-spores can develop as the sporophytes (dashed line) under some conditions (Arun et al., 2013). PS, plurilocular sporangia; US, unilocular sporangia; PG, plurilocular gametangia; SCM, sporophyte condition medium; R!, meiotic reduction; F!, gametes fusion. Reproduced from Peters et al. (2008).

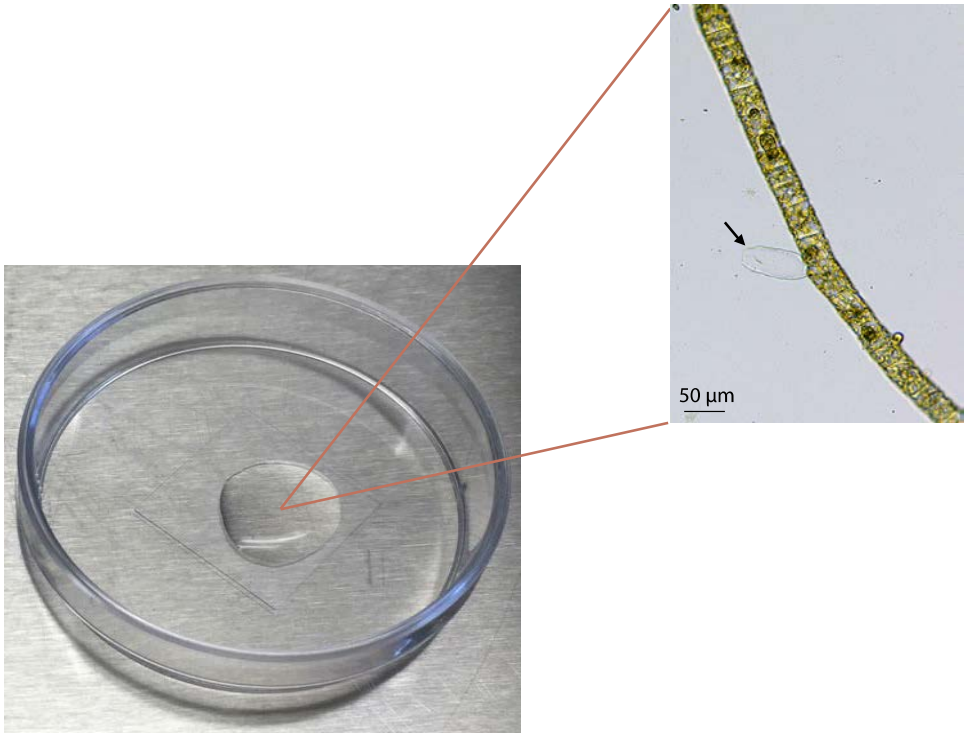


**Figure 2. Release of meio-spores from unilocular sporangia**. After dissection, a piece of upright filament carrying one or more unilocular sporangia is transferred to a small drop on a coverslip placed inside a Petri dish. Three drops of PES are placed around the edge of the Petri dish to keep the chamber moist and the Petri dish is sealed with parafilm. The insert shows a piece of sporophyte upright filament with a unilocular sporangium (arrow) that has released its meio-spores into the test medium. Scale bar: 50 µm.

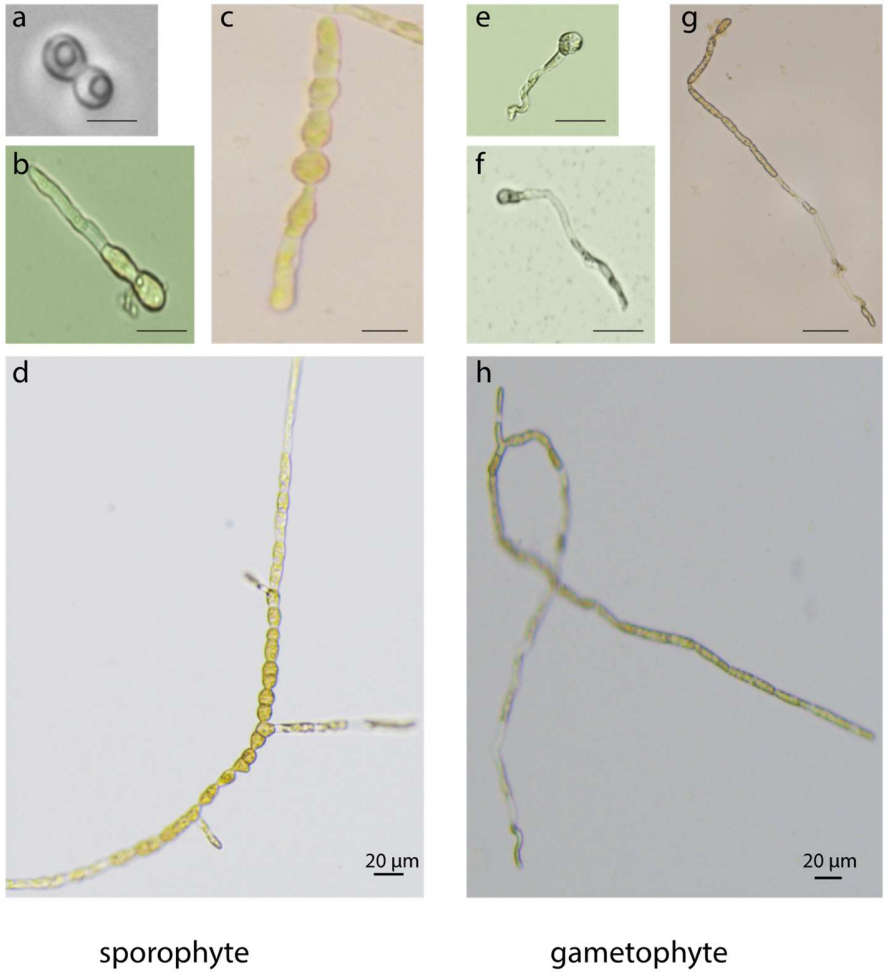


**Figure 3. Morphological differences between gametophytes (normal development, right) and sporophytes (modified development, left) derived from SCM-treated meio-spores.** Meio-spores were incubated in SCM for three days and then grown in PES. (a) and (e) two cell stages of the sporophyte (symmetrical cell division) and the gametophyte (asymmetrical cell division), respectively. (b) and (f) sporophyte and gametophyte germlings, respectively, after about 3 days in SCM. (c) and (g) sporophyte and gametophyte germlings, respectively, after about 5 days in SCM. (d) and (h) sporophyte and gametophyte germlings, respectively, after about 14 days in SCM. Scale bars: 20 µm.

## Discussion and future work

Development of the protocol described in this chapter involved selection of an optimal strain for the production of the bioassay material (meio-spores) and optimisation of multiple steps of the bioassay process. The wild type *Ectocarpus* strain Ec32 is a good choice for bioassay experiments because it has a very low (essentially 0%) background of heteroblasty, minimising the occurrence of false positives. Optimal release of meio-spores from unilocular sporangia was induced by exposure to strong light intensity overnight. Another important factor was that meio-spore release occurred directly into the test solution (SCM), ensuring that the treatment occurred from the earliest steps of germination. Removal of filaments with empty unilocular sporangia after meio-spore release was also important to avoid possible false positives. Finally, the amount of variation in the responses of meio-spores to test solutions was reduced by eliminating unilocular sporangia that did not release within 48h. This optimised bioassay was successfully applied to optimise production of active SCM and for the preliminary characterisation of the diffusible factor. The standardised bioassay provides a stable and rapid method to detect diffusible factor activity whilst minimising the amount of bioassay test work required for each analysis. This protocol will be a valuable tool for future research aimed at characterising the diffusible factor.

# Chapter III

# Characterisation of a diffusible factor that induces gametophyte-to-sporophyte developmental reprogramming in *Ectocarpus*

*Ectocarpus* is a filamentous brown alga with a haploid-diploid life cycle involving alternation between two independent and morphologically distinct multicellular generations: the diploid sporophyte and the haploid gametophyte (Bothwell et al., 2010). The sporophyte produces haploid spores through meiotic divisions and these develop as male or female gametophytes, which then produce male or female gametes. Recent work has shown that alternation of generations in *Ectocarpus* is under the control of two TALE HD transcription factors (ORO and SAM) (Arun et al., 2019; Coelho et al., 2011) but developmental fate can also be influenced non-cell autonomously by a diffusible factor produced by the sporophyte, which causes major developmental reprogramming in gametophyte cells (Arun et al., 2013). This chapter will present optimisation of the production and detection of the sporophyte-inducing diffusible factor, together with preliminary experiments aimed at characterising the factor biochemically. Our results indicate that the factor is a large molecule and a broad protein sequencing approach identified a candidate protein which is predicted to be an arabinogalactan protein (AGP) and to be involved in cell wall metabolism. Additional experiments, such as treatment with proteinase K and heating to 121°C, provided further information about the nature of the diffusible factor. Based on the hypothesis that the factor may correspond to an AGP, experiments were also carried out in which meio-spores were incubated with the plant AGP preparation gum arabic or the plant arabinogalactan preparation larcoll. Characterisation of the sporophyte-inducing diffusible factor was the main objective of this Ph.D project. This chapter has been prepared in the form of a manuscript.

# Evidence that an arabinogalactan-protein-like factor induces gametophyte to sporophyte switching in the brown alga *Ectocarpus*

**Haiqin Yao[1], Delphine Scornet[1], Murielle Jam[2], Cecile Hervé[2], Philippe Potin[3], Lydie Oliveira Correia[4], Susana M. Coelho[1,*], J. Mark Cock[1,*]**

[1]Algal Genetics group, CNRS, Sorbonne Université, UPMC University Paris 06, UMR 8227, Integrative Biology of Marine Models, Station Biologique de Roscoff, CS 90074, F-29688, Roscoff, France

[2] Marine Glycobiology, CNRS, Sorbonne Université, UPMC University Paris 06, UMR 8227, Integrative Biology of Marine Models, Station Biologique de Roscoff, CS 90074, F-29688, Roscoff, France

[3]Algal Biology and Enviromental interactions, CNRS, Sorbonne Université, UPMC University Paris 06, UMR 8227, Integrative Biology of Marine Models, Station Biologique de Roscoff, CS 90074, F-29688, Roscoff, France

[4]Micalis Institute, PAPPSO, INRA, AgroParisTech, Université Paris-Saclay, 78350, Jouy-en-Josas, France

[*]Authors for correspondence (cock@sb-roscoff.fr, coelho@sb-roscoff.fr), joint last authors.

Keywords: arabinogalactan protein; diffusible factor; *Ectocarpus*; life cycle; sporophyte

## Abstract

The haploid-diploid life cycle of the filamentous brown alga *Ectocarpus* involves alternation between two independent and morphologically distinct multicellular generations, the sporophyte and the gametophyte. The sporophyte generation has been shown to secrete a diffusible factor that induces meiotic spores to switch from the gametophyte to the sporophyte developmental program. Here, we determine optimal conditions for production, storage and detection of this factor and show that it is a heat-resistant, high molecular weight molecule. Several lines of evidence suggest that the factor may be an arabinogalactan-protein-like molecule and,

remarkably, incubation of meio-spores with plant arabinogalactan proteins (gum arabic) or arabinogalactans (larcoll) mimicked the effect of treatment with sporophyte-conditioned medium, inducing switching to the sporophyte program.

## Introduction

Most eukaryotic life cycles involve an alternation between haploid and diploid phases, with the transitions between ploidy states occurring as a result of meiotic division (ploidy reduction) and gamete fusion, or syngamy (increased ploidy) (Coelho et al., 2007). Multicellular photosynthetic organisms with haploid-diploid life cycles produce two distinct multicellular generations, one during each phase of the life cycle: diploid, spore-producing sporophytes and haploid, gamete-producing gametophytes (Cock et al., 2014; Coelho et al., 2007). The majority of brown algae have this type of haploid-diploid life cycle and one of these species, the filamentous brown alga *Ectocarpus*, is being used as a model system to study life cycle regulation (Cock et al., 2014; Peters et al., 2004a). *Ectocarpus* has a complex life cycle (Müller, 1967). In addition to the basic sexual life cycle, involving an alternation between gametophyte and sporophyte generations, several asexual variations have been observed in culture, including parthenogenetic development of gametes that fail to encounter and fuse with a gamete of the opposite sex (Müller, 1967). Interestingly, germinating parthenogenetic gametes deploy the sporophyte program, despite being haploid, to produce partheno-sporophyte individuals that are morphologically indistinguishable from diploid sporophytes. One important conclusion that can be drawn from the existence of haploid partheno-sporophytes is that life cycle generation (i.e. deployment of a gametophyte or a sporophyte bodyplan) is not determined by ploidy (haploid or diploid phase) and that these two features of the life cycle can be uncoupled under certain circumstances (Bothwell et al., 2010; Müller, 1967). This conclusion is supported by the existence of genetic mutants that cause switching between life cycle generations, independent of the ploidy of the mutant individual (Arun et al., 2019; Coelho et al., 2011). Genetic analysis of life cycle mutants of this type has demonstrated that the deployment of the sporophyte program in *Ectocarpus* is under the control of two homeodomain transcription factors (HD TFs) of the three amino acid loop extension (TALE) class, which have been named OUROBOROS (ORO) and SAMSARA (SAM),

Coelho et al., 2011). These transcription factors appear to be derived from an extremely ancient life cycle regulation system and to be distantly related to HD TF life cycle regulators in other eukaryotic supergroups such as specific KNOX and BEL class proteins in the green lineage (Viridiplantae).

Further evidence for the independence of life cycle generation and ploidy was provided by the identification of a sporophyte-inducing factor that is secreted into the surrounding seawater medium by *Ectocarpus* sporophytes in culture (Arun et al., 2013). When meio-spores, which normally develop to produce the gametophyte generation, are allowed to germinate in the presence of this diffusible factor, a proportion of the resulting germlings deploy the sporophyte developmental pathway. Interestingly, meio-spores carrying either *oro* or *sam* mutations are insensitive to the action of the diffusible, sporophyte-inducing factor (Arun et al., 2019; Arun et al., 2013), indicating that the *ORO* and *SAM* genes are necessary for developmental reprogramming to occur. ORO and SAM may therefore be part of the regulatory network trigged by the sporophyte-inducing factor.

The objective of this study was to further characterise the diffusible sporophyte-inducing factor. After optimising production, storage and bioassay of the factor, we carried out a number of analyses aimed at providing further information about its biochemical nature. We obtained evidence that the sporophyte-inducing factor is a high molecular weight molecule that is resistant to high temperature and protease treatment. Despite its insusceptibility to protease treatment, we found several indications that the factor may correspond to an arabinogalactan protein (AGP): 1) mass spectrometry analysis of partially purified (ultrafiltrated) sporophyte-conditioned medium (SCM) identified 36 proteins, one of which is predicted to contain an AGP core protein domain, 2) AGP glycan epitopes were detected in a concentrated SCM preparation using immunoblotting, 3) SCM activity was reduced following incubation with an AGP-reactive Yariv reagent and 4) the biological activity of the sporophyte-inducing factor could be mimicked by the addition of either a preparation of land plant AGPs (gum arabic) or arabinogalactans (larcoll).

## Results

### Rapidly released meio-spores are more responsive to the sporophyte-inducing diffusible factor

Arun et al. (2013) demonstrated that *Ectocarpus* sporophytes secrete a diffusible factor that induces meio-spores to switch from the gametophyte to the sporophyte developmental program. With the objective of further characterising this diffusible factor, we first aimed to determine optimal conditions for its production and assay. The physiological state of a sporophyte can influence unilocular sporangium production and function, leading to developmental abnormalities of the sporangium and often delayed or dysfunctional release of meio-spores. To assess the effect of meio-spore quality on detection of the diffusible factor, we compared batches of unilocular sporangia that had released after 12-24 h, 24-48 h or >48 h of incubation in SCM to determine whether the time taken to release the spores influenced the proportion of meio-spores that were converted to the sporophyte generation (Figure 1). This analysis indicated that rapidly released meio-spores (i.e. within 24 h) were more sensitive to the diffusible factor than meio-spores whose release had been delayed (i.e. taking >48 h; Wilcoxon test, $p$-value <0.01). Based on this observation, whenever possible, subsequent experiments were carried out with meio-spores that had been released within 48 h of transfer of the micro-dissected unilocular sporangia to the test conditions.

### The sporophyte-inducing diffusible factor is stable when stored at 4°C or at -20°C

To test the stability of the sporophyte-inducing factor, SCM was stored at either 4°C or at -20°C and its activity tested after different time periods (Figure 2A). The results of this analysis indicated that the factor was stable for at least eight weeks at 4°C. Similarly, storage at -20° for one to five weeks did not result in a decrease in the activity of the diffusible factor (Figure 2B).

**Effect of sporophyte culture conditions on the production of the sporophyte-inducing diffusible factor**

We next tested whether the conditions under which the sporophyte material was cultivated influenced production of the diffusible factor. To test whether diffusible factor production was influenced by the length of time the sporophyte material was maintained in culture, volumes of 160 ml of Provasoli-enriched natural seawater (PES) in 150 mm Petri dishes were inoculated with about $10^6$ gametes and the resulting partheno-sporophytes were cultivated for different times under standard conditions. The SCM samples were removed after four, six, eight and ten weeks and assayed for diffusible factor activity (Figure 3A). This experiment indicated that SCM contained the highest activities after six to eight weeks of culture, with the activity diminishing in older cultures.

To test the effect of light intensity, volumes of 160 ml PES in 150 mm Petri dishes were inoculated with 100 µl aliquots of gametes (about $10^6$ cells) and the resulting partheno-sporophytes grown either under low (2-3 µM photons/$m^2$·s), medium (15-16 µM photons/$m^2$·s) or high light (25-30 µM photons/$m^2$·s) conditions (12h:12h light: dark). SCM was collected after 4 weeks of culture and assayed for the diffusible factor (Figure 3B). There were no significant differences between the detected levels of diffusible factor produced by the cultures that were grown under the three light conditions (Wilcoxon-test, *p*-value>0.05).

Taken together, these experiments indicated that production of the diffusible factor was not effected by light intensity, but note that cultures can be maintained for longer under low light intensity. Cultures were therefore grown for five to six weeks under low light intensity to produce SCM for subsequent experiments.

**The diffusible factor is a large molecule**

As a first step towards investigating the biochemical nature of the diffusible factor, we used ultrafiltration to estimate its molecular size. SCM was filtered through an ÄKTA™ flux ultrafiltration system using filters with different molecular size cut-offs to prepare different size

fractions (Figure 4A). Bioassay testing of the different size fractions indicated that the diffusible factor had a molecular size of greater than 50 and that at least part of the activity had a molecular size of less than 100 kDa (Figure 4B).

**Mass spectrometry analysis of proteins in concentated SCM**

To further characterise the high molecular weight fraction, 200 ml of SCM were processed with a Falcon filter system to concentrate >30 kDa components. Coomassie blue staining of the concentrated SCM sample after separation on SDS-PAGE (Figure 5A) revealed several high molecular weight bands of greater than 50 kDa (i.e. in the active size range determined by ultrafiltration experiments, Figure 4B). Liquid chromatography mass spectrometry/mass spectrometry (LC-MS/MS) analysis of the SDS-PAGE bands identified peptides corresponding to 36 different proteins (Table 1). Most of these proteins detected were predicted to be secreted proteins based on the presence of a putative signal peptide. Interestingly, the list of proteins that had been detected included a mannuronan C5-epimerase (locusID Ec-20_004700, Figure 5B), which had been reported to contain three chimeric AGP backbone motifs (Hervé et al., 2016).

**The sporophyte-inducing diffusible factor is resistant to autoclaving and proteinase K treatment**

To characterise the diffusible factor further, we determined whether it was stable when treated with high temperature or subjected to protease digestion. SCM was either autoclaved or digested by incubation at 37°C in the presence of 100 µg/ml proteinase K followed by autoclaving to denature the enzyme. Figure 6 shows that the diffusible factor was resistant to both autoclaving and proteinase K treatment. Surprisingly, the activity of the factor significantly increased following proteinase K treatment (Wilcoxon-test, $p$-value<0.05).

This result of this experiment suggested that the diffusible factor may not be a protein but note that alternative interpretations of these results are possible. For example, the factor could be a complex molecule such as a glycoprotein, with the protein part of the molecule being either inaccessible to proteinase K or unnecessary for the factor's activity. This interpretation would be

meio-spores with larcoll also induced a significant level of switching to the sporophyte program compared to the control treatment ($p$-value <0.05; Figure 9B).

## Discussion

Genetic experiments have shown that the switch from the gametophyte to the sporophyte generation in *Ectocarpus* is controlled by two TALE HD TFs, OUROBOROS and SAMSARA (Arun et al., 2019; Coelho et al., 2011) but this switch can also be influenced by a non-cell autonomous, sporophyte-inducing factor that is secreted into the medium by the sporophyte generation (Arun et al., 2013). The experiments carried out here were aimed at further characterising this diffusible factor. We show that light intensity does not significantly influence production of the diffusible factor but at lower light intensities the algae to grow more slowly allowing them to be maintained at higher densities for longer periods of time. *Ectocarpus* sporophytes normally become sexually mature after three to four weeks under normal light and, therefore, cultures cannot be maintained for long periods under these conditions. We also showed that SCM did not lose its activity when stored for 8 weeks at either 4°C or -20°C.

Further characterisation of the SCM indicated that the sporophyte-inducing factor was resistant to heat (121°C for 30 min) and proteinase K treatment and that the factor was a large molecular weight molecule, greater than 50 kDa in size. Mass spectrometry analysis identified 36 different proteins in concentrated SCM, including a mannuronan C5-epimerase (locusID Ec-20_004700) that has been reported to contain chimeric AGP backbone motifs (Hervé et al., 2016). Brown algal cell walls play an important role in conferring resistance to mechanical stress and protection from predators (Popper et al., 2011b). They are mainly composed of alginates and sulphated fucans and therefore differ markedly in their composition from the cell walls of land plants (Hervé et al., 2016). Mannuronan C5-epimerase acts on alginate, altering its mechanical properties by converting β-D-mannuronate to its epimer α-L-guluronate (Fischl et al., 2016; Nyvall et al., 2003). The mannuronan C5-epimerase protein Ec-20_004700 is predicted to contain wall sensing component (WSC) domains, in addition to its catalytic domain. WSC domains have been associated with cell wall sensing (Ohsawa et al., 2017; Oide et al., 2019) and resistance to

various stress conditions (Dupres et al., 2009; Lodder et al., 1999; Lommel et al., 2004). WSC domain proteins were first described as cell surface sensors in the yeast *Saccharomyces cerevisiae*, where they are involved in evaluating cell wall status and transmitting this information to the cell wall integrity (CWI) signalling pathway (Philip and Levin, 2001). Similarly, there is evidence that the putative *Aspergillus nidulans* WSC domain stress sensors WscA and WscB are involved in CWI under hypo-osmotic and acid pH condition (Futagami et al., 2011) and that *Pichia pastoris* Wsc1 and Wsc3 function as methanol-sensors during growth on methanol (Ohsawa et al., 2017). Fungal WSC contribute to protein anchoring and plant colonization through their ability to bind a variety of cell wall polysaccharides from plants and/or fungi including β-1,3-glucans, xylans and chitin (Oide et al., 2019; Wawra et al., 2019). In *Ectocarpus,* the WSC domain family is one of the largest protein domain families, with 115 genes containing at least one WSC module. Three of the 28 mannuronan C5-epimerase enzymes in *Ectocarpus* are predicted to possess WSC domains and, while their biochemical function has not been yet elucidated, these motifs may act as cell wall-binding domains, possibly targeting alginate (Michel et al., 2010).

One particularly interesting feature of the mannuronan C5-epimerase that was detected in ultrafiltrated SCM (encoded by the gene with LocusID Ec-20_004700) was the presence of three AGP backbone motifs. AGPs are large molecular weight glycoproteins (from 50 to more than 200 kDa) that were initially detected in land plant cell surfaces. These molecules have been shown to play crucial roles during development and reproduction in the land plant lineage (Fu et al., 2007; Nathan Hancock et al., 2005; Seifert and Roberts, 2007). Developmental switches that appear to be influenced by AGPs in land plants include, for example, the acquisition of embryogenic capacity in *Daucus carota* (Kreuger and van Holst, 1993; van Hengel et al., 2001), the role of the AGP-like protein xylogen in xylem formation in *Zinnia* and *Arabidopsis* (Motose et al., 2004), the role of AGP18 in the selection of viable megaspores in *Arabidopsis* (Demesa-Arevalo and Vielle-Calzada, 2013), the role of the fasciclin-like AGP FLA4/SOS5 in root elongation in *Arabidopsis* (Shi et al., 2003) and the role of AGP1 in moss apical cell expansion (Lee et al., 2005). The phenotype associated with AGP18 is particularly interesting as this

glycoprotein acts at the transition from the sporophyte to the gametophyte generation and loss of AGP18 leads to an arrest of gametogenesis (Acosta-Garcia and Vielle-Calzada, 2004).

AGPs have also been shown to act as signal molecules during fertilisation. For example, tobacco TTS, which is produced by the stylar transmitting tissue, appears to act as a signalling factor to guide pollen tube growth (Cheung et al., 1995) and, in the land plant *Torenia fournieri*, ovular methyl-glucuronosyl arabinogalactan (AMOR) induces competency of the pollen tube to respond to ovular attractant peptides (Jiao et al., 2017; Mizukami et al., 2016).

In contrast to the situation for land plants, evidence for the presence of chimeric AGPs in brown algae has only been described recently. Hervé et al. (2016) identified multiple genes in the *Ectocarpus* genome that were predicted to encode AGP-like core proteins. This study also presented evidence that AGP-like proteins are developmentally regulated during *Fucus* development and those developmental abnormalities occur if the action of these proteins is inhibited by the addition of AGP-reactive Yariv reagents.

In the current study, anti-AGP antibodies detected AGP glycan epitopes in SCM and addition of the Yariv reagent β-glucosyl to SCM led to an inhibition of its sporophyte-inducing activity. Moreover, incubation of meio-spores with plant AGPs (gum arabic) or arabinogalactans (larcoll) mimicked the effect of treatment with SCM. The ability of the land-plant-derived extracts gum arabic and larcoll to induce a specific developmental switch to the sporophyte program in brown algal gametophyte initial cells may seem surprising but note that cross-species effects of AGPs have been reported previously, at least within the land plant lineage. For example, gum arabic has been shown to enhance microspore embryogenesis in wheat (Letarte et al., 2006). Taken together, these observations indicate that the sporophyte-inducing factor is likely to be a large, AGP-like molecule that is resistant to heat treatment and digestion with proteinase K.

The lack of susceptibility of the sporophyte-inducing factor to proteinase K and heat treatment could be interpreted as an argument against the factor corresponding to an AGP but note that plant AGPs with similar heat and protease tolerances have been described. For example, xylogen has been shown to be heat resistant, although its activity is eliminated by proteases (Motose et al.,

2001). AMOR was found to be both heat stable (100°C for 10 min) and maintained its activity following treatment with proteinase K. For the latter, a disaccharide, methyl-glucuronosyl galactose (4-Me-GlcA-b-(1/6)-Gal), was synthesised and shown to exhibit AMOR activity, suggesting that the protein moiety may not be important for the observed biological activity (Mizukami et al., 2016). By analogy, it is therefore possible that the active moiety of the *Ectocarpus* sporophyte-inducing factor may be a saccharide molecule.

In conclusion, this study has optimized conditions for the production of the sporophyte-inducing factor and has provided some initial information about its molecular nature that will be important for future attempts to purify the factor. Several different approaches provided evidence that the factor may be an AGP or an AGP-like molecule. Future work will be aimed at characterising the exact molecular nature of the factor and at investigating how the factor functions to induce the sporophyte program. On a broader scale, characterisation of the *Ectocarpus* factor may provide a starting point for the characterisation of analogous factors in other eukaryotic lineages. For example, moss sporophytes have been reported to produce a diffusible factor that induces apogamous sporophyte formation (Bauer, 1959) but the nature of this factor has not been investigated.

## Material and Methods

### Biological material and preparation of SCM

*Ectocarpus* sp. strain Ec32 was cultivated in Provasoli-enriched natural seawater (PES) under standard culture conditions at 13°C, with a 12h/12h day/night cycle of white fluorescent light at 20 µM photons/$m^2$·s (Coelho et al., 2012b).

The standard conditions for the production of SCM involved inoculating 160 ml of PES in a 150 mm Petri dish with about $10^6$ gametes of partheno-sporophyte thalli and cultivating for 4 to 6 weeks under low light conditions (2-3 µM photons/$m^2$·s). Variations on this procedure were used to test the effect of light intensity, culture density and culture time on SCM production. The

alternative light conditions used were medium light (15-16 µM photons/$m^2$·s) and high light (25-30 µM photons/$m^2$·s).

To produce large volumes of SCM, 10 L bottles of PES were inoculated with 0.5 g of partheno-sporophyte material and cultured under low light conditions with aeration by pumping air through a 0.2 µm filter. In this bottle system, cultures grown for between four and 11 weeks produce SCM with diffusible factor activity.

SCM was recovered by filtering cultures through a reusable coffee filter (12.5 cm Finlandek permanent coffee filter) to remove most of the partheno-sporophyte tissue and then filtering through a 40 µm cell strainer (Falcon 40 µm Nylon cell strainer) to remove any remaining algal cells and a 0.22 µm syringe filter (Millipore Millex-GP polyethersulphone membrane) to remove bacteria. The SCM was then either used immediately or stored at 4°C.

**Bioassay for the diffusible sporophyte-inducing factor**

Test samples were either diluted in PES or, when used undiluted, enriched in micronutrients by addition of Provasoli solution to 1x final concentration. One or more unilocular sporangia were micro-dissected from fertile partheno-sporophyte thalli under a binocular microscope and placed in 300 µl of these preparations so that the meio-spores were released directly into the test solution. Each 300 µl droplet represented a replicate assay of the test solution. The preparations were incubated overnight in very high light (35 µM photons/$m^2$·s) to promote meio-spore release. Empty unilocular sporangia were removed after release of the meio-spores. The numbers of gametophytes and sporophytes were scored four to seven days later based on germling morphology (Peters et al., 2008) using an inverted light microscope (Olympus CKX41). In some cases when the meio-spores grew poorly, an additional 300 µl of the test preparation was added to the drop and culture continued.

**Proteinase K and UV treatment of SCM**

SCM was incubated with 100 µg/ml proteinase K at 37°C for 1 h and then autoclaved at 121°C for 30 min. Heat treated SCM was autoclaved at 121°C for 30 min. Provasoli solution was added

to the samples from both experiments to 1x final concentration before carrying out bioassays for the diffusible factor.

**Size fractionation by ultrafiltration**

SCM was pre-filtered through a 0.22 µm filtration system (Stericup and Steritop, 500 ml Millipore Express PLUSE 0.22 µm PES) before ultrafiltration. Ultrafiltration was then carried out using an ÄKTA$^{TM}$ flux (GE Healthcare BioSciences Uppsala, Sweden) equipped with a 100 kDa, a 50 kDa or a 10 kDa cartridge. Batches of pre-filtered SCM, were gradually fed into the starting reservoir in order to maintain a constant volume of about 300 ml which was cycled through the filter resin, with the filtrate being collected separately during the cycling. The 10-50 kDa size range was obtained by filtering the flow-through from a 50 kDa filter filtration through a 10 kDa filter as a second step, retaining the retentate (Figure 4A). Concentrated retentates were designated uf-SCM for ultra-filtrated SCM. To assay the activity of the diffusible factor, uf-SCM preparations were diluted in PES to obtain a concentration equivalent to 1X SCM.

**Dot immunoblot analyses with anti-AGP antibodies**

Serial dilutions of each test sample (five five-fold dilution steps) were carried out and 1 µL aliquots of each dilution spotted onto nitrocellulose membranes (Amersham) along with equivalent dilutions of a gum arabic solution (starting concentration 1 mg/ml) as a positive control. The prints were allowed to dry and blocked with 5% of milk powder in Phosphate Buffer saline solution (PBS/MP Biomedicals). The samples were then probed with the rat anti-AGP monoclonal antibodies (Plant Probes, Leeds, UK) JIM8, JIM13, JIM16, JIM4, LM2, LM14 and MAC207 diluted 10-fold in PBS/MP (Moller et al., 2007). After washing, anti-rat-HRP (diluted 1000-fold) was added in PBS/MP. After washing, antibody-epitope interactions were detected using a luminescent ECL substrate (BioRad) and a Fusion FX.XT-820.EPI/20M system (Vilber Lourmat, France).

**Yariv reagent tests**

β-D-glucosyl (βGlc-Y) or β-D-mannosyl (βMan-Y) Yariv reagents (Biosupplies Pty Ltd, Melbourne, Australia) were added to Provasoli-enriched SCM at final concentrations of 2 µg/ml before carrying out diffusible factor bioassays.

**SCM analysis by SDS-PAGE**

An initial volume of 200 ml SCM was concentrated using two Amicon® Ultra-15 30 kDa centrifugal filters by sequentially centrifuging 15 ml aliquots for 8 min at 3500 rpm. Each of the retentates (1.5 ml for each of the two filters) was then washed with 100 ml MilliQ $H_2O$ by adding batches of 15 ml and centrifuging each time for 8 min at 3500 rpm. The final retentate, a total of 2 ml from the two filters was freeze-dried and redissolved in 10 µl MilliQ $H_2O$ and 2 µl of 6x protein loading buffer (360 mM Tris-HCl pH 6.8, 45% Glycerol, 9% SDS, 9% DTT, 0.12% Bromophenol Blue). Twelve microlitres of this sample was heated to 100°C for 10 min before loading on a sodium dodecyl sulphate polyacrylamide gel electrophoresis (SDS-PAGE, 12% w/v) gel (Brunelle and Green, 2014) and run at 120 V. Gels were stained with Coomassie blue for 1h then washed three times in 20% ethanol/10% acetic acid.

**Protein digestion and MS de *novo* sequencing analysis**

Protein bands were excised from an SDS-PAGE gel and digested as described (Rosenfeld et al., 1992). Gel pieces were washed with 50 µl of 10% formic acid/40% ethanol, then twice for 15 min with 50 µl of 50% acetonitrile (ACN)/50 mM sodium bicarbonate ($NH_4HCO_3$). The gel pieces were incubated in 10 mM dithiothreitol at 56°C to reduce any disulphide bridges and the cysteines then alkylated with 50 mM iodoacetate for 1 h at room temperature. The gel pieces were washed with 50 µl 50% ACN/50 mM $NH_4HCO_3$ then with 50 µl of ACN and dried. The dried fragments were digested overnight at 37°C with 100 ng of trypsin and the digestion stopped by adding 0.1% trifluoroacetic acid (TFA). Peptides were extracted with 40% ACN/0.1% TFA, dried in a speed vac, redissolved in 20µl of loading buffer (2% ACN/0.1% FA) and 6 µl loaded on an LC-MS/MS system.

Mass spectrometry analysis was performed at the Paris Sud Ouest PAPPSO proteomics core facility (http://papso.inra.fr). LC-MS/MS analyses were performed using an Ultimate 3000 RSLC system (Thermo Scientific) coupled to a LTQ-orbitrap discovery mass spectrometer (Thermo Scientific) by a nanoelectrospray ion source. Protein digests were injected and preconcentrated on a precolumn (Acclaim PepMap C18 particle 5 µm size, 5 mm length, 300 µm i.d., Thermo Fisher Scientific) at 20 µL/min with 0.08% TFA in 2% ACN for 2 min, followed by separation on a reverse phase separating column (Acclaim PepMap RSLC nanoViper, C18 particle 2 µm size, 150 mm length, 75 µm i.d., Thermo Fisher Scientific). Buffers were 0.1 % formic acid in 98% water (solvent A) and 0.1% formic acid in 80% ACN (solvent B). The peptides were eluted with a multi-step gradient of from 1% to 35% of solvent B for 34.5 min at 300 nL/min for a total run of 42 min. MS scans were acquired in a mass range of 300-1400 m/z at a resolution of 15000 in the orbitrap analyser. The 8 most intense ions were selected for CID MS/MS with a normalised collision energy of 35 in the ion trap.

All MS/MS spectra were searched against the *Ectocarpus* v2 genome database using X!TandemPipeline (version 3.4.3), the open search engine developped by PAPPSO (http://pappso.inra.fr/bioinfo/xtandempipeline/). Precursor mass tolerance was 10 ppm and fragment mass tolerance was 0.5 Da. Data filtering was achieved according to a peptide E-value < 0.01, protein E-value < $10e^{-4}$ and to a minimum of two identified peptides per protein.

**Acknowledgements**

This work was supported by the Centre National de la Recherche Scientifique, the European Research Council (grant agreement 638240) and Sorbonne University. Support was also provided by the French National Research Agency via the investment expenditure programme IDEALG (ANR-10-BTBR-04-02). HY was supported by a grant from the Chinese Scholarship Council (grant number 201608310119).

## References


Acosta-Garcia, G., Vielle-Calzada, J.P., 2004. A classical arabinogalactan protein is essential for the initiation of female gametogenesis in *Arabidopsis*. Plant Cell 16, 2614-2628.

Arun, A., Coelho, S.M., Peters, A.F., Bourdareau, S., Peres, L., Scornet, D., Strittmatter, M., Lipinska, A.P., Yao, H., Godfroy, O., Montecinos, G.J., Avia, K., Macaisne, N., Troadec, C., Bendahmane, A., Cock, J.M., 2019. Convergent recruitment of TALE homeodomain life cycle regulators to direct sporophyte development in land plants and brown algae. Elife 8.

Arun, A., Peters, N.T., Scornet, D., Peters, A.F., Mark Cock, J., Coelho, S.M., 2013. Non-cell autonomous regulation of life cycle transitions in the model brown alga *Ectocarpus*. New Phytol 197, 503-510.

Bauer, L., 1959. Auslösung apogamer Sporogonbildung am Regenerationsprotonema von Laubmoosen durch einen vom Muttersporogon abgegebenen Faktor. Naturwissenschaften 46, 154-155.

Bothwell, J.H., Marie, D., Peters, A.F., Cock, J.M., Coelho, S.M., 2010. Role of endoreduplication and apomeiosis during parthenogenetic reproduction in the model brown alga *Ectocarpus*. New Phytologist 188, 111-121.

Cheung, A.Y., Wang, H., Wu, H.-m., 1995. A floral transmitting tissue-specific glycoprotein attracts pollen tubes and stimulates their growth. Cell 82, 383-393.

Cock, J.M., Godfroy, O., Macaisne, N., Peters, A.F., Coelho, S.M., 2014. Evolution and regulation of complex life cycles: a brown algal perspective. Curr Opin Plant Biol 17, 1-6.

Coelho, S.M., Godfroy, O., Arun, A., Le Corguillé, G., Peters, A.F., Cock, J.M., 2011. *OUROBOROS* is a master regulator of the gametophyte to sporophyte life cycle transition in the brown alga *Ectocarpus*. Proceedings of the National Academy of Sciences 108, 11518-11523.

Coelho, S.M., Peters, A.F., Charrier, B., Roze, D., Destombe, C., Valero, M., Cock, J.M., 2007. Complex life cycles of multicellular eukaryotes: new approaches based on the use of model organisms. Gene 406, 152-170.

Coelho, S.M., Scornet, D., Rousvoal, S., Peters, N.T., Dartevelle, L., Peters, A.F., Cock, J.M., 2012. How to cultivate *Ectocarpus*. Cold Spring Harb Protoc 2012, 258-261.

Demesa-Arevalo, E., Vielle-Calzada, J.P., 2013. The classical arabinogalactan protein AGP18 mediates megaspore selection in *Arabidopsis*. Plant Cell 25, 1274-1287.

Dupres, V., Alsteens, D., Wilk, S., Hansen, B., Heinisch, J.J., Dufrene, Y.F., 2009. The yeast Wsc1 cell surface sensor behaves like a nanospring in vivo. Nat Chem Biol 5, 857-862.

Fischl, R., Bertelsen, K., Gaillard, F., Coelho, S., Michel, G., Klinger, M., Boyen, C., Czjzek, M., Hervé, C., 2016. The cell-wall active mannuronan C5-epimerases in the model brown alga *Ectocarpus*: From gene context to recombinant protein. Glycobiology 26, 973-983.

Fu, H., Yadav, M.P., Nothnagel, E.A., 2007. *Physcomitrella patens* arabinogalactan proteins contain abundant terminal 3-O-methyl-L-rhamnosyl residues not found in angiosperms. Planta 226, 1511.

Futagami, T., Nakao, S., Kido, Y., Oka, T., Kajiwara, Y., Takashita, H., Omori, T., Furukawa, K., Goto, M., 2011. Putative stress sensors WscA and WscB are involved in hypo-osmotic and acidic pH stress tolerance in *Aspergillus nidulans*. Eukaryotic cell 10, 1504-1515.

Gane, A.M., Craik, D., Munro, S.L., Howlett, G.J., Clarke, A.E., Bacic, A., 1995. Structural analysis of the carbohydrate moiety of arabinogalactan-proteins from stigmas and styles of *Nicotiana alata*. Carbohydrate Research 277, 67-85.

Hervé, C., Simeon, A., Jam, M., Cassin, A., Johnson, K.L., Salmean, A.A., Willats, W.G., Doblin, M.S., Bacic, A., Kloareg, B., 2016. Arabinogalactan proteins have deep roots in eukaryotes:

identification of genes and epitopes in brown algae and their role in *Fucus serratus* embryo development. New Phytol 209, 1428-1441.

Jiao, J., Mizukami, A.G., Sankaranarayanan, S., Yamguchi, J., Itami, K., Higashiyama, T., 2017. Structure-activity relation of AMOR sugar molecule that activates pollen-tubes for ovular guidance. Plant physiology 173, 354-363.

Johnson, K.L., Jones, B.J., Bacic, A., Schultz, C.J., 2003. The fasciclin-like arabinogalactan proteins of *Arabidopsis*. A multigene family of putative cell adhesion molecules. Plant physiology 133, 1911-1925.

Kreuger, M., van Holst, G.-J., 1993. Arabinogalactan proteins are essential in somatic embryogenesis of *Daucus carota L*. Planta 189, 243-248.

Lee, K.J., Sakata, Y., Mau, S.L., Pettolino, F., Bacic, A., Quatrano, R.S., Knight, C.D., Knox, J.P., 2005. Arabinogalactan proteins are required for apical cell extension in the moss *Physcomitrella patens*. Plant Cell 17, 3051-3065.

Letarte, J., Simion, E., Miner, M., Kasha, K.J., 2006. Arabinogalactans and arabinogalactan-proteins induce embryogenesis in wheat (*Triticum aestivum L.)* microspore culture. Plant cell reports 24, 691.

Lodder, A.L., Lee, T.K., Ballester, R., 1999. Characterization of the Wsc1 protein, a putative receptor in the stress response of *Saccharomyces cerevisiae*. Genetics 152, 1487-1499.

Lommel, M., Bagnat, M., Strahl, S., 2004. Aberrant processing of the WSC family and Mid2p cell surface sensors results in cell death of *Saccharomyces cerevisiae* O-mannosylation mutants. Molecular and cellular biology 24, 46-57.

Müller, D.G., 1967. Generationswechsel, kernphasenwechsel und sexualität der braunalge *Ectocarpus siliculosus* im kulturversuch. Planta 75, 39-54.

Michel, G., Tonon, T., Scornet, D., Cock, J.M., Kloareg, B., 2010. The cell wall polysaccharide metabolism of the brown alga Ectocarpus siliculosus. Insights into the evolution of extracellular matrix polysaccharides in Eukaryotes. New Phytol 188, 82-97.

Mizukami, A.G., Inatsugi, R., Jiao, J., Kotake, T., Kuwata, K., Ootani, K., Okuda, S., Sankaranarayanan, S., Sato, Y., Maruyama, D., Iwai, H., Garenaux, E., Sato, C., Kitajima, K., Tsumuraya, Y., Mori, H., Yamaguchi, J., Itami, K., Sasaki, N., Higashiyama, T., 2016. The AMOR Arabinogalactan Sugar Chain Induces Pollen-Tube Competency to Respond to Ovular Guidance. Curr Biol 26, 1091-1097.

Moller, I., Sørensen, I., Bernal, A.J., Blaukopf, C., Lee, K., Øbro, J., Pettolino, F., Roberts, A., Mikkelsen, J.D., Knox, J.P., 2007. High ‐ throughput mapping of cell ‐ wall polymers within and between plants using novel microarrays. The Plant Journal 50, 1118-1128.

Motose, H., Sugiyama, M., Fukuda, H., 2001. An arabinogalactan protein (s) is a key component of a fraction that mediates local intercellular communication involved in tracheary element differentiation of *zinnia* mesophyll cells. Plant and Cell Physiology 42, 129-137.

Motose, H., Sugiyama, M., Fukuda, H., 2004. A proteoglycan mediates inductive interaction during plant vascular development. Nature 429, 873.

Nathan Hancock, C., Kent, L., McClure, B.A., 2005. The stylar 120 kDa glycoprotein is required for S ‐ specific pollen rejection in *Nicotiana*. The Plant Journal 43, 716-723.

Nyvall, P., Corre, E., Boisset, C., Barbeyron, T., Rousvoal, S., Scornet, D., Kloareg, B., Boyen, C., 2003. Characterization of Mannuronan C-5-Epimerase Genes from the Brown Alga *Laminaria digitata*. Plant Physiology 133, 726-735.

Ohsawa, S., Yurimoto, H., Sakai, Y., 2017. Novel function of W sc proteins as a methanol ‐ sensing machinery in the yeast *P ichia pastoris*. Molecular microbiology 104, 349-363.

Oide, S., Tanaka, Y., Watanabe, A., Inui, M., 2019. Carbohydrate-binding property of a cell wall integrity and stress response component (WSC) domain of an alcohol oxidase from the rice blast pathogen *Pyricularia oryzae*. Enzyme Microb Technol 125, 13-20.

Paulsen, B.S., Craik, D.J., Dunstan, D.E., Stone, B.A., Bacic, A., 2014. The Yariv reagent: behaviour in different solvents and interaction with a gum arabic arabinogalactan-protein. Carbohydr Polym 106, 460-468.

Peters, A.F., Marie, D., Scornet, D., Kloareg, B., Mark Cock, J., 2004. Proposal of *Ectocarpus siliculosus* (Ectocarpales, Phaeophyceae) as a model organism for brown algal genetics and genomics 1, 2. Journal of Phycology 40, 1079-1088.

Peters, A.F., Scornet, D., Ratin, M., Charrier, B., Monnier, A., Merrien, Y., Corre, E., Coelho, S.M., Cock, J.M., 2008. Life-cycle-generation-specific developmental processes are modified in the immediate upright mutant of the brown alga *Ectocarpus siliculosus*. Development 135, 1503-1512.

Philip, B., Levin, D.E., 2001. Wsc1 and Mid2 are cell surface sensors for cell wall integrity signaling that act through Rom2, a guanine nucleotide exchange factor for Rho1. Molecular and cellular biology 21, 271-280.

Popper, Z.A., Michel, G., Hervé, C., Domozych, D.S., Willats, W.G., Tuohy, M.G., Kloareg, B., Stengel, D.B., 2011. Evolution and diversity of plant cell walls: from algae to flowering plants. Annual review of plant biology 62, 567-590.

Seifert, G.J., Roberts, K., 2007. The biology of arabinogalactan proteins. Annu. Rev. Plant Biol. 58, 137-161.

Shi, H., Kim, Y., Guo, Y., Stevenson, B., Zhu, J.-K., 2003. The *Arabidopsis SOS5* locus encodes a putative cell surface adhesion protein and is required for normal cell expansion. The Plant Cell 15, 19-32.

Tan, L., Showalter, A.M., Egelund, J., Hernandez-Sanchez, A., Doblin, M.S., Bacic, A.F., 2012. Arabinogalactan-proteins and the research challenges for these enigmatic plant cell surface proteoglycans. Frontiers in Plant Science 3, 140.

van Hengel, A.J., Tadesse, Z., Immerzeel, P., Schols, H., Van Kammen, A., de Vries, S.C., 2001. N-acetylglucosamine and glucosamine-containing arabinogalactan proteins control somatic embryogenesis. Plant Physiology 125, 1880-1890.

Wawra, S., Fesel, P., Widmer, H., Neumann, U., Lahrmann, U., Becker, S., Hehemann, J.H., Langen, G., Zuccaro, A., 2019. FGB1 and WSC3 are in planta-induced *beta*-glucan-binding fungal lectins with different functions. New Phytol 222, 1493-1506.

Yang, L.F., Lu, W.D., Yang, S.S., 2007. Analysis of protein expression profiles of *Halobacillus dabanensis* D-8 T under optimal and high salinity conditions. Current microbiology 54, 20-26.

## Table

**Table 1. Proteins detected in concentrated sporophyte-conditioned medium by mass spectrometry.** Proteins detected following SDS-PAGE, excision of bands >50 kDa and mass spectrometry. SP, signal peptide; TM, transmembrane domain; WSC, cell-wall integrity and stress-response component 1 domain; MC5E, mannuronan C-5-epimerase; AGP, arabinogalactan protein; G/SdH, glucose/sorbosone dehydrogenase; PLF/V, pectin lyase fold/virulence factor; PS8/S53, petidase S8/S53; HIP, high-CO2 inducible periplasmic; PKinase, protein kinase; RCC1, regulator of chromosome condensation; SBBP, six-bladed beta-propeller, TolB-like; Gal, galactose-binding; AP, alkaline-phosphatase-like; SGNH, SGNH hydrolase-type esterase; HLRR, hypothetical leucine-rich repeat; vWA, von Willebrand factor type A; FA58C, Coagulation factor 5/8 C-terminal type domain; HP, Haem peroxidase; CA, carbonic anhydrase; GH114, N-terminal glycosyl-hydrolase-114-associated domain; nd, none detected.

| Description | Locus ID | Domains | Major Component |
|---|---|---|---|
| Mannuronan C-5-epimerases | Ec-20_004700 | SP, 2xWSC, MC5E, AGP | No |
| | Ec-00_006370 | SP, MC5E | Yes |
| | Ec-00_006380 | SP, MC5E | Yes |
| | Ec-11_000400 | SP, MC5E | Yes |
| | Ec-27_006700 | SP, MC5E | Yes |
| | Ec-18_000130 | MC5E | Yes |
| | Ec-00_010800 | TM, 2xWSC, MC5E | Yes |
| | Ec-18_000150 | SP, MC5E | No |
| Carbohydrate-binding WSC domain protein | Ec-17_000970 | SP, WSC | Yes |
| Glucose/Sorbosone dehydrogenase and WSC domain protein | Ec-00_007780 | SP, G/SdH, 5xWSC | Yes |
| | Ec-09_000520 | SP, G/SdH, WSC | Yes |
| | Ec-13_003060 | SP, G/SdH, 3xWSC | No |
| High-$CO_2$ inducible periplasmic domain protein | Ec-26_006220 | SP, HIP | Yes |
| Pectin lyase fold proteins | Ec-03_002910 | SP, PLF/V | No |
| | Ec-22_003520 | SP, PLF/V | Yes |
| Seven-bladed beta-propeller domain receptor kinase | Ec-22_003740 | SP, RCC1, TM, PKinase | Yes |
| TolB-like six-bladed beta-propeller proteins | Ec-15_001700 | SP, SBBP | Yes |
| | Ec-02_001340 | SP, SBBP | No |
| Galactose-binding domain-like proteins | Ec-21_001340 | SP, 3xGal, PLF/V | No |
| | Ec-21_001320 | SP, Gal, PLF/V | No |
| | Ec-21_001360 | SP, 3xGal, PLF/V | Yes |
| | Ec-21_001350 | SP, 2xGal, PLF/V | Yes |
| Seven-bladed beta-propeller domain protein | Ec-16_004480 | SP, RCC1, TM | Yes |
| Secreted protein similar to EsV-1-163 | Ec-26_002660 | SP | No |
| | Ec-26_005190 | SP | No |
| asn/thr-rich large protein family protein | Ec-02_004700 | SP | No |
| Secreted alkaline phosphatase | Ec-01_007880 | SP, AP | Yes |
| KP-43 peptidase | Ec-06_007900 | PS8/S53, Gal | No |
| SGNH hydrolase-type esterase domain | Ec-09_000420 | SP, SGNH | No |
| Hypothetical leucine rich repeat protein | Ec-09_004400 | SP, Gal, FA58C, LRR | No |
| Von Willebrand factor type A domain protein | Ec-21_003770 | vWA | No |
| Catalase (imm downregulated 7) | Ec-26_000310 | SP, HP | Yes |
| FAS1 domain protein | Ec-27_005070 | FAS1, TM | Yes |
| carbonic anhydrase alpha type | Ec-27_005680 | SP, CA | No |
| conserved unknown protein | Ec-05_001620 | SP | Yes |
| GH114 glycosyl-hydrolase | Ec-28_003870 | GH114 | Yes |

## Figures

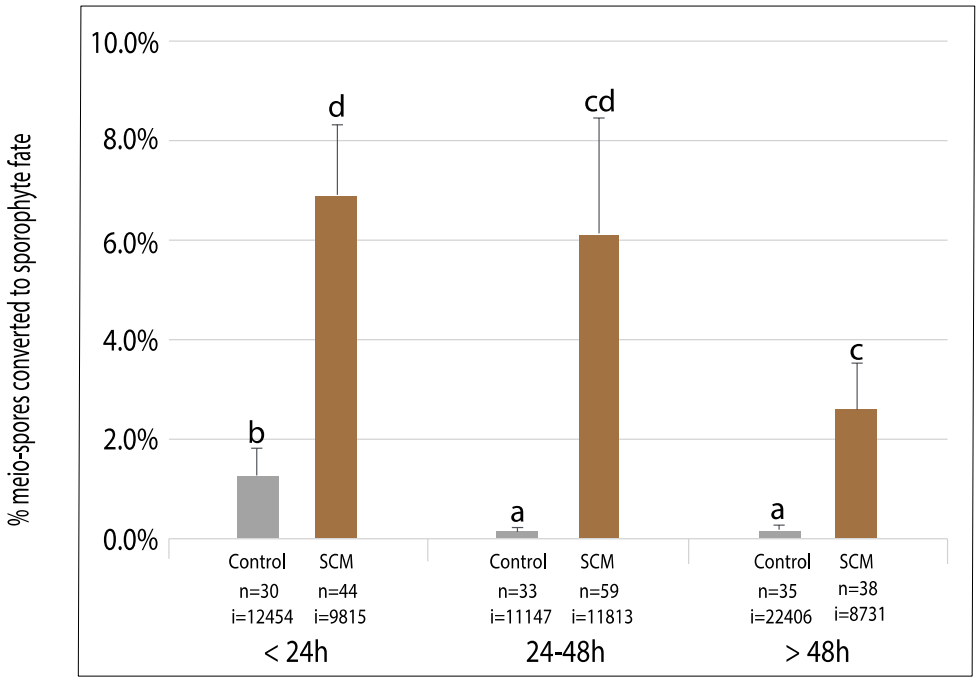


**Figure 1. Effect of unilocular sporangium release time on meio-spore susceptibility to the diffusible sporophyte-inducing factor.** Percent of germlings that exhibited sporophyte morphology following the release of meio-spores from unilocular sporangia 12-24 h, 24-48 h or >48 h after dissection and transfer to either SCM or to PES as a negative control. Error bars indicate standard error of the mean, letters above bars indicate significant differences ($p$-value<0.05). PES, Provasoli-enriched natural seawater; SCM, sporophyte-condition medium; n, number of replicates; i, number of individual germlings counted.

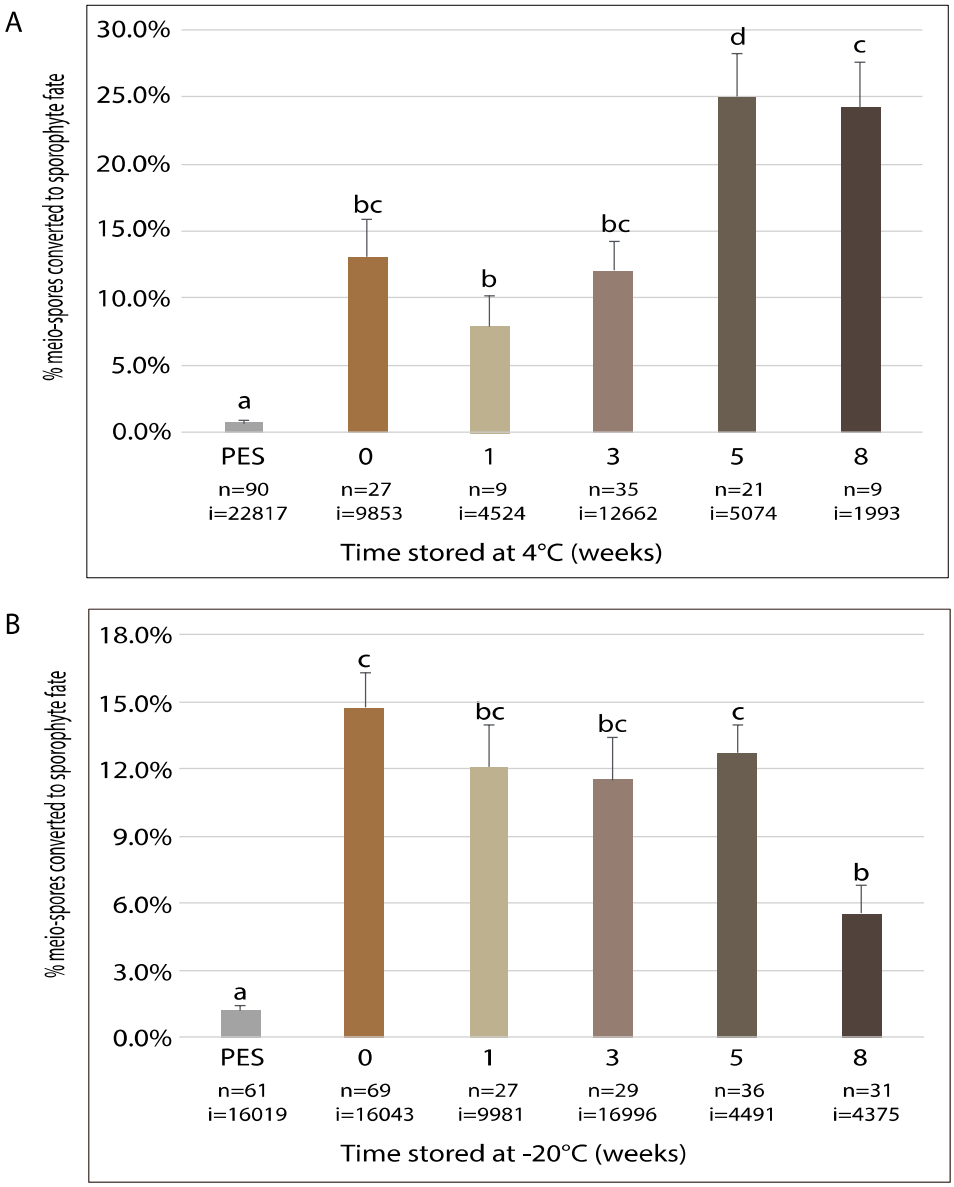


**Figure 2. The sporophyte-inducing factor is stable when SCM is stored at 4°C or -20°C.** A. Bioassay activity after storage at 4°C. B. Bioassay activity after storage at -20°C. Error bars indicate standard error of the mean, letters above bars indicate significant differences ($p$-value<0.05). PES, Provasoli-enriched natural seawater; SCM, sporophyte-condition medium; n, number of replicates; i, number of individual germlings counted.

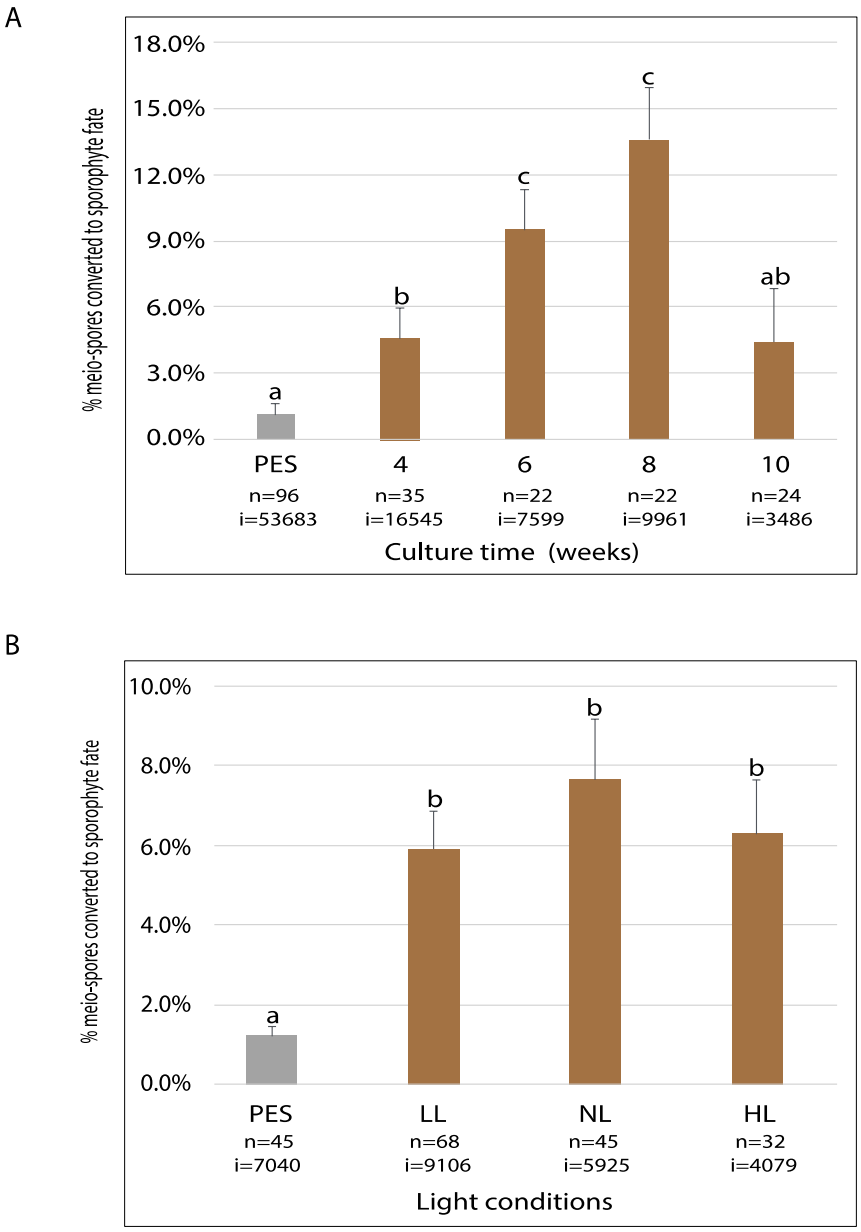


**Figure 3. Effect of sporophyte culture conditions on production of the sporophyte-inducing diffusible factor.** A. Effect of time in culture, B. Effect of light intensity. Error bars indicate standard error of the mean, letters above bars indicate significant differences ($p$-value<0.05). PES, Provasoli-enriched natural seawater; LL, low light; NL, normal light; HL, high light; n, number of replicates; i, number of individual germlings counted.

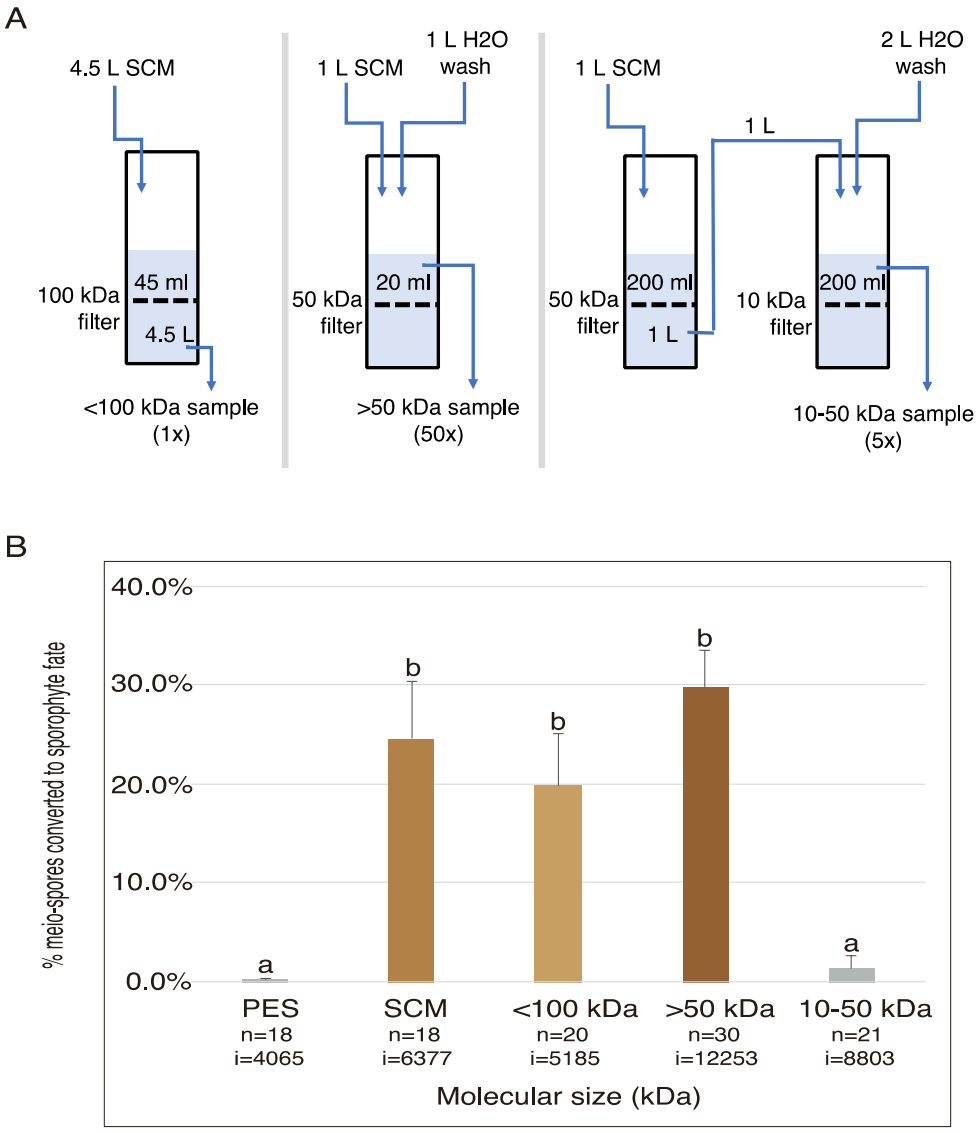


**Figure 4. Sporophyte-inducing activity of different SCM size fractions.** A. Size fractionation of SCM using ultrafiltration. The diagrams indicate input, flow through and retentate volumes. Washes with deionised water were carried out after completion of SCM filtration and the retentate volumes correspond to the final volumes after washing where relevant. B. SCM size fractions, separated by ultrafiltration, were tested on meio-spores for sporophyte-inducing activity. All samples were diluted to a concentration equivalent to 1X SCM before carrying out the bioassays. Error bars indicate standard error of the mean, letters above bars indicate significant differences ($p$-value<0.05). PES, Provasoli-enriched natural seawater; SCM, sporophyte-condition medium; n, number of replicates; i, number of individual germlings counted.

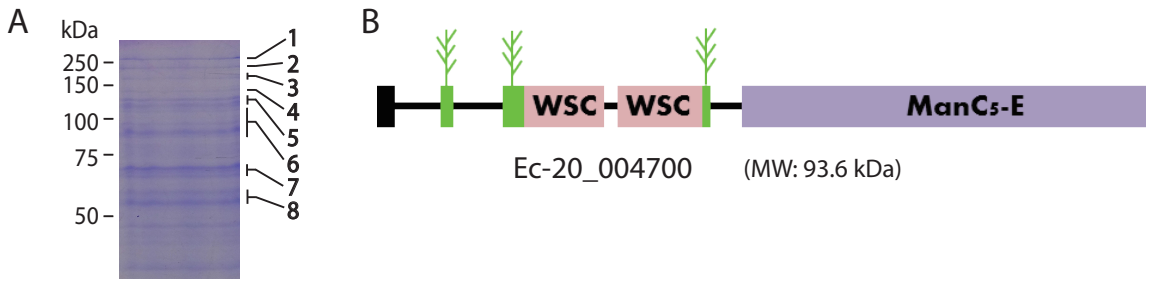


**Figure 5. Identification of candidate proteins for the diffusible sporophyte-inducing factor by mass spectroscopy analysis of protein bands detected in the >30 kDa fraction of concentrated SCM.** A. Coomassie stained SDS-PAGE gel showing the protein bands detected in concentrated SCM. Numbers and bars on the right indicate the fragments that were excised for mass spectrometry analysis. B. Domain structure of the Ec-20_004700 protein. Green boxes indicate AGP protein cores with putative glycan decoration. The Ec-20_004700 protein was detected in band 4.

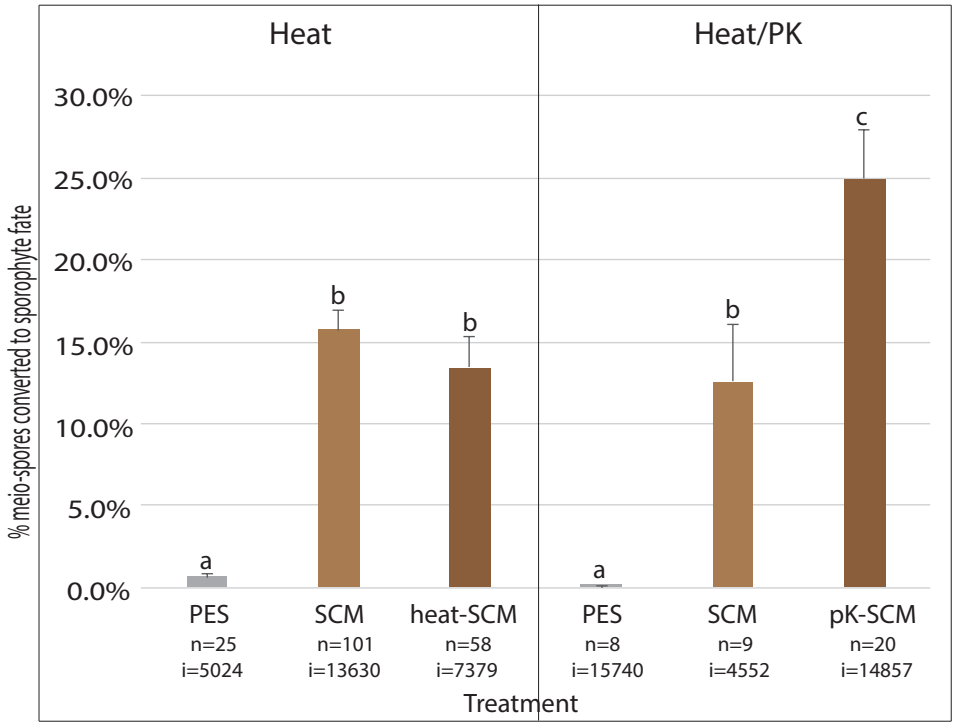


**Figure 6. Effect of heat and proteinase K treatment on the sporophyte-inducing factor.** SCM was autoclaved at 121°C for 20 min (right panel) or incubated with proteinase K (100 µg/ml) at 37°C for 1h followed by autoclaving at 121°C for 20 min (left panel). Error bars indicate standard error of the mean, letters above bars indicate significant differences ($p$-value<0.05). PES, Provasoli-enriched natural seawater; SCM, sporophyte-condition medium; n, number of replicates; i, number of individual germlings counted.

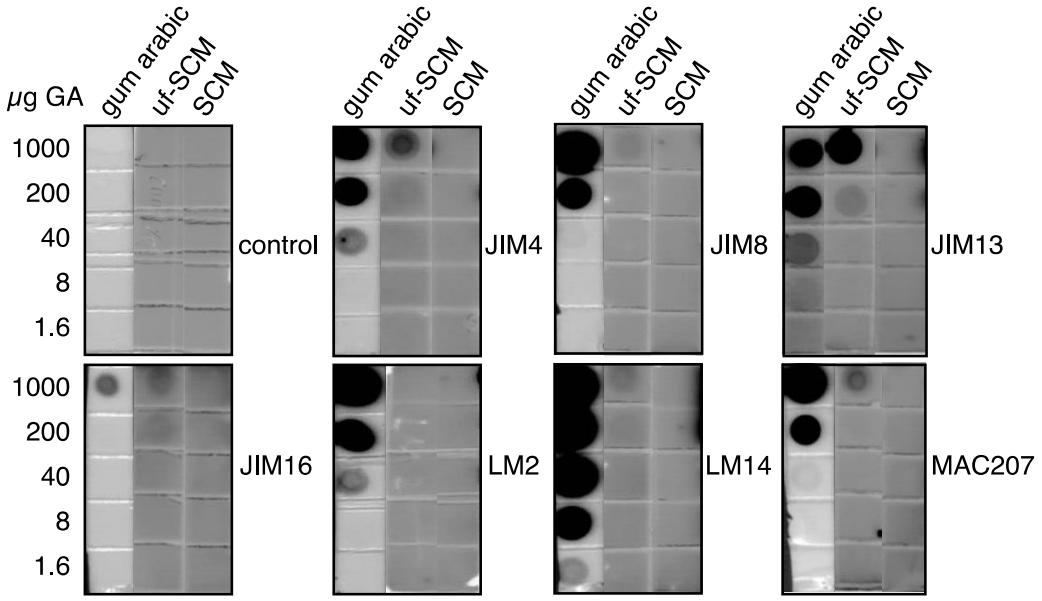


**Figure 7. Detection of AGP epitopes in sporophyte-conditioned medium.** Samples were serially diluted in five steps of five-fold dilution and 1 µl of each dilution spotted for testing with the anti-AGP monoclonal antibodies JIM4, JIM8, JIM13, JIM16, LM2, LM14 and MAC207. Gum arabic (starting concentration 1 mg/ml) was used as a positive control. Molecules >50 kDa were 400-fold more concentrated in the neat uf-SCM sample compared to the neat SCM sample. SCM, sporophyte-conditioned medium; uf-SCM, ultrafiltrated SCM; control, no primary antibody.

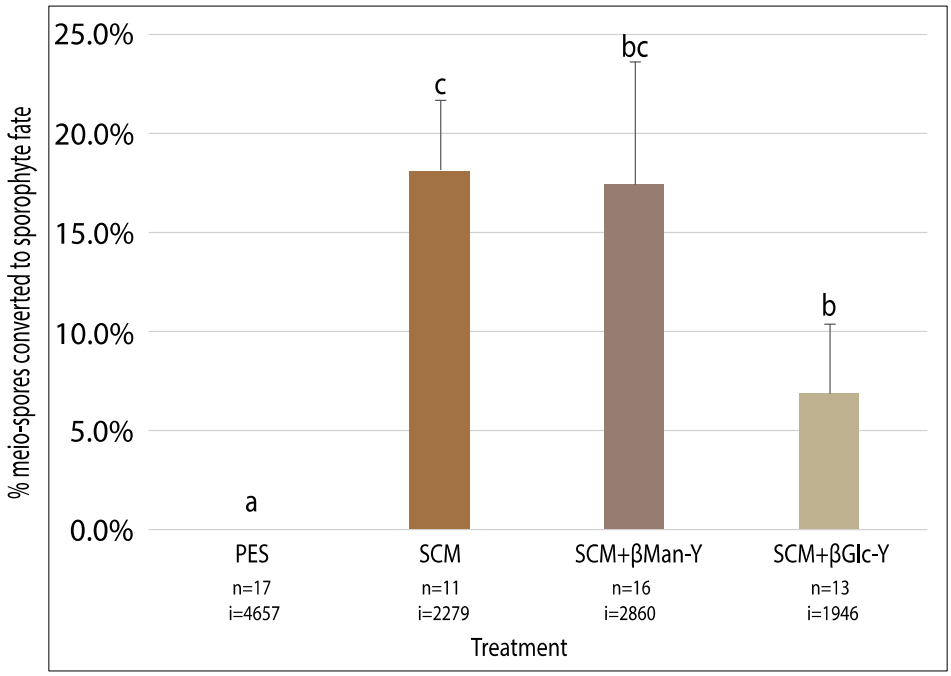


**Figure 8. Inhibition of the sporophyte-inducing activity of SCM following addition of a Yariv reagent.** SCM was incubated with either β-D-glucosyl Yariv reagent or with β-D-mannosyl-Yariv reagent as a control. Error bars indicate standard error of the mean, letters above bars indicate significant differences ($p$-value<0.05). PES, Provasoli-enriched natural seawater; SCM, sporophyte-conditioned medium; βGlc-Y, β-D-glucosyl Yariv reagent; βMan-Y, β-D-mannosyl Yariv reagent; n, number of replicates; i, number of individual germlings counted.

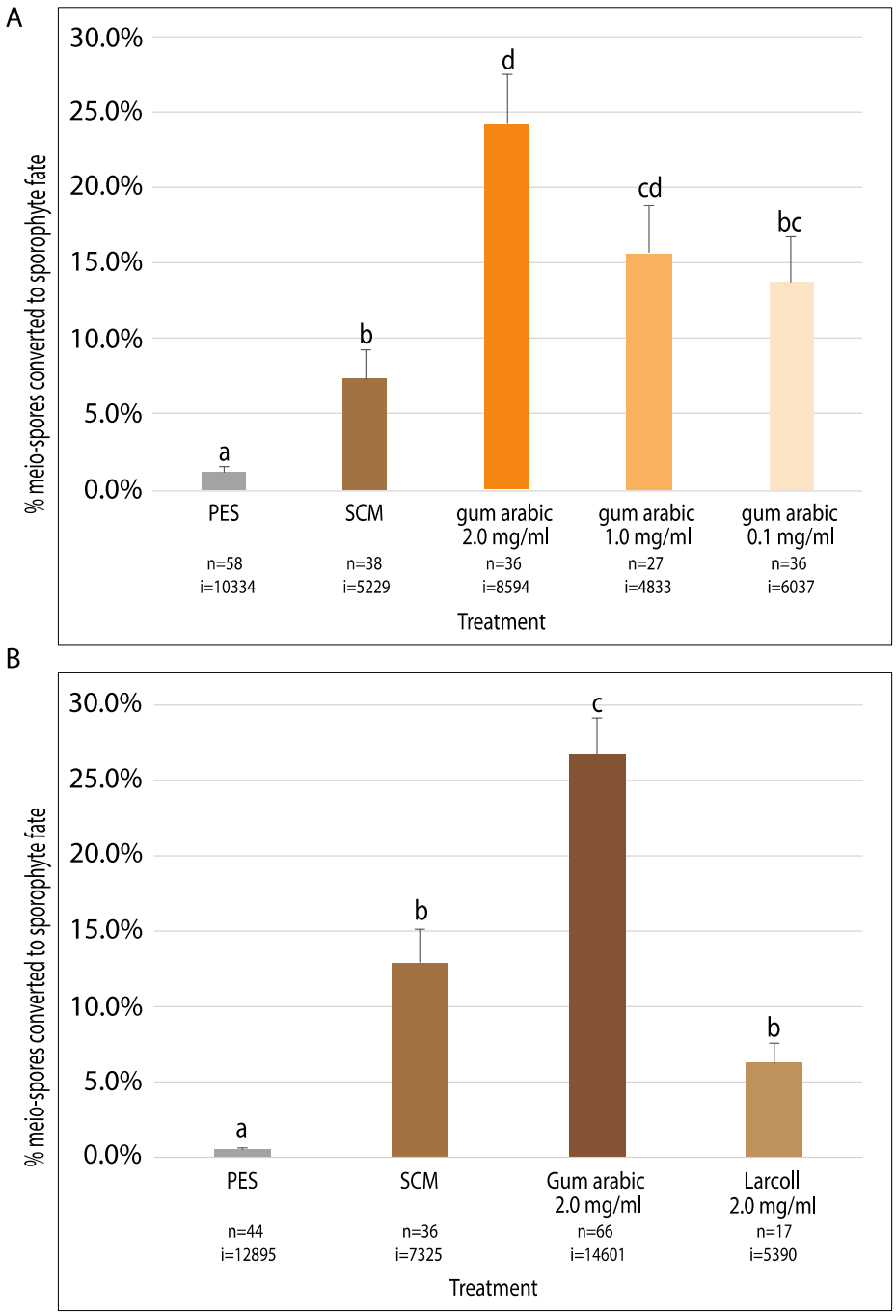


**Figure 9. Plant AGPs (gum arabic) mimics the effect of SCM, inducing meio-spores to switch to the sporophyte generation.** A. Meio-spores were treated with different concentrations of gum arabic or with SCM or PES as positive and negative controls, respectively. B. Meio-spores were treated with larcoll or gum arabic or with SCM or PES as positive and negative controls, respectively. Error bars indicate standard error of the mean, letters above bars indicate significant differences ($p$-value<0.05). PES, Provasoli-enriched natural seawater; SCM, sporophyte-conditioned medium; n, number of replicates; i, number of individual germlings counted.

## Discussion and perspectives

In this chapter, meio-spores were used to detect the bioactivity of the diffusible, sporophyte-inducing factor produced by *Ectocarpus* sporophytes. Meio-spores normally germinate to produce gametophytes after they are released from the unilocular sporangia but a proportion of meio-spores undergo the sporophyte developmental process in the presence of the diffusible factor or sporophyte tissue (Arun et al., 2019; Arun et al., 2013). As the diffusible factor is secreted into the culture medium by the sporophyte, the bioassay experiments were carried out by incubating meio-spores with sporophyte-conditioned medium (SCM) or other treatment media. We determined optimal conditions for the production of the sporophyte-inducing factor and carried out a primary characterisation of the factor. The physiological condition of meio-spores was shown to play a crucial role in detection of the diffusible factor, as poor condition affected the sensitivity of meio-spores to the factor. The data in this chapter demonstrated that meio-spores released less than 48h after isolation were more sensitive to the factor.

Experiments in which sporophytes were cultured at various light levels or for different lengths of time indicated that light intensity does not significantly influence sporophyte-inducing factor production. However, cultures grown under low light can be maintained for longer than those grown under high light intensity because, under the latter conditions, sporophytes mature after four weeks in culture and produce unilocular sporangia that release meio-spores, which develop as gametophytes. Therefore, pure sporophyte cultures cannot be maintained for long periods under low light conditions. This has an indirect effect on production of the sporophyte-inducing factor because experiments on the effect of sporophyte culture time showed that significant activity of the diffusible factor was detected after four weeks of culture but that the level increased with culture time up to eight weeks. These experiments indicated that the diffusible factor is produced by adult sporophytes.

Primary characterisation of the diffusible factor indicated that it was a heat-resistant, high molecular weight molecule. Mass spectrometry (MS) analysis identified a candidate protein which contained an arabinogalactan protein (AGP) core protein domain. Moreover, AGP glycan

epitopes were detected in SCM, supporting a hypothesis that the factor may be related to AGPs. AGPs are components of land plant cell surfaces and are hydroxyproline-rich glycoproteins, consisting of about 90% carbohydrate (Tan et al., 2012). They can bind to Yariv reagents. Although the molecular mechanisms of action of AGPS remain elusive (Hervé et al., 2016; Paulsen et al., 2014), they have been shown to have important functions in the green lineage. AGPs are involved in numerous developmental processes, including regulation of plant reproduction, e.g. initiation of male and female gametogenesis (Acosta-Garcia and Vielle-Calzada, 2004; Dresselhaus and Coimbra, 2016; Leszczuk et al., 2019), promotion of pollen tube growth and guidance and pollen grain development (Cheung et al., 1995; Coimbra et al., 2009; Lee et al., 2008a; Levitin et al., 2008; Mollet et al., 2002; Pereira et al., 2006; Wu et al., 1995; Wu et al., 2000), plant growth and development, e.g. cell expansion, secretion and programmed cell death (Chaves et al., 2002; Cruz‐Garcia et al., 2005; Gao and Showalter, 1999; Lee et al., 2008a; Lee et al., 2005; Lind et al., 1996; Nathan Hancock et al., 2005; Xu et al., 2008; Yang and Showalter, 2007), somatic embryogenesis of *Daucus carota* (Van Hengel et al., 2002), root growth and development of *A. thaliana* (Van Hengel and Roberts, 2003), signalling in tobacco and *Torenia fournieri* (Cheung et al., 1995; Jiao et al., 2017; Mizukami et al., 2016; Schultz et al., 1998), *Zinnia* xylem differentiation (Motose et al., 2004) and other developmental procees, e.g. resistance to Agro-bacterium tumefaciens-mediated infection (Gaspar et al., 2004), hormone responses in *Cucumber* (Park et al., 2003), salt tolerance and cell wall plasticity (Lamport et al., 2006; Shi et al., 2003). Further evidence linking the diffusible sporophyte-inducing factor to AGPs came from bioassay experiments involving incubation of meio-spores with an AGP-reactive Yariv reagent, which resulted in reduced activity of the factor. Furthermore, when either plant AGPs (gum arabic) or an arabinogalactan preparation (larcoll) were added to Provasoli-enriched seawater (PES), these mimicked the effect of the sporophyte-inducing factor. Taken together these experiments strongly indicate that the diffusible factor may be a type of AGP or at least is likely to contain arabinose and galactose residues within its composition.

Production and detection of the diffusible sporophyte-inducing factor are not straightforward due to problems of stability and the complicated, quantitative nature of the meio-spore-base bioassay. Nonetheless, the experiments described in this chapter provided important new information about

the factor and lay a foundation for future work. An important future objective will be to carry out further experiments aimed at characterising the exact biochemical nature of the diffusible factor such as biochemical purification the factor and deglycosylation experiments aimed at investigating the role of carbohydrate moieties. Finally, it would also be interesting to carry out experiments aimed at testing the activity of SCM or gum arabic on the meio-spores of other brown algal species, for example *Saccharina japonica*, which is of economic interest.

# Chapter IV

# Convergent recruitment of TALE homeodomain life cycle regulators to direct sporophyte development in land plants and brown algae

## Introduction

The life cycles of all sexual eukaryotes involve an alternation between two processes: meiosis and syngamy, which lead to the production of haploid cells (gametes) and diploid cells (zygotes), respectively. Multicellular development (mitotic cell divisions without cell separation) can occur during the haploid phase (haplontic life cycles), the diploid phase (diplontic life-cycles) or during both phases (haplo-diplontic life-cycles) (Bourdareau, 2018). Most brown algae have haploid-diplontic life cycles involving an alternation between gametophyte and sporophyte generations (Silberfeld et al., 2010). However, the molecular mechanisms that underlie this alternation is remain unclear (Cock et al., 2014). *Ectocarpus* is a filamentous brown alga, with free-living, independent gametophyte and sporophyte generations (Russell, 1967). The two generations exhibit some marked differences in morphogenesis and functions (Coelho et al., 2012a; Lipinska et al., 2019). *Ectocarpus* was the first brown alga to be sequenced and has been adopted as a genetic model organism for the brown algae (Cock et al., 2015; Cock et al., 2010; Coelho et al., 2012a; Peters et al., 2004a). Numerous molecular and genetic tools are available for this model

this model species. One particularly interesting feature is parthenogenesis, during which unfused gametes develop as haploid sporophyte, facilitating mutant screens because mutations affecting sporophyte development are directly expressed phenotypically in haploid partheno-sporophytes. Using this model system, several life-cycle and developmental mutants have been identified including the *immediate upright* (*imm*), *ouroboros* (*oro*) and *samsara* (*sam*) mutants (Arun et al., 2019; Coelho et al., 2011; Macaisne et al., 2017; Peters et al., 2008). Overall, *Ectocarpus* represents a good organism to study eukaryotic life cycles. Work on *Ectocarpus* has shown that the alternation between generations in *Ectocarpus* both by genetic factors and by a non-cell-autonomous, diffusible factor produced by the sporophyte (Arun et al., 2013). This chapter will present the characterisation of two life-cycle-related genes, *ORO* and *SAM*, that code for the TALE HD transcription factors ORO and SAM respectively. The manuscript presented in this chapter has been published in the journal eLife (Arun et al., 2019). My contribution to this work was to investigate the susceptibility of the *sam* mutant to treatment with the diffusible factor with the aim of understanding the developmental pathway triggered by this factor.

eLIFE elifesciences.org

RESEARCH ARTICLE

# Convergent recruitment of TALE homeodomain life cycle regulators to direct sporophyte development in land plants and brown algae

**Alok Arun[1†‡], Susana M Coelho[1†], Akira F Peters[2], Simon Bourdareau[1], Laurent Pérès[1], Delphine Scornet[1], Martina Strittmatter[1§], Agnieszka P Lipinska[1], Haiqin Yao[1], Olivier Godfroy[1], Gabriel J Montecinos[1], Komlan Avia[#], Nicolas Macaisne[¶], Christelle Troadec[3], Abdelhafid Bendahmane[3], J Mark Cock***

[1]Sorbonne Université, CNRS, Algal Genetics Group, Integrative Biology of Marine Models (LBI2M), Station Biologique de Roscoff (SBR), Roscoff, France; [2]Bezhin Rosko, Santec, France; [3]Institut National de la Recherche Agronomique (INRA), Institute of Plant Sciences Paris-Saclay (IPS2), CNRS, Université Paris-Sud, Orsay, France

***For correspondence:** cock@sb-roscoff.fr

[†]These authors contributed equally to this work

**Present address:** [‡]Institute of Sustainable Biotechnology, Department of Science and Technology, Inter American University of Puerto Rico, Barranquitas Campus, Puerto Rico, United States; [§]CNRS, Sorbonne Université, UPMC University Paris 06, UMR 7144, Adaptation and Diversity in the Marine Environment, Station Biologique de Roscoff, Roscoff, France; [#]Agroécologie, AgroSup Dijon, INRA, Univ. Bourgogne, University Bourgogne Franche-Comté, Dijon, France; [¶]Magee-Womens Research Institute, University of Pittsburgh School of Medicine, Pittsburgh, United States

**Competing interests:** The authors declare that no competing interests exist.

**Funding:** See page 17

**Received:** 24 October 2018
**Accepted:** 13 January 2019
**Published:** 15 January 2019

**Reviewing editor:** Sheila McCormick, University of California, Berkeley, United States



**Abstract** Three amino acid loop extension homeodomain transcription factors (TALE HD TFs) act as life cycle regulators in green algae and land plants. In mosses these regulators are required for the deployment of the sporophyte developmental program. We demonstrate that mutations in either of two TALE HD TF genes, *OUROBOROS* or *SAMSARA*, in the brown alga *Ectocarpus* result in conversion of the sporophyte generation into a gametophyte. The OUROBOROS and SAMSARA proteins heterodimerise in a similar manner to TALE HD TF life cycle regulators in the green lineage. These observations demonstrate that TALE-HD-TF-based life cycle regulation systems have an extremely ancient origin, and that these systems have been independently recruited to regulate sporophyte developmental programs in at least two different complex multicellular eukaryotic supergroups, Archaeplastida and Chromalveolata.
DOI: https://doi.org/10.7554/eLife.43101.001

## Introduction

Developmental processes need to be precisely coordinated with life cycle progression. This is particularly important in multicellular organisms with haploid-diploid life cycles, where two different developmental programs, corresponding to the sporophyte and gametophyte, need to be deployed appropriately at different time points within a single life cycle. In the unicellular green alga *Chlamydomonas*, plus and minus gametes express two different HD TFs of the three amino acid loop extension (TALE) family called Gsm1 and Gsp1 (***Lee et al., 2008***). When two gametes fuse to form a zygote, these two proteins heterodimerise and move to the nucleus, where they orchestrate the diploid phase of the life cycle. Gsm1 and Gsp1 belong to the knotted-like homeobox (KNOX) and BEL TALE HD TF classes, respectively. In the multicellular moss *Physcomitrella patens*, deletion of two KNOX genes, *MKN1* and *MKN6*, blocks initiation of the sporophyte program leading to conversion of this generation of the life cycle into a diploid gametophyte (***Sakakibara et al., 2013***). Similarly, the moss BEL class gene *BELL1* is required for induction of the sporophyte developmental program and ectopic expression of *BELL1* in gametophytic tissues induces the development of apogametic sporophytes during the gametophyte generation of the life cycle (***Horst et al., 2016***). In mosses, therefore, the KNOX and BEL class life cycle regulators have been recruited to act as master

**eLife digest** Brown algae and land plants are two groups of multicellular organisms that have been evolving independently for over a billion years. Their last common ancestor is thought to have existed as a single cell; then, complex multicellular organisms would have appeared separately in each lineage. Comparing brown algae and land plants therefore helps us understand the rules that guide how multicellular organisms evolve from single-celled ancestors.

During their life cycles, both brown algae and land plants alternate between two multicellular forms: the gametophyte and the sporophyte. The gametophyte develops sexually active reproductive cells, which, when they merge, create the sporophyte. In turn, spores produced by the sporophyte give rise to the gametophyte. Specific developmental programs are deployed at precise points in the life cycle to make either a sporophyte or a gametophyte.

Two proteins known as TALE HD transcription factors help to control the life cycle of single-celled algae related to land plants. Similar proteins are also required for the sporophyte to develop at the right time in land plants known as mosses. This suggests that, when multicellular organisms emerged in this lineage, life cycle TALE HD transcription factors were recruited to orchestrate the development of the sporophyte. However, it was not clear whether TALE HD transcription factors play equivalent roles in other groups, such as brown algae.

To address this question, Arun, Coelho et al. examined two mutants of the brown alga *Ectocarpus*, which produce gametophytes when the non-mutated alga would have made sporophytes. Genetic analyses revealed that these mutated brown algae carried changes in two genes that encode TALE HD transcription factors, indicating that these proteins also regulate the formation of sporophytes in brown algae. Taken together, the results suggest that TALE HD transcription factors were originally tasked with controlling life cycles, and then have been independently harnessed in both land plants and brown algae to govern the formation of sporophytes. This means that, regardless of lineage, the same fundamental forces may be shaping the evolutionary paths that lead to multicellular organisms.

Proteins similar to TALE HD transcription factors also regulate life cycles in other groups such as fungi and social amoebae, which indicates that their role is very ancient. It now remains to be explored whether such proteins control life cycles and developmental programs in other multicellular organisms, such as animals.

DOI: https://doi.org/10.7554/eLife.43101.002

regulators of the sporophyte developmental program, coupling the deployment of this program with life cycle progression. *P. patens* KNOX and BEL proteins have been shown to form heterodimers (**Horst et al., 2016**) and it is therefore possible that life cycle regulation also involves KNOX/BEL heterodimers in this species.

The filamentous alga *Ectocarpus* has emerged as a model system for the brown algae (**Cock et al., 2015**; **Coelho et al., 2012**). This alga has a haploid-diploid life cycle that involves alternation between multicellular sporophyte and gametophyte generations (**Figure 1A**). A mutation at the *OUROBOROS* (*ORO*) locus has been shown to cause the sporophyte generation to be converted into a fully functional (gamete-producing) gametophyte (**Figure 1B**) (**Coelho et al., 2011**). This mutation therefore induces a phenotype that is essentially identical to that observed with the *P. patens mkn1 mkn6* double mutant, but in an organism from a distinct eukaryotic supergroup (the stramenopiles), which diverged from the green lineage over a billion years ago (**Eme et al., 2014**).

Here we identify mutations at a second locus, *SAMSARA*, that also result in conversion of the sporophyte generation into a gametophyte. Remarkably, both *OUROBOROS* and *SAMSARA* encode TALE HD TFs and the two proteins associate to form a heterodimer. These observations indicate that TALE-HD-TF-based life cycle regulatory systems have very deep evolutionary origins and that they have been independently recruited in at least two eukaryotic supergroups to act as master regulators of sporophyte developmental programs.

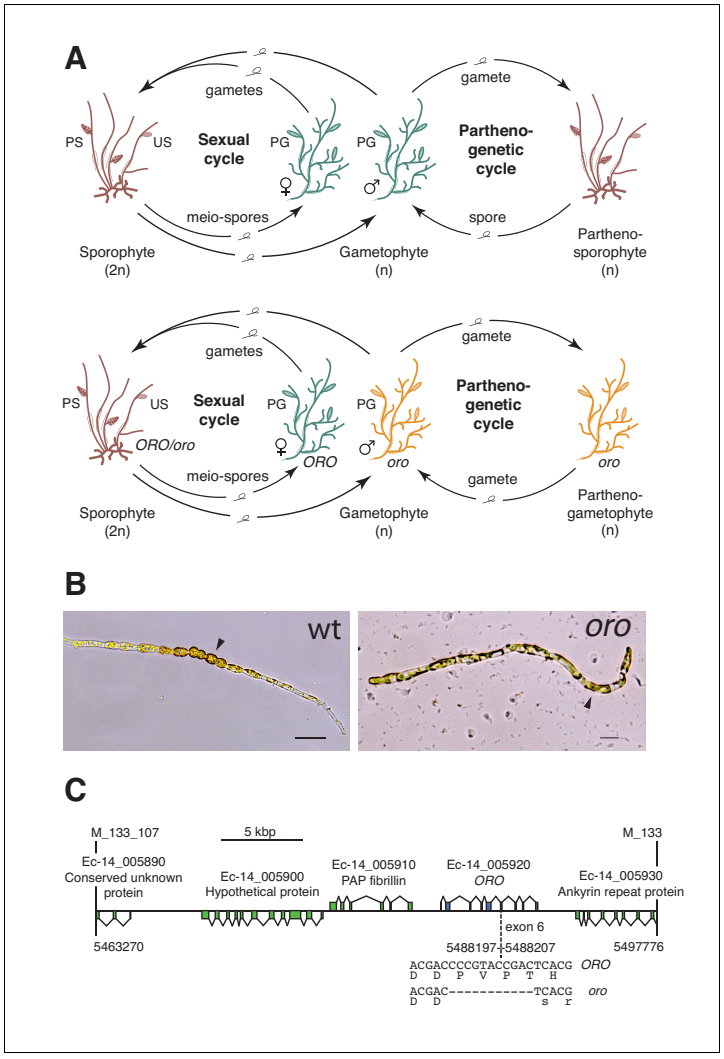


**Figure 1.** The *oro* life cycle mutation corresponds to a TALE homeodomain transcription factor gene. (**A**) Life cycles of wild type and *oro* mutant *Ectocarpus*. The wild type sexual cycle (upper panel) involves production of meio-spores by the diploid sporophyte via meiosis in unilocular (single-chambered) sporangia (US). The meio-spores develop as haploid, dioicous (male and female) gametophytes. The gametophytes produce gametes in plurilocular (multichambered) gametangia (PG), which fuse to produce a diploid sporophyte. Gametes that fail to fuse can develop parthenogenetically to produce a partheno-sporophyte, which can produce spores by apomeiosis or following endoreduplication to engender a new generation of gametophytes. PS, plurilocular sporangium (asexual reproduction). Gametes of the *oro* mutant (lower panel) are unable to initiate the sporophyte program and develop parthenogenetically to produce partheno-gametophytes. The mutation is recessive so a cross with a wild type gametophyte produces a heterozygous diploid sporophyte with a wild type phenotype. (**B**) Young gamete-derived parthenotes of wild type and *oro* strains. Arrowheads indicate round, thick-walled cells typical of the sporophyte for the wild type and long, wavy cells typical of the gametophyte for the *oro* mutant. Scale bars: 20 µm. (**C**) Representation of the interval on chromosome 14 between the closest recombining markers to the *ORO* locus (M_133_107 and M_133) showing the position of the single mutation within the mapped interval.
DOI: https://doi.org/10.7554/eLife.43101.003

## Results

### Two TALE homeodomain transcription factors direct sporophyte development in *Ectocarpus*

The *ORO* gene was mapped to a 34.5 kbp (0.45 cM) interval on chromosome 14 using a segregating family of 2000 siblings derived from an *ORO* x *oro* cross and a combination of amplified fragment

length polymorphism (AFLP) (**Vos et al., 1995**) and microsatellite markers. Resequencing of the 34.5 kbp interval in the *oro* mutant showed that it contained only one mutation: an 11 bp deletion in exon six of the gene with the LocusID Ec-14_005920, which encodes a TALE homeodomain transcription factor. (**Figure 1C**).

A visual screen of about 14,000 UV-mutagenised germlings identified three additional life cycle mutants (designated *samsara-1, samsara-2* and *samsara-3,* abbreviated as *sam-1, sam-2* and *sam-3*). The *sam* mutants closely resembled the *oro* mutant in that gamete-derived parthenotes did not adopt the normal sporophyte pattern of development but rather resembled gametophytes. Young, germinating individuals exhibited the wavy pattern of filament growth typical of the gametophyte and, at maturity, never produced unilocular sporangia (the reproductive structures where meiosis occurs; **Figure 1A**), a structure that is uniquely observed during the sporophyte generation (**Figure 2A–C**; **Figure 2—figure supplement 1**). Moreover, the *sam* mutants exhibited a stronger negative phototrophic response to unilateral light than wild type sporophytes (**Figure 2D**), a feature typical of gametophytes (**Peters et al., 2008**) that was also observed for the *oro* mutant (**Coelho et al., 2011**).

Genetic crosses confirmed that the *sam* mutants were fully functional (i.e. gamete-producing) gametophytes and complementation analysis indicated that the mutations were not located at the same genetic locus as the *oro* mutation (**Supplementary file 1**). Interestingly, hybrid sporophytes that were heterozygous for the *sam* mutations failed to produce functional unilocular sporangia. Wild type unilocular sporangia contain about a hundred haploid meio-spores produced by a single meiotic division followed by several rounds of mitotic divisions, whereas unilocular sporangia of *SAM/sam* heterozygotes never contained more than four nuclei indicating that abortion was either concomitant with or closely followed meiosis (**Figure 2F**). This indicated either a dominant effect of the *sam* mutations in the fertile sporophyte or abortion of the sporangia due to arrested development of the two (haploid) meiotic daughter cells that carried the mutant *sam* allele. Note that no meiotic defects were observed in heterozygous sporophytes carrying the *oro* mutation.

*Ectocarpus* sporophytes produce a diffusible factor that induces gametophyte initial cells or protoplasts of mature gametophyte cells to switch to the sporophyte developmental program (**Arun et al., 2013**). The *oro* mutant is not susceptible to this diffusible factor (*oro* protoplasts regenerate as gametophytes in sporophyte-conditioned medium) indicating that *ORO* is required for the diffusible factor to direct deployment of the sporophyte developmental pathway (**Arun et al., 2013**). We show here that the *sam-1* mutant is also resistant to the action of the diffusible factor. Congo red staining of individuals regenerated from *sam-1* protoplasts that had been treated with the diffusible factor detected no sporophytes, whereas control treatment of wild type gametophyte-derived protoplasts resulted in the conversion of 7.5% of individuals into sporophytes (**Figure 2E**, **Supplementary file 2**). Therefore, in order to respond to the diffusible factor, cells must possess functional alleles of both *ORO* and *SAM*.

The *Ectocarpus* genome contains two TALE HD TFs in addition to the *ORO* gene. Resequencing of these genes in the three *sam* mutants identified three genetic mutations, all of which were predicted to severely affect the function of Ec-27_006660 (**Figure 2G**). The identification of three disruptive mutations in the same gene in the three independent *sam* mutants strongly indicates that these are the causative lesions. Ec-27_006660 was therefore given the gene name *SAMSARA (SAM).*

*ORO* and *SAM* transcripts were most abundant in gametes (**Figure 3A**), consistent with a role in initiating sporophyte development following gamete fusion. Interestingly, transcripts of both *ORO* and *SAM* were detected in both male and female gametes indicating that gametes of both sexes carry both ORO and SAM proteins. This situation therefore appears to differ from that observed in *Chlamydomonas* where GSP1 and GSM1 are expressed uniquely in the plus and minus gametes, respectively (**Lee et al., 2008**). Whilst we cannot rule out the possibility that post-transcriptional regulatory processes result in *ORO* and *SAM* exhibiting sex-specific patterns of gamete expression, genetic evidence also supports a bi-sexual pattern of expression, at least for *ORO*, because complementation was observed when both male and female strains carrying the *oro* mutation were crossed with wild type strains (**Supplementary file 1**). This would not be expected if the ORO protein were supplied to the zygote uniquely by the male or the female gamete.

Quantitative PCR experiments demonstrated that sporophyte and gametophyte marker genes (**Peters et al., 2008**) were down- and up-regulated, respectively, in *sam* mutant lines (**Figure 3B**), as was previously demonstrated for the *oro* mutant (**Coelho et al., 2011**).

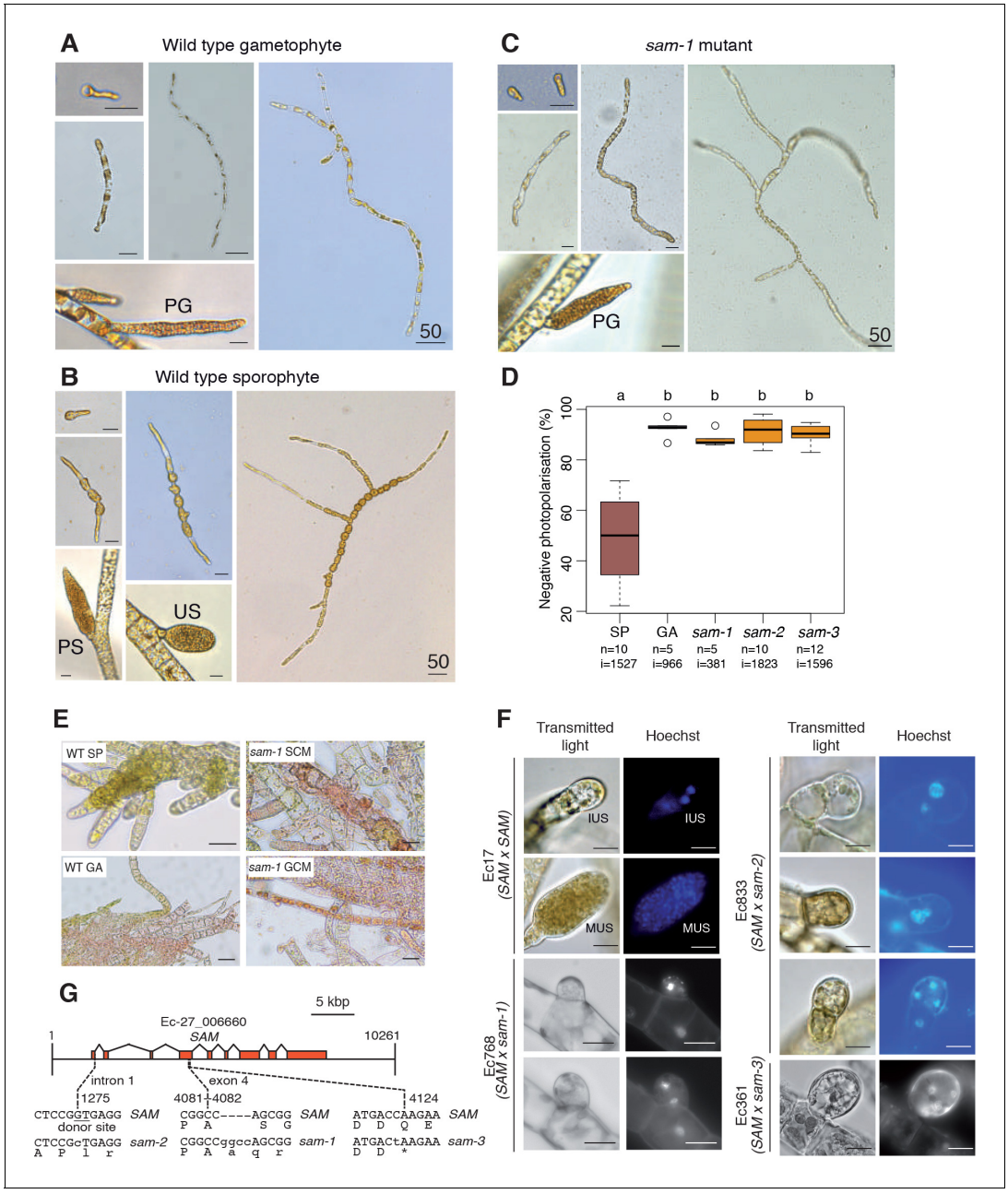


**Figure 2.** Phenotypic and genetic characterisation of *sam* life cycle mutants. (**A-C**) The *sam-1* mutant exhibits gametophyte-like morphological characteristics. Different stages of (**A**) wild type gametophyte (strain Ec32), (**B**) wild type partheno-sporophyte (strain Ec32) and (**C**) *sam-1* mutant (strain Ec374). PG, plurilocular gametangia; PS, plurilocular sporangium; US, unilocular sporangium. (**D**) *sam* mutants exhibit a gametophyte-like photopolarisation response to unidirectional light. Letters above the boxplot indicate significant differences (Wilcoxon test, p-value<0.01). n, number of replicates; i, number of individuals scored. (**E**) Representative images of congo red staining showing that the *sam-1* mutant protoplasts are resistant to treatment with sporophyte conditioned medium (SCM). GCM, control gametophyte conditioned medium. (**F**) Abortion of unilocular sporangia in *sam-1*, *sam-2* or *sam-3* mutant sporophytes. Images are representative of n = 19 (Ec17), n = 23 (Ec768), n = 20 (Ec833) and n = 14 (Ec361) unilocular sporangia. IUS, immature unilocular sporangium; MUS, mature unilocular sporangium. (**G**) Locations of the three *sam* mutations within the *SAM* gene. Scale bars: 20 µm (or 50 µm if indicated by 50).

DOI: https://doi.org/10.7554/eLife.43101.004

The following figure supplement is available for figure 2:

**Figure supplement 1.** Morphological characteristics of *sam* mutants.

DOI: https://doi.org/10.7554/eLife.43101.005

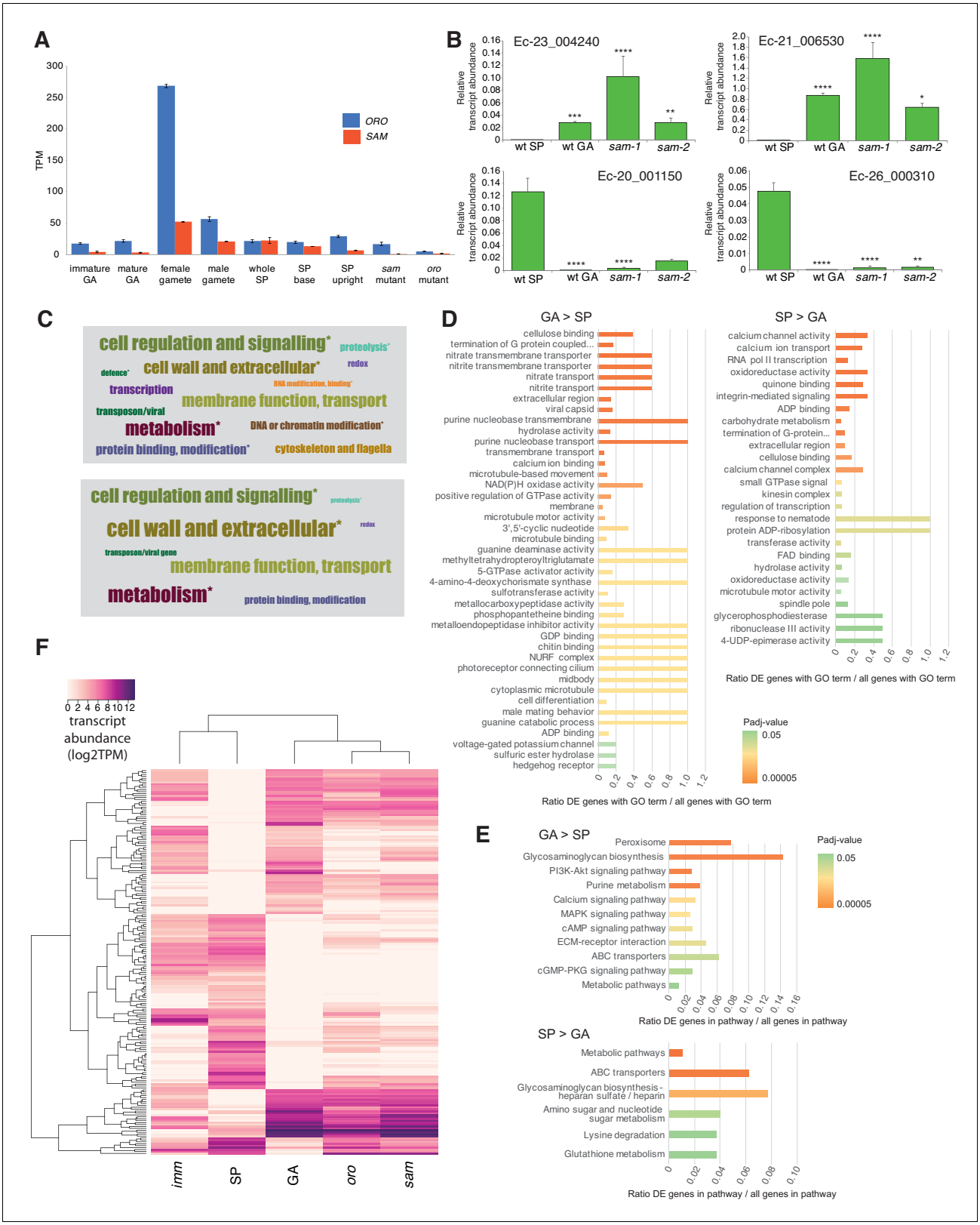


**Figure 3.** Gene expression analysis. (**A**) Abundance of *ORO* and *SAM* transcripts during different stages of the life cycle. Error bars, standard error of the mean (SEM); TPM, transcripts per million. (**B**) Quantitative reverse transcription PCR analysis of generation marker genes. The graphs indicate mean values ± standard error of transcript abundances for two gametophyte marker genes, Ec-23_004240 and Ec-21_006530, and two sporophyte marker genes, Ec-20_001150 and Ec-26_000310. Data from five independent experiments. *p≤0.05, **p≤0.01, ***p≤0.001, ****p≤0.0001. (**C**) Word cloud

*Figure 3 continued on next page*

*Figure 3 continued*

representations of the relative abundances (log2 gene number) of manually assigned functional categories in the set of genes that were differential regulated between the sporophyte and gametophyte generations (upper panel) and in the subset of those genes that encode secreted proteins (lower panel). Asterisks indicate functional categories that were significantly over- or under-represented in the two datasets. (**D-E**) Significantly overrepresented GO terms (**D**) and KEGG pathways (**E**) associated with generation-biased genes. (**F**) Expression patterns of the 200 most strongly generation-biased genes. *oro*, *oro* mutant; *sam*, *sam* mutant; *imm*, *immediate upright* mutant; GA: gametophyte; SP: sporophyte.

DOI: https://doi.org/10.7554/eLife.43101.006

The following figure supplement is available for figure 3:

**Figure supplement 1.** Evidence for the production of full-length *ORO* and *SAM* transcripts during the gametophyte generation.

DOI: https://doi.org/10.7554/eLife.43101.007

## *ORO* and *SAM* regulate the expression of sporophyte generation genes

To investigate the genetic mechanisms underlying the switch from the gametophyte to the sporophyte program directed by the *ORO* and *SAM* genes, we characterised the gene expression networks associated with the two generations of the *Ectocarpus* life cycle. Comparative analysis of RNA-seq data for duplicate cultures of wild type sporophytes and wild type gametophytes grown under identical conditions (libraries GBP-5 and GBP-6 and libraries GBP-7 and GBP-8 in ***Supplementary file 9***, respectively) identified 1167 genes that were differentially regulated between the two generations (465 upregulated in the sporophyte and 702 upregulated in the gametophyte; ***Supplementary file 3***). The predicted functions of these generation-biased genes were analysed using a system of manually-assigned functional categories, together with analyses based on GO terms and KEGG pathways. The set of generation-biased genes was significantly enriched in genes belonging to two of the manually-assigned categories: 'Cell wall and extracellular' and 'Cellular regulation and signalling' and for genes of unknown function (***Figure 3C***, ***Supplementary file 3***). Enriched GO terms also included several signalling- and cell wall-associated terms and terms associated with membrane transport (***Figure 3D***, ***Supplementary file 4***). The gametophyte-biased gene set was enriched for several cell signalling KEGG pathways whereas the sporophyte-biased gene set was enriched for metabolic pathways (***Figure 3E***, ***Supplementary file 5***). We also noted that the generation-biased genes included 23 predicted transcription factors and ten members of the EsV-1–7 domain family (***Macaisne et al., 2017***) (***Supplementary file 3***). The latter were significantly enriched in the sporophyte-biased gene set ($\chi 2$ test p=0.001).

Both the sporophyte-biased and the gametophyte-biased datasets were enriched in genes that were predicted to encode secreted proteins (Fisher's Exact Test $p=2.02e^{-8}$ and $p=4.14e^{-6}$, respectively; ***Supplementary file 3***). Analysis of GO terms associated with the secreted proteins indicated a similar pattern of enrichment to that observed for the complete set of generation-biased genes (terms associated with signalling, cell wall and membrane transport; ***Supplementary file 4***). ***Figure 3C*** illustrates the relative abundances of manually-assigned functional categories represented in the generation-biased genes predicted to encode secreted proteins.

The lists of differentially expressed genes identified by the above analysis were used to select 200 genes that showed strong differential expression between the sporophyte and gametophyte generations. The pattern of expression of the 200 genes was then analysed in parthenotes of the *oro* and *sam* mutants and of a third mutant, *immediate upright* (*imm*), which does not cause switching between life cycle generations (***Macaisne et al., 2017***), as a control. ***Figure 3F*** shows that mutation of either *ORO* or *SAM* leads to upregulation of gametophyte generation genes and downregulation of sporophyte generation genes, consistent with the switch from sporophyte to gametophyte phenotypic function. Moreover, *oro* and *sam* mutants exhibited similar patterns of expression but the patterns were markedly different to that of the *imm* mutant. Taken together with the morphological and reproductive phenotypes of the *oro* and *sam* mutants, this analysis supports the conclusion that *ORO* and *SAM* are master regulators of the gametophyte-to-sporophyte transition.

## The ORO and SAM proteins interact in vitro

HD TFs that act as life cycle regulators or mating type determinants often form heterodimeric complexes (***Banham, 1995***; ***Horst et al., 2016***; ***Hull et al., 2005***; ***Kämper et al., 1995***; ***Lee et al., 2008***). The ORO and SAM proteins were also shown to be capable of forming a stable heterodimer

using an in vitro pull-down approach (***Figure 4***). Deletion analysis indicated that the interaction between the two proteins was mediated by their homeodomains.

## Evolutionary origins and domain structure of the *ORO* and *SAM* genes

Analysis of sequence databases indicated that all brown algae possess three HD TFs, all of the TALE class, including orthologues of ORO and SAM (***Figure 5A***, ***Supplementary file 6***). Comparison of brown algal ORO and SAM orthologues identified conserved domains both upstream and downstream of the HDs in both ORO and SAM (***Figure 5B,C***). These domains do not correspond to any known domains in public domain databases and were not found in any other proteins in the public sequence databases. In particular, we did not detect any clear similarity with HD-associated domains that have been shown to be deeply conserved across eukaryotic TALE HD TFs (***Bürglin, 1997***; ***Joo et al., 2018***) but we cannot rule out the possibility that the ORO and SAM proteins possess

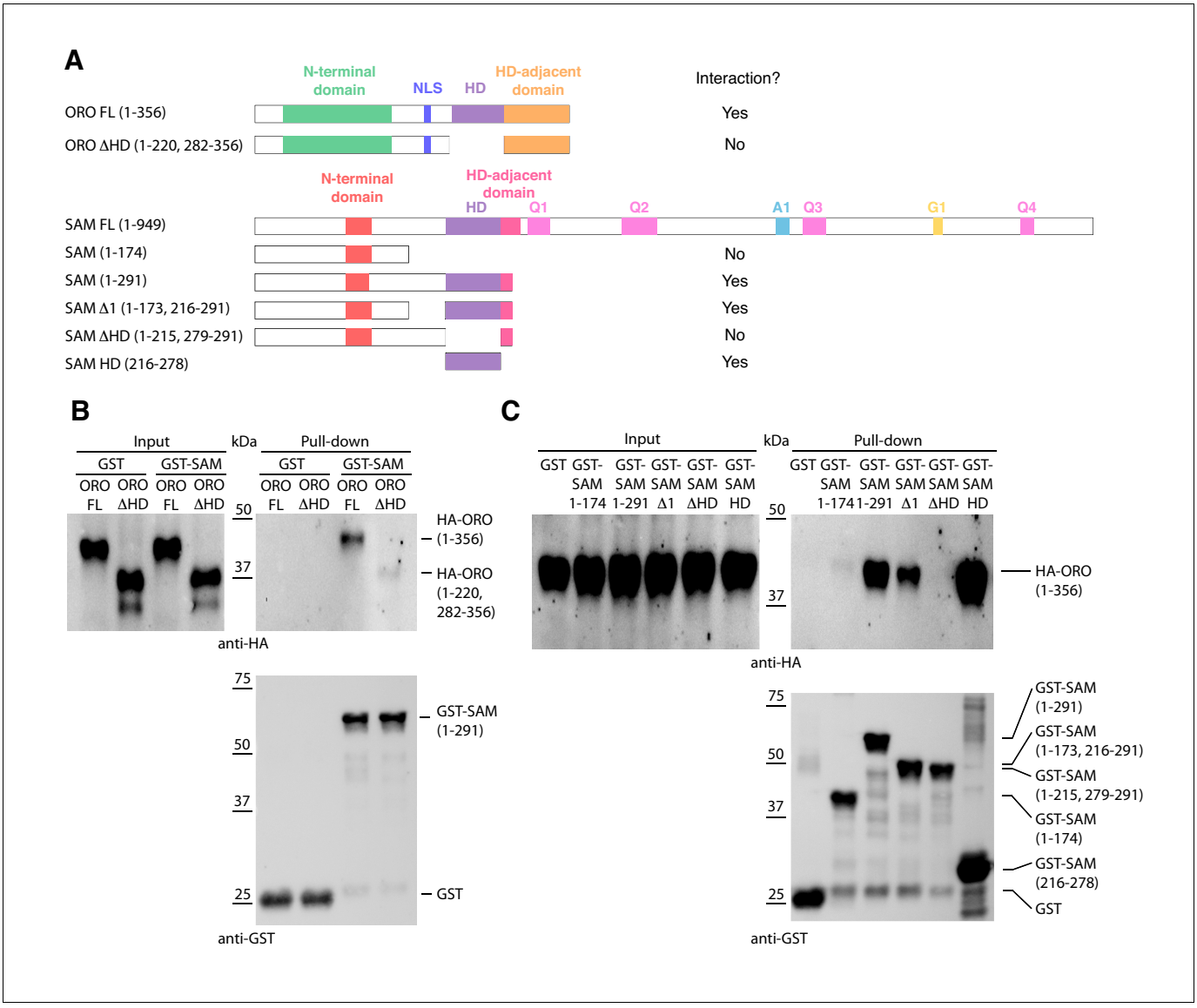


**Figure 4.** Detection of ORO-SAM heterodimerisation in vitro using a pull-down assay. (**A**) ORO and SAM constructs used for the pull-down experiments. (**B**) Pull-down assay between SAM and different versions of the ORO protein. (**C**) Pull-down assay between different versions of the SAM protein and full-length ORO protein. Note that all ORO proteins were fused with the HA epitope. FL, full-length; HD, homeodomain.
DOI: https://doi.org/10.7554/eLife.43101.008

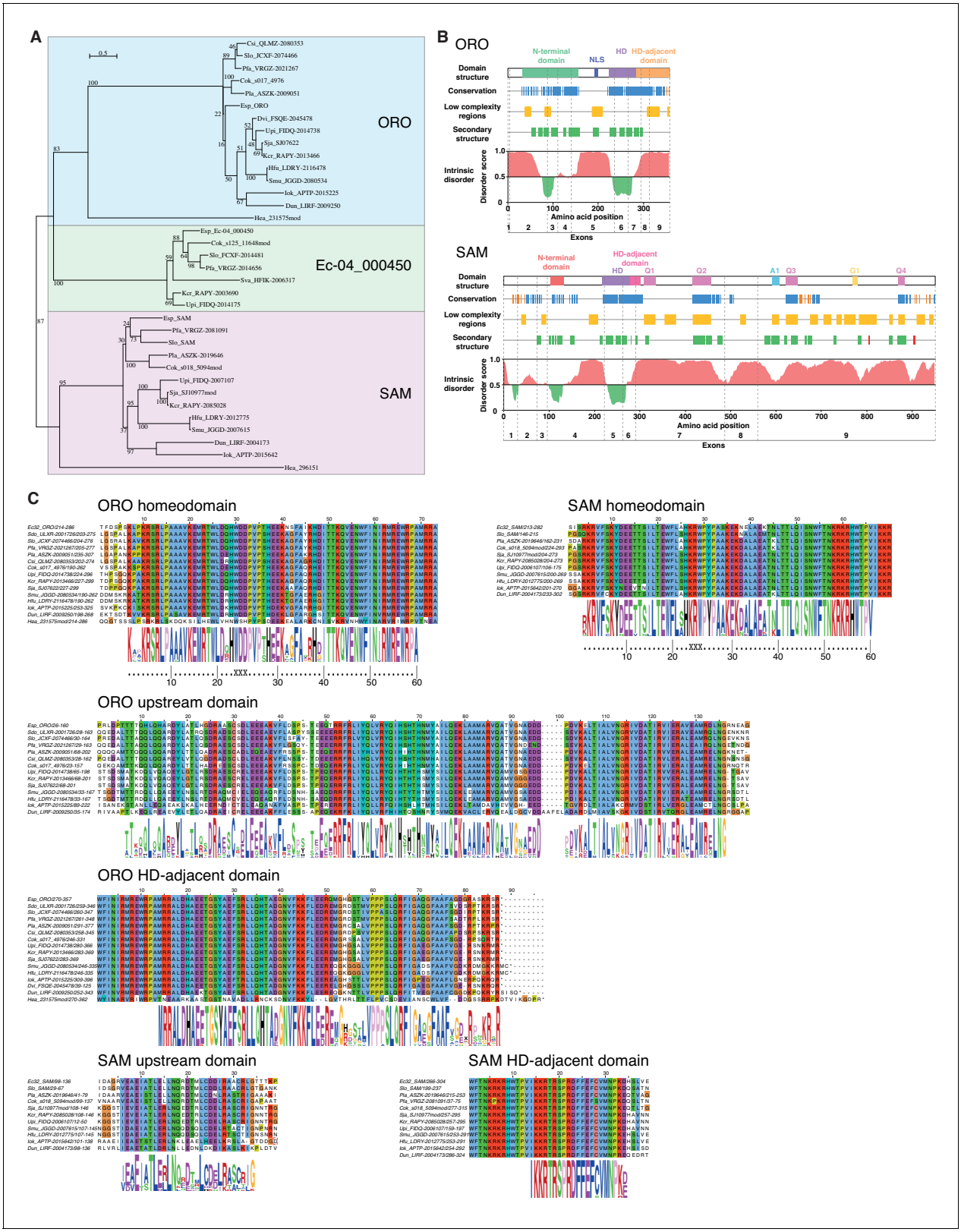


**Figure 5.** ORO and SAM conservation and domain structure. (**A**) Unrooted maximum likelihood tree of ORO, SAM and Ec-04_000450 orthologues from diverse brown algal species and the raphidophyte *Heterosigma akashiwo*. (**B**) Domain structure of the ORO and SAM TALE homeodomain transcription factors. Conservation: strong (blue), less strong (orange), secondary structure: α-helix (green), β-strand (red). Q1-4, A1 and G1: regions rich in glutamine, alanine and glycine, respectively. (**C**) Conserved domains in ORO and SAM proteins. Cok, *Cladosiphon okamuranus*; Csi, *Colpomenia sinuosa*; Dvi,

*Figure 5 continued on next page*

*Figure 5 continued*

*Desmarestia viridis*; Dun, *Dictyopteris undulata*; Esp, *Ectocarpus* sp.; Hea, *Heterosigma akashiwo*; Hfu, *Hizikia fusiformis*; Iok, *Ishige okamurai*; Kcr, *Kjellmaniella crassifolia*; Pfa, *Petalonia fascia*; Pla, *Punctaria latifolia*; Sja, *Saccharina japonica*; Smu, *Sargassum muticum*; Sva, *Sargassum vachellianum*; Sdo, *Scytosiphon dotyi*; Slo, *Scytosiphon lomentaria*; Upi, *Undaria pinnatifida*.

DOI: https://doi.org/10.7554/eLife.43101.009

The following figure supplement is available for figure 5:

**Figure supplement 1.** Intron conservation in homeobox genes.

DOI: https://doi.org/10.7554/eLife.43101.010

highly diverged versions of these domains. The HD was the only domain that was common to both the ORO and SAM proteins (***Figure 5***).

To identify more distantly-related orthologues of ORO and SAM, we searched a broad range of stramenopile TALE HD TFs for the presence of characteristic ORO and SAM protein domains. Only one non-brown-algal protein, from the raphidophyte *Heterosigma akashiwo*, possessed similarity to these domains, allowing it to be classed tentatively as an ORO orthologue (gene identifier 231575mod; ***Figure 5A,C***, ***Supplementary file 6***). The transcriptome of this strain also included a truncated TALE HD TF transcript similar to SAM but more complete sequence data will be required to confirm orthology with SAM (gene identifier 296151; ***Figure 5A***, ***Supplementary file 6***). This analysis allowed the origin of ORO to be traced back to the common ancestor with the raphidophytes (about 360 Mya; ***Brown and Sorhannus, 2010***) but the rate of divergence of the non-HD regions of ORO and SAM precluded the detection of more distantly related orthologues. An additional search based on looking for TALE HD TF genes with intron positions corresponding to those of *ORO* and *SAM* did not detect any further orthologues (***Figure 5—figure supplement 1***).

## Discussion

The analysis presented here demonstrates that two TALE HD TFs, which are capable of forming a heterodimer, are required for the deployment of the sporophyte program during the life cycle of the brown alga *Ectocarpus*. The parallels with life cycle regulation in the green lineage, where TALE HD TFs have also been shown to regulate deployment of the sporophyte program (***Horst et al., 2016***; ***Sakakibara et al., 2013***), are striking. Knockout of the KNOX class TALE HD TF genes *MKN1* and *MKN6* in *Physcomitrella patens* result in conversion of the sporophyte generation into a functional gametophyte (***Sakakibara et al., 2013***), essentially the same phenotype as that observed with *Ectocarpus oro* or *sam* mutants despite the fact that more than a billion years of evolution separate the two lineages (***Eme et al., 2014***) and that the two lineages independently evolved complex multicellularity. The similarities between life cycle regulators in the two eukaryotic supergroups suggests that they are derived from a common ancestral system that would therefore date back to early eukaryotic evolution. The ancient origin of this life cycle regulatory system is further supported by the fact that distantly-related homeodomain or homeodomain-like proteins act as mating type factors in both fungi and social amoebae (***Hedgethorne et al., 2017***; ***Hull et al., 2005***; ***Nasmyth and Shore, 1987***; ***Van Heeckeren et al., 1998***). Moreover, in Basidiomycetes these proteins regulate multiple aspects of sexual development including the formation of filaments, basidia and spores indicating recurrent recruitment as developmental regulators (***Banham, 1995***; ***Hull et al., 2005***; ***Kämper et al., 1995***).

It has been proposed that the ancestral function of homeodomain-based life cycle regulators was to detect syngamy and to implement processes specific to the diploid phase of the life cycle such as repressing gamete formation and initiating meiosis (***Perrin, 2012*** and references therein). With the emergence of complex, multicellular organisms, it would not have been surprising if additional processes such as developmental networks had come under the control of these regulators as this would have ensured that those developmental processes were deployed at the appropriate stage of the life cycle (***Cock et al., 2014***). Indeed, it has been suggested that modifications to homeodomain-based regulatory circuits may have played an important role in the emergence of sporophyte complexity in the green lineage (***Bowman et al., 2016***; ***Lee et al., 2008***). Key events may have included the replacement of the Gsp1-like class of BELL-related1 genes with alternative (true BEL-class) proteins and diversification of both the true BEL-class and the KNOX-class TALE HD TFs. In

particular, the emergence and subfunctionalisation of two KNOX subfamilies early in streptophyte evolution is thought to have facilitated the evolution of more complex sporophyte transcriptional networks (**Furumizu et al., 2015**; **Sakakibara et al., 2013**). In the brown algae, ORO and SAM also function as major developmental regulators but, in this lineage, the emergence of a multicellular sporophyte has not been associated with a marked expansion of the TALE HD TF family. However, there does appear to have been considerable divergence of the ORO and SAM protein sequences during brown algal evolution, perhaps reflecting the evolution of new functions associated with multicellular development and divergence of the sporophyte and gametophyte developmental programs.

Heterodimerisation appears to be a conserved feature of brown algal and green lineage TALE HD TFs (**Figure 4** and **Lee et al., 2008**) despite the lack of domain conservation. However, in *Ectocarpus* heterodimerisation involves the ORO and SAM HDs whereas in *Chlamydomonas*, it is the KNOX1 and KNOX2 domains of Gsm1 that interact with the C-terminal region of Gsp1 (which includes the HD, Ala and DE domains). In *Chlamydomonas*, the Gsp1 and Gsm1 proteins are carried specifically by plus and minus gametes, respectively, so that dimerisation of the two proteins allows the organism to detect syngamy and therefore the transition from a haploid to a diploid state. Based on transcript detection (**Figure 3A**) and genetic analysis (**Supplementary file 1**), *ORO* and *SAM* do not appear to exhibit sex-specific patterns of expression in gametes. This also appears to be the case in *P. patens*, where both the class 2 KNOX proteins MKN1 and MKN6 and the BEL proteins BELL1 and BELL2 are expressed in the egg (**Horst et al., 2016**; **Sakakibara et al., 2013**). It is not known whether these proteins are also expressed in the sperm, although BELL1 appears not to be (**Horst et al., 2016** but see **Ortiz-Ramírez et al., 2017**). Taken together, these observations suggest that novel mechanisms may lead to the activation of TALE HD TF life cycle regulators in groups that have evolved complex multicellularity. In *P. patens*, the glutamate receptor GLR2 may be a component of such a mechanism (**Ortiz-Ramírez et al., 2017**). It is perhaps not unexpected that the recruitment of TALE HD TFs to act as master regulators of complex developmental programs should be associated with a modification of the regulation of these systems themselves. Moreover, modified regulation of these TALE HD TFs may have had advantages in terms of life cycle flexibility. For example, in *Ectocarpus*, it would not be possible to deploy the sporophyte program in parthenogenetic gametes if gamete fusion was strictly required to create an ORO-SAM heterodimer.

Interestingly, diploid sporophytes heterozygous for *sam* mutations exhibited abortive development of unilocular sporangia at a stage corresponding to the meiotic division of the mother cell. At first sight it might seem surprising that a gene should play an important role both directly following the haploid to diploid transition (initiation of sporophyte development) and at the opposite end of the life cycle, during the diploid to haploid transition (meiosis). However, these phenotypes make more sense when viewed from an evolutionary perspective, if the ORO SAM system originally evolved as a global regulator of diploid phase processes.

There is now accumulating evidence for an ancient role for HD TFs in life cycle regulation in both the bikont and unikont branches of the eukaryotic tree of life (**Hedgethorne et al., 2017**; **Horst et al., 2016**; **Hull et al., 2005**; **Lee et al., 2008**; **Sakakibara et al., 2013** and this study). We show here that these systems have been adapted to coordinate life cycle progression and development in at least two multicellular eukaryotic lineages (land plants and brown algae). The recruitment of TALE HD TFs as sporophyte program master regulators in both the brown and green lineages represents a particularly interesting example of latent homology, where the shared ancestral genetic toolkit constrains the evolutionary process in two diverging lineages leading to convergent evolution of similar regulatory systems (**Nagy et al., 2014**). The identification of such constraints through comparative analysis of independent complex multicellular lineages provides important insights into the evolutionary processes underlying the emergence of complex multicellularity. One particularly interesting outstanding question is whether HD TFs also play a role in coordinating life cycle progression and development in animals? Analysis of the functions of TALE HD TFs in unicellular relatives of animals may help provide some insights into this question.

## Materials and methods

### Key resources table

| Reagent type (species) or resource | Designation | Source or reference | Identifiers | Additional information |
|---|---|---|---|---|
| Commercial assay or kit | GoTaq-polymerase | Promega | Promega:M3001 | |
| Commercial assay or kit | Qiagen RNeasy Plant mini kit | Qiagen | Qiagen:74903 | |
| Commercial assay or kit | ImPro-II Reverse Transcription System | Promega | Promega:A3800 | |
| Commercial assay or kit | MagneGST™ Pull-Down System | Promega | Promega:V8870 | |
| Commercial assay or kit | TNT Coupled Wheat Germ Extract System | Promega | Promega:L4130 | |
| Commercial assay or kit | Clarity™ chemiluminescent detection | Biorad | Biorad:1705060S | |
| Chemical compound, drug | Congo red | Sigma | Sigma:C6767-25G | |
| Chemical compound, drug | anti-GST antibody | Ozyme | Ozyme:91G1 | |
| Software, algorithm | RStudio Version 1.1.463 | RStudio | RRID:SCR_000432 | http://www.rstudio.com/ |
| Software, algorithm | GraphPad Prism5 | GraphPad | | http://graphpad.com/scientific-software/prism |
| Software, algorithm | Trimmomatic | Trimmomatic | RRID:SCR_011848 | http://www.usadellab.org/cms/index.php?page=trimmomatic |
| Software, algorithm | Tophat2 | Tophat | RRID:SCR_013035 | https://ccb.jhu.edu/software/tophat/index.shtml |
| Software, algorithm | HTSeq | HTSeq | RRID:SCR_005514 | http://htseq.readthedocs.io/en/release_0.9.1/ |
| Software, algorithm | DESeq2 | Bioconductor | RRID:SCR_015687 | https://bioconductor.org/packages/release/bioc/html/DESeq2.html |
| Software, algorithm | Heatplus package for R | Bioconductor 10.18129/B9.bioc.Heatplus | | http://bioconductor.org/packages/release/bioc/html/Heatplus.html |
| Software, algorithm | ColorBrewer | ColorBrewer project | | http://colorbrewer.org |
| Software, algorithm | Blast2GO | Blast2GO | RRID:SCR_005828 | http://www.blast2go.com/b2ghome |
| Software, algorithm | Hectar | DOI: 10.1186/1471-2105-9-393 | | http://webtools.sb-roscoff.fr/root?tool_id=abims_hectar |
| Software, algorithm | Blast | National Center for Biotechnology Information | | https://blast.ncbi.nlm.nih.gov/Blast.cgi |
| Software, algorithm | HMMsearch | EBI | | https://www.ebi.ac.uk/Tools/hmmer/search/hmmsearch |
| Software, algorithm | GenomeView | GenomeView | RRID:SCR_012968 | http://genomeview.org/ |
| Software, algorithm | MEGA7 | DOI: 10.1093/molbev/msr121 | | https://www.megasoftware.net/ |

*Continued on next page*

*Continued*

| Reagent type (species) or resource | Designation | Source or reference | Identifiers | Additional information |
|---|---|---|---|---|
| Software, algorithm | RAxML | DOI: 10.1002/0471250953.bi0614s51 | RRID:SCR_006086 | https://github.com/stamatak/standard-RAxML |
| Software, algorithm | Jalview | | RRID:SCR_006459 | http://www.jalview.org/ |
| Software, algorithm | WebLogo | | RRID:SCR_010236 | http://weblogo.berkeley.edu |
| Software, algorithm | SPINE-D | DOI: 10.1080/073911012010525022 | | http://sparks-lab.org/SPINE-D/ |
| Software, algorithm | SEG | PMID:7952898 | | http://www.biology.wustl.edu/gcg/seg.html |
| Software, algorithm | PSIPRED | DOI: 10.1093/nar/gkt381 | RRID:SCR_010246 | http://bioinf.cs.ucl.ac.uk/psipred/ |

## Treatment with the sporophyte-produced diffusible factor

Sporophyte-conditioned medium, gametophyte-conditioned medium and protoplasts were produced as previously described (***Arun et al., 2013***). Protoplasts were allowed to regenerate either in sporophyte-conditioned medium supplemented with osmoticum or in gametophyte-conditioned supplemented with osmoticum as a control. Congo red staining was used to distinguish sporophytes from gametophytes (***Arun et al., 2013***). At least 60 individuals were scored per treatment per experiment. Results are representative of three independent experiments.

## Mapping of genetic loci

The *oro* mutation has been shown to behave as a single-locus, recessive, Mendelian factor (***Coelho et al., 2011***). AFLP analysis was carried out essentially as described by ***Vos et al. (1995)***. DNA was extracted from 50 wild type and 50 *oro* individuals derived from a cross between the outcrossing line Ec568 (***Heesch et al., 2010***) and the *oro* mutant Ec494 (***Coelho et al., 2011***; ***Supplementary file 1***). Equal amounts of DNA were combined into two pools, for bulk segregant analysis. Pre-selective amplification was carried out with an *Eco*RI-anchored primer and an *Mse*I-anchored primer, each with one selective nucleotide, in five different combinations (*Eco*RI +T/*Mse*I +G; *Eco*RI +T/*Mse*I +A; *Eco*RI +C/*Mse*I +G; *Eco*RI +C/*Mse*I +A; *Eco*RI +A/*Mse*I +C). These reactions were diluted 1:150 for the selective amplifications. The selective amplifications used an *Eco*RI-anchored primer and an *Mse*I-anchored primer, each with three selective nucleotides, in various different combinations. The PCR conditions for both steps were 94˚C for 30 s, followed by 20 cycles of DNA amplification (30 s at 94˚C, 1 min at 56˚C and 1 min at 72˚C) and a 5 min incubation at 72˚C except that this protocol was preceded by 13 touchdown cycles involving a decrease of 0.7˚C per cycle for the selective amplifications. PCR products were analysed on a LI-COR apparatus. This analysis identified two flanking AFLP markers located at 20.3 cM and 21.1 cM on either side of the *ORO* locus. For 23 (12 *oro* and 11 wild type) of the 100 individuals, no recombination events were detected within the 41.4 cM interval between the two markers. Screening of these 23 individuals (11 wild type and 12 *oro*) with the microsatellite markers previously developed for a sequence-anchored genetic map (***Heesch et al., 2010***) identified one marker within the 41.4 cM interval (M_512) and located the *ORO* locus to near the bottom of chromosome 14 (***Cormier et al., 2017***).

Fine mapping employed a segregating population of 2000 individuals derived from the cross between the outcrossing line Ec568 and the *oro* mutant line (Ec494) and an additional 11 microsatellite markers within the mapping interval (***Supplementary file 7***) designed based on the *Ectocarpus* genome sequence (***Cock et al., 2010***). PCR reactions contained 5 ng of template DNA, 1.5 µl of 5xGoTaq reaction buffer, 0.25 units of GoTaq-polymerase (Promega), 10 nmol $MgCl_2$, 0.25 µl of dimethyl sulphoxide, 0.5 nmol of each dNTP, 2 pmol of the reverse primer, 0.2 pmol of the forward primer (which included a 19-base tail that corresponded to a nucleotide sequence of the M13

bacteriophage) and 1.8 pmol of the fluorescence marked M13 primer. The PCR conditions were 94˚C for 4 min followed by 13 touch-down cycles (94˚C for 30 s, 65–54˚C for 1 min and 72˚C for 30 s) and 25 cycles at 94˚C for 30 s, 53˚C for 1 min and 72˚C for 30 s. Samples were genotyped by electrophoresis on an ABI3130xl Genetic Analyser (Applied Biosystems) followed by analysis with Genemapper version 4.0 (Applied Biosystems). Using the microsatellite markers, the *oro* mutation was mapped to a 34.5 kbp (0.45 cM) interval, which contained five genes. Analysis of an assembled, complete genome sequence for a strain carrying the *oro* mutation (strain Ec597; European Nucleotide Archive PRJEB1869; **Ahmed et al., 2014**) together with Sanger method resequencing of ambiguous regions demonstrated that there was only one mutation within the mapped interval: an 11 bp deletion in the gene with the LocusID Ec-14_005920.

## Reconstruction and sequence correction of the *ORO* and *SAM* loci

The sequence of the 34.5 kbp mapped interval containing the *ORO* gene (chromosome 27, 5463270–5497776) in the wild type *Ectocarpus* reference strain Ec32 included one short region of uncertain sequence 1026 bp downstream of the end of the *ORO* open reading frame. The sequence of this region was completed by PCR amplification and Sanger sequencing and confirmed by mapping Illumina read data to the corrected region. The corrected *ORO* gene region has been submitted to Genbank under the accession number KU746822.

Comparison of the reference genome (strain Ec32) supercontig that contains the *SAM* gene (sctg_251) with homologous supercontigs from several independently assembled draft genome sequences corresponding to closely related *Ectocarpus* sp. strains (**Ahmed et al., 2014**; **Cormier et al., 2017**) indicated that sctg_251 was chimeric and that the first three exons of the *SAM* gene were missing. The complete *SAM* gene was therefore assembled and has been submitted to Genbank under the accession number KU746823.

## Quantitative reverse transcriptase polymerase chain reaction analysis of mRNA abundance

Total RNA was extracted from wild-type gametophytes and partheno-sporophytes (Ec32) and from *sam-1* (Ec374) and *sam-2* (Ec364) partheno-gametophytes using the Qiagen RNeasy Plant mini kit and any contaminating DNA was removed by digestion with Ambion Turbo DNase (Life Technologies). The generation marker genes analysed were Ec-20_001150 and Ec-26_000310 (sporophyte markers), and Ec-23_004240 and Ec-21_006530 (gametophyte markers), which are referred to as *IDW6, IDW7, IUP2* and *IUP7* respectively, in **Peters et al. (2008)**. Following reverse transcription of 50–350 ng total RNA with the ImPro-II TM Reverse Transcription System (Promega), quantitative RT-PCR was performed on a LightCycler 480 II instrument (Roche). Reactions were run in 10 µl containing 5 ng cDNA, 500 nM of each oligo and 1x LightCycler 480 DNA SYBR Green I mix (Roche). The sequences of the oligonucleotides used are listed in **Supplementary file 8**. Pre-amplification was performed at 95˚C for 5 min, followed by the amplification reaction consisting of 45 cycles of 95˚C for 10 s, 60˚C for 30 s and 72˚C for 15 s with recording of the fluorescent signal after each cycle. Amplification specificity and efficiency were checked using a melting curve and a genomic DNA dilution series, respectively, and efficiency was always between 90% and 110%. Data were analysed using the LightCycler 480 software (release 1.5.0). A pair of primers that amplified a fragment which spanned intron 2 of the *SAM* gene was used to verify that there was no contaminating DNA (**Supplementary file 1**-table supplement 8). Standard curves generated from serial dilutions of genomic DNA allowed quantification for each gene. Gene expression was normalized against the reference gene *EEF1A2*. Three technical replicates were performed for the standard curves and for each sample. Statistical analysis (Kruskal-Wallis test and Dunn's Multiple Comparison Post Test) was performed using the software GraphPad Prism5.

## RNA-seq analysis

RNA for RNA-seq analysis was extracted from duplicate samples (two biological replicates) of approximately 300 mg (wet weight) of tissue either using the Qiagen RNeasy plant mini kit with an on-column Deoxyribonuclease I treatment or following a modified version (**Peters et al., 2008**) of the protocol described by **Apt et al. (1995)**. Briefly, this second protocol involved extraction with a cetyltrimethylammonium bromide (CTAB)-based buffer and subsequent phenol-chloroform

purification, LiCl-precipitation, and DNAse digestion (Turbo DNAse, Ambion, Austin, TX, USA) steps. RNA quality and concentration was then analysed on a 1.5% agarose gel stained with ethidium bromide and a NanoDrop ND-1000 spectrophotometer (NanoDrop products, Wilmington, DE, USA). Between 21 and 93 million sequence reads were generated for each sample on an Illumina Hiseq2000 platform (**Supplementary file 9**). Raw reads were quality trimmed with Trimmomatic (leading and trailing bases with quality below three and the first 12 bases were removed, minimum read length 50 bp) (**Bolger et al., 2014**). High score reads were aligned to the *Ectocarpus* reference genome (**Cock et al., 2010**; available at Orcae; **Sterck et al., 2012**) using Tophat2 with the Bowtie2 aligner (**Kim et al., 2013**). The mapped sequencing data was then processed with HTSeq (**Anders et al., 2014**) to obtain counts for sequencing reads mapped to exons. Expression values were represented as TPM and TPM >1 was applied as a filter to remove noise.

Differential expression was detected using the DESeq2 package (Bioconductor; **Love et al., 2014**) using an adjusted p-value cut-off of 0.05 and a minimal fold-change of two. Genes that were differentially expressed in the gametophyte- and sporophyte generations were identified using duplicate RNA-seq datasets for whole gametophytes (GBP-5 and GBP-6, **Supplementary file 9**) and whole sporophytes (GBP-7 and GBP-8, **Supplementary file 9**) that had been grown in parallel under identical culture conditions. Heatmaps were generated using the Heatplus package for R (**Ploner, 2015**) and colour schemes selected from the ColorBrewer project (http://colorbrewer.org).

The entire set of 16,724 protein-coding genes in the *Ectocarpus* Ec32 genome were manually assigned to one of 22 functional categories (**Supplementary file 10**) and this information was used to determine whether sets of differentially expressed genes were enriched in particular functional categories compared to the entire nuclear genome ($\chi^2$ test). Blast2GO (**Conesa and Götz, 2008**) was used to detect enrichment of GO-terms associated with the genes that were consistently up- or downregulated in pairwise comparisons of the wild type gametophyte, the *sam* mutant and the *oro* mutant with the wild type sporophyte. Significance was determined using a Fisher exact test with an FDR corrected p-value cutoff of 0.05. Sub-cellular localisations of proteins were predicted using Hectar (**Gschloessl et al., 2008**). Sets of secreted proteins corresponded to those predicted to possess a signal peptide or a signal anchor.

## Expression of *ORO* and *SAM* during the gametophyte generation

Gametophytes carrying *oro* or *sam* mutations did not exhibit any obvious phenotypic defects, despite the fact that both genes are expressed during this generation (although *SAM* expression was very weak). In *P. patens,* GUS fusion experiments failed to detect expression of KNOX genes in the gametophyte but RT-PCR analysis and cDNA cloning has indicated that KNOX (and BEL) transcripts are expressed during this generation (**Champagne and Ashton, 2001**; **Sakakibara et al., 2013**; **Sakakibara et al., 2008**). However, no phenotypes were detected during the haploid protonema or gametophore stages in KNOX mutant lines (**Sakakibara et al., 2013**; **Sakakibara et al., 2008**; **Singer and Ashton, 2007**) and the RT-PCR only amplified certain regions of the transcripts. Consequently, these results have been interpreted as evidence for the presence of partial transcripts during the gametophyte generation. To determine whether the *ORO* and *SAM* transcripts produced in *Ectocarpus* were incomplete, RNA-seq data from male and female, immature and mature gametophytes was mapped onto the *ORO* and *SAM* gene sequences. This analysis indicated that full-length transcripts of both the *ORO* and *SAM* genes are produced during the gametophyte generation (**Figure 3—figure supplement 1**).

## Detection of protein-protein interactions

Pull-down assays were carried out using the MagneGST™ Pull-Down System (Promega, Madison, WI) by combining human influenza hemagglutinin (HA)-tagged and glutathione S-transferase (GST) fusion proteins. In vitro transcription/translation of HA-tagged ORO proteins was carried out using the TNT Coupled Wheat Germ Extract System (Promega, Madison, WI). GST-tagged SAM proteins were expressed in *Escherichia coli*. Protein production was induced by adding IPTG to a final concentration of 2 mM and shaking for 20 hr at 16˚C. After the capture phase, beads were washed four times with 400 µL of washing buffer (0.5% IGEPAL, 290 mM NaCl, 10 mM KCl, 4.2 mM $Na_2HPO_4$, 2 mM $KH_2PO_4$, at pH 7.2) at room temperature. Beads were then recovered in SDS-PAGE loading buffer, and proteins analysed by SDS-PAGE followed by Clarity™ chemiluminescent detection

(Biorad, Hercules, CA). The anti-HA antibody (3F10) was purchased from Roche, and the anti-GST antibody (91G1) from Ozyme.

## Searches for HD proteins from other stramenopile species

Searches for homeodomain proteins from additional brown algal or stramenopile species were carried out against the NCBI, Uniprot, oneKP (**Matasci et al., 2014**) and iMicrobe databases and against sequence databases for individual brown algal (*Saccharina japonica*, **Ye et al., 2015**; *Cladosiphon okamuranus*, **Nishitsuji et al., 2016**) and stramenopile genomes (*Nannochloropsis oceanica, Aureococcus anophagefferens, Phaeodactylum tricornutum, Thalassiosira pseudonana, Pseudo-nitzschia multiseries*) and transcriptomes (*Vaucheria litorea, Heterosigma akashiwo*) using both Blast (Blastp or tBlastn) and HMMsearch with a number of different alignments of brown algal TALE HD TF proteins. As the homeodomain alone does not provide enough information to construct well-supported phylogenetic trees, searches for ORO and SAM orthologues were based on screening for the presence of the additional protein domains conserved in brown algal ORO and SAM proteins.

As intron position and phase was strongly conserved between the homeoboxes of *ORO* and *SAM* orthologues within the brown algae, this information was also used to search for ORO and SAM orthologues in other stramenopile lineages. However, this analysis failed to detect any additional candidate *ORO* or *SAM* orthologues. These observations are consistent with a similar analysis of plant homeobox introns, which showed that intron positions were strongly conserved in recently diverged classes of homeobox gene but concluded that homeobox introns were of limited utility to deduce ancient evolutionary relationships (**Mukherjee et al., 2009**).

GenomeView (**Abeel et al., 2012**) was used together with publically available genome and RNA-seq sequence data (**Nishitsuji et al., 2016**; **Ye et al., 2015**) to improve the gene models for some of the brown algal TALE HD TFs (indicated in **Supplementary file 6** by adding the suffix 'mod' for modified to the protein identifier).

All the stramenopile species analysed in this study possessed at least two TALE HD TFs, with some species possessing as many as 14 (**Supplementary file 6**). Note that genomes of several diverse stramenopile lineages outside the brown algae were predicted to encode proteins with more than one HD (**Supplementary file 6**). It is possible that these proteins have the capacity to bind regulatory sequences in a similar manner to heterodimers of proteins with single HDs.

## Phylogenetic analysis and protein analysis and comparisons

Multiple alignments were generated with Muscle in MEGA7 (**Tamura et al., 2011**). Phylogenetic trees were then generated with RAxML (**Stamatakis, 2015**) using 1000 bootstrap replicates and the most appropriate model based on an analysis in MEGA7. Domain alignments were constructed in Jalview (http://www.jalview.org/) and consensus sequence logos were generated with WebLogo (http://weblogo.berkeley.edu/logo.cgi). Intrinsic disorder in protein folding was predicted using SPINE-D (**Zhang et al., 2012**), low complexity regions with SEG (default parameters, 12 amino acid window; **Wootton, 1994**) and secondary structure with PSIPRED (**Buchan et al., 2013**).

## ORO and SAM domain structure

The conserved domains that flank the homeodomains in the ORO and SAM proteins share no detectable similarity with domains that are associated with TALE HDs in the green (Viridiplantae) lineage, such as the KNOX, ELK and BEL domains. Interestingly, both the ORO and SAM proteins possess regions that are predicted to be highly disordered (**Figure 5B**). Intrinsically disordered region are a common feature in transcription factors and the flexibility conferred by these regions is thought to allow them to interact with a broad range of partners (**Niklas et al., 2015**), a factor that may be important for master developmental regulators such as the ORO and SAM proteins.

# Acknowledgements

We thank the ABiMS platform (Roscoff Marine Station) for providing computing facilities and support.

# Additional information


## Funding

| Funder | Grant reference number | Author |
|---|---|---|
| Centre National de la Recherche Scientifique | | Alok Arun<br>Susana M Coelho<br>Akira F Peters<br>Simon Bourdareau<br>Laurent Pérès<br>Delphine Scornet<br>Martina Strittmatter<br>Agnieszka P Lipinska<br>Haiqin Yao<br>Olivier Godfroy<br>Gabriel J Montecinos<br>Komlan Avia<br>Nicolas Macaisne<br>Christelle Troadec<br>Abdelhafid Bendahmane<br>J Mark Cock |
| Agence Nationale de la Recherche | ANR-10-BLAN-1727 | J Mark Cock |
| Interreg Program France (Channel)-England | Marinexus | J Mark Cock |
| University Pierre and Marie Curie | | Alok Arun<br>Susana M Coelho<br>Akira F Peters<br>Simon Bourdareau<br>Laurent Pérès<br>Delphine Scornet<br>Martina Strittmatter<br>Agnieszka P Lipinska<br>Haiqin Yao<br>Olivier Godfroy<br>Gabriel J Montecinos<br>Komlan Avia<br>Nicolas Macaisne<br>J Mark Cock |
| European Research Council | 638240 | Susana M Coelho |
| European Commission | European Erasmus Mundus program | J Mark Cock |
| China Scholarship Council | | J Mark Cock |
| Agence Nationale de la Recherche | ANR-10-BTBR-04-01 | J Mark Cock |
| Agence Nationale de la Recherche | ANR-10-LABX-40 | Abdelhafid Bendahmane |
| European Research Council | ERC-SEXYPARTH | Abdelhafid Bendahmane |

The funders had no role in study design, data collection and interpretation, or the decision to submit the work for publication.


## Author contributions

Alok Arun, Formal analysis, Investigation, Writing—review and editing; Susana M Coelho, Formal analysis, Supervision, Funding acquisition, Investigation, Project administration, Writing—review and editing; Akira F Peters, Delphine Scornet, Resources, Investigation, Writing—review and editing; Simon Bourdareau, Laurent Pérès, Martina Strittmatter, Haiqin Yao, Olivier Godfroy, Gabriel J Montecinos, Nicolas Macaisne, Christelle Troadec, Investigation, Writing—review and editing; Agnieszka P Lipinska, Komlan Avia, Formal analysis, Writing—review and editing; Abdelhafid Bendahmane, Resources, Validation, Project administration, Writing—review and editing; J Mark Cock,

Conceptualization, Formal analysis, Supervision, Funding acquisition, Validation, Investigation, Writing—original draft, Project administration, Writing—review and editing


### Author ORCIDs

Susana M Coelho http://orcid.org/0000-0002-9171-2550
Laurent Pérès http://orcid.org/0000-0001-6016-4785
Komlan Avia http://orcid.org/0000-0001-6212-6774
Nicolas Macaisne https://orcid.org/0000-0002-0109-9845
J Mark Cock http://orcid.org/0000-0002-2650-0383



### Decision letter and Author response

Decision letter https://doi.org/10.7554/eLife.43101.079
Author response https://doi.org/10.7554/eLife.43101.080


## Additional files

### Supplementary files

- Supplementary file 1. *Ectocarpus* strains used in this study.
DOI: https://doi.org/10.7554/eLife.43101.011
- Supplementary file 2. Congo red staining of wild type or *sam-1* protoplasts following regeneration in sporophyte-conditioned medium (SCM) or gametophyte-conditioned medium (GCM).
DOI: https://doi.org/10.7554/eLife.43101.012
- Supplementary file 3. Analysis of genes that are differentially expressed in the gametophyte and sporophyte generations.
DOI: https://doi.org/10.7554/eLife.43101.013
- Supplementary file 4. Gene ontology analysis of the gametophyte versus sporophyte differentially regulated genes.
DOI: https://doi.org/10.7554/eLife.43101.014
- Supplementary file 5. Kyoto encyclopaedia of genes and genomes (KEGG) pathway analysis of the gametophyte versus sporophyte differentially regulated genes.
DOI: https://doi.org/10.7554/eLife.43101.015
- Supplementary file 6. TALE homeodomain transcription factors in brown algae and other stramenopiles.
DOI: https://doi.org/10.7554/eLife.43101.016
- Supplementary file 7. New microsatellite markers developed to map the *ORO* gene.
DOI: https://doi.org/10.7554/eLife.43101.017
- Supplementary file 8. Oligonucleotides used for the qRT-PCR analysis.
DOI: https://doi.org/10.7554/eLife.43101.018
- Supplementary file 9. *Ectocarpus* RNA-seq data used in this study.
DOI: https://doi.org/10.7554/eLife.43101.019
- Supplementary file 10. Manual functional assignments and Hectar subcellular targeting predictions for all *Ectocarpus* nucleus-encoded proteins
DOI: https://doi.org/10.7554/eLife.43101.020
- Transparent reporting form
DOI: https://doi.org/10.7554/eLife.43101.021

### Data availability

All the sequencing data that has been generated by or used in this study is described in Supplementary file 9. SRA accession numbers are provided for all samples. Genbank accession numbers for the corrected ORO and SAM genes are provided in the results section.

The following datasets were generated:

| Author(s) | Year | Dataset title | Dataset URL | Database and Identifier |
|---|---|---|---|---|
| Arun A, Coelho SM, Peters AF, Bourdareau S, Pérès L, Scornet D, Strittmatter M, Lipinska AP, Yao H, Godfroy O, Montecinos GJ, Avia K, Macaisne N, Troadec C, Bendahmane A, Cock JM | 2018 | GBP-5 | https://www.ncbi.nlm.nih.gov/sra/SRR5241401 | NCBI Sequence Read Archive, SRR5241401 |
| Arun A, Coelho SM, Peters AF, Bourdareau S, Pérès L, Scornet D | 2018 | GBP-6 | https://www.ncbi.nlm.nih.gov/sra/SRR5241402 | NCBI Sequence Read Archive, SRR5241402 |
| Arun A, Coelho SM, Peters AF, Bourdareau S, Pérès L, Scornet D, Strittmatter M, Lipinska AP, Yao H, Godfroy O, Montecinos GJ, Avia K, Macaisne N, Troadec C, Bendahmane A, Cock JM | 2018 | GPO-32 | https://www.ncbi.nlm.nih.gov/sra/SRR5242540 | NCBI Sequence Read Archive, SRR5242540 |
| Arun A, Coelho SM, Peters AF, Bourdareau S, Pérès L, Scornet D, Strittmatter M, Lipinska AP, Yao H, Godfroy O, Montecinos GJ, Avia K, Macaisne N, Troadec C, Bendahmane A, Cock JM | 2018 | GPO-33 | https://www.ncbi.nlm.nih.gov/sra/SRR5242545 | NCBI Sequence Read Archive, SRR5242545 |
| Arun A, Coelho SM, Peters AF, Bourdareau S, Pérès L, Scornet D, Strittmatter M, Lipinska AP, Yao H, Godfroy O, Montecinos GJ, Avia K, Macaisne N, Troadec C, Bendahmane A, Cock JM | 2018 | GPO-30 | https://www.ncbi.nlm.nih.gov/sra/SRR5242538 | NCBI Sequence Read Archive, SRR5242538 |
| Arun A, Coelho SM, Peters AF, Bourdareau S, Pérès L, Scornet D, Strittmatter M, Lipinska AP, Yao H, Godfroy O, Montecinos GJ, Avia K, Macaisne N, Troadec C, Bendahmane A, Cock JM | 2018 | GPO-31 | https://www.ncbi.nlm.nih.gov/sra/SRR5242539 | NCBI Sequence Read Archive, SRR5242539 |
| Arun A, Coelho SM, Peters AF, Bourdareau S, Pérès L, Scornet D, Strittmatter M, Lipinska AP, Yao H, Godfroy O, Montecinos GJ, Avia K, Macaisne N, | 2018 | GPO-47 | https://www.ncbi.nlm.nih.gov/sra/SRR5242548 | NCBI Sequence Read Archive, SRR5242548 |

| | | | | |
|---|---|---|---|---|
| Troadec C, Bendahmane A, Cock JM | | | | |
| Arun A, Coelho SM, Peters AF, Bourdareau S, Pérès L, Scornet D, Strittmatter M, Lipinska AP, Yao H, Godfroy O, Montecinos GJ, Avia K, Macaisne N, Troadec C, Bendahmane A, Cock JM | 2018 | GPO-48 | https://www.ncbi.nlm.nih.gov/sra/SRR5242549 | NCBI Sequence Read Archive, SRR5242549 |
| Arun A, Coelho SM, Peters AF, Bourdareau S, Pérès L, Scornet D, Strittmatter M, Lipinska AP, Yao H, Godfroy O, Montecinos GJ, Avia K, Macaisne N, Troadec C, Bendahmane A, Cock JM | 2018 | GPO-49 | https://www.ncbi.nlm.nih.gov/sra/SRR5242551 | NCBI Sequence Read Archive, SRR5242551 |
| Arun A, Coelho SM, Peters AF, Bourdareau S, Pérès L, Scornet D, Strittmatter M, Lipinska AP, Yao H, Godfroy O, Montecinos GJ, Avia K, Macaisne N, Troadec C, Bendahmane A, Cock JM | 2018 | GPO-50 | https://www.ncbi.nlm.nih.gov/sra/SRR5242552 | NCBI Sequence Read Archive, SRR5242552 |
| Arun A, Coelho SM, Peters AF, Bourdareau S, Pérès L, Scornet D | 2018 | Corrected ORO gene region | https://www.ncbi.nlm.nih.gov/nuccore/KU746822 | NCBI Genbank, KU746822 |
| Arun A, Coelho SM, Peters AF, Bourdareau S, Pérès L, Scornet D, Strittmatter M, Lipinska AP, Yao H, Godfroy O, Montecinos GJ, Avia K, Macaisne N, Troadec C, Bendahmane A, Cock JM | 2018 | Complete Sam gene | https://www.ncbi.nlm.nih.gov/nuccore/KU746823 | NCBI Genbank, KU746823 |

The following previously published datasets were used:

| Author(s) | Year | Dataset title | Dataset URL | Database and Identifier |
|---|---|---|---|---|
| Macaisne N | 2017 | GBP-3 | https://www.ncbi.nlm.nih.gov/sra/SRR3108628 | NCBI Sequence Read Archive, SRR3108628 |
| Macaisne N, Liu F, Scornet D, Peters AF, Lipinska A, Perrineau M-M, Henry A, Strittmatter M, Coelho SM, Cock JM | 2017 | GBP-4 | https://www.ncbi.nlm.nih.gov/sra/SRR3108629 | NCBI Sequence Read Archive, SRR3108629 |
| Cormier A, Avia K, Sterck L, Derrien T, Wucher V, Andres | 2017 | GBP-7 | https://www.ncbi.nlm.nih.gov/sra/SRR3108630 | NCBI Sequence Read Archive, SRR3108630 |

| | | | | |
|---|---|---|---|---|
| G, Monsoor M, Godfroy O, Lipinska A, Perrineau M-M, Van De Peer Y, Hitte C, Corre E, Coelho SM, Cock JM | | | | |
| Cormier A, Avia K, Sterck L, Derrien T, Wucher V, Andres G, Monsoor M, Godfroy O, Lipinska A, Perrineau M-M, Van De Peer Y, Hitte C, Corre E, Coelho SM, Cock JM | 2017 | GBP-8 | https://www.ncbi.nlm.nih.gov/sra/SRR3108631 | NCBI Sequence Read Archive, SRR3108631 |
| Cormier A, Avia K, Sterck L, Derrien T, Wucher V, Andres G, Monsoor M, Godfroy O, Lipinska A, Perrineau M-M, Van De Peer Y, Hitte C, Corre E, Coelho SM, Cock JM | 2017 | GBP-16 | https://www.ncbi.nlm.nih.gov/sra/SRR3108632 | NCBI Sequence Read Archive, SRR3108632 |
| Cormier A, Avia K, Sterck L, Derrien T, Wucher V, Andres G, Monsoor M, Godfroy O, Lipinska A, Perrineau M-M, Van De Peer Y, Hitte C, Corre E, Coelho SM, Cock JM | 2017 | GBP-17 | https://www.ncbi.nlm.nih.gov/sra/SRR3108633 | NCBI Sequence Read Archive, SRR3108633 |
| Cormier A, Avia K, Sterck L, Derrien T, Wucher V, Andres G, Monsoor M, Godfroy O, Lipinska A, Perrineau M-M, Van De Peer Y, Hitte C, Corre E, Coelho SM, Cock JM | 2017 | GBP-18 | https://www.ncbi.nlm.nih.gov/sra/SRR3108626 | NCBI Sequence Read Archive, SRR3108626 |
| Cormier A, Avia K, Sterck L, Derrien T, Wucher V, Andres G, Monsoor M, Godfroy O, Lipinska A, Perrineau M-M, Van De Peer Y, Hitte C, Corre E, Coelho SM, Cock JM | 2017 | GBP-19 | https://www.ncbi.nlm.nih.gov/sra/SRR3108627 | NCBI Sequence Read Archive, SRR3108627 |
| Ahmed S, Cock JM, Pessia E, Luthringer R, Cormier A, Robuchon M, Sterck L, Peters AF, Dittami SM, Corre E, Valero M, Aury JM, Roze D, Van de Peer Y, Bothwell J, Marais GA, Coelho SM | 2014 | GPO-32 | https://www.ncbi.nlm.nih.gov/sra/SRR5242540 | NCBI Sequence Read Archive, SRR5242540 |
| Ahmed S, Cock JM, Pessia E, Lu- | 2014 | GPO-33 | https://www.ncbi.nlm.nih.gov/sra/SRR5242545 | NCBI Sequence Read Archive, |

| | | | | |
|---|---|---|---|---|
| thringer R, Cormier A, Robuchon M, Sterck L, Peters AF, Dittami SM, Corre E, Valero M, Aury JM, Roze D, Van de Peer Y, Bothwell J, Marais GA, Coelho SM | | | | SRR5242545 |
| Ahmed S, Cock JM, Pessia E, Luthringer R, Cormier A, Robuchon M, Sterck L, Peters AF, Dittami SM, Corre E, Valero M, Aury JM, Roze D, Van de Peer Y, Bothwell J, Marais GA, Coelho SM | 2014 | GPO-30 | https://www.ncbi.nlm.nih.gov/sra/SRR5242538 | NCBI Sequence Read Archive, SRR5242538 |
| Ahmed S, Cock JM, Pessia E, Luthringer R, Cormier A, Robuchon M, Sterck L, Peters AF, Dittami SM, Corre E, Valero M, Aury JM, Roze D, Van de Peer Y, Bothwell J, Marais GA, Coelho SM | 2014 | GPO-31 | https://www.ncbi.nlm.nih.gov/sra/SRR5242539 | NCBI Sequence Read Archive, SRR5242539 |
| Lipinska A, Cormier A, Luthringer R, Peters AF, Corre E, Gachon CMM, Cock JM, Coelho SM | 2015 | GPO-47 | https://www.ncbi.nlm.nih.gov/sra/SRR5242548 | NCBI Sequence Read Archive, SRR5242548 |
| Lipinska A, Cormier A, Luthringer R, Peters AF, Corre E, Gachon CMM, Cock JM, Coelho SM | 2015 | GPO-48 | https://www.ncbi.nlm.nih.gov/sra/SRR5242549 | NCBI Sequence Read Archive, SRR5242549 |
| Lipinska A, Cormier A, Luthringer R, Peters AF, Corre E, Gachon CMM, Cock JM, Coelho SM | 2015 | GPO-49 | https://www.ncbi.nlm.nih.gov/sra/SRR5242551 | NCBI Sequence Read Archive, SRR5242551 |
| Lipinska A, Cormier A, Luthringer R, Peters AF, Corre E, Gachon CMM, Cock JM, Coelho SM | 2015 | GPO-50 | https://www.ncbi.nlm.nih.gov/sra/SRR5242552 | NCBI Sequence Read Archive, SRR5242552 |

## References

**Abeel T**, Van Parys T, Saeys Y, Galagan J, Van de Peer Y. 2012. GenomeView: a next-generation genome browser. *Nucleic Acids Research* **40**:e12. DOI: https://doi.org/10.1093/nar/gkr995, PMID: 22102585

**Ahmed S**, Cock JM, Pessia E, Luthringer R, Cormier A, Robuchon M, Sterck L, Peters AF, Dittami SM, Corre E, Valero M, Aury JM, Roze D, Van de Peer Y, Bothwell J, Marais GA, Coelho SM. 2014. A haploid system of sex determination in the Brown alga *Ectocarpus* sp. *Current Biology* **24**:1945–1957. DOI: https://doi.org/10.1016/j.cub.2014.07.042, PMID: 25176635

**Anders S**, Pyl ST, Huber W. 2014. HTSeq — A Python framework to work with high-throughput sequencing data. *BioRxiv*. DOI: https://doi.org/10.1101/002824

**Apt KE**, Clendennen SK, Powers DA, Grossman AR. 1995. The gene family encoding the fucoxanthin chlorophyll proteins from the Brown alga *macrocystis pyrifera*. *MGG Molecular & General Genetics* **246**:455–464. DOI: https://doi.org/10.1007/BF00290449, PMID: 7891659

**Arun A**, Peters NT, Scornet D, Peters AF, Mark Cock J, Coelho SM. 2013. Non-cell autonomous regulation of life cycle transitions in the model Brown alga *Ectocarpus*. *New Phytologist* **197**:503–510. DOI: https://doi.org/10.1111/nph.12007, PMID: 23106314

**Banham AH**. 1995. An N-Terminal dimerization domain permits homeodomain proteins to choose compatible partners and initiate sexual development in the mushroom *coprinus cinereus*. *The Plant Cell Online* **7**:773–783. DOI: https://doi.org/10.1105/tpc.7.6.773

**Bolger AM**, Lohse M, Usadel B. 2014. Trimmomatic: a flexible trimmer for illumina sequence data. *Bioinformatics* **30**:2114–2120. DOI: https://doi.org/10.1093/bioinformatics/btu170, PMID: 24695404

**Bowman JL**, Sakakibara K, Furumizu C, Dierschke T. 2016. Evolution in the cycles of life. *Annual Review of Genetics* **50**:133–154. DOI: https://doi.org/10.1146/annurev-genet-120215-035227, PMID: 27617970

**Brown JW**, Sorhannus U. 2010. A molecular genetic timescale for the diversification of autotrophic stramenopiles (Ochrophyta): substantive underestimation of putative fossil ages. *PLoS ONE* **5**:e12759. DOI: https://doi.org/10.1371/journal.pone.0012759, PMID: 20862282

**Buchan DW**, Minneci F, Nugent TC, Bryson K, Jones DT. 2013. Scalable web services for the PSIPRED protein analysis workbench. *Nucleic Acids Research* **41**:W349–W357. DOI: https://doi.org/10.1093/nar/gkt381, PMID: 23748958

**Bürglin TR**. 1997. Analysis of TALE superclass homeobox genes (MEIS, PBC, KNOX, iroquois, TGIF) reveals a novel domain conserved between plants and animals. *Nucleic Acids Research* **25**:4173–4180. DOI: https://doi.org/10.1093/nar/25.21.4173, PMID: 9336443

**Champagne CEM**, Ashton NW. 2001. Ancestry of KNOX genes revealed by bryophyte (*physcomitrella patens*) homologs. *New Phytologist* **150**:23–36. DOI: https://doi.org/10.1046/j.1469-8137.2001.00076.x

**Cock JM**, Sterck L, Rouzé P, Scornet D, Allen AE, Amoutzias G, Anthouard V, Artiguenave F, Aury JM, Badger JH, Beszteri B, Billiau K, Bonnet E, Bothwell JH, Bowler C, Boyen C, Brownlee C, Carrano CJ, Charrier B, Cho GY, et al. 2010. The *ectocarpus* genome and the independent evolution of multicellularity in brown algae. *Nature* **465**:617–621. DOI: https://doi.org/10.1038/nature09016, PMID: 20520714

**Cock JM**, Godfroy O, Macaisne N, Peters AF, Coelho SM. 2014. Evolution and regulation of complex life cycles: a Brown algal perspective. *Current Opinion in Plant Biology* **17**:1–6. DOI: https://doi.org/10.1016/j.pbi.2013.09.004, PMID: 24507487

**Cock JM**, Godfroy O, Strittmatter M, Scornet D, Uji T, Farnham G, Peters AF, Coelho SM. 2015. Emergence of *Ectocarpus* as a model system to study the evolution of complex multicellularity in the brown algae. In: Ruiz-Trillo I, Nedelcu A. M (Eds). *Evolutionary Transitions to Multicellular Life*. Dordrecht: Springer. p. 153–162. DOI: https://doi.org/10.1007/978-94-017-9642-2_8

**Coelho SM**, Godfroy O, Arun A, Le Corguille G, Peters AF, Cock JM. 2011. *OUROBOROS* is a master regulator of the gametophyte to sporophyte life cycle transition in the Brown alga *Ectocarpus*. *PNAS* **108**:11518–11523. DOI: https://doi.org/10.1073/pnas.1102274108

**Coelho SM**, Scornet D, Rousvoal S, Peters NT, Dartevelle L, Peters AF, Cock JM. 2012. *Ectocarpus*: a model organism for the Brown algae. *Cold Spring Harbor Protocols* **2012**:pdb.emo065821. DOI: https://doi.org/10.1101/pdb.emo065821, PMID: 22301644

**Conesa A**, Götz S. 2008. Blast2GO: a comprehensive suite for functional analysis in plant genomics. *International Journal of Plant Genomics* **2008**:1–12. DOI: https://doi.org/10.1155/2008/619832

**Cormier A**, Avia K, Sterck L, Derrien T, Wucher V, Andres G, Monsoor M, Godfroy O, Lipinska A, Perrineau MM, Van De Peer Y, Hitte C, Corre E, Coelho SM, Cock JM. 2017. Re-annotation, improved large-scale assembly and establishment of a catalogue of noncoding loci for the genome of the model Brown alga *Ectocarpus*. *New Phytologist* **214**:219–232. DOI: https://doi.org/10.1111/nph.14321, PMID: 27870061

**Eme L**, Sharpe SC, Brown MW, Roger AJ. 2014. On the age of eukaryotes: evaluating evidence from fossils and molecular clocks. *Cold Spring Harbor Perspectives in Biology* **6**:a016139. DOI: https://doi.org/10.1101/cshperspect.a016139

**Furumizu C**, Alvarez JP, Sakakibara K, Bowman JL. 2015. Antagonistic roles for KNOX1 and KNOX2 genes in patterning the land plant body plan following an ancient gene duplication. *PLOS Genetics* **11**:e1004980. DOI: https://doi.org/10.1371/journal.pgen.1004980, PMID: 25671434

**Gschloessl B**, Guermeur Y, Cock JM. 2008. HECTAR: a method to predict subcellular targeting in heterokonts. *BMC Bioinformatics* **9**:393. DOI: https://doi.org/10.1186/1471-2105-9-393, PMID: 18811941

**Hedgethorne K**, Eustermann S, Yang JC, Ogden TEH, Neuhaus D, Bloomfield G. 2017. Homeodomain-like DNA binding proteins control the haploid-to-diploid transition in *dictyostelium*. *Science Advances* **3**:e1602937. DOI: https://doi.org/10.1126/sciadv.1602937, PMID: 28879231

**Heesch S**, Cho GY, Peters AF, Le Corguillé G, Falentin C, Boutet G, Coëdel S, Jubin C, Samson G, Corre E, Coelho SM, Cock JM. 2010. A sequence-tagged genetic map for the Brown alga *Ectocarpus siliculosus* provides large-scale assembly of the genome sequence. *New Phytologist* **188**:42–51. DOI: https://doi.org/10.1111/j.1469-8137.2010.03273.x, PMID: 20456050

**Horst NA**, Katz A, Pereman I, Decker EL, Ohad N, Reski R. 2016. A single homeobox gene triggers phase transition, embryogenesis and asexual reproduction. *Nature Plants* **2**:15209. DOI: https://doi.org/10.1038/nplants.2015.209, PMID: 27250874

**Hull CM**, Boily MJ, Heitman J. 2005. Sex-specific homeodomain proteins Sxi1alpha and Sxi2a coordinately regulate sexual development in *cryptococcus neoformans*. *Eukaryotic Cell* **4**:526–535. DOI: https://doi.org/10.1128/EC.4.3.526-535.2005, PMID: 15755915

**Joo S**, Wang MH, Lui G, Lee J, Barnas A, Kim E, Sudek S, Worden AZ, Lee JH. 2018. Common ancestry of heterodimerizing TALE homeobox transcription factors across metazoa and archaeplastida. *BMC Biology* **16**: 136. DOI: https://doi.org/10.1186/s12915-018-0605-5, PMID: 30396330

**Kämper J**, Reichmann M, Romeis T, Bölker M, Kahmann R. 1995. Multiallelic recognition: nonself-dependent dimerization of the bE and bW homeodomain proteins in *Ustilago maydis*. *Cell* **81**:73–83. DOI: https://doi.org/10.1016/0092-8674(95)90372-0, PMID: 7720075

**Kim D**, Pertea G, Trapnell C, Pimentel H, Kelley R, Salzberg SL. 2013. TopHat2: accurate alignment of transcriptomes in the presence of insertions, deletions and gene fusions. *Genome Biology* **14**:R36. DOI: https://doi.org/10.1186/gb-2013-14-4-r36, PMID: 23618408

**Lee JH**, Lin H, Joo S, Goodenough U. 2008. Early sexual origins of homeoprotein heterodimerization and evolution of the plant KNOX/BELL family. *Cell* **133**:829–840. DOI: https://doi.org/10.1016/j.cell.2008.04.028, PMID: 18510927

**Love MI**, Huber W, Anders S. 2014. Moderated estimation of fold change and dispersion for RNA-seq data with DESeq2. *Genome Biology* **15**:550. DOI: https://doi.org/10.1186/s13059-014-0550-8, PMID: 25516281

**Macaisne N**, Liu F, Scornet D, Peters AF, Lipinska A, Perrineau MM, Henry A, Strittmatter M, Coelho SM, Cock JM. 2017. The *ectocarpus IMMEDIATE UPRIGHT* gene encodes a member of a novel family of cysteine-rich proteins with an unusual distribution across the eukaryotes. *Development* **144**:409–418. DOI: https://doi.org/10.1242/dev.141523, PMID: 28049657

**Matasci N**, Hung LH, Yan Z, Carpenter EJ, Wickett NJ, Mirarab S, Nguyen N, Warnow T, Ayyampalayam S, Barker M, Burleigh JG, Gitzendanner MA, Wafula E, Der JP, dePamphilis CW, Roure B, Philippe H, Ruhfel BR, Miles NW, Graham SW, et al. 2014. Data access for the 1,000 plants (1KP) project. *GigaScience* **3**:17. DOI: https://doi.org/10.1186/2047-217X-3-17, PMID: 25625010

**Mukherjee K**, Brocchieri L, Bürglin TR. 2009. A comprehensive classification and evolutionary analysis of plant homeobox genes. *Molecular Biology and Evolution* **26**:2775–2794. DOI: https://doi.org/10.1093/molbev/msp201, PMID: 19734295

**Nagy LG**, Ohm RA, Kovács GM, Floudas D, Riley R, Gácser A, Sipiczki M, Davis JM, Doty SL, de Hoog GS, Lang BF, Spatafora JW, Martin FM, Grigoriev IV, Hibbett DS. 2014. Latent homology and convergent regulatory evolution underlies the repeated emergence of yeasts. *Nature Communications* **5**:4471. DOI: https://doi.org/10.1038/ncomms5471, PMID: 25034666

**Nasmyth K**, Shore D. 1987. Transcriptional regulation in the yeast life cycle. *Science* **237**:1162–1170. DOI: https://doi.org/10.1126/science.3306917, PMID: 3306917

**Niklas KJ**, Bondos SE, Dunker AK, Newman SA. 2015. Rethinking gene regulatory networks in light of alternative splicing, intrinsically disordered protein domains, and post-translational modifications. *Frontiers in Cell and Developmental Biology* **3**:8. DOI: https://doi.org/10.3389/fcell.2015.00008, PMID: 25767796

**Nishitsuji K**, Arimoto A, Iwai K, Sudo Y, Hisata K, Fujie M, Arakaki N, Kushiro T, Konishi T, Shinzato C, Satoh N, Shoguchi E. 2016. A draft genome of the Brown alga, *Cladosiphon okamuranus*, S-strain: a platform for future studies of 'mozuku' biology. *DNA Research* **23**:561–570. DOI: https://doi.org/10.1093/dnares/dsw039, PMID: 27501718

**Ortiz-Ramírez C**, Michard E, Simon AA, Damineli DSC, Hernández-Coronado M, Becker JD, Feijó JA. 2017. GLUTAMATE RECEPTOR-LIKE channels are essential for chemotaxis and reproduction in mosses. *Nature* **549**: 91–95. DOI: https://doi.org/10.1038/nature23478, PMID: 28737761

**Perrin N**. 2012. What uses are mating types? The "developmental switch" model. *Evolution* **66**:947–956. DOI: https://doi.org/10.1111/j.1558-5646.2011.01562.x, PMID: 22486681

**Peters AF**, Scornet D, Ratin M, Charrier B, Monnier A, Merrien Y, Corre E, Coelho SM, Cock JM. 2008. Life-cycle-generation-specific developmental processes are modified in the *immediate upright* mutant of the brown alga *Ectocarpus siliculosus*. *Development* **135**:1503–1512. DOI: https://doi.org/10.1242/dev.016303, PMID: 18339673

**Ploner A**. 2015. Heatplus: Heatmaps with row and/or column covariates and colored clusters. *R Package Version 2.22.0*.

**Sakakibara K**, Nishiyama T, Deguchi H, Hasebe M. 2008. Class 1 KNOX genes are not involved in shoot development in the moss Physcomitrella Patens but do function in sporophyte development. *Evolution & Development* **10**:555–566. DOI: https://doi.org/10.1111/j.1525-142X.2008.00271.x, PMID: 18803774

**Sakakibara K**, Ando S, Yip HK, Tamada Y, Hiwatashi Y, Murata T, Deguchi H, Hasebe M, Bowman JL. 2013. KNOX2 genes regulate the haploid-to-diploid morphological transition in land plants. *Science* **339**:1067–1070. DOI: https://doi.org/10.1126/science.1230082, PMID: 23449590

**Singer SD**, Ashton NW. 2007. Revelation of ancestral roles of KNOX genes by a functional analysis of physcomitrella homologues. *Plant Cell Reports* **26**:2039–2054. DOI: https://doi.org/10.1007/s00299-007-0409-5, PMID: 17724598

**Stamatakis A**. 2015. Using RAxML to infer phylogenies. *Current Protocols in Bioinformatics* **51**:6.14.1–6.14.6. DOI: https://doi.org/10.1002/0471250953.bi0614s51

**Sterck L**, Billiau K, Abeel T, Rouzé P, Van de Peer Y. 2012. ORCAE: online resource for community annotation of eukaryotes. *Nature Methods* **9**:1041. DOI: https://doi.org/10.1038/nmeth.2242, PMID: 23132114

**Tamura K**, Peterson D, Peterson N, Stecher G, Nei M, Kumar S. 2011. MEGA5: molecular evolutionary genetics analysis using maximum likelihood, evolutionary distance, and maximum parsimony methods. *Molecular Biology and Evolution* **28**:2731–2739. DOI: https://doi.org/10.1093/molbev/msr121, PMID: 21546353

**Van Heeckeren WJ**, Dorris DR, Struhl K. 1998. The mating-type proteins of fission yeast induce meiosis by directly activating mei3 transcription. *Molecular and Cellular Biology* **18**:7317–7326. DOI: https://doi.org/10.1128/MCB.18.12.7317, PMID: 9819418

**Vos P**, Hogers R, Bleeker M, Reijans M, van de Lee T, Hornes M, Frijters A, Pot J, Peleman J, Kuiper M. 1995. AFLP: a new technique for DNA fingerprinting. *Nucleic Acids Research* **23**:4407–4414. DOI: https://doi.org/10.1093/nar/23.21.4407, PMID: 7501463

**Wootton JC**. 1994. Non-globular domains in protein sequences: automated segmentation using complexity measures. *Computers & Chemistry* **18**:269–285. DOI: https://doi.org/10.1016/0097-8485(94)85023-2, PMID: 7952898

**Ye N**, Zhang X, Miao M, Fan X, Zheng Y, Xu D, Wang J, Zhou L, Wang D, Gao Y, Wang Y, Shi W, Ji P, Li D, Guan Z, Shao C, Zhuang Z, Gao Z, Qi J, Zhao F. 2015. *Saccharina* genomes provide novel insight into kelp biology. *Nature Communications* **6**:6986. DOI: https://doi.org/10.1038/ncomms7986, PMID: 25908475

**Zhang T**, Faraggi E, Xue B, Dunker AK, Uversky VN, Zhou Y. 2012. SPINE-D: accurate prediction of short and long disordered regions by a single neural-network based method. *Journal of Biomolecular Structure and Dynamics* **29**:799–813. DOI: https://doi.org/10.1080/073911012010525022, PMID: 22208280

## Discussion and perspectives

The haploid-diploid life cycle of the brown alga *Ectocarpus* is complex (Coelho et al., 2007), involving alternation between two multicellular generations, the gametophyte and the sporophyte. Alternation between life cycle generations has been shown to be under the control of genetic factors. The genetic analysis of two *Ectocarpus* life-cycle mutants, *oro* and *sam*, described in this chapter demonstrated that *ORO* and *SAM* belong to the TALE HD TF gene family, which includes genes that also act as life cycle regulators in green algae and land plants (Arun et al., 2019; Derelle et al., 2007; Lee et al., 2008b; Sakakibara et al., 2013). During the *Ectocarpus* life cycle the ORO and SAM proteins, which are capable of forming a heterodimer in a similar manner to TALE HD TF life cycle regulators in the green lineage (Horst et al., 2016; Lee et al., 2008b), are required for the deployment of the sporophyte program. This similarity between life cycle regulators in brown algae and plants suggests they are derived from a common ancestral system that would therefore date back to early eukaryotic evolution. This is a remarkable conclusion considering that multicellularity evolved independently in these two lineages and that brown algae and land plants have been evolving independently for over a billion years (Eme et al., 2014). Similar systems, with roles in the regulation of life-cycle-related process have been reported in two other groups, the fungi and the social amoebae (Hedgethorne et al., 2017; Hull et al., 2005; Nasmyth and Shore, 1987; van Heeckeren et al., 1998), supporting the conclusion that these genes represent an ancient life cycle regulatory system.

Life cycle alternation in *Ectocarpus* can also be influenced by a non-cell autonomous, diffusible factor that induces gametophyte initial cells (meio-spores) or gametophyte-derived protoplasts to switch to the sporophyte developmental pathway (Arun et al., 2013). However, the nature of the sporophyte-inducing factor and the mechanism by which it mediates the gametophyte-to-sporophyte transition are not clear. The *oro* and *sam* mutations cause the sporophyte generation to be converted into a fully functional gametophyte but experiments involving treatment of protoplasts from these gametophytes with sporophyte-conditioned medium have demonstrated that these gametophyte individuals are not sensitive to the sporophyte-inducing diffusible factor (Arun et al., 2019; Coelho et al., 2011). This lack of sensitivity to the factor was observed with

both *oro* and *sam* mutant lines (Arun et al., 2019; Coelho et al., 2011). These observations suggest that functional *ORO* and *SAM* genes are necessary for the sporophyte-inducing diffusible factor to induce a switch to the sporophyte developmental pathway and therefore that ORO and SAM may act downstream of the factor in the signalling pathway that leads to this switch. One interesting objective for the future would be to investigate the relationship between the sporophyte-inducing factor and ORO/ SAM using the yeast two-hybrid system. To carry out this experiment, we would first need to know the nature of the diffusible factor.

# Chapter V

# Mutations in the *BASELESS* gene affect initial cell fate determination in *Ectocarpus* sp.

The life cycle of the brown alga *Ectocarpus* involves an alternation between two independent generations, the sporophyte and the gametophyte (Cock et al., 2014; Coelho et al., 2007). These two organisms share the same genome but have different morphologies (e.g. cell morphologies, vegetative structures and reproductive structures) and different patterns of initial cell division (Peters et al., 2008). The initial cell division of the sporophyte is symmetrical, in contrast to the asymmetric division observed in the gametophyte (Peters et al., 2008). The symmetrical initial cell division of the sporophyte results in all cells having a basal fate during early development, while the asymmetrical initial cell division in the gametophyte results in the establishment of basal and apical cell fates from the first stages of development (Godfroy et al., 2017). Events in the initial cell therefore play a crucial role in the differentiation of *Ectocarpus* generations since they determine which daughter cells undergo which (generation-specific) developmental program. Similarly, in most flowering plants, asymmetric division of the initial cell plays an important role in establishing the apical (shoot) – basal (root) axis of the mature plant, influencing the shape and early development of the embryo and generating cell-type diversity (Kimata et al., 2019; ten Hove and Heidstra, 2008). In addition, this type of cell division involves movement of the nucleus and other organelles, vacuole enlargement, and microtubule reorganization (Kimata et al., 2016).

There is clear evidence for extrinsic signals that orient or create asymmetries during plant development (Dong et al., 2009). In two well-established systems of polarity-generating families, Rho GTPases of plants (ROPs) and the PIN family of auxin transporters (Feraru and Friml, 2008; Fu et al., 2005; Yang and Fu, 2007), the hormone auxin plays an important role in regulating tissue and organ polarity (Benková et al., 2003; Feraru and Friml, 2008). In plants, auxin is required for embryogenesis (Schmidt et al., 1994), including establishment of the apical-basal axis (Friml, 2003) and bilateral symmetry (Liu et al., 1993), and for the positioning of apical organs (Reinhardt 2000), organ initiation and development. During *Arabidopsis* development, auxin defects in the *gnom* (Shevell et al., 2000; Shevell et al., 1994) and *pin* mutants affect the correct positioning of cell division planes (Dhonukshe et al., 2005). Signals that control animal asymmetric division have been characterised (Goldstein and Macara, 2007; Knoblich, 2008; Zhong and Chia, 2008) but homologs of known animal or fungal cell polarity regulators have not been shown to exist in land plants. However, plants employ a novel molecule, BREAKING OF ASYMMETRY IN THE STOMATAL (BASL), and novel mechanisms to create asymmetries. In asymmetrically dividing stomatal-lineage cells, BASL accumulates as a polarized crescent at the cell periphery before division and then localizes differentially to the nucleus and a peripheral crescent in self-renewing cells and their sisters after division (Dong et al., 2009). Stomata are vital to plant survival (Raven, 2002), their development, which follows the asymmetric division of the initiation cell (meristemoid mother) described above, is negatively regulated by the *YODA (YDA)* gene. Interestingly, this gene had also been identified as a site of mutations that affect early embryo development. Normally, the *Arabidopsis* zygote undergoes an asymmetric cell division to form a small apical cell that develops as an embryo and a large lower cell that develops as a suspensor. *yda* mutants fail to form a suspensor and the embryo incorporates the lower cell lineage (Gray and Hetherington, 2004).

In the brown alga *Fucus,* and in land plants, the zygote cell divides asymmetrically to establish an apical-basal axis (Berger et al., 1994; Bouget et al., 1996; Brownlee and Bouget, 1998). In *Ectocarpus,* asymmetrical initial cell division is normally only observed during the gametophyte generation, but it also occurs in the sporophyte of the *imm* mutant, resulting in a gametophyte-like germination pattern (Peters et al., 2008). Another *Ectocarpus* mutant with a defect in initial

cell division has been identified recently (Godfroy et al. (2017). *distag* (*dis*) mutants fail to develop basal systems (rhizoids in the gametophyte and prostrate filaments in the sporophyte) and their zygotes have disordered microtubule networks, large cell size, altered Golgi structure and mispositioned nuclei and centrioles. This chapter focuses on two *Ectocarpus* mutant strains (*bas-1* and *bas-2*) which exhibit phenotypes very similar to *dis* mutants. The *baseless* (*bas*) mutants fail to develop any of the basal structures normally observed in wild type strains and are affected during both the gametophyte and the sporophyte generations. In *bas* mutants, the initial cells of both gametophyte and sporophyte directly develop as upright filaments, without the formation of a basal system (rhizoid in the gametophyte or prostrate filaments in the sporophyte). The *BAS* gene encodes a protein phosphatase 2A regulatory subunit type B" with EF-hand-domains. The aim of this study was to characterise the *BAS* gene to further our understanding of the molecular mechanisms underlying initial cell division during both the sporophyte and gametophyte generations in *Ectocarpus*.

This chapter is presented in the form of a manuscript that will be submitted for publication. My contribution to this work included the generation of genetic material for the *bas* mutants such as creation of a segregating population from the sporophyte Ec805 (a strain derived from a *bas-1* x *dis-1* cross) for genetic characterization, observation of the phenotypes associated with both *bas-1* and *bas-2* during both the sporophyte and gametophyte generations, and the development of PCR markers for candidate mutations that were then validated using mutant and wild type strains and a small segregating population.

# Mutations in the *BASELESS* gene affect initial cell fate determination in *Ectocarpus* sp.

**Olivier Godfroy[1], Haiqin Yao[1], Akira F. Peters[2], Delphine Scornet[1], Sebastien Colin[1], Nana Kinoshita[3], Chikako Nagasato[3], Taizo Motomura[3], J. Mark Cock[1*], Susana M. Coelho[1*]**

[1]Sorbonne Université, UPMC Univ Paris 06, CNRS, Algal Genetics Group, UMR 8227, Integrative Biology of Marine Models, Station Biologique de Roscoff, CS 90074, F-29688, Roscoff, France. [2]Bezhin Rosko, 29250 Santec, France, [3]Muroran Marine Station, Hokkaido University, Japan

[*]Correspondence: coelho@sb-roscoff.fr; cock@sb-roscoff.fr

Keywords: *BASELESS* gene; cell fate; asymmetric cell division; *Ectocarpus*

## Summary

The first mitotic division of the initial cell is a key event in all multicellular organisms and is usually concomitant with the establishment of major developmental axes and cell fates. The filamentous brown alga *Ectocarpus* has a haploid-diploid life cycle that involves the development of two multicellular generations, the sporophyte and the gametophyte. An earlier analysis showed that *distag* (*dis*) mutants, which lack a functional TBCCd1 protein, exhibit multiple cellular defects during the first division of the initial cell and subsequently fail to produce basal structures (rhizoids and prostrate filaments) during both the sporophyte and the gametophyte generations. Here we show that mutations in the *BASELESS* (*BAS*) gene result in very similar phenotypes to those observed in the *dis* mutants at both the cellular and morphological levels, including cytoskeletal defects during initial cell division and complete loss of basal systems during both generations of the life cycle. Cloning-by-sequencing revealed that *BAS* encodes a type B" regulatory subunit of protein phosphatase 2A. The high level of similarity of the *dis* and *bas* mutant phenotypes suggests that TBCCd1 and PP2A are two essential components of the cellular

machinery that regulates the division of the initial cell and mediates the establishment of basal cell fate in the developing thallus.

## Introduction

In most eukaryotes, the asymmetric division of the zygote is crucial to shaping the early development of the embryo and further developmental patterns of the adult organism (reviewed in Rensing, 2016; Radoeva et al., 2019). In *Arabidopsis thaliana*, for instance, asymmetrical division of the zygote produces the root and shoot cell lineages. The establishment of the zygote polarity is well described and under the control of MAP-kinases and transcription factors (review in Bayer et al 2017 COPB) and asymmetric cell division involves the movement of the nucleus and other organelles, enlargement of the vacuole, and reorganization of microtubules (Kimata et al., 2016).

The mechanisms underlying body pattern formation in multicellular plants and animals are well understood but research has lagged behind for the third most complex group of multicellular eukaryotes, the brown algae. These organisms display a remarkable diversity or morphologies and rival land plants in terms of their complexity and size (Charrier et al., 2012, 2008). The brown algae offer an interesting contrast to animal and plant body plan formation because of their phylogenetic position and the fact that they evolved complex multicellularity independently from those groups. Moreover, body pattern formation is particularly interesting to study in organisms whose life cycles alternate between two generations, the sporophyte and the gametophyte. In brown algae, the two generations are independent and often very distinct morphologically. The same genome, therefore, regulates the set-up of two independent and distinct developmental programs from two different types of initial cells, opening interesting questions on the molecular control of alternation of generations (Arun et al., 2019; Coelho et al., 2011, 2007). Furthermore, gametophytes and sporophytes of brown algae develop from single cells outside of the parent organism, indicating that they likely establish polarity in a cell-autonomous manner, without the involvement of factors delivered from the parental tissues, simplifying the study of polarity, axis establishment and body plan formation.

Investigations using the classical model brown alga *Fucus* have shown that asymmetrical first cell division is driven by apical-basal polarity established within the zygotic cell (Bouget et al., 1998; Goodner and Quatrano, 1993). The daughter cells further divide to produce the apical and basal systems of the alga, the thallus and the rhizoid, respectively (Brownlee and Bouget, 1998). Studies using *Fucus* zygotes have underlined the role of calcium asymmetries, mRNA distribution and position-dependent information from the cell wall (involving an unknown diffusible apoplastic factor) in the determination of the fate of the basal and apical systems (Berger et al., 1994; Bouget et al., 1996; Brownlee and Bouget, 1998).

More recently, *Ectocarpus* has emerged as a suitable model to look at the molecular mechanisms underlying first cell division and impact on body pattern formation in the brown algae and research on this algae has been largely facilitated by existing genetic and genomic tools (Cock et al., 2010; Peters et al., 2004) and the regularity of the first cell division that characterise the early stages of development of both the gametophyte and sporophyte generations. In this organism, the sporophyte generation initiates from a single cell that undergoes a symmetrical initial cell division to produce two daughter cells with similar fates, i.e., both divide to produce the network of filaments that constitutes the basal system, firmly attaching the alga to the substrate (Godfroy et al., 2017; Peters et al., 2008). The apical system (composed of upright filaments) is initiated later in the development of the sporophyte generation, once the basal system is relatively dense. The gametophyte generation, in contrast, exhibits an asymmetrical initial cell division that produces a basal rhizoid cell and an apical cell, the latter further dividing to form the apical system of upright filaments. The upright filaments bear the reproductive structures (plurilocular gametangia, which produce the gametes by mitosis).

Earlier work identified an *Ectocarpus* mutant that does not produce rhizoids (Godfroy et al., 2017). *distag (dis)* mutant gametophytes and sporophytes are unable to develop basal systems (rhizoids in the gametophyte, prostrate filaments in the sporophyte). Consistent with the establishment of polarity before the first cell division, *dis* mutants exhibit a strong phenotype in the initial cell, with disordered microtubule networks (more clusters of microtubules), larger cell size, altered Golgi structure and mispositioned nuclei and centrioles. The cell division plane,

however, is normal and the cellular defects are only observed during the first cell divisions indicating that *DIS* function is specific to the initial cell. *DIS* encodes a Tubulin Binding Cofactor C (TBCC) domain protein of the TBCCd1 class, with conserved roles in the organisation of cellular architecture animal and plants (André et al., 2013; Feldman and Marshall, 2009; Gonçalves et al., 2010).

Here, we report the identification the *BASELESS* (*BAS*) locus in *Ectocarpus*. *baseless* mutants exhibit phenotypes that closely resemble those of *distag* mutants, including an atypical initial cell division that leads to failure to deploy a basal system in the adult organism, abnormal cellular features such as disorganised microtubule cytoskeleton and loss of bipolar germination. *BAS* encodes a protein phosphatase 2A regulatory subunit type B" with EF-hand domains. Together, our results are consistent with BAS playing a key role in initial cell division and basal cell fate determination during both the gametophyte and sporophyte generations of the *Ectocarpus* life cycle.

## Results

### *baseless* mutants lack a basal system during both the sporophyte and gametophyte generations

During the *Ectocarpus* gametophyte generation, the apical/basal axis is established in the initial cell, prior to the first cell division (Godfroy et al., 2017; Peters et al., 2008). The two cells derived from the division of the initial cell develop as two germ tubes, and establish a rhizoid (a basal, root-like organ) and an upright filamentous thallus (an apical, shoot-like organ) (Figure 1). The first cell division of the sporophyte generation, in contrast, produces two daughter cells with similar morphology and equivalent cell fates. These two cells then divide to produce a prostrate filament, which branches to establish the basal system. The basal system firmly attaches the individual to the substrate (Peters et al., 2008). During the sporophyte generation, an extensive, prostrate basal system is first formed, followed by the growth of the apical system whichconsists of upright filaments that grow up into the medium. Reproductive structures (unilocular sporangia in sporophytes and plurilocular gametangia in gametophytes) are produced principally on the

A screen of a large population of individuals mutagenised by ultraviolet (UV) irradiation identified two mutant strains (Ec800 and Ec801; Table S1) that failed to develop any of the basal structures normally observed during either the gametophyte or the sporophyte generation of wild type strains. Initial cells of Ec800 and Ec801 gametophytes immediately developed as apical upright filament cells and no rhizoid cells were produced. Similarly, during the sporophyte generation, neither mutant strain produced the network of prostrate filaments typical of the wild type sporophyte and, instead, the first divisions of the sporophyte initial cell directly produced an upright filament (Figure 1).

In wild-type *Ectocarpus*, secondary rhizoids, which are analogous to the adventitious roots produced from the stems of some land plants (Atkinson et al 2014), are produced from apical upright filament cells at a late stage of development (Peters et al., 2008). The Ec800 and Ec801 mutants did not produce secondary rhizoids during either the sporophyte or the gametophyte generations (Figure 1). Hence, production of all basal, attachment structures, both primary and secondary, was abolished in these mutants. Taking into account these phenotypes, the Ec800 and Ec801 mutants were named *baseless-1* (*bas-1*) and *baseless-2* (*bas-2*).

The establishment of reproductive structures on apical systems in both the gametophyte and sporophyte generations was unaffected, and the mutants were fully fertile after three weeks in culture (Figure 1).

**_bas_ mutants exhibit reduced bipolar germination compared with wild type strains**

In wild type *Ectocarpus*, the majority of the initial cells (91%) of the sporophyte generation exhibit a bipolar pattern of germination, with two germ tubes emerging from opposite poles of the initial cell (Figure 1U; Peters et al., 2008). In contrast, only 21% of the initial cells of *bas-1* sporophytes exhibited this bipolar pattern of germination, the remaining 79% undergoing unipolar germination (Figure 1U). The proportion of the *bas-1* sporophytes that exhibited a bipolar germination pattern (Fig. 1U) produced one or more enlarged and abnormally shaped cells at the extremity where the second germ tube would normally emerge, possibly

corresponding to an aborted basal system (Figure 1O). Similar phenotypes were observed for *bas-2* sporophytes (not shown).

### *bas-1* and *bas-2* resemble *dis* mutants but are unaffected in the *DIS* gene

The phenotypes of *bas-1* and *bas-2* strongly resembled that of the *dis* mutant (Godfroy et al., 2017). The *dis* mutant also fails to produce any basal structures, during both the sporophyte and gametophyte generations, and lacks secondary rhizoids, again during both generations. Sporophytes resulting from crosses between the *bas-1* strain Ec800 and strains carrying either the *dis-1* or *dis-2* allele had wild type phenotypes (Figure S1), indicating complementation and therefore that the *DIS* gene was not mutated in the *bas-1* mutants.

### Disorganisation of the microtubule cytoskeleton in *bas* mutant initial cells

Mutations at the *DIS* locus strongly affect the organisation of the microtubule cytoskeleton (Godfroy et al., 2017). Because of the similarity between the morphological phenotypes of *bas* and *dis* mutants, we investigated the distribution of the microtubule network during early development of *bas* mutants compared with wild type germlings (Figure 2). The microtubule cytoskeleton was markedly disorganised in the *bas* mutants, with supernumerary microtubule filaments and an overall disordered network. However, we did not detect any abnormalities in terms of the positioning of the cell division plane, all mutants *bas* initial cells produced a cell division plane perpendicular to the growing axis (Figure 1U).

### Genetic analysis and identification of the *BAS* gene

Sporophytes can be cultivated through multiple asexual generations via the production of mito-spores (Figure 1). The Bas$^{-}$ mutant phenotype was stable through 10 rounds of asexual generations via mito-spores.

A male *bas-1* gametophyte (strain Ec800) was crossed with a wild-type outcrossing female gametophyte (strain Ec568; (Coelho et al., 2011; Peters et al., 2008) (Supplemental Table 1 and Figure S1)). The resulting sporophyte (Ec805) exhibited a wild type pattern of development, indicating that the *bas-1* mutation was recessive. A segregating population of 38 individuals derived from this cross consisted of 16 and 22 phenotypically wild-type and mutant individuals, respectively, consistent with a 1:1 segregation ratio and Mendelian inheritance of a single-locus recessive mutation ($\chi 2$ test = 0.947, df = 1, P value = 0.330) (Table S4).

**_BAS_ encodes a protein phosphatase 2A type B" regulatory subunit**

A cloning-by-sequencing approach (see methods for details) identified a candidate locus on chromosome 21 for the location of the *bas-1* and *bas-2* mutations (Figure 3). Whole genome resequencing (WGS) was carried out for the Ec800 and Ec801 mutants and the data compared to the wild type *Ectocarpus* sp. Ec32 reference genome. More than 41,000 putative variants were detected for each mutant. Those variants were compared to a list of 567,532 variants called during the analysis of 14 other mutant lines that showed a range of different phenotypes. This approach allowed the identification of 827 and 769 variants that were unique to the Ec800 and Ec801 mutants, respectively. Quality filtering of those variants (see methods for details) resulted in 118 putative mutations for the Ec800 and Ec801 strains, respectively, corresponding to one mutation every 1.7 to 3 Mb of genome. Of these 185 putative mutations, 26 and 15 were in coding regions (CDS) (22%) in Ec800 and Ec801, respectively. Two single nucleotide transitions affected the same gene (*Ec-21_001770*): a transition from T to C at position 2,806,985 was identified in the *bas-1* mutant (strain Ec800) and a G to A transition at position 2,807,321 in the *bas-2* mutant (strain Ec801) (Figure 3).

The *Ec-21_001770* gene encodes a protein of 646 amino-acids similar to protein phosphatase 2A regulatory subunit type B" proteins. This polypeptide contains three predicted functional domains: a disordered region between positions 50 to 185 and two EF-hand domains at positions 280 to 370 and 380 to 550. The *bas-1* mutation affects the first EF-hand, replacing the positively charged lysine residue with a negatively charged glutamic acid (K302E). This modification of electric charge may disrupt domain folding and/or function. The *bas-2* mutant carries a non-sense

mutation that creates a premature stop codon at position 190 of the protein. This mutation is predicted to result in the production of a truncated protein that lacks EF-hand domains (Figure 3).

**Analysis of *BAS* expression during the *Ectocarpus* life cycle**

RNA-seq data (Bourdareau, 2018; Coelho et al., 2011; Godfroy et al., 2017; Macaisne et al., 2017) were analysed to investigate *BAS* gene expression during the *Ectocarpus* life cycle. *BAS* transcripts were detected throughout development, during both the gametophyte and sporophyte generations (Figure 4). The *BAS* transcript was most abundant at the gamete stage, just before germination of the gametes, but was also abundant during the first three cell divisions of the partheno-sporophyte (Figure 4A). This pattern of expression is consistent with a role of BAS in the early divisions of the initial cells of the partheno-sporophyte generation. Note that it is currently not possible to extract RNA from early stage gametophytes, precluding the possibility to study gene expression at this stage of development.

The strikingly similar phenotypes of *dis* and *bas* mutants suggest that the products of the two genes may play roles in common cellular processes. If this is the case, we reasoned that loss of one of the genes might lead to an alteration of the expression pattern of the other. However, analysis of previously generated *dis* RNA-seq data (Godfroy et al., 2017) indicated to investigate the expression of *BAS* in a *dis* background. This analysis showed that the presence of a mutation at the *dis* locus had no effect on expression of the *BAS* gene (Figure 4B). The *immediate upright* mutant also affects the phenotype of the basal system, although the phenotype is specific to the sporophyte generation, where the extensive basal system is converted to a rhizoid-like structure. We therefore also tested whether the *imm* mutation had any effect on the expression of the *BAS* gene. Figure 2B shows that there was no significant difference in *BAS* transcript abundance in *imm* partheno-sporophytes compared to the wild type.

**Discussion**

The two *Ectocarpus* mutants identified in this study, *bas-1* and *bas-2*, lack basal systems during both the gametophyte and the sporophyte generations of the life cycle. Analysis of initial cells of

*bas* mutant sporophytes showed that the morphological phenotype was associated with several cellular anomalies during germination and the first cell division, including disorganisation of the microtubule network, an increase in the number of microtubule bundles and unipolar, rather than bi-polar, germination patterns.

Very similar morphological and cellular phenotypes were observed for *dis* mutant strains (Godfroy et al., 2017) suggesting that *BAS* and *DIS* may be involved in similar cellular processes. *DIS* is predicted to encode a TBCCd1 protein (Godfroy et al., 2017) whereas *BIS* is predicted to encode a PP2A regulatory B" subunit (Figure 3).

TBCCd1 shares similarity with TBCC, which is a component of the complex (TBCA to TBCE) that mediates dimerisation of α and β tubulin subunits to form microtubules (Tian et al., 1996; Nithianantham et al., 2015). However, TBCCd1 lacks a conserved arginine residue that is essential for TBCC activity and is unable to complement TBCC in yeast indicating that the two proteins may have different biochemical functions (Gonçalves et al., 2010). TBCCd1 has been localized to both the centrosome and the Golgi in humans, *Chlamydomonas*, and trypanosomes and there is evidence that TBCCd1 plays important roles in positioning organelles within the cells of these diverse organisms (Feldman and Marshall, 2009; André et al., 2013; Gonçalves et al., 2010). However, the molecular mechanisms underlying these cellular phenotypes are unclear and they may not involve direct effects on microtubule assembly (Gonçalves et al., 2010).

PP2A phosphatases are involved in diverse cellular processes and constitute a major component of cellular serine/threonine phosphatase activity, dephosphorylating several hundred cellular substrates (Wlodarchak and Xing, 2016; Reynhout and Janssens, 2019). In animals, for example, PP2A, together with PP1, accounts for more than 90% of cellular serine/threonine phosphatase activity. PP2A phosphatases are protein complexes and are usually composed of three subunits, a catalytic C subunit, a scaffolding A subunit and a regulatory B subunit (Wlodarchak and Xing, 2016). Most species have multiple forms of each subunit and there are four distinct classes of the B subunit (B/B55/PR55, B′/B56/PR61, B″/PR72 and B‴/Striatin), which are unrelated at the sequence level. The BAS protein is predicted to belong to the B" class. In animals PP2A has been

implicated in the reorganization of several cellular structures. For example, during mitosis PP2A plays key roles in nuclear envelope breakdown, rearrangement of intracellular organelles such as the endoplasmic reticulum and the Golgi apparatus and events during chromosome segregation through effects on assembly of the mitotic spindle and attachment of cytoplasmic microtubules to kinetochores (reviewed in Wlodarchak and Xing, 2016 and Wurzenberger and Gerlich, 2011). In the land plant *Arabidopsis,* a PP2A regulatory B" subunit, FASS/TON2, is essential for the reorganisation of cortical microtubular arrays into a dense preprophase band preceding cell division (Spinner et al. 2012). FASS-containing PP2A complexes are targeted to microtubules through an association with TONNEAU1 (TON1) and TON1-recruiting motif protein (TRM) (Spinner et al. 2012).

Therefore both TBCCd1 and PP2A have been linked to cytoskeleton function and both proteins have been shown to play important roles in the regulation of cellular architecture in diverse eukaryotic systems. These observations are consistent with the pleiotropic cellular phenotypes of both the *dis* and *bas* mutants. We suggest that the observed morphological and cell fate (loss of basal cells) phenotypes of the *bas* and *dis* mutants are a consequence of cellular defects during the first cell division, perhaps through disruption of the distribution of hypothetical cell-fate-determining factors during this critical step of development (see model proposed by Godfroy et al., 2017). Further analysis of the biochemical functions of BAS and DIS will be necessary to test this hypothesis.

## Methods

### UV Mutagenesis and isolation of mutant strains

Strain cultivation, genetic crosses, raising of sporophytes from zygotes, and isolation of meiotic families were performed as described previously (Coelho et al., 2012a, 2012d, Godfroy et al 2017). *Ectocarpus* sp. gametes are able to develop parthenogenically to produce haploid partheno-sporophytes, which are identical morphologically to the sporophytes that develop from diploid zygotes (Peters et al., 2008; Coelho et al., 2011). This phenomenon was exploited to screen directly, in a haploid population, for mutants affected in early sporophyte development.

UV mutagenesis of gametes was performed as described previously (Coelho et al., 2011; Godfroy et al., 2017, 2015) and mutant partheno-sporophytes lacking basal structures were identified by visual screening under a light microscope.

**Genetic analysis of bas mutants**

Genetic crosses were performed as in Coelho et al., 2012. The *bas-1* mutant (Ec800) was crossed with the outcrossing line Ec568 to generate a segregating population of 38 individuals. Each of the 38 individuals was derived from a different unilocular sporangium (each unilocular sporangium contains 50–100 meio-spores, derived from single meiosis followed by at least five mitotic divisions). The meio-spores germinated to produce gametophytes, which were isolated and allowed to produce gametes which germinated parthenogenically. The resulting partheno-sporophytes were then observed under a light microscope to determine whether they exhibited the $Bas^{-}$ phenotype.

**Identification of candidate mutations**

Genomic DNA from Ec800 and Ec801 strains was sequenced on an Illumina HiSeq4000 platform ($1/12^{th}$ lane; 2x150nt paired-end; 8.5 and 7.95 Gbp of data respectively; Fasteris, Switzerland). After quality cleaning using the Trimmomatic (Bolger et al., 2014), the reads were mapped onto the *Ectocarpus* sp. reference genome (Cormier et al., 2017) using Bowtie2 (Langmead and Salzberg, 2012). Coverage depth and breadth were, respectively, 34x and 96.83% for Ec800 and 32x and 96.81% for Ec801 (Table S1). Variants were called and counted using bcftools mpileup (http://samtools.github.io/). These variants were compared with a list of variants identified in genome sequence data for 14 other *Ectocarpus* mutant lines in order to remove false positive mutations due, for example, to errors in the reference genome sequence. Variants unique to strains Ec800 and Ec801 were quality filtered based on coverage depth (±50% of the genome mean), mapping quality (>20), and variant quality (>50), variant frequency (>0.9) and variant support in both sequencing directions. A home-made python script allowed the identification of

variants in coding regions (CDS) and the effect of each CDS mutation on the predicted protein was accessed manually. A schema of the approach is used depicted in Figure S2.

**Electron Microscopy Analysis of Cellular Ultrastructure**

Medium containing mature *bas* partheno-sporophytes was pipetted onto a plastic film (gel support films; ATTO). The film was cut into <1-cm side triangles, and these were attached to Petri dishes by adhesive tape. Two days after the release of mitospores from plurilocular sporangia, the resulting germlings, which were attached to the triangles, were rapidly immersed in liquid propane cooled to −180°C by liquid nitrogen, and immediately transferred into liquid nitrogen. The samples were submerged in substitution solution containing 2% osmium tetroxide with acetone at −80°C for 2 d, at −40°C for 2 h, and at 4°C for 2 h. Finally, the temperature of the samples was gradually allowed to rise to room temperature, and they were then washed with acetone several times. The gel support films were infiltrated and embedded in Spurr's low-viscosity resin (Polysciences) on aluminium foil dishes. The films with the samples were turned inside out on the upper surface of the resin. Serial sections were cut with a diamond knife on an Ultracut ultramicrotome (Reichert-Jung) and mounted on Formvar-coated slot grids. Sections were stained with TI blue (Nisshin EM) and lead citrate and observed using an electron microscope (JEM-1011; JEOL).

**Immunostaining**

*Ectocarpus* samples were processed as described by Coelho et al. (2012b) using a protocol adapted from Bisgrove and Kropf (1998). Briefly, *Ectocarpus* cells were settled on cover slips and at appropriate times after settlement were rapidly frozen in liquid nitrogen and fixed in 2.5% glutaraldehyde and 3.2% paraformaldehyde for 1 h, then washed in PBS and treated with 5% triton overnight. Samples were then rinsed in PBS and 100 mM $NaBH_4$ was added for 4 h. Cell walls were degraded with cellulase (1% w/v) and hemicellulase (4% w/v) for 1 h, and the preparation was then rinsed with PBS and blocked overnight in 2.5% non-fat dry milk in PBS. Samples were treated with an anti-tubulin antibody (1/200th, DM1A; Sigma-Aldrich) at 20°C overnight and then treated with the secondary antibody (AlexaFluor 488-conjugated goat anti-

mouse IgG; Sigma-Aldrich; 1:1000 in PBS) at 20°C overnight. The preparation was rinsed with PBS and blocked overnight in 2.5% non-fat dry milk in PBS and then treated with an anti-centrin antibody (1/1000th anticentrin 1 ab11257; Abcam) at 20°C overnight, followed by the secondary antibody (1/1000th AlexaFluor 555-conjugated goat anti-rabbit IgG; Sigma-Aldrich) for 8 h. Samples were stained with 4′,6-diamidino-2-phenylindole (DAPI; 0.5 µg/mL in PBS) for 10 min at room temperature and mounted in ProLong Gold (Invitrogen).

**Confocal Microscopy**

Confocal microscopy was conducted using an inverted SP8 laser scanning confocal microscope (Leica Microsystems) equipped with a compact supply unit which integrates a LIAchroic scan head, several laser lines (405 and 488 nm), and standard photomultiplier tube detectors. We used the oil immersion lens HC PL APO 63×/1.40 OIL CS2. The scanning speed was set at 400 Hz unidirectional. The pinhole was adjusted to one Airy unit for all channels. The spatial sampling rate was optimized according to Niquist criteria, generating a 0.058 × 0.058 × 0.299-µm voxel size (xyz). The Z-stack height fitted the specimen thickness. A two-step sequential acquisition was designed to collect the signal from three or four channels. The first step recorded the anti-tubulin fluorescence signal (excitation, 488 nm; emission, 530 nm) and the transmitted light. The second step acquired the DAPI fluorescence signal (excitation, 405 nm; emission, 415–480 nm). Signal intensity was averaged three times. The Fiji software was used to optimize the raw images, including maximum intensity projection and de-noising (3*3 median filter). For any given data, both wild-type and mutant images were analysed simultaneously with similar settings.

**Acknowledgements**

This work was supported by the CNRS, Sorbonne Université and the ERC (grant agreement 638240). HY was supported by a grant from the China Scholarship Council (grant number 201608310119).

**References**

André, J., Harrison, S., Towers, K., Qi, X., Vaughan, S., McKean, P.G., Ginger, M.L., 2013. The tubulin cofactor C family member TBCCD1 orchestrates cytoskeletal filament formation. J Cell Sci 126, 5350-5356.

Arun, A., Coelho, S.M., Peters, A.F., Bourdareau, S., Pérès, L., Scornet, D., Strittmatter, M., Lipinska, A.P., Yao, H., Godfroy, O., 2019. Convergent recruitment of TALE homeodomain life cycle regulators to direct sporophyte development in land plants and brown algae. eLife 8, e43101.

Atkinson, J.A., Rasmussen, A., Traini, R., Voss, U., Sturrock, C., Mooney, S.J., Wells, D.M., Bennett, M.J., 2014. Branching Out in Roots: Uncovering Form, Function, and Regulation. Plant Physiology 166, 538-550.

Bayer, M., Slane, D., Juergens, G., 2017. Early plant embryogenesis—dark ages or dark matter? Current opinion in plant biology 35, 30-36.

Berger, F., Taylor, A., Brownlee, C., 1994. Cell fate determination by the cell wall in early *Fucus* development. Science 263, 1421-1423.

Bisgrove, S.R., Kropf, D.L., 1998. Alignment of Centrosomal and Growth Axes Is a Late Event during Polarization of *Pelvetia compressa* Zygotes. Developmental biology 194, 246-256.

Bolger, A.M., Lohse, M., Usadel, B., 2014. Trimmomatic: a flexible trimmer for Illumina sequence data. Bioinformatics 30, 2114-2120.

Bouget, F.-Y., Berger, F., Brownlee, C., 1998. Position dependent control of cell fate in the *Fucus* embryo: role of intercellular communication. Development 125, 1999-2008.

Bouget, F.-Y., Gerttula, S., Shaw, S.L., Quatrano, R.S., 1996. Localization of actin mRNA during the establishment of cell polarity and early cell divisions in *Fucus* embryos. The Plant Cell 8, 189-201.

Bourdareau, S., 2018. Genetic and epigenetic control of life cycle transitions in the brown alga *Ectocarpus* sp. Sorbonne Université.

Brownlee, C., Bouget, F.-Y., 1998. Polarity determination in *Fucus*: From zygote to multicellular embryo, Seminars in cell & developmental biology. Elsevier, pp. 179-185.

Charrier, B., Coelho, S.M., Le Bail, A., Tonon, T., Michel, G., Potin, P., Kloareg, B., Boyen, C., Peters, A.F., Cock, J.M., 2008. Development and physiology of the brown alga *Ectocarpus siliculosus*: two centuries of research. New Phytol 177, 319-332.

Charrier, B., Le Bail, A., de Reviers, B., 2012. Plant Proteus: brown algal morphological plasticity and underlying developmental mechanisms. Trends in Plant Science 17, 468-477.

Cock, J.M., Sterck, L., Rouze, P., Scornet, D., Allen, A.E., Amoutzias, G., Anthouard, V., Artiguenave, F., Aury, J.M., Badger, J.H., Beszteri, B., Billiau, K., Bonnet, E., Bothwell, J.H., Bowler, C., Boyen, C., Brownlee, C., Carrano, C.J., Charrier, B., Cho, G.Y., Coelho, S.M., al., e., 2010. The *Ectocarpus* genome and the independent evolution of multicellularity in brown algae. Nature 465, 617-621.

Coelho, S.M., Godfroy, O., Arun, A., Le Corguillé, G., Peters, A.F., Cock, J.M., 2011. *OUROBOROS* is a master regulator of the gametophyte to sporophyte life cycle transition in the brown alga *Ectocarpus*. Proceedings of the National Academy of Sciences 108, 11518-11523.

Coelho, S.M., Scornet, D., Rousvoal, S., Peters, N., Dartevelle, L., Peters, A.F., Cock, J.M., 2012a. Genetic crosses between *Ectocarpus* strains. Cold Spring Harbor Protocols 2012, pdb. prot067942.

Coelho, S.M., Scornet, D., Rousvoal, S., Peters, N., Dartevelle, L., Peters, A.F., Cock, J.M., 2012b. Immunostaining of *Ectocarpus* cells. Cold Spring Harb Protoc 2012, 369-372.

Coelho, S.M., Scornet, D., Rousvoal, S., Peters, N.T., Dartevelle, L., Peters, A.F., Cock, J.M., 2012c. How to cultivate *Ectocarpus*. Cold Spring Harb Protoc 2012, 258-261.

Coelho, S.M.B., Brownlee, C., Bothwell, J.H.F., 2007. A tip-high, $Ca^{2+}$-interdependent, reactive oxygen species gradient is associated with polarized growth in *Fucus* serratus zygotes. Planta 227, 1037-1046.

Cormier, A., Avia, K., Sterck, L., Derrien, T., Wucher, V., Andres, G., Monsoor, M., Godfroy, O., Lipinska, A., Perrineau, M.M., 2017. Re‐annotation, improved large‐scale assembly and establishment of a catalogue of noncoding loci for the genome of the model brown alga *Ectocarpus*. New Phytologist 214, 219-232.

Feldman, J.L., Marshall, W.F., 2009. *ASQ2* encodes a TBCC-like protein required for mother-daughter centriole linkage and mitotic spindle orientation. Current biology 19, 1238-1243.

Godfroy, O., Peters, A.F., Coelho, S.M., Cock, J.M., 2015. Genome-wide comparison of ultraviolet and ethyl methanesulphonate mutagenesis methods for the brown alga *Ectocarpus*. Mar Genomics 24 Pt 1, 109-113.

Godfroy, O., Uji, T., Nagasato, C., Lipinska, A.P., Scornet, D., Peters, A.F., Avia, K., Colin, S., Mignerot, L., Motomura, T., Cock, J.M., Coelho, S.M., 2017. DISTAG/TBCCd1 is required for basal cell fate determination in *Ectocarpus*. The Plant Cell 29, 3102-3122.

Gonçalves, J., Nolasco, S., Nascimento, R., Fanarraga, M.L., Zabala, J.C., Soares, H., 2010. TBCCD1, a new centrosomal protein, is required for centrosome and Golgi apparatus positioning. EMBO reports 11, 194-200.

Goodner, B., Quatrano, R.S., 1993. *Fucus* embryogenesis: A model to study the establishment of polarity. The Plant Cell 5, 1471.

Kimata, Y., Higaki, T., Kawashima, T., Kurihara, D., Sato, Y., Yamada, T., Hasezawa, S., Berger, F., Higashiyama, T., Ueda, M., 2016. Cytoskeleton dynamics control the first asymmetric cell division in *Arabidopsis* zygote. Proceedings of the National Academy of Sciences 113, 14157-14162.

Langmead, B., Salzberg, S.L., 2012. Fast gapped-read alignment with Bowtie 2. Nature methods 9, 357.

Macaisne, N., Liu, F., Scornet, D., Peters, A.F., Lipinska, A., Perrineau, M.M., Henry, A., Strittmatter, M., Coelho, S.M., Cock, J.M., 2017. The *Ectocarpus IMMEDIATE UPRIGHT* gene encodes a member of a novel family of cysteine-rich proteins with an unusual distribution across the eukaryotes. Development 144, 409-418.

Nithianantham, S., Le, S., Seto, E., Jia, W., Leary, J., Corbett, K.D., Moore, J.K., Al-Bassam, J., 2015. Tubulin cofactors and Arl2 are cage-like chaperones that regulate the soluble αβ-tubulin pool for microtubule dynamics. Elife 4, e08811.

Peters, A.F., Marie, D., Scornet, D., Kloareg, B., Mark Cock, J., 2004. Proposal of *Ectocarpus siliculosus* (Ectocarpales, Phaeophyceae) as a model organism for brown algal genetics and genomics 1, 2. Journal of Phycology 40, 1079-1088

Peters, A.F., Scornet, D., Ratin, M., Charrier, B., Monnier, A., Merrien, Y., Corre, E., Coelho, S.M., Cock, J.M., 2008. Life-cycle-generation-specific developmental processes are modified in the *immediate upright* mutant of the brown alga *Ectocarpus siliculosus*. Development 135, 1503-1512.

Radoeva, T., Vaddepalli, P., Zhang, Z., Weijers, D., 2019. Evolution, Initiation, and Diversity in Early Plant Embryogenesis. Developmental cell 50, 533-543.

Rensing, S.A., 2016. (Why) does evolution favour embryogenesis? Trends in plant science 21, 562-573.

Reynhout, S., Janssens, V., 2019. Physiologic functions of PP2A: Lessons from genetically modified mice. Biochimica et Biophysica Acta (BBA)-Molecular Cell Research 1866, 31-50.

Spinner, L., Gadeyne, A., Belcram, K., Goussot, M., Moison, M., Duroc, Y., Eeckhout, D., De Winne, N., Schaefer, E., Van De Slijke, E., 2013. A protein phosphatase 2A complex spatially controls plant cell division. Nature communications 4, 1863.

Tian, G., Huang, Y., Rommelaere, H., Vandekerckhove, J., Ampe, C., Cowan, N.J., 1996. Pathway leading to correctly folded β-tubulin. Cell 86, 287-296.

Wlodarchak, N., Xing, Y., 2016. PP2A as a master regulator of the cell cycle. Critical reviews in biochemistry and molecular biology 51, 162-184.

Wurzenberger, C., Gerlich, D.W., 2011. Phosphatases: providing safe passage through mitotic exit. Nature reviews Molecular cell biology 12, 469.

**Figure legends**

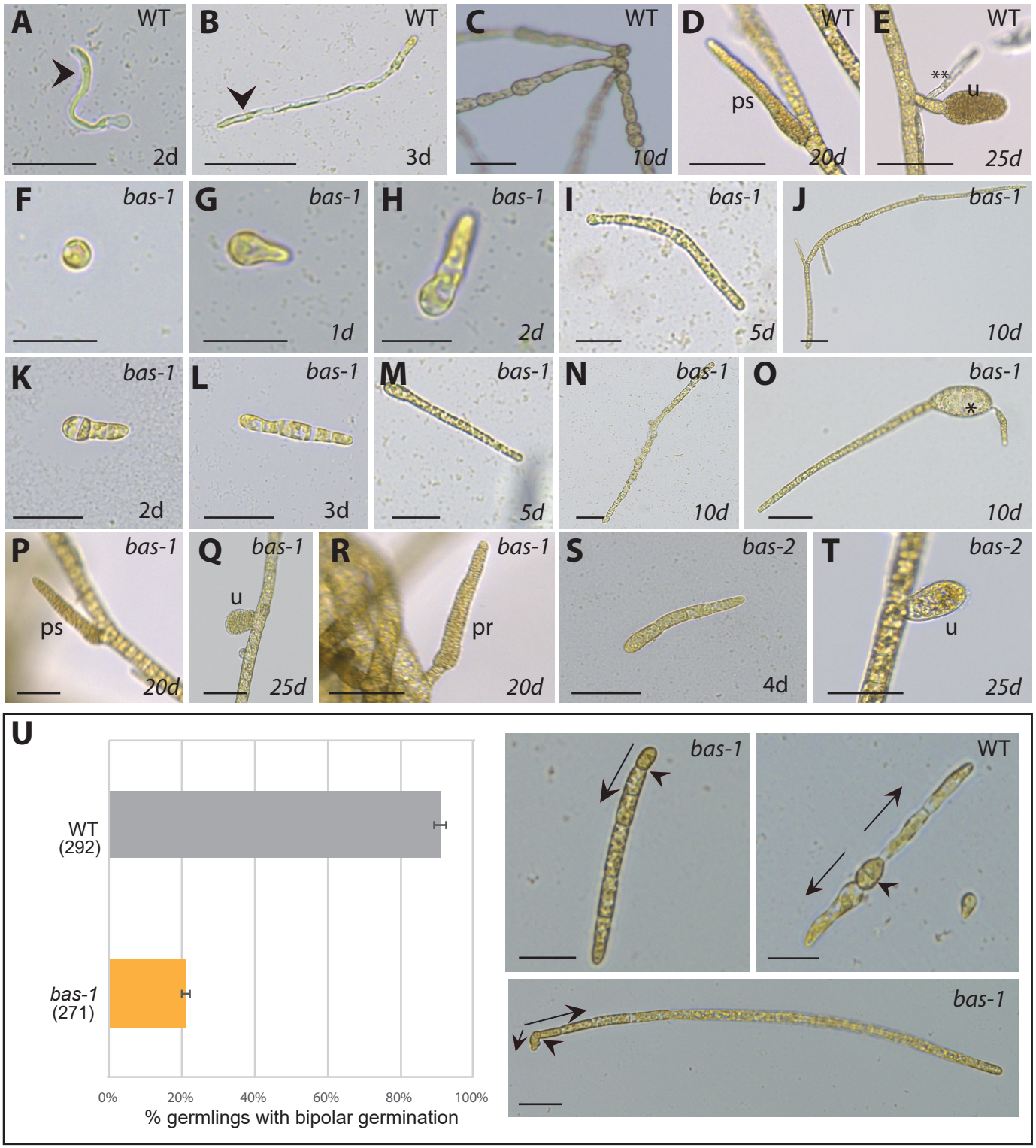


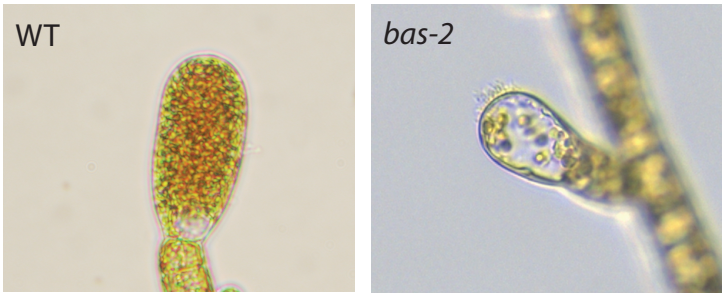

**Figure 1. Phenotypes of *bas* mutants.** A) Wild type gametophyte germling, the arrowhead indicates the rhizoid cell (basal structure). B) Three day-old wild type gametophyte, the arrowhead indicates the rhizoid. C) Wild type sporophyte generation composed of round prostrate filaments firmly attached to the substrate. D) Wild type plurilocular sporangium containing mitotic spores, produced after 20 days in culture. E) Wild type unilocular sporangium (where meiosis takes place) produced after 25 days in culture. A secondary rhizoid is indicated by **. (F-J) Development of the gametophyte generation of the *bas-1* mutant. (K-N) Development of the sporophyte generation of *bas-1* mutant. O) Occasionally, the mutant strains produced enlarged, abnormal cells (asterisk). P) Plurilocular sporangium on a *bas-1* mutant sporophyte. Q) Unilocular sporangium on a *bas-1* mutant sporophyte. R) Plurilocular gametangium on a fertile *bas-1* gametophyte. S) Initial cell division of a *bas-2* gametophyte. T) Unilocular sporangium on a mature *bas-2* sporophyte (about 3 weeks after initial cell germination). U) Proportions of 10 day-old *bas-1* and wild type germlings that exhibited unipolar germination. Plots represent the mean and SE of five replicate cultures, the total number of germlings scored are indicated in brackets. The photographs are of representative *bas-1* and wild type (WT) germlings, exhibiting uni- (one arrow) or bi-polar (two arrows) germination, respectively. Arrows indicate the direction of germination. Note that, in the *bas-1* mutant, following the first cell division, one of the daughter cells continues to divide to produce an upright filament but division of the other daughter cell is arrested. Arrowheads indicate the cell division plane, which is perpendicular to the growth axis both in the bas mutants and in the wild type. ps, plurilocular sporangium; pg, plurilocular gametangium; u, unilocular sporangium. Scale bars=20 um.

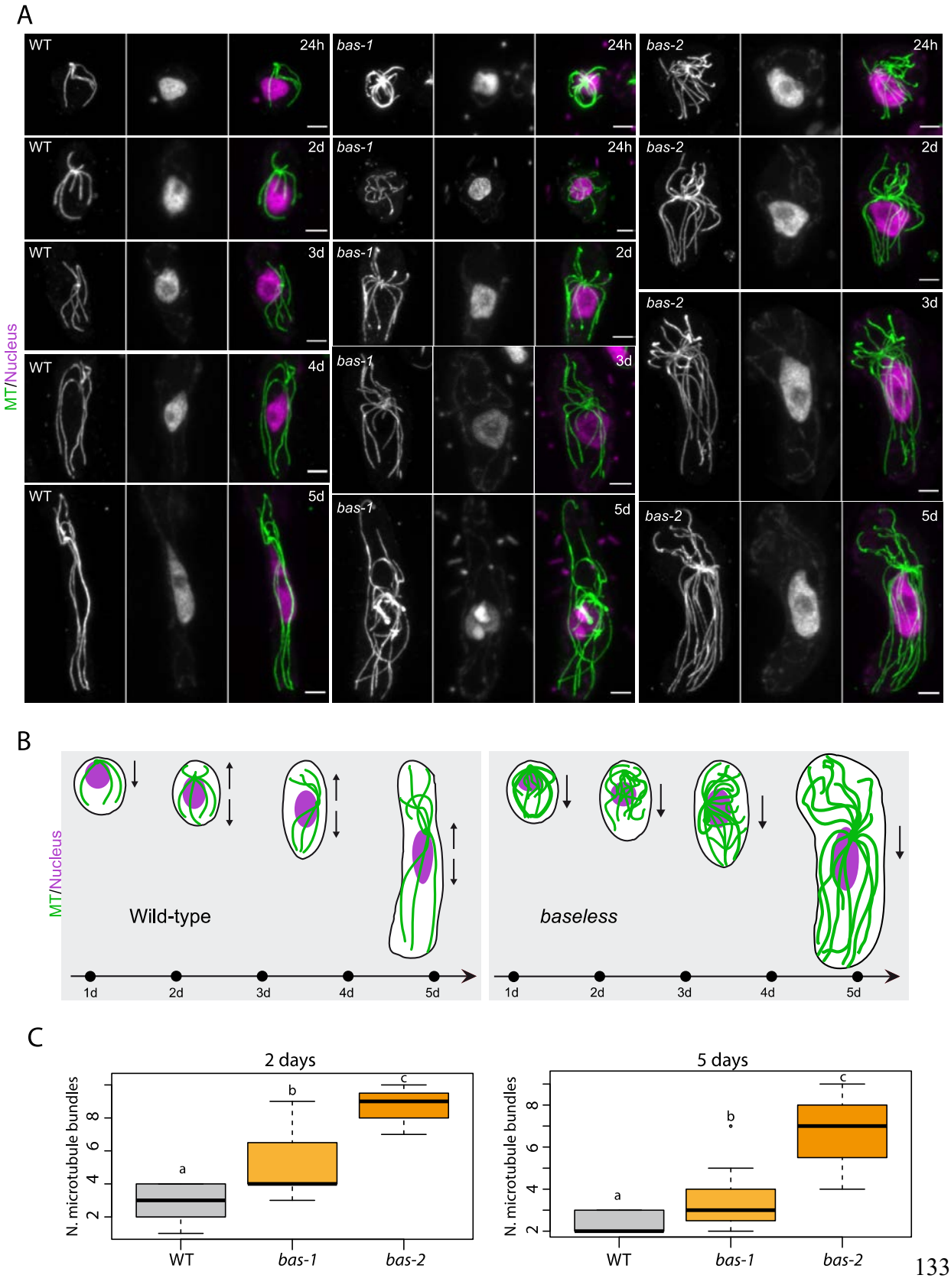
A
WT
bas-1
bas-2
24h
2d
3d
4d
5d
MT/Nucleus
B
MT/Nucleus
Wild-type
baseless
1d
2d
3d
4d
5d
C
2 days
5 days
N. microtubule bundles
a
b
c
WT
bas-1
bas-2

**Figure 2. The organization of the microtubule cytoskeleton is affected in *bas* mutant germinating cells.** A) Confocal maximum z-projections showing representative cells of wild type, *bas-1*, and *bas-2* partheno-sporophytes (derived from mito-spores) at several stages of early development (24h, 2-5 days). Microtubules (MT) were immunostained with an anti-tubulin antibody (green). Nuclear DNA was counterstained with DAPI (mauve). Microtubule (MT) bundles were wavy and more abundant in both *bas-1* and *bas-2* mutant cells compared with the wild type during the germination of the initial cell. B) Cartoons summarising the stages shown in A) in wild type and *bas* mutants. C) Number of microtubule bundles during germination in wild type (WT), *bas-1* and bas-2 mutants at 2 days and 5 days of germination of the initial cell of the sporophyte generation. Number of bundles were counted.

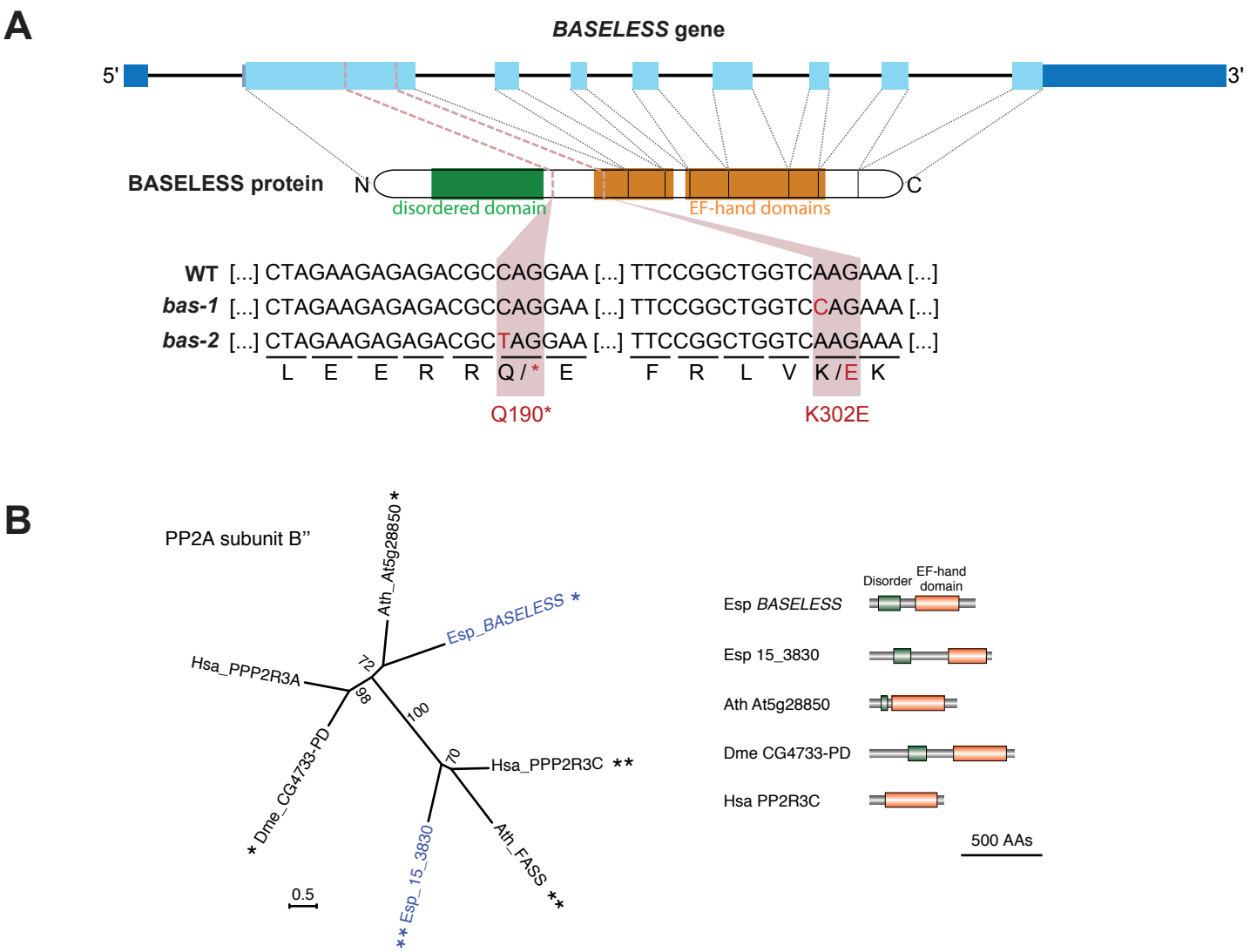
A
BASELESS gene
5'
3'
BASELESS protein
N
C
disordered domain
EF-hand domains
WT [...] CTAGAAGAGAGACGCCAGGAA [...] TTCCGGCTGGTCAAGAAA [...]
bas-1 [...] CTAGAAGAGAGACGCCAGGAA [...] TTCCGGCTGGTCCAGAAA [...]
bas-2 [...] CTAGAAGAGAGACGCTAGGAA [...] TTCCGGCTGGTCAAGAAA [...]
L E E R R Q / * E F R L V K / E K
Q190*
K302E
B
PP2A subunit B"
Ath_At5g28850 *
Esp_BASELESS *
Hsa_PPP2R3A
Hsa_PPP2R3C **
* Dme_CG4733-PD
** Esp_15_3830
Ath_FASS **
0.5
Disorder
EF-hand domain
Esp BASELESS
Esp 15_3830
Ath At5g28850
Dme CG4733-PD
Hsa PP2R3C
500 AAs
PP2A subunit B
* Ath_PP2AB2
Esp_06_8320 *
* Hsa_PPP2R2B
Nca_NCAS0B05510
* Dme_tws
Sce_CDC55 *
0.1
PP2A subunit B'
Esp_25_3320
Esp_03_3760 *
Ec-14_0006
Tgo_BN1205_005480
Ath_At3g26020
Sce_YOR014Wp-like *
* Ath_At3g09880
Hsa_PPP2R5D
Dme_wrd *
Hsa_PPP2R5E *
1.0
PP2A subunit A
* Esp_12_3710
Esp_14_6920
Sce_TPD3
* Ath_At3g25800
Hsa_PP2R1B
PP2A subunit C
Ath_PP2A4 *
Esp_07_6920
Ath_PP2A1
* Esp_23_0740
Dme_mts *
Hsa_PPP2CA *
* Sce_PPH22

**Figure 3. Identification of mutations in the *BAS* gene and identification of protein phosphate 2A subunits in *Ectocarpus*.** A) Diagram showing the domain structure of the *BAS* gene, indicating the positions of the *bas-1* and *bas-2* mutations. The point mutation in exon 2 in *bas-1* results a lysine (K) being replaced with a glutamate (E) residue, whereas the point mutation in *bas-2* results in the introduction of a stop codon into the coding region of the gene (represented by an asterisk). Dark-blue boxes represent untranslated regions, and light-blue indicates protein-coding exons. B) *Ectocarpus* protein phosphatase 2A subunits. Unrooted maximum likelihood trees of PPA2A subunits (LG+G model). Only bootstrap (1000 repetitions) values of >50 are shown. *Ectocarpus* proteins are shown in blue. Asterisks and double asterisks indicate best species-to-species reciprocal Blastp matches with the *Ectocarpus* protein. The *Ectocarpus* genome does not encode an orthologue of PP2A subunit B'''/striatin. The domain structures of five PP2A subunit B'' proteins are shown with the EF-hand domains in brown and disordered domains in green. AA, amino acid; Esp, *Ectocarpus* sp.; Tgo, *Toxoplasma gondii*; Ath, *Arabidopsis thaliana*; Hsa, *Homo sapiens*; Dme, *Drosophila melanogaster*; Sce, *Sccharomyces cerevisiae*; Nca, *Naumovozyma castelli*. *Ectocarpus* locus ID are abbreviated as in the following example: *Esp_14_3830*, *Ectocarpus* sp. *Ec-15_003830*.

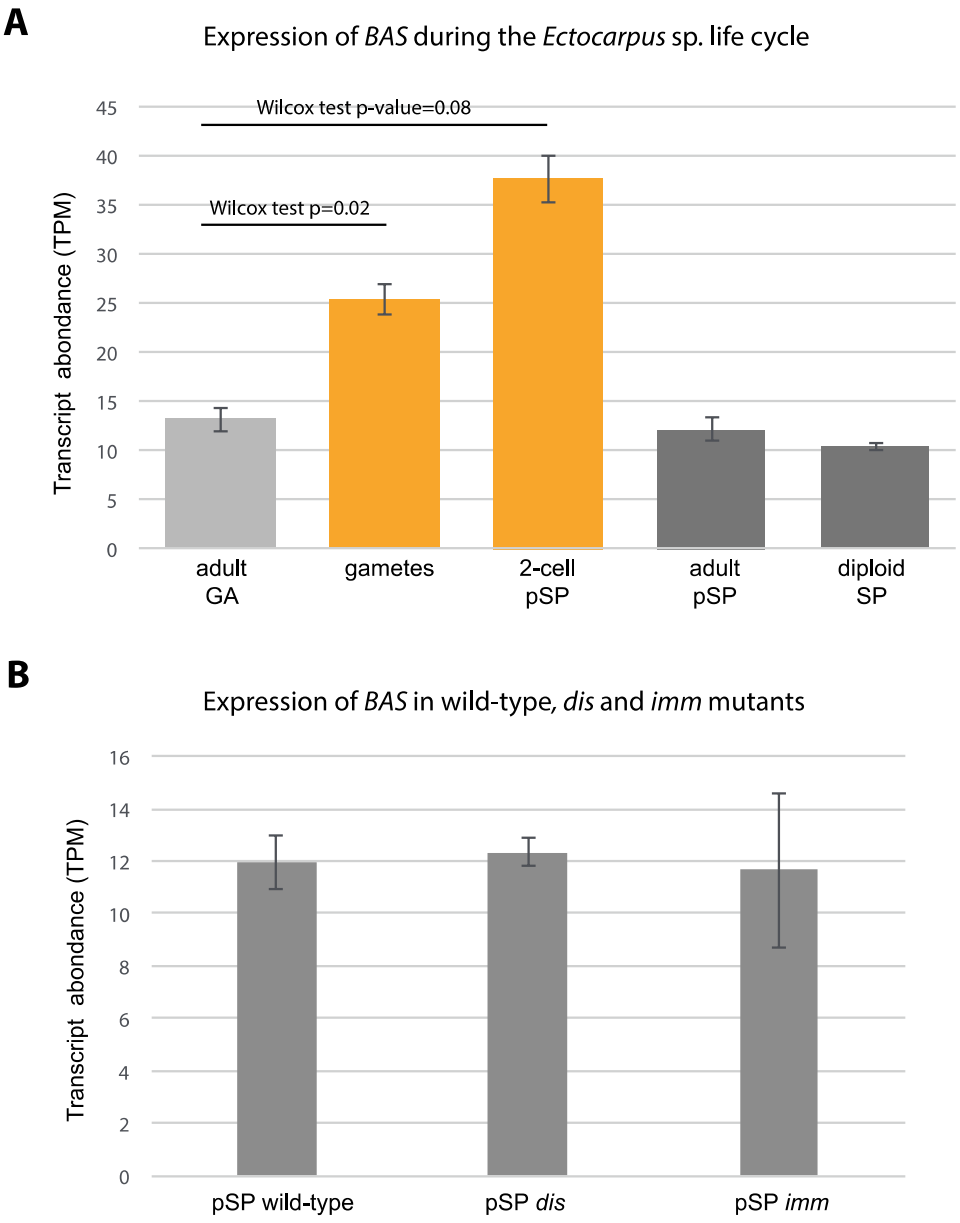


**Figure 4. Abundance of the BAS transcript (measured as transcripts per million, TPM) during the life cycle of *Ectocarpus* and in developmental mutants.** A) BAS transcript abundance during several developmental stages of the sporophyte and gametophyte generations of wild type *Ectocarpus* sp.. Note the increased abundance of the BAS transcript in gametes and during the early stages of sporophyte development. GA: gametophyte, pSP: partheno-sporophyte; SP: diploid sporophyte. Significant differences in expression (pairwise Wilcoxon test) are indicated above the plots. *=*p*-value<0.05, **=*p*-value<0.005. B) Abundance of the BAS transcript in wild type partheno-sporophytes compared with *distag* (*dis*) and *immediate upright* (*imm*) mutants. The plots were generated by averaging the TPMs of several developmental stages of wild-type, *dis* and *imm* partheno-sporophytes.

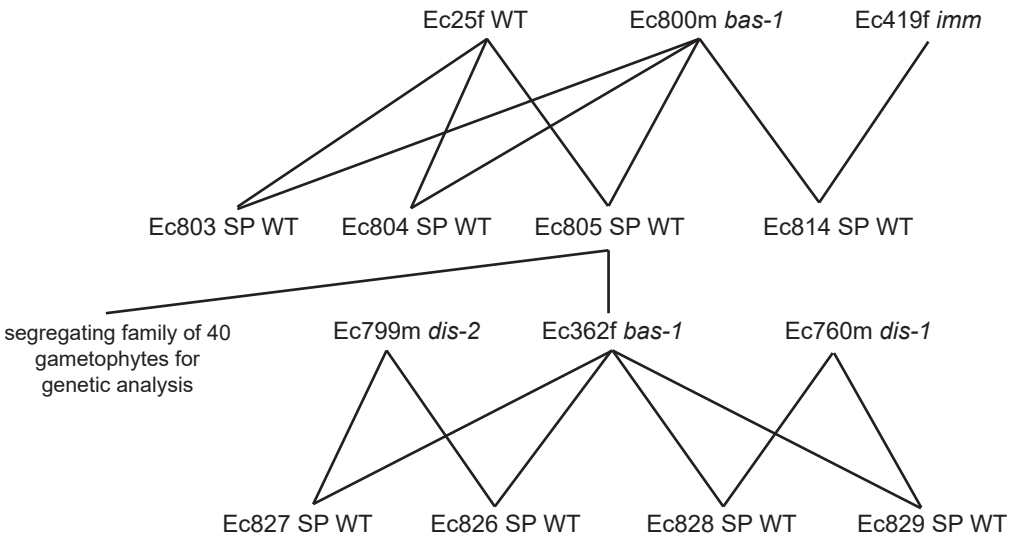


**Figure S1. Pedigree of the *Ectocarpus* strains used in this study.** SP, diploid, hybrid sporophyte; WT, wild type; m, male; f, female.

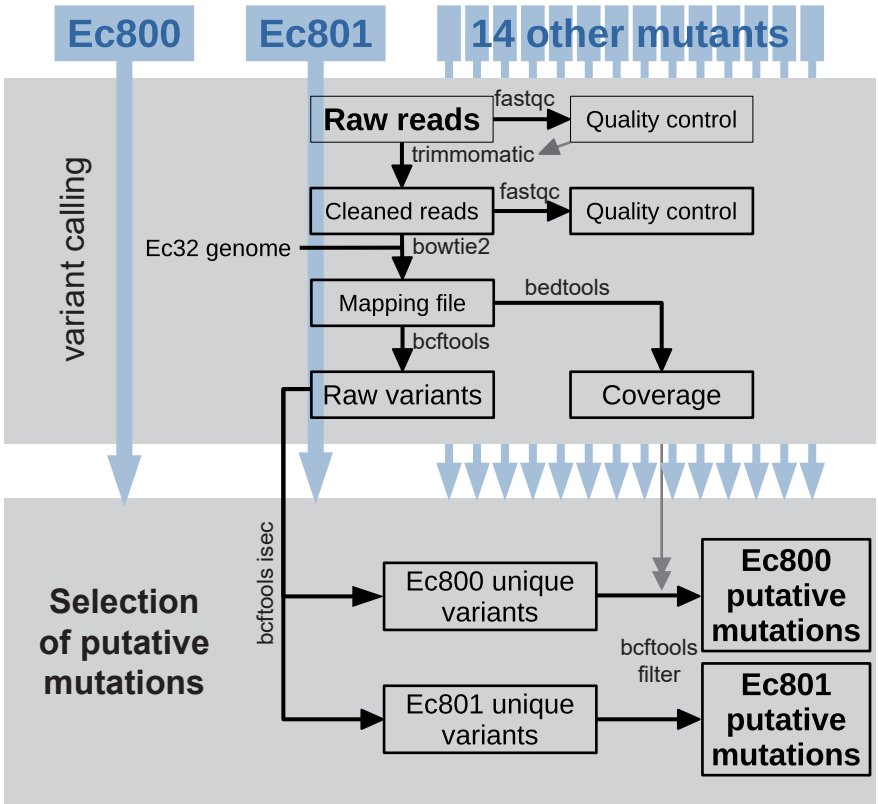


**Figure S2. Schematic diagram of the approach used to detect putative mutations in the genomes of Ec800 and Ec801.**

## Discussion and perspectives

*Ectocarpus bas* mutants lack basal systems during the early stage development of both the gametophyte and the sporophyte generations. The phenotypes of the two allelic forms (*bas1* and *bas2*) were characterised in this chapter revealing that their microtubules were disorganised, that they had supernumerary microtubules and that they exhibited unipolar instead of bipolar generation. Candidate mutations were identified by whole genome sequencing genomic, revealing that the two mutants were affected in the same gene. The protein encoded by *BAS* therefore plays a key role in initial cell division and basal cell fate determination during the two generations of the *Ectocarpus*.

The similarity between the phenotypes of *bas* and *dis* mutants suggest that the two genes may act in similar cellular processes. A third mutant, *imm*, also exhibits defects during initial cell division, involving convertion from asymmetric to symmetric division and resulting in the apical cell immediately developing as an upright filament. The abundance of the *BAS* transcript was not affected in *dis* or *imm* mutants, suggesting that BAS may act upstream of DIS and IMM in the same pathway or that BAS acts in a different pathway to DIS or IMM.

The *BAS* gene encodes a protein phosphatase 2A regulatory subunit type B" with EF-hand ($Ca^{2+}$-binding) domains. EF-hand-containing proteins are ubiquitous in eukaryotes, consistent with $Ca^{2+}$ being involved in many developmental processes (Day et al., 2002; Michiels et al., 2002). Hazak et al. (2019) reported that auxin induces specific $Ca^{2+}$ signalling patterns and that these patterns are spatially consistent with the expression pattern of auxin-related genes in *Arabidopsis* roots. These observations emphasise the functions of EF-hand $Ca^{2+}$-binding proteins as transducers of auxin-regulated gene expression linked to cell fate determination in plants. Calcium also acts as a secondary messenger in the CLV3/CLV1 signal transduction system, which controls gene expression and stem cell fate in the shoot apical meristem of *Arabidopsis* (Chou et al., 2016). Finally, calcium is involved in cellular pathways in the zygote of the brown alga *Fucus*, where it plays a crucial role in cell signalling during embryogenesis and in the response to stress (Coelho et al., 2008; Coelho et al., 2002; Quatrano, 1997).

In the *bas* mutants, the absence of the basal system is undoubtedly caused by an atypical initial cell division. In *dis* mutants, the cell division plane is normal and the cellular phenotype (disordered microtubule cytoskeleton) was only observed during the initial cell division. Furthermore, the absence of a basal system in both the sporophyte and gametophyte generations of the life cycle, suggests that *BAS*, like *DIS*, has a specific function during the initial cell division and plays a crucial role in basal system formation during the two generations of the *Ectocarpus* life cycle. The atypical initial cell divisions observed in both *bas* and *dis* mutants may be a result of disorganization of the microtubule cytoskeleton given that the microtubule cytoskeleton functions in cell division, trafficking, and cell morphogenesis. In addition, a protein phosphatase 2A (PP2A) with the B" regulatory subunit (similar to that encoded by *BAS*) specifically promotes microtubule branching nucleation in *Arabidopsis* (Kirik et al., 2012). In animals, PP2A/Bα, a major protein PP2A holoenzyme, binds to and dephosphorylates tau, and regulates microtubule stability (Sontag et al., 2012). Taken together, these observations indicate that basal cell fate determination is intrinsically linked to the microtubule cytoskeleton.

The phenotype of *bas* mutants is similar to that of the *dis* mutants but we only investigated the microtubule distribution at the cellular level during the initial cell division. In the future, it would be interesting to investigate the structure of Golgi, the position of nuclei and centrioles to further compare with *dis* mutant phenotypes. Moreover, further genetic analyses could be implemented to investigate the functional relationship between *BAS* and *DIS*.

# Chapter VI

# General Discussion and Perspectives

**Regulation of life cycle alternation**

Genetic characterisation (described in Chapter IV) revealed that two TALE homeodomain transcription factors regulate the transition from the gametophyte to the sporophyte generation in *Ectocarpus* (Arun et al., 2019). Homeodomain or homeodomain-like proteins have been implicated in mating-type determination and/or life cycle regulation in several organisms from widely distributed groups in the eukaryotic tree, including the green alga *Chlamydomonas reinhardtii*, the moss *Physcomitrella patens*, the fungus *Cryptococcus neoformans* and the social amoeba *Dictyostelium discoideum* (Hedgethorne et al., 2017; Horst and Reski, 2016; Hull et al., 2005; Lee et al., 2008a; Sakakibara et al., 2013). In the *Chlamydomonas* mating-type system, two different TALE homeodomain transcription factors are carried by the male and female gametes, respectively. These two proteins can only dimerise when the haploid gametes fuse to form a diploid zygote. This dimerisation event is therefore used to signal to the cell that it has transitioned from the haploid to the diploid phase. In *Ectocapus*, mutation of either of the two TALE homeodomain transcription factor genes, *OUROBOROS* (*ORO*) (Coelho et al., 2011) or *SAMSARA* (*SAM*) (Arun et al., 2019), results in a switch from the sporophyte generation to a full functional gametophyte generation. In these mutants, the transition from sporophyte to gametophyte is not associated with a change in ploidy demonstrating that alternation of generation during the life cycle is not strictly determined by ploidy (Cock et al., 2014). Interestingly, both *ORO* and *SAM* are expressed in both male and female gametes, i.e. there is not the sex-limited pattern of expression that was observed for the *Chlamydomonas* mating-type system genes (Fig. 1). In the moss *Physcomitrella patens* the TALE homeodomain transcription factors life cycle regulations *KNOX* and *BELL* do not show sex-specific patterns of expression, which is different to the pattern of expression observed in *Chlamydomonas*. We therefore suggested that the expression patterns of *ORO* and *SAM* may have been modified during evolution (Arun et al., 2019) to ensure that both the male and female gametes carry both homeodomain transcription factors and, therefore, are capable of initiating the sporophyte program during parthenogenesis. This may have been an important factor in the evolution of the complex life cycles of both *Ectocarpus* and mosses, allowing the combination of a sexual cycle with an asexual, parthenogenetic cycle (Fig. 1).

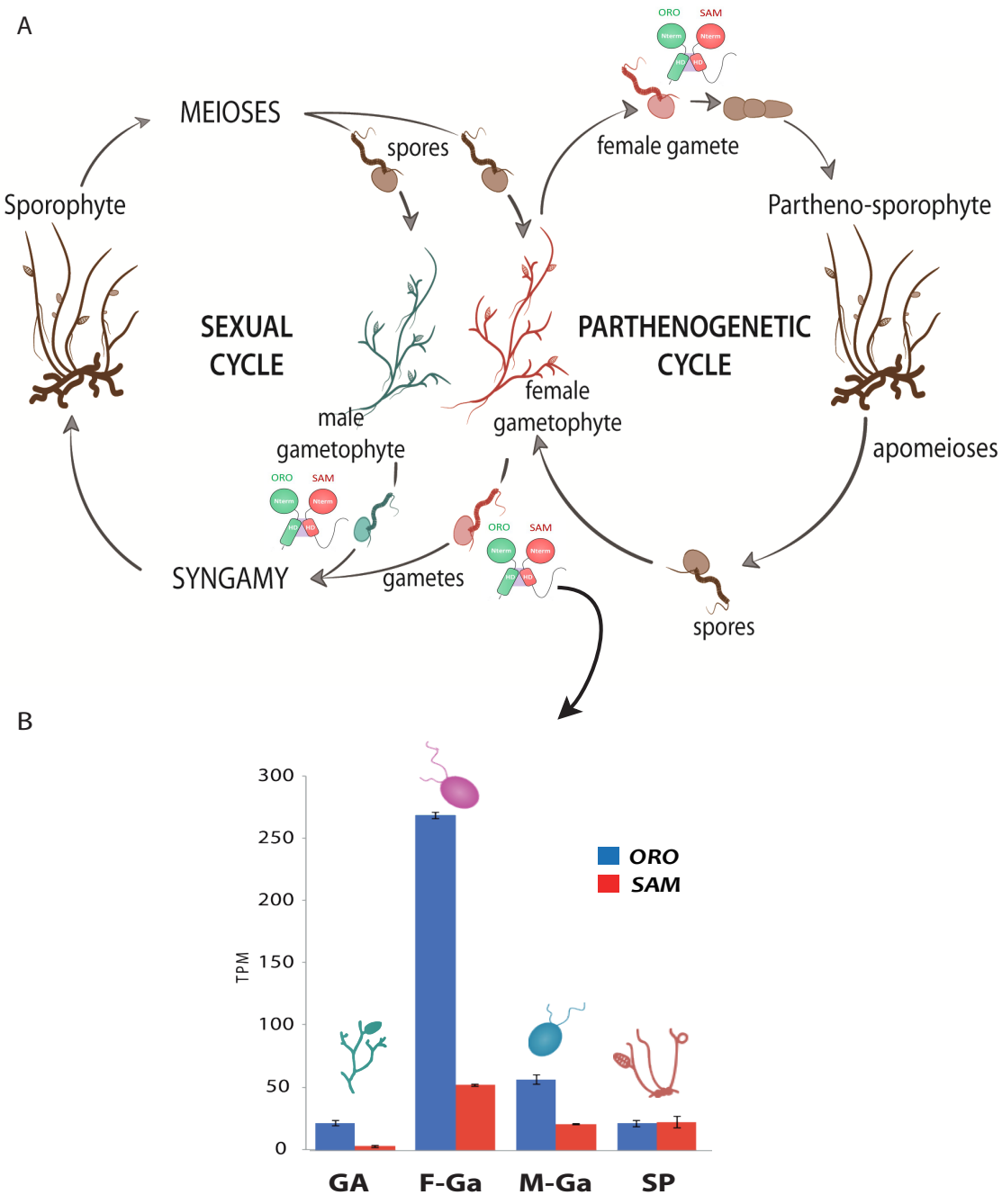


**Figure 1. Regulation of life cycle alternation by the TALE HD TFs, ORO and SAM.** *Ectocarpus* life cycle showing the sexual and parthenogenetic cycles on the left and right, respectively (A). In some strains, unfertilised male gametes can also enter the parthenogenetic asexual cycle (not shown). *ORO* and *SAM* are both expressed in both male and female gametes (B). GA: gametophyte; F-Ga: female gamete; M-Ga: male gamete; SP: sporophyte.

In addition to the genetic regulation of life cycle transitions via ORO and SAM, our work has shown that a diffusible, sporophyte-inducing factor influences the gametophyte-to-sporophyte transition of the *Ectocarpus* life cycle. The diffusible factor appears to be secreted into the culture medium by the sporophyte filaments and induces up to 30% of meio-spores (Arun et al., 2013) to convert from the gametophyte to the sporophyte generation in a non-cell autonomous manner. The work that was carried out to characterise this factor is described in Chapter III. The sporophyte-inducing factor is not the only diffusible factor produced by brown algae, these organisms are known to produce several other diffusible molecules such as sex pheromones (see table 1); for example, ectocarpene in *Ectocarpus siliculosus*, which is produced by the female gametes and acts as a male gamete attractant (Jaenicke, 1977; Müller et al., 1971). On a broader level, many marine species produce chemical signals and defence metabolites, such as kairomones, dimethyl sulfide (DMS) (Pohnert et al., 2007) and N-acyl homoserine lactone (AHL). These molecules mediate interactions between species and have been observed in both coastal and open water environments (Joint et al., 2002). Interestingly, a diffusible molecule with an equivalent function to the *Ectocarpus* sporophyte-inducing factor (i.e. conversion from the gametophyte to the sporophyte program) has been reported in another eukaryotic lineage, the mosses (Bauer, 1959). In this latter system, moss sporophytes produce a diffusible factor that induces apogamous sporophyte formation but the nature of the factor is not clear.

**Table 1. Male-attracting pheromones produced by females of brown algae.** (Maier, 1995)

| Class | Species | Sex attractant | Properties |
|---|---|---|---|
| Phaeophyceae | *Ectocarpus siliculosus* | Ectocarpene | Hydrocarbon, $C_{11}H_{16}$ |
| | *Cutleria multifida* | Multifidene | Hydrocarbon, $C_{11}H_{16}$ |
| | *Fucus serratus* | Fucoserratene | Hydrocarbon, $C_8H_{12}$ |

In chapter IV, we show that mutations at the *ORO* and *SAM* loci render strains unsusceptible to the diffusible sporophyte-inducing factor (Arun et al., 2019; Arun et al., 2013) indicating that the diffusible factor probably acts upstream of the ORO and SAM proteins in the pathway that leads to induction of the sporophyte developmental program. One important question is: What is the

role (if any) of the diffusible factor in regulating the *Ectocarpus* life cycle in the field? For example, does the factor accumulate to sufficient concentrations in proximity to sporophytes in the field to influence the development of released meio-spores? One factor that may play a role in this respect is the tendency for *Ectocarpus* to grow in small rock pools where there may be more capacity to accumulate a secreted factor, under certain tide conditions, than in open water. Another possibility that needs to be investigated is whether the factor plays an "endocrine" role, for example in maintaining sporophyte cell identities within a developing sporophyte.

Some significant advances have been made in the characterisation of the diffusible sporophyte-inducing factor (presented in Chapter III) but the exact biochemical nature of this factor still remains to be elucidated. Using the protocols available at the beginning of the thesis work, considerable difficulties were encountered with the collection of active diffusible factor, requiring growth of multiple cultures under various conditions and the carrying out of multiple bioassays to detect activity. Difficulties were associated both with the production and the detection of the factor. For the production step, various culture parameters including inoculum size, the growth stage of the material, light intensity and culture time may influence the production of the diffusible factor. Initially, cultures were started from gametes, which develop as partheno-sporophytes via parthenogenesis. However, the inoculum is difficult to determine with this method. Excess inoculum led to sporophytes being in poor condition (swollen cells were observed under the microscope) after 4 weeks in culture. In addition, very young sporophytes produce a less diffusible factor. Also, with low amounts of inoculum sporophytes become mature in culture, producing unilocular sporangia that release meio-spores. These meio-spores then develop as gametophytes and it is therefore not possible to maintain the pure sporophyte cultures under these culture conditions.

Several factors were identified that could influence the detection of the diffusible factor including the physical state of the unilocular sporangia, the time at which the unilocular sporangia were isolated and the time taken for the unilocular sporangia to release. Furthermore, the ability of each meio-spore to respond to the diffusible factor appears to be variable, necessitating analysis of a large number of cells. These various problems were overcome by optimising production

conditions and by establishing a statistically robust bioassay system for detecting the factor. The optimisation experiments were inspired by the studies reported by Kochert and Yates (1974), who purified and partially characterised a sexual inducer that is released into the culture medium by male *Volvox* colonies, initiating transition to sexuality in colonies of a wide range of *Volvox* species and by that of Zsebo et al. (1990), who identified a growth factor (stem cell factor) from buffalo rat liver-condition medium with potent synergistic activity in semisolid bone marrow cultures in conjunction with colony-stimulating factors.

The bioassay system (described in chapter II) for the *Ectocarpus* diffusible sporophyte-inducing factor involves incubating haploid meio-spores in Provasoli-enriched sporophyte-condition medium or other test media. One advantage of this system is that meio-spores are released directly into the test medium, ensuring that the cells receive the treatment before they synthesise any cell wall. The absence of a cell wall is important because cells (meio-spores or gametophyte-derived protoplasts) become resistant to the diffusible factor about 48h after release/isolation and this time corresponds to the beginning of cell wall synthesis (Arun et al., 2013). In relation to this time constraint, we took care to use only unilocular sporangia that released within 2 days after isolation for the bioassay. The mechanism of the acquired resistance to the diffusible factor was not investigated during this study but the link with cell wall synthesis is intriguing in the light of the implication of cell walls in developmental processes in both the brown algae (for example in *Fucus*, where rhizoid cell fate is induced in thallus cells by contact with the cell wall) (Berger et al., 1994; Bouget et al., 1998; Kropf et al., 1993; Kropf et al., 1988) and land plants (*Arabidopsis*), where the orientation of microfibrils in walls influences the direction of cell growth (Hamant et al., 2010). The cell wall could influence the action of the diffusible sporophyte-condition factor in several different ways. For example, the cell wall could act as a physical barrier, preventing the diffusible factor from interacting with its target in the cell. However, this hypothesis would only work if the distances between the polymers that make up the cell walls are sufficiently small to prevent the passage of the diffusible factor or if the factor is absorbed onto the filaments. Alternatively, the cell wall may have an indirect effect, for example, by playing a regulatory role, making the target cell resistant to the factor or locking the cell into the gametophyte fate. Note, however, the cell wall does not appear to be necessary to

maintain gametophyte fate because (wall-less) gametophyte-derived protoplasts regenerate as gametophytes (Arun et al., 2013). One possible approach to test the hypotheses that the cell wall acts as a barrier, preventing the factor from targeting the cell, would be to microinject (Bouget et al., 1998) the diffusible factor into unilocular sporangia at the syncytial stage. Other techniques that could be used include isotope labelling to track the metabolism of the diffusible factor in the cell or immunodetection to localise the diffusible factor in the cell. However, all of these approaches would be technically difficult, given the variable response to the factor, and some of them would require a better understanding of the nature of the diffusible factor and the development of new tools such as antibodies.

Note that we used haploid partheno-sporophytes to produce meio-spores but this stage of the life cycle is phenotypically identical to diploid sporophytes (Peters et al., 2008) so the use of haploid sporophyte individuals is not expected to have any repercussions for the bioassay.

We noted some disadvantages with the current bioassay system, in particular, problems were encountered with bacterial infections resulting in some of the tests needing to be eliminated. Also, whilst the small quantity of medium used is advantageous for observation of the developing germlings, the medium can become rapidly exhausted, impacting cell growth and development. The experiments aimed at optimising SCM focused on culture time and the level of light intensity but additional parameters such as modifying the size of the inoculum of adult sporophyte use to start the cultures may reduce the time required for SCM production. In summary, the current optimised production conditions and bioassay enabled us to carry out work on the diffusible factor but further optimisation would facilitate future experiments. In particular, one major constraint of the system is that a large number of tests are required to obtain statistically meaningful results. Any future improvements that would allow diffusible factor activity to be measured robustly with fewer assays would greatly facilitate work with the factor.

Several lines of evidence indicated that the diffusible sporophyte-inducing factor may be an AGP or an AGP-like molecule. This is interesting because AGPs have only recently been characterised in brown algae and because these recent analyses have also linked brown algal AGPs with developmental processes. In terrestrial plants, these molecules have been shown to play crucial

roles in diverse developmental and reproductive processes (Fu et al., 2007; Nathan Hancock et al., 2005; Seifert et al., 2014). Brown algal AGPs are unusual in that they are chimeric and present novel domain structures compared to the AGPs of land plants Hervé et al. (2016). Hervé et al. (2016) presented evidence that AGP-like proteins are developmentally regulated during *Fucus* development and that the developmental abnormalities occur if the action of these proteins is inhibited by the addition of AGP-reactive Yariv reagents. Therefore, if the *Ectocarpus* diffusible factor does correspond to an AGP, it may be one of several brown algal AGPs with roles in the control of developmental processes. One possible objective for the future would be to test the effects of AGPs extracted from the cell walls of other brown algae (e.g. *Fucus* or *Saccharina*) on developmental processes during the gametophyte and sporophyte generations in *Ectocarpus,* particularly during early development of initial cells such as meio-spores or zygotes. Tests could involve AGP treatments plus the addition of AGPs together with Yariv reagent as a negative control. Fischl et al. (2016) described 12 ManC5-E genes, most of which were expressed during both generations of the life cycle. However, four of the ManC5-E genes were preferentially expressed during the gametophyte generation (Fig. 2). It would be interesting to explore the distribution patterns of these AGPs during early development of the gametophyte and to investigate the phenotypes of gametophytes in which the action of AGPs is blocked, for example by addition of Yariv reagent. If current efforts to develop a gene knockdown method based on CRISPR-Cas9 are successful (Y. Badis, personal communication), this would represent a means to specifically silence AGP genes providing direct information about their functions.

It is interesting that the diffusible sporophyte-inducing factor was resistant to heating and proteinase K treatment. This was also the case for the AGP methyl-glucuronosyl arabinogalactan (AMOR) and Motose et al. (2001) were able to demonstrate that the active moiety of the molecule was a disaccharide: methyl-glucuronosyl galactose (4-Me-GlcA-b-(1/6)-Gal). By analogy, it is possible that the active moiety of the *Ectocarpus* sporophyte-inducing factor may be a saccharide molecule and future experiments could be designed to test this possibility. In the future, it would be interesting to treat the *Ectocarpus* diffusible factor with deglycosylase to remove the sugar chains and then bioassay the sugar and proteins fractions separately.

Characterisation of the diffusible factor would be greatly facilitated if it could be obtained in pure form. A number of experiments were carried out during the thesis with the aim of purifying the factor using combinations of gel filtration and ion-exchange chromatography (Annexe 1) but no conclusive results were obtained. Possible reasons for the failure of these experiments may have been very low diffusible factor concentrations in eluted fractions, perhaps exacerbated by adsorption of the factor onto surfaces during the purification procedure (a common problem with AGPs) and loss of activity due to degradation during purification. One important objective for the future will be to optimise the purification protocol in order to purify the diffusible factor. In addition, it would be very interesting to test whether other brown algal species produce an equivalent molecule and whether such molecules are active across species or are species-specific. Indeed, if species with large sporophyte thalli, such as kelps are shown to produce diffusible sporophyte-inducing factors, this may facilitate purification by allowing the production of large quantities of SCM.

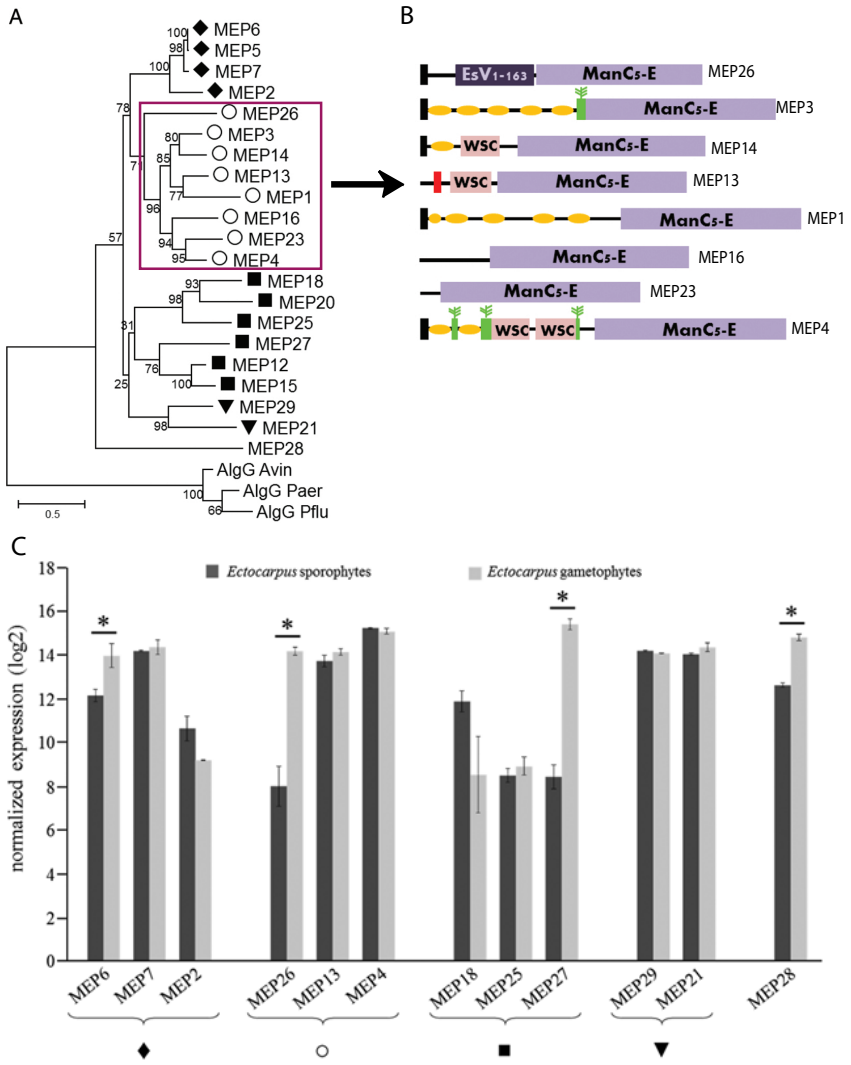


**Figure 2. The *Ectocarpus* ManC5-E family.** (A) Phylogenetic tree of *Ectocarpus* ManC5-E proteins. Numbers indicate the bootstrap values from the maximum likelihood analysis. The sequences belonging to the four main clusters are marked by different symbols (black diamond, open circle, black square and black triangle). (B) Domain structure of the ManC5-E proteins marked by an open circle. Putative structures of the encoded proteins are shown with the signal peptide (black box), the catalytic ManC5-E domain, WSC domains, the AGP protein core featuring the glycan decoration (green "wattle blossom" shape), the MUF (yellow oval) and a transmembrane domain (red box). Protein lengths are proportionally to scale. (C) Microarray analysis of the abundance of ManC5-E transcripts in *Ectocarpus* sporophytes versus gametophytes, using microarray data from Coelho et al. (2011). Data are means of three independent biological replicates ± SE. Asterisks indicate significant differences (t-test, $p$-value<0.05). Reproduced from Fischl et al. (2016).

**Division of the initial cell of the sporophyte generation**

In this thesis, we characterised the *BASELESS* (*BAS*) gene (Chapter V), which plays a key role during early development. Mutations in this gene resulted in defects in initial cell divisions during early development of both the gametophyte and the sporophyte generations causing them to fail to form basal structures (a rhizoid in the gametophyte and prostrate filaments in the sporophyte). During the gametophyte generation, asymmetric division of the initial cell was lost and was replaced by unipolar germination to produce just one cell type: cylindrical upright filament cells. Asymmetric cell division is a ubiquitous mechanism that is required for the development of multicellular organisms, representing the first stage of the differentiation process (Dong et al., 2009). Asymmetric division of the initial cell is crucial for the early development of the animal and plant embryos, setting the conditions for the formation of tissue layers and cell-types (ten Hove and Heidstra, 2008). Asymmetric cell divisions have been shown to play crucial roles in cell-fate determination in diverse domains of the tree of life including, for example, polar growth in yeast (Feierbach and Chang, 2001), and asymmetric cell division in bacteria (Ben-Yehuda and Losick, 2002), flies and worms (Gönczy, 2008).

Microtubule distribution during the early development of the *bas* mutant indicated that the filaments were disorganised compared with wild type germlings. The atypical initial cell division phenotype exhibited by the *bas* mutant was very similar to that observed with the *dis* mutant (Godfroy et al., 2017), which also exhibits disorganisation of the microtubule cytoskeleton. Interestingly, microtubule arrangement defects have been shown to be associated with abnormal cell shapes in the *Arabidopisis fass* mutant (Kirik et al., 2012). In the future, it would be interesting to carry out additional experiments to investigate the structure of the Golgi and the position of nuclei and centrioles in *bas* initial cells because these features were also modified in the *dis* mutant. Importantly, asymmetrical division involves the movement of the nucleus and other organelles, enlargement of the vacuole and reorganization of microtubules (Kimata et al., 2016) suggesting links between these various phenotypes. This thesis analysed *BAS* gene expression during the *Ectocarpus* life cycle, including in *dis* and *imm* backgrounds, use RNA-seq data (Bourdareau, 2018; Coelho et al., 2011; Godfroy et al., 2017; Macaisne et al., 2017). These

analyses suggested that the *BAS* transcript was abundant during early cell division in the partheno-sporophyte generation, but neither the *dis* nor the *imm* mutations affected its expression. In the future, more work is needed to investigate the relationships between these three genes.

Genetic analysis showed that two *bas* mutations (*bas-1* and *bas-2*) were located in the gene *Ec-21_001770*, which encodes a protein phosphatase 2A (PP2A) regulatory subunit type B" with EF-hand domains. An EF-hand has a small, partially hydrophobic core, that binds calcium. In many proteins with this domain, the EF-hand binds to $Ca^{2+}$ which is acting as a second messenger (Kawasaki et al., 1998). In the future, we plan to further investigate the function of *Ec-21_001770* in *Ectocarpus*. It would be particularly interesting to understand the relationship between BAS (i.e. PP2A) and DIS (TBCCd1). Because the phenotypes of both classes of mutation are very similar, the proteins may be involved in similar processes during the initial cell division in *Ectocarpus*.

# References

Acosta-Garcia, G., Vielle-Calzada, J.P., 2004. A classical arabinogalactan protein is essential for the initiation of female gametogenesis in *Arabidopsis*. Plant Cell 16, 2614-2628.

Ahmed, S., Cock, J.M., Pessia, E., Luthringer, R., Cormier, A., Robuchon, M., Sterck, L., Peters, A.F., Dittami, S.M., Corre, E., 2014. A haploid system of sex determination in the brown alga *Ectocarpus sp*. Current biology 24, 1945-1957.

Ale, M.T., Mikkelsen, J.D., Meyer, A.S., 2011. Important determinants for fucoidan bioactivity: A critical review of structure-function relations and extraction methods for fucose-containing sulfated polysaccharides from brown seaweeds. Marine drugs 9, 2106-2130.

Anderson, J.B., Sirjusingh, C., Ricker, N., 2004. Haploidy, diploidy and evolution of antifungal drug resistance in *Saccharomyces cerevisiae*. Genetics 168, 1915-1923.

Arun, A., 2012. Analyse génétique et moléculaire de la régulation du cycle de vie chez l'algue brune *Ectocarpus siliculosis*. Paris 6.

Arun, A., Coelho, S.M., Peters, A.F., Bourdareau, S., Pérès, L., Scornet, D., Strittmatter, M., Lipinska, A.P., Yao, H., Godfroy, O., 2019. Convergent recruitment of TALE homeodomain life cycle regulators to direct sporophyte development in land plants and brown algae. eLife 8, e43101.

Arun, A., Peters, N.T., Scornet, D., Peters, A.F., Mark Cock, J., Coelho, S.M., 2013. Non-cell autonomous regulation of life cycle transitions in the model brown alga *Ectocarpus*. New Phytol 197, 503-510.

Avia, K., Coelho, S.M., Montecinos, G.J., Cormier, A., Lerck, F., Mauger, S., Faugeron, S., Valero, M., Cock, J.M., Boudry, P., 2017. High-density genetic map and identification of QTLs for responses to temperature and salinity stresses in the model brown alga *Ectocarpus*. Scientific reports 7, 43241.

Baldauf, S.L., 2008. An overview of the phylogeny and diversity of eukaryotes. Journal of Systematics and Evolution 46, 263-273.

Banks, J.A., 1999. Gametophyte development in ferns. Annual review of plant biology 50, 163-186.

Bauer, L., 1959. Auslösung apogamer Sporogonbildung am Regenerationsprotonema von Laubmoosen durch einen vom Muttersporogon abgegebenen Faktor. Naturwissenschaften 46, 154-155.

Belanger, K.D., Quatrano, R.S., 2000. Polarity: the role of localized secretion. Current opinion in plant biology 3, 67-72.

Bell, G., 1994. The comparative biology of the alternation of generations. Lectures on mathematics in the life sciences: theories for the evolution of haploid-diploid life cycles: Am Math Soc, Providence, RI, 1-26.

Ben-Yehuda, S., Losick, R., 2002. Asymmetric cell division in *B. subtilis* involves a spiral-like intermediate of the cytokinetic protein FtsZ. Cell 109, 257-266.

Benková, E., Michniewicz, M., Sauer, M., Teichmann, T., Seifertová, D., Jürgens, G., Friml, J., 2003. Local, efflux-dependent auxin gradients as a common module for plant organ formation. Cell 115, 591-602.

Berger, F., Taylor, A., Brownlee, C., 1994. Cell fate determination by the cell wall in early *Fucus* development. Science 263, 1421-1423.

Berglin, M., Delage, L., Potin, P., Vilter, H., Elwing, H., 2004. Enzymatic cross-linking of a phenolic polymer extracted from the marine alga *Fucus serratus*. Biomacromolecules 5, 2376-2383.

Berney, C., Pawlowski, J., 2006. A molecular time-scale for eukaryote evolution recalibrated with the continuous microfossil record. Proceedings of the Royal Society B: Biological Sciences 273, 1867-1872.

Bisgrove, S.R., Kropf, D.L., 2001. Cell wall deposition during morphogenesis in fucoid algae. Planta 212, 648-658.

Bothwell, J.H., Marie, D., Peters, A.F., Cock, J.M., Coelho, S.M., 2010. Role of endoreduplication and apomeiosis during parthenogenetic reproduction in the model brown alga *Ectocarpus*. New Phytologist 188, 111-121.

Bouget, F.-Y., Berger, F., Brownlee, C., 1998. Position dependent control of cell fate in the *Fucus* embryo: role of intercellular communication. Development 125, 1999-2008.

Bouget, F.-Y., Gerttula, S., Shaw, S.L., Quatrano, R.S., 1996. Localization of actin mRNA during the establishment of cell polarity and early cell divisions in *Fucus* embryos. The Plant Cell 8, 189-201.

Bourdareau, S., 2018. Genetic and epigenetic control of life cycle transitions in the brown alga *Ectocarpus* sp. Sorbonne Université.

Bowman, J.L., Floyd, S.K., Sakakibara, K., 2007. Green genes—comparative genomics of the green branch of life. Cell 129, 229-234.

Brownlee, C., 2002. Role of the extracellular matrix in cell–cell signalling: paracrine paradigms. Current opinion in plant biology 5, 396-401.

Brownlee, C., Bouget, F.-Y., 1998. Polarity determination in Fucus: From zygote to multicellular embryo, Seminars in cell & developmental biology. Elsevier, pp. 179-185.

Brunelle, J.L., Green, R., 2014. One-dimensional SDS-polyacrylamide gel electrophoresis (1D SDS-PAGE), Methods in enzymology, vol. 541. Elsevier, pp. 151-159.

Burki, F., Kaplan, M., Tikhonenkov, D.V., Zlatogursky, V., Minh, B.Q., Radaykina, L.V., Smirnov, A., Mylnikov, A.P., Keeling, P.J., 2016. Untangling the early diversification of eukaryotes: a phylogenomic study of the evolutionary origins of Centrohelida, Haptophyta and Cryptista. Proceedings of the Royal Society B: Biological Sciences 283, 20152802.

Burki, F., Shalchian-Tabrizi, K., Minge, M., Skjæveland, Å., Nikolaev, S.I., Jakobsen, K.S., Pawlowski, J., 2007. Phylogenomics reshuffles the eukaryotic supergroups. PloS one 2, e790.

Callow, M.E., Coughlan, S., Evans, L., 1978. The role of Golgi bodies in polysaccharide sulphation in Fucuszygotes. Journal of cell science 32, 337-356.

Cavalier-Smith, T., Fiore-Donno, A.M., Chao, E., Kudryavtsev, A., Berney, C., Snell, E.A., Lewis, R., 2015. Multigene phylogeny resolves deep branching of Amoebozoa. Molecular phylogenetics and evolution 83, 293-304.

Charles, B.H., 1985. Introduction to the algae: structure and reproduction.

Chaudhury, A.M., Ming, L., Miller, C., Craig, S., Dennis, E.S., Peacock, W.J., 1997. Fertilization-independent seed development in *Arabidopsis thaliana*. Proceedings of the National Academy of Sciences 94, 4223-4228.

Chaves, I., Regalado, A.P., Chen, M., Ricardo, C.P., Showalter, A.M., 2002. Programmed cell death induced by (β‐d‐galactosyl) 3 Yariv reagent in *Nicotiana tabacum* BY‐2 suspension‐cultured cells. Physiologia Plantarum 116, 548-553.

Cheung, A.Y., Wang, H., Wu, H.-m., 1995. A floral transmitting tissue-specific glycoprotein attracts pollen tubes and stimulates their growth. Cell 82, 383-393.

Chou, H., Zhu, Y., Ma, Y., Berkowitz, G.A., 2016. The CLAVATA signaling pathway mediating stem cell fate in shoot meristems requires $Ca^{2+}$ as a secondary cytosolic messenger. The Plant Journal 85, 494-506.

Cock, J.M., Godfroy, O., Macaisne, N., Peters, A.F., Coelho, S.M., 2014. Evolution and regulation of complex life cycles: a brown algal perspective. Curr Opin Plant Biol 17, 1-6.

Cock, J.M., Godfroy, O., Strittmatter, M., Scornet, D., Uji, T., Farnham, G., Peters, A.F., Coelho, S.M., 2015. Emergence of *Ectocarpus* as a model system to study the evolution of complex multicellularity in the brown algae, Evolutionary transitions to multicellular life. Springer, pp. 153-162.

Cock, J.M., Sterck, L., Rouze, P., Scornet, D., Allen, A.E., Amoutzias, G., Anthouard, V., Artiguenave, F., Aury, J.M., Badger, J.H., Beszteri, B., Billiau, K., Bonnet, E., Bothwell, J.H., Bowler, C., Boyen, C., Brownlee, C., Carrano, C.J., Charrier, B., Cho, G.Y., Coelho, S.M., al., e., 2010. The *Ectocarpus* genome and the independent evolution of multicellularity in brown algae. Nature 465, 617-621.

Coelho, S.M., Brownlee, C., Bothwell, J.H., 2008. Feedback control of reactive oxygen and $Ca^{2+}$ signalling during brown algal embryogenesis. Plant signaling & behavior 3, 570-572.

Coelho, S.M., Godfroy, O., Arun, A., Le Corguillé, G., Peters, A.F., Cock, J.M., 2011. *OUROBOROS* is a master regulator of the gametophyte to sporophyte life cycle transition in the brown alga *Ectocarpus*. Proceedings of the National Academy of Sciences 108, 11518-11523.

Coelho, S.M., Peters, A.F., Charrier, B., Roze, D., Destombe, C., Valero, M., Cock, J.M., 2007. Complex life cycles of multicellular eukaryotes: new approaches based on the use of model organisms. Gene 406, 152-170.

Coelho, S.M., Scornet, D., Rousvoal, S., Peters, N.T., Dartevelle, L., Peters, A.F., Cock, J.M., 2012a. *Ectocarpus*: a model organism for the brown algae. Cold Spring Harb Protoc 2012, 193-198.

Coelho, S.M., Scornet, D., Rousvoal, S., Peters, N.T., Dartevelle, L., Peters, A.F., Cock, J.M., 2012b. How to cultivate *Ectocarpus*. Cold Spring Harb Protoc 2012, 258-261.

Coelho, S.M., Taylor, A.R., Ryan, K.P., Sousa-Pinto, I., Brown, M.T., Brownlee, C., 2002. Spatiotemporal patterning of reactive oxygen production and $Ca^{2+}$ wave propagation in *Fucus* rhizoid cells. The Plant Cell 14, 2369-2381.

Coimbra, S., Costa, M., Jones, B., Mendes, M.A., Pereira, L.G., 2009. Pollen grain development is compromised in *Arabidopsis agp6 agp11* null mutants. Journal of Experimental Botany 60, 3133-3142.

Colin, C., Leblanc, C., Michel, G., Wagner, E., Leize-Wagner, E., Van Dorsselaer, A., Potin, P., 2005. Vanadium-dependent iodoperoxidases in *Laminaria digitata*, a novel biochemical function diverging from brown algal bromoperoxidases. JBIC Journal of Biological Inorganic Chemistry 10, 156-166.

Cormier, A., Avia, K., Sterck, L., Derrien, T., Wucher, V., Andres, G., Monsoor, M., Godfroy, O., Lipinska, A., Perrineau, M.M., 2017. Re‐annotation, improved large‐scale assembly and establishment of a catalogue of noncoding loci for the genome of the model brown alga *Ectocarpus*. New Phytologist 214, 219-232.

Couceiro, L., Le Gac, M., Hunsperger, H.M., Mauger, S., Destombe, C., Cock, J.M., Ahmed, S., Coelho, S.M., Valero, M., Peters, A.F., 2015. Evolution and maintenance of haploid–diploid life cycles in natural populations: The case of the marine brown alga *Ectocarpus*. Evolution 69, 1808-1822.

Cronshaw, J., Myers, A., Preston, R., 1958. A chemical and physical investigation of the cell walls of some marine algae. Biochimica et biophysica acta 27, 89-103.

Cruz‐Garcia, F., Nathan Hancock, C., Kim, D., McClure, B., 2005. Stylar glycoproteins bind to S‐RNase in vitro. The Plant Journal 42, 295-304.

d'Amato, F., 1977. Nuclear cytology in relation to development. CUP Archive.

Day, I.S., Reddy, V.S., Ali, G.S., Reddy, A., 2002. Analysis of EF-hand-containing proteins in *Arabidopsis*. Genome biology 3, research0056. 0051.

de Reviers, B., 2006. Biologia e filogenia das algas. Artmed Editora.

Demesa-Arevalo, E., Vielle-Calzada, J.P., 2013. The classical arabinogalactan protein AGP18 mediates megaspore selection in *Arabidopsis*. Plant Cell 25, 1274-1287.

Deniaud-Bouët, E., Kervarec, N., Michel, G., Tonon, T., Kloareg, B., Hervé, C., 2014. Chemical and enzymatic fractionation of cell walls from Fucales: insights into the structure of the extracellular matrix of brown algae. Annals of botany 114, 1203-1216.

Derelle, R., Lopez, P., Guyader, H.L., Manuel, M., 2007. Homeodomain proteins belong to the ancestral molecular toolkit of eukaryotes. Evolution & development 9, 212-219.

Destombe, C., Godin, J., Lefebvre, C., Dehorter, O., Vernet, P., 1992. Differences in dispersal abilities of haploid and diploid spores of *Gracilaria verrucosa* (Gracilariales, Rhodophyta). Botanica Marina 35, 93-98.

Dhonukshe, P., Kleine-Vehn, J., Friml, J., 2005. Cell polarity, auxin transport, and cytoskeleton-mediated division planes: who comes first? Protoplasma 226, 67-73.

Dittami, S.M., Scornet, D., Petit, J.-L., Ségurens, B., Da Silva, C., Corre, E., Dondrup, M., Glatting, K.-H., König, R., Sterck, L., 2009. Global expression analysis of the brown alga *Ectocarpus siliculosus* (Phaeophyceae) reveals large-scale reprogramming of the transcriptome in response to abiotic stress. Genome biology 10, R66.

Dolan, L., 2009. Body building on land—morphological evolution of land plants. Current opinion in plant biology 12, 4-8.

Dong, J., MacAlister, C.A., Bergmann, D.C., 2009. BASL controls asymmetric cell division in *Arabidopsis*. Cell 137, 1320-1330.

Dresselhaus, T., Coimbra, S., 2016. Plant reproduction: AMOR enables males to respond to female signals. Curr Biol 26, R321-323.

Dupres, V., Alsteens, D., Wilk, S., Hansen, B., Heinisch, J.J., Dufrene, Y.F., 2009. The yeast Wsc1 cell surface sensor behaves like a nanospring in vivo. Nat Chem Biol 5, 857-862.

Ebel, C., Mariconti, L., Gruissem, W., 2004. Plant retinoblastoma homologues control nuclear proliferation in the female gametophyte. Nature 429, 776.

Eme, L., Sharpe, S.C., Brown, M.W., Roger, A.J., 2014. On the age of eukaryotes: evaluating evidence from fossils and molecular clocks. Cold Spring Harbor Perspectives in Biology 6, a016139.

Feierbach, B., Chang, F., 2001. Roles of the fission yeast formin for3p in cell polarity, actin cable formation and symmetric cell division. Current Biology 11, 1656-1665.

Feraru, E., Friml, J., 2008. PIN polar targeting. Plant Physiology 147, 1553-1559.

Fischl, R., Bertelsen, K., Gaillard, F., Coelho, S., Michel, G., Klinger, M., Boyen, C., Czjzek, M., Herve, C., 2016. The cell-wall active mannuronan C5-epimerases in the model brown alga *Ectocarpus*: From gene context to recombinant protein. Glycobiology 26, 973-983.

Fowler, J.E., Quatrano, R.S., 1997. Plant cell morphogenesis: plasma membrane interactions with the cytoskeleton and cell wall. Annual review of cell and developmental biology 13, 697-743.

Friml, J., 2003. Auxin transport—shaping the plant. Current opinion in plant biology 6, 7-12.

Fritsch, F.E., 1935. Structure and reproduction of the algae.

Fu, H., Yadav, M.P., Nothnagel, E.A., 2007. *Physcomitrella patens* arabinogalactan proteins contain abundant terminal 3-O-methyl-L-rhamnosyl residues not found in angiosperms. Planta 226, 1511.

Fu, Y., Gu, Y., Zheng, Z., Wasteneys, G., Yang, Z., 2005. *Arabidopsis* interdigitating cell growth requires two antagonistic pathways with opposing action on cell morphogenesis. Cell 120, 687-700.

Futagami, T., Nakao, S., Kido, Y., Oka, T., Kajiwara, Y., Takashita, H., Omori, T., Furukawa, K., Goto, M., 2011. Putative stress sensors WscA and WscB are involved in hypo-osmotic and acidic pH stress tolerance in *Aspergillus nidulans*. Eukaryotic cell 10, 1504-1515.

Gönczy, P., 2008. Mechanisms of asymmetric cell division: flies and worms pave the way. Nature reviews Molecular cell biology 9, 355.

Gane, A.M., Craik, D., Munro, S.L., Howlett, G.J., Clarke, A.E., Bacic, A., 1995. Structural analysis of the carbohydrate moiety of arabinogalactan-proteins from stigmas and styles of *Nicotiana alata*. Carbohydrate Research 277, 67-85.

Gao, M., Showalter, A.M., 1999. Yariv reagent treatment induces programmed cell death in *Arabidopsis* cell cultures and implicates arabinogalactan protein involvement. The Plant Journal 19, 321-331.

Gaspar, Y.M., Nam, J., Schultz, C.J., Lee, L.-Y., Gilson, P.R., Gelvin, S.B., Bacic, A., 2004. Characterization of the *Arabidopsis* lysine-rich arabinogalactan-protein *AtAGP17* mutant (*rat1*) that results in a decreased efficiency of Agrobacterium transformation. Plant Physiology 135, 2162-2171.

Gillissen, B., Bergemann, J., Sandmann, C., Schroeer, B., Bölker, M., Kahmann, R., 1992. A two-component regulatory system for self/non-self recognition in *Ustilago maydis*. Cell 68, 647-657.

Gleeson, P.A., Jermyn, M.A., Clarke, A.E., 1979. Isolation of an arabinogalactan protein by lectin affinity chromatography on tridacnin-sepharose 4B. Analytical biochemistry 92, 41-45.

Godfroy, O., Uji, T., Nagasato, C., Lipinska, A.P., Scornet, D., Peters, A.F., Avia, K., Colin, S., Mignerot, L., Motomura, T., Cock, J.M., Coelho, S.M., 2017. DISTAG/TBCCd1 is required for basal cell fate determination in *Ectocarpus*. The Plant Cell 29, 3102-3122.

Goldstein, B., Macara, I.G., 2007. The PAR proteins: fundamental players in animal cell polarization. Developmental cell 13, 609-622.

Goutte, C., Johnson, A.D., 1988. a1 protein alters the DNA binding specificity of α2 repressor. Cell 52, 875-882.

Graham, L.K., Wilcox, L.W., 2000. The origin of alternation of generations in land plants: a focus on matrotrophy and hexose transport. Philosophical Transactions of the Royal Society of London. Series B: Biological Sciences 355, 757-767.

Gray, J.E., Hetherington, A.M., 2004. Plant development: YODA the stomatal switch. Current Biology 14, R488-R490.

Guitton, A.-E., Berger, F., 2004. Control of reproduction by Polycomb Group complexes in animals and plants. International Journal of Developmental Biology 49, 707-716.

Hackett, J.D., Yoon, H.S., Li, S., Reyes-Prieto, A., Rümmele, S.E., Bhattacharya, D., 2007. Phylogenomic analysis supports the monophyly of cryptophytes and haptophytes and the association of rhizaria with chromalveolates. Molecular Biology and Evolution 24, 1702-1713.

Haerizadeh, F., Wong, C.E., Bhalla, P.L., Gresshoff, P.M., Singh, M.B., 2009. Genomic expression profiling of mature soybean (Glycine max) pollen. BMC Plant Biology 9, 25.

Hamant, O., Traas, J., Boudaoud, A., 2010. Regulation of shape and patterning in plant development. Current opinion in genetics & development 20, 454-459.

Hawkes, M., 1990. Reproductive strategies. Biology of the Red Algae., 455-476.

Hazak, O., Mamon, E., Lavy, M., Sternberg, H., Behera, S., Schmitz-Thom, I., Bloch, D., Dementiev, O., Gutman, I., Danziger, T., Schwarz, N., Abuzeineh, A., Mockaitis, K., Estelle, M., Hirsch, J.A., Kudla, J., Yalovsky, S., 2019. A novel $Ca^{2+}$-binding protein that can rapidly transduce auxin responses during root growth. PLoS Biol 17, e3000085.

Hedgethorne, K., Eustermann, S., Yang, J.-C., Ogden, T.E., Neuhaus, D., Bloomfield, G., 2017. Homeodomain-like DNA binding proteins control the haploid-to-diploid transition in *Dictyostelium*. Science Advances 3, e1602937.

Heesch, S., Cho, G.Y., Peters, A.F., Le Corguillé, G., Falentin, C., Boutet, G., Coëdel, S., Jubin, C., Samson, G., Corre, E., 2010. A sequence‐tagged genetic map for the brown alga Ectocarpus siliculosus provides large‐scale assembly of the genome sequence. New Phytologist 188, 42-51.

Herth, W., Schnepf, E., 1982. Chitin-fibril formation in algae, Cellulose and other natural polymer systems. Springer, pp. 185-206.

Hervé, C., Simeon, A., Jam, M., Cassin, A., Johnson, K.L., Salmean, A.A., Willats, W.G., Doblin, M.S., Bacic, A., Kloareg, B., 2016. Arabinogalactan proteins have deep roots in eukaryotes: identification of genes and epitopes in brown algae and their role in *Fucus serratus* embryo development. New Phytol 209, 1428-1441.

Hoek, C., Mann, D., Jahns, H.M., Jahns, M., 1995. Algae: an introduction to phycology. Cambridge university press.

Hofmeister, W., 1851. Vergleichende Untersuchungen der Keimung, Entfaltung und Fruchtbildung höherer Kryptogamen:(*Moose, Farne, Equisetaceen, Rhizocarpeen und Lycopodiaceen*) und der Samenbildung der Coniferen. Hofmeister.

Honys, D., Twell, D., 2003. Comparative analysis of the *Arabidopsis* pollen transcriptome. Plant physiology 132, 640-652.

Honys, D., Twell, D., 2004. Transcriptome analysis of haploid male gametophyte development in *Arabidopsis*. Genome biology 5, R85.

Horst, N.A., Katz, A., Pereman, I., Decker, E.L., Ohad, N., Reski, R., 2016. A single homeobox gene triggers phase transition, embryogenesis and asexual reproduction. Nature Plants 2, 15209.

Horst, N.A., Reski, R., 2016. Alternation of generations - unravelling the underlying molecular mechanism of a 165-year-old botanical observation. Plant Biol (Stuttg) 18, 549-551.

Hughes, J.S., Otto, S.P., 1999. Ecology and the evolution of biphasic life cycles. The American Naturalist 154, 306-320.

Hull, C.M., Boily, M.-J., Heitman, J., 2005. Sex-specific homeodomain proteins Sxi1α and Sxi2a coordinately regulate sexual development in *Cryptococcus neoformans*. Eukaryotic cell 4, 526-535.

Jaenicke, L., 1977. Sex hormones of brown algae. Naturwissenschaften 64, 69-75.

Jiao, J., Mizukami, A.G., Sankaranarayanan, S., Yamguchi, J., Itami, K., Higashiyama, T., 2017. Structure-activity relation of AMOR sugar molecule that activates pollen-tubes for ovular guidance. Plant physiology 173, 354-363.

Johnson, K.L., Jones, B.J., Bacic, A., Schultz, C.J., 2003. The fasciclin-like arabinogalactan proteins of *Arabidopsis*. A multigene family of putative cell adhesion molecules. Plant physiology 133, 1911-1925.

Joint, I., Tait, K., Callow, M.E., Callow, J.A., Milton, D., Williams, P., Cámara, M., 2002. Cell-to-cell communication across the prokaryote-eukaryote boundary. Science 298, 1207-1207.

Kües, U., Richardson, W., Tymon, A.M., Mutasa, E.S., Göttgens, B., Gaubatz, S., Gregoriades, A., Casselton, L.A., 1992. The combination of dissimilar alleles of the A alpha and A beta gene

complexes, whose proteins contain homeo domain motifs, determines sexual development in the mushroom *Coprinus cinereus*. Genes & development 6, 568-577.

Köhler, C., Hennig, L., Spillane, C., Pien, S., Gruissem, W., Grossniklaus, U., 2003. The Polycomb-group protein MEDEA regulates seed development by controlling expression of the MADS-box gene PHERES1. Genes & Development 17, 1540-1553.

Küpper, F.C., Kloareg, B., Guern, J., Potin, P., 2001. Oligoguluronates elicit an oxidative burst in the brown algal kelp *Laminaria digitata*. Plant physiology 125, 278-291.

Kawai, H., Hanyuda, T., Draisma, S.G., Müller, D.G., 2007. Molecular phylogeny of *Discosporangium Mesarthrocarpum* (Phaeophyceae) with a reinstatement of the order *Discosporangiales* 1 Journal of phycology 43, 186-194.

Kawasaki, H., Nakayama, S., Kretsinger, R., 1998. Classification and evolution of EF-hand proteins. Biometals 11, 277-295.

Kimata, Y., Higaki, T., Kawashima, T., Kurihara, D., Sato, Y., Yamada, T., Hasezawa, S., Berger, F., Higashiyama, T., Ueda, M., 2016. Cytoskeleton dynamics control the first asymmetric cell division in *Arabidopsis* zygote. Proceedings of the National Academy of Sciences 113, 14157-14162.

Kimata, Y., Kato, T., Higaki, T., Kurihara, D., Yamada, T., Segami, S., Morita, M.T., Maeshima, M., Hasezawa, S., Higashiyama, T., 2019. Polar vacuolar distribution is essential for accurate asymmetric division of *Arabidopsis* zygotes. Proceedings of the National Academy of Sciences 116, 2338-2343.

Kirik, A., Ehrhardt, D.W., Kirik, V., 2012. *TONNEAU2/FASS* regulates the geometry of microtubule nucleation and cortical array organization in interphase *Arabidopsis* cells. Plant Cell 24, 1158-1170.

Kloareg, B., Quatrano, R., 1988. Structure of the cell walls of marine algae and ecophysiological functions of the matrix polysaccharides. Oceanography and Marine Biology: an annual review. 26, 259-315.

Knoblich, J.A., 2008. Mechanisms of asymmetric stem cell division. Cell 132, 583-597.

Knoll, A.H., 2011. The multiple origins of complex multicellularity. Annual Review of Earth and Planetary Sciences 39, 217-239.

Kochert, G., Yates, I., 1974. Purification and partial characterization of a glycoprotein sexual inducer from *Volvox carteri*. Proceedings of the National Academy of Sciences 71, 1211-1214.

Kreuger, M., van Holst, G.-J., 1993. Arabinogalactan proteins are essential in somatic embryogenesis of *Daucus carota L*. Planta 189, 243-248.

Kropf, D.L., Coffman, H.R., Kloareg, B., Glenn, P., Allen, V.W., 1993. Cell wall and rhizoid polarity in *Pelvetia* embryos. Developmental biology 160, 303-314.

Kropf, D.L., Kloareg, B., Quatrano, R.S., 1988. Cell wall is required for fixation of the embryonic axis in *Fucus* zygotes. Science 239, 187-190.

Lamport, D.T., Kieliszewski, M.J., Showalter, A.M., 2006. Salt stress upregulates periplasmic arabinogalactan proteins: using salt stress to analyse AGP function. New Phytologist 169, 479-492.

Langdale, J.A., 2008. Evolution of developmental mechanisms in plants. Current opinion in genetics & development 18, 368-373.

Lee, C.B., Swatek, K.N., McClure, B., 2008a. Pollen proteins bind to the C-terminal domain of *Nicotiana alata* pistil arabinogalactan proteins. Journal of Biological Chemistry 283, 26965-26973.

Lee, J.-H., Lin, H., Joo, S., Goodenough, U., 2008b. Early Sexual Origins of Homeoprotein Heterodimerization and Evolution of the Plant KNOX/BELL Family. Cell 133, 829-840.

Lee, K.J., Sakata, Y., Mau, S.L., Pettolino, F., Bacic, A., Quatrano, R.S., Knight, C.D., Knox, J.P., 2005. Arabinogalactan proteins are required for apical cell extension in the moss *Physcomitrella patens*. Plant Cell 17, 3051-3065.

Leszczuk, A., Szczuka, E., Zdunek, A., 2019. Arabinogalactan proteins: Distribution during the development of male and female gametophytes. Plant Physiol Biochem 135, 9-18.

Letarte, J., Simion, E., Miner, M., Kasha, K.J., 2006. Arabinogalactans and arabinogalactan-proteins induce embryogenesis in wheat (*Triticum aestivum L.)* microspore culture. Plant cell reports 24, 691.

Levitin, B., Richter, D., Markovich, I., Zik, M., 2008. Arabinogalactan proteins 6 and 11 are required for stamen and pollen function in *Arabidopsis*. The Plant Journal 56, 351-363.

Lewis, L.A., McCourt, R.M., 2004. Green algae and the origin of land plants. American journal of botany 91, 1535-1556.

Lind, J.L., Bönig, I., Clarke, A.E., Anderson, M.A., 1996. A style-specific 120-kDa glycoprotein enters pollen tubes of *Nicotiana alata* in vivo. Sexual Plant Reproduction 9, 75-86.

Lipinska, A.P., Serrano-Serrano, M.L., Cormier, A., Peters, A.F., Kogame, K., Cock, J.M., Coelho, S.M., 2019. Rapid turnover of life-cycle-related genes in the brown algae. Genome Biol 20, 35.

Liu, C., Xu, Z., Chua, N.-h., 1993. Auxin polar transport is essential for the establishment of bilateral symmetry during early plant embryogenesis. The Plant Cell 5, 621-630.

Lodder, A.L., Lee, T.K., Ballester, R., 1999. Characterization of the Wsc1 protein, a putative receptor in the stress response of *Saccharomyces cerevisiae*. Genetics 152, 1487-1499.

Lommel, M., Bagnat, M., Strahl, S., 2004. Aberrant processing of the WSC family and Mid2p cell surface sensors results in cell death of *Saccharomyces cerevisiae* O-mannosylation mutants. Molecular and cellular biology 24, 46-57.

Luthringer, R., Lipinska, A.P., Roze, D., Cormier, A., Macaisne, N., Peters, A.F., Cock, J.M., Coelho, S.M., 2015. The pseudoautosomal regions of the U/V sex chromosomes of the brown alga *Ectocarpu*s exhibit unusual features. Molecular biology and evolution 32, 2973-2985.

Ma, J., Skibbe, D.S., Fernandes, J., Walbot, V., 2008. Male reproductive development: gene expression profiling of maize anther and pollen ontogeny. Genome biology 9, R181.

Mabeau, S., Kloareg, B., 1987. Isolation and analysis of the cell walls of brown algae: *Fucus spiralis, F. ceranoides, F. vesiculosus, F. serratus, Bifurcaria bifurcata* and *Laminaria digitata*. Journal of Experimental Botany 38, 1573-1580.

Mable, B.K., Otto, S.P., 1998. The evolution of life cycles with haploid and diploid phases. BioEssays 20, 453-462.

Macaisne, N., Liu, F., Scornet, D., Peters, A.F., Lipinska, A., Perrineau, M.M., Henry, A., Strittmatter, M., Coelho, S.M., Cock, J.M., 2017. The *Ectocarpus IMMEDIATE UPRIGHT* gene encodes a member of a novel family of cysteine-rich proteins with an unusual distribution across the eukaryotes. Development 144, 409-418.

Menand, B., Yi, K., Jouannic, S., Hoffmann, L., Ryan, E., Linstead, P., Schaefer, D.G., Dolan, L., 2007. An ancient mechanism controls the development of cells with a rooting function in land plants. Science 316, 1477-1480.

Michel, G., Tonon, T., Scornet, D., Cock, J.M., Kloareg, B., 2010. Central and storage carbon metabolism of the brown alga *Ectocarpus siliculosus*: insights into the origin and evolution of storage carbohydrates in Eukaryotes. New Phytologist 188, 67-81.

Michiels, J., Xi, C., Verhaert, J., Vanderleyden, J., 2002. The functions of $Ca^{2+}$ in bacteria: a role for EF-hand proteins? Trends in microbiology 10, 87-93.

Mignerot, L., Avia, K., Luthringer, R., Lipinska, A.P., Peters, A.F., Cock, J.M., Coelho, S.M., 2019. A key role for sex chromosomes in the regulation of parthenogenesis in the brown alga *Ectocarpus*. PLoS genetics 15, e1008211.

Mignerot, L., Coelho, S.M., 2016. The origin and evolution of the sexes: Novel insights from a distant eukaryotic linage. C R Biol 339, 252-257.

Mizukami, A.G., Inatsugi, R., Jiao, J., Kotake, T., Kuwata, K., Ootani, K., Okuda, S., Sankaranarayanan, S., Sato, Y., Maruyama, D., Iwai, H., Garenaux, E., Sato, C., Kitajima, K., Tsumuraya, Y., Mori, H., Yamaguchi, J., Itami, K., Sasaki, N., Higashiyama, T., 2016. The AMOR arabinogalactan sugar chain induces pollen-tube competency to respond to ovular guidance. Curr Biol 26, 1091-1097.

Moller, I., Sørensen, I., Bernal, A.J., Blaukopf, C., Lee, K., Øbro, J., Pettolino, F., Roberts, A., Mikkelsen, J.D., Knox, J.P., 2007. High‐throughput mapping of cell‐wall polymers within and between plants using novel microarrays. The Plant Journal 50, 1118-1128.

Mollet, J.-C., Kim, S., Jauh, G.-Y., Lord, E.M., 2002. Arabinogalactan proteins, pollen tube growth, and the reversible effects of Yariv phenylglycoside. Protoplasma 219, 89-98.

Mosquna, A., Katz, A., Decker, E.L., Rensing, S.A., Reski, R., Ohad, N., 2009. Regulation of stem cell maintenance by the Polycomb protein FIE has been conserved during land plant evolution. Development 136, 2433-2444.

Motose, H., Sugiyama, M., Fukuda, H., 2001. An arabinogalactan protein (s) is a key component

of a fraction that mediates local intercellular communication involved in tracheary element differentiation of *zinnia* mesophyll cells. Plant and Cell Physiology 42, 129-137.

Motose, H., Sugiyama, M., Fukuda, H., 2004. A proteoglycan mediates inductive interaction during plant vascular development. Nature 429, 873.

Müller, D., 1974. Sexual reproduction and isolation of a sex attractant in *Cutleria multifida* (Smith) Grey.(Phaeophyta). Biochemie und Physiologie der Pflanzen 165, 212-215.

Müller, D., Jaenicke, L., Donike, M., Akintobi, T., 1971. Sex attractant in a brown alga: chemical structure. Science 171, 1132-1132.

Müller, D.G., 1964. Life-cycle of *Ectocarpus siliculosus* from Naples, Italy. Nature 203, 1402.

Müller, D.G., 1967. Generationswechsel, Kernphasenwechsel und Sexualität der Braunalge *Ectocarpus siliculosus* im Kulturversuch. Planta 75, 39-54.

Müller, D.G., Jaenicke, L., 1973. Fucoserraten, the female sex attractant of *Fucus serratus* L.(Phaeophyta). FEBS letters 30, 137-139.

Nam, J., Nei, M., 2005. Evolutionary change of the numbers of homeobox genes in bilateral animals. Molecular biology and evolution 22, 2386-2394.

Nasmyth, K., Shore, D., 1987. Transcriptional regulation in the yeast life cycle. Science 237, 1162-1170.

Nathan Hancock, C., Kent, L., McClure, B.A., 2005. The stylar 120 kDa glycoprotein is required for S‐specific pollen rejection in *Nicotiana*. The Plant Journal 43, 716-723.

Niklas, K.J., Kutschera, U., 2010. The evolution of the land plant life cycle. New Phytologist 185, 27-41.

Niklas, K.J., Newman, S.A., 2013. The origins of multicellular organisms. Evolution & development 15, 41-52.

Nishiyama, T., Fujita, T., Shin, T., Seki, M., Nishide, H., Uchiyama, I., Kamiya, A., Carninci, P., Hayashizaki, Y., Shinozaki, K., 2003. Comparative genomics of *Physcomitrella patens* gametophytic transcriptome and *Arabidopsis thaliana*: implication for land plant evolution. Proceedings of the National Academy of Sciences 100, 8007-8012.

Nyvall, P., Corre, E., Boisset, C., Barbeyron, T., Rousvoal, S., Scornet, D., Kloareg, B., Boyen, C., 2003. Characterization of Mannuronan C-5-Epimerase Genes from the Brown Alga *Laminaria digitata*. Plant Physiology 133, 726-735.

Ohad, N., Margossian, L., Hsu, Y.-C., Williams, C., Repetti, P., Fischer, R.L., 1996. A mutation that allows endosperm development without fertilization. Proceedings of the National Academy of Sciences 93, 5319-5324.

Ohad, N., Yadegari, R., Margossian, L., Hannon, M., Michaeli, D., Harada, J.J., Goldberg, R.B., Fischer, R.L., 1999. Mutations in *FIE*, a WD polycomb group gene, allow endosperm development without fertilization. The Plant Cell 11, 407-415.

Ohsawa, S., Yurimoto, H., Sakai, Y., 2017. Novel function of Wsc proteins as a methanol‐sensing machinery in the yeast *Pichia pastoris*. Molecular microbiology 104, 349-363.

Oide, S., Tanaka, Y., Watanabe, A., Inui, M., 2019. Carbohydrate-binding property of a cell wall integrity and stress response component (WSC) domain of an alcohol oxidase from the rice blast pathogen *Pyricularia oryzae*. Enzyme Microb Technol 125, 13-20.

Okano, Y., Aono, N., Hiwatashi, Y., Murata, T., Nishiyama, T., Ishikawa, T., Kubo, M., Hasebe, M., 2009. A polycomb repressive complex 2 gene regulates apogamy and gives evolutionary

insights into early land plant evolution. Proceedings of the National Academy of Sciences 106, 16321-16326.

Orr, H.A., Otto, S.P., 1994. Does diploidy increase the rate of adaptation? Genetics 136, 1475-1480.

Otto, S.P., Gerstein, A.C., 2008. The evolution of haploidy and diploidy. Current Biology 18, R1121-R1124.

Paciorek, T., Bergmann, D.C., 2010. The secret to life is being different: asymmetric divisions in plant development. Current opinion in plant biology 13, 661-669.

Parfrey, L.W., Lahr, D.J., Knoll, A.H., Katz, L.A., 2011. Estimating the timing of early eukaryotic diversification with multigene molecular clocks. Proceedings of the National Academy of Sciences 108, 13624-13629.

Park, M.H., Suzuki, Y., Chono, M., Knox, J.P., Yamaguchi, I., 2003. *CsAGP1*, a gibberellin-responsive gene from cucumber hypocotyls, encodes a classical arabinogalactan protein and is involved in stem elongation. Plant physiology 131, 1450-1459.

Paulsen, B.S., Craik, D.J., Dunstan, D.E., Stone, B.A., Bacic, A., 2014. The Yariv reagent: behaviour in different solvents and interaction with a gum arabic arabinogalactan-protein. Carbohydr Polym 106, 460-468.

Peng, H.B., Jaffe, L.F., 1976. Cell-wall formation in *Pelvetia* embryos. A freeze-fracture study. Planta 133, 57-71.

Pereira, L.G., Coimbra, S., Oliveira, H., Monteiro, L., Sottomayor, M., 2006. Expression of arabinogalactan protein genes in pollen tubes of *Arabidopsis thaliana*. Planta 223, 374-380.

Pereira, M.S., Mulloy, B., Mourão, P.A., 1999. Structure and anticoagulant activity of sulfated fucans. Comparison between the regular, repetitive, and linear fucans from echinoderms with the

more heterogeneous and branched polymers from brown algae. Journal of Biological Chemistry 274, 7656-7667.

Perrot, V., Richerd, S., Valéro, M., 1991. Transition from haploidy to diploidy. Nature 351, 315.

Peters, A.F., Marie, D., Scornet, D., Kloareg, B., Mark Cock, J., 2004a. Proposal of *Ectocarpus siliculosus* (Ectocarpales, Phaeophyceae) as a model organism for brown algal genetics and genomics. Journal of Phycology 40, 1079-1088.

Peters, A.F., Ramírez, M.E., 2001. Molecular phylogeny of small brown algae, with special reference to the systematic position of *Caepidium antarcticum* (Adenocystaceae, Ectocarpales). Cryptogamie Algologie 22, 187-200.

Peters, A.F., Scornet, D., Müller, D.G., Kloareg, B., Cock, J.M., 2004b. Inheritance of organelles in artificial hybrids of the isogamous multicellular chromist alga *Ectocarpus siliculosus* (Phaeophyceae). European journal of phycology 39, 235-242.

Peters, A.F., Scornet, D., Ratin, M., Charrier, B., Monnier, A., Merrien, Y., Corre, E., Coelho, S.M., Cock, J.M., 2008. Life-cycle-generation-specific developmental processes are modified in the immediate upright mutant of the brown alga *Ectocarpus siliculosus*. Development 135, 1503-1512.

Philip, B., Levin, D.E., 2001. Wsc1 and Mid2 are cell surface sensors for cell wall integrity signaling that act through Rom2, a guanine nucleotide exchange factor for Rho1. Molecular and cellular biology 21, 271-280.

Pina, C., Pinto, F., Feijó, J.A., Becker, J.D., 2005. Gene family analysis of the *Arabidopsis* pollen transcriptome reveals biological implications for cell growth, division control, and gene expression regulation. Plant physiology 138, 744-756.

Pohnert, G., Steinke, M., Tollrian, R., 2007. Chemical cues, defence metabolites and the shaping of pelagic interspecific interactions. Trends in Ecology & Evolution 22, 198-204.

Popper, Z.A., Bootten, T., Harris, P., Melton, L., Newman, R., 2011a. The Plant Cell Wall. Springer.

Popper, Z.A., Michel, G., Hervé, C., Domozych, D.S., Willats, W.G., Tuohy, M.G., Kloareg, B., Stengel, D.B., 2011b. Evolution and diversity of plant cell walls: from algae to flowering plants. Annual review of plant biology 62, 567-590.

Quatrano, R., 1997. Cortical asymmetries direct the establishment of cell polarity and the plane of cell division in the *Fucus* embryo, Cold Spring Harbor symposia on quantitative biology. Cold Spring Harbor Laboratory Press, pp. 65-70.

Quatrano, R.S., Stevens, P.T., 1976. Cell wall assembly in *Fucus* zygotes: I. Characterization of the polysaccharide components. Plant Physiology 58, 224-231.

Raper, J.R., Flexer, A.S., 1970. The road to diploidy with emphasis on a detour, Symp. Soc. Gen. Microbiol, pp. 401-432.

Raven, J.A., 2002. Selection pressures on stomatal evolution. New Phytologist 153, 371-386.

Reinhardt, D., Mandel, T., Kuhlemeier, C., 2000. Auxin regulates the initiation and radial position of plant lateral organs. The Plant Cell 12, 507-518.

Reyes-Prieto, A., Weber, A.P., Bhattacharya, D., 2007. The origin and establishment of the plastid in algae and plants. Annu. Rev. Genet. 41, 147-168.

Richerd, S., Couvet, D., Valéro, M., 1993. Evolution of the alternation of haploid and diploid phases in life cycles. II. Maintenance of the haplo‐diplontic cycle. Journal of Evolutionary Biology 6, 263-280.

Roberts, K., Phillips, J., Hills, G., 1974. Structure, composition and morphogenesis of the cell wall of *Chlamydomonas reinhardii*. VI. The flagellar collar. Micron (1969) 5, 341-357.

Roe, K.E., 1975. Origin of the alternation of generations in plants: reconsideration of the traditional theories. Biologist.

Rosenfeld, J., Capdevielle, J., Guillemot, J.C., Ferrara, P., 1992. In-gel digestion of proteins for internal sequence analysis after one-or two-dimensional gel electrophoresis. Analytical biochemistry 203, 173-179.

Russell, G., 1967. The ecology of some free-living Ectocarpaceae. Helgoländer wissenschaftliche Meeresuntersuchungen 15, 155.

Sakai, T., Ishizuka, K., Shimanaka, K., Ikai, K., Kato, I., 2003. Structures of oligosaccharides derived from *Cladosiphon okamuranus* fucoidan by digestion with marine bacterial enzymes. Marine Biotechnology 5, 536-544.

Sakakibara, K., Ando, S., Yip, H.K., Tamada, Y., Hiwatashi, Y., Murata, T., Deguchi, H., Hasebe, M., Bowman, J.L., 2013. *KNOX2* genes regulate the haploid-to-diploid morphological transition in land plants. Science 339, 1067-1070.

Sano, R., Juárez, C.M., Hass, B., Sakakibara, K., Ito, M., Banks, J.A., Hasebe, M., 2005. *KNOX* homeobox genes potentially have similar function in both diploid unicellular and multicellular meristems, but not in haploid meristems. Evolution & development 7, 69-78.

Schiefthaler, U., Balasubramanian, S., Sieber, P., Chevalier, D., Wisman, E., Schneitz, K., 1999. Molecular analysis of *NOZZLE*, a gene involved in pattern formation and early sporogenesis during sex organ development in *Arabidopsis thaliana*. Proceedings of the National Academy of Sciences 96, 11664-11669.

Schmidt-Nielsen, K., 1997. Animal physiology: adaptation and environment. Cambridge University Press.

Schmidt, E.D., de Jong, A.J., de Vries, S.C., 1994. Signal molecules involved in plant embryogenesis. Plant molecular biology 26, 1305-1313.

Schoenwaelder, M.E., Wiencke, 2000. Phenolic compounds in the embryo development of several northern hemisphere fucoids. Plant Biology 2, 24-33.

Schultz, C., Gilson, P., Oxley, D., Youl, J., Bacic, A., 1998. GPI-anchors on arabinogalactan-proteins: implications for signalling in plants. Trends in Plant Science 3, 426-431.

Seifert, G.J., Roberts, K., 2007. The biology of arabinogalactan proteins. Annu. Rev. Plant Biol. 58, 137-161.

Seifert, G.J., Xue, H., Acet, T., 2014. The *Arabidopsis thaliana FASCICLIN LIKE ARABINOGALACTAN PROTEIN* 4 gene acts synergistically with abscisic acid signalling to control root growth. Ann Bot 114, 1125-1133.

Shaw, A.J., Szövényi, P., Shaw, B., 2011. Bryophyte diversity and evolution: windows into the early evolution of land plants. American Journal of Botany 98, 352-369.

Shepherd, J.C., McGinnis, W., Carrasco, A.E., De Robertis, E.M., Gehring, W.J., 1984. Fly and frog homoeo domains show homologies with yeast mating type regulatory proteins. Nature 310, 70.

Shevell, D.E., Kunkel, T., Chua, N.-H., 2000. Cell wall alterations in the *Arabidopsis emb30* mutant. The Plant Cell 12, 2047-2059.

Shevell, D.E., Leu, W.-M., Gillmor, C.S., Xia, G., Feldmann, K.A., Chua, N.-H., 1994. *EMB30* is essential for normal cell division, cell expansion, and cell adhesion in *Arabidopsis* and encodes a protein that has similarity to Sec7. Cell 77, 1051-1062.

Shi, H., Kim, Y., Guo, Y., Stevenson, B., Zhu, J.-K., 2003. The *Arabidopsis SOS5* locus encodes a putative cell surface adhesion protein and is required for normal cell expansion. The Plant Cell 15, 19-32.

Silberfeld, T., Leigh, J.W., Verbruggen, H., Cruaud, C., de Reviers, B., Rousseau, F., 2010. A multi-locus time-calibrated phylogeny of the brown algae (Heterokonta, Ochrophyta, Phaeophyceae): Investigating the evolutionary nature of the “brown algal crown radiation”. Molecular Phylogenetics and Evolution 56, 659-674.

Silberfeld, T., Rousseau, F., de Reviers, B., 2014. An updated classification of brown algae (Ochrophyta, Phaeophyceae). Cryptogamie, Algologie 35, 117-157.

Simpson, A.G., Inagaki, Y., Roger, A.J., 2005. Comprehensive multigene phylogenies of excavate protists reveal the evolutionary positions of “primitive” eukaryotes. Molecular Biology and Evolution 23, 615-625.

Sontag, J.-M., Nunbhakdi-Craig, V., White, C.L., Halpain, S., Sontag, E., 2012. The protein phosphatase PP2A/Bα binds to the microtubule-associated proteins tau and MAP2 at a motif also recognized by the kinase fyn implications for tauopathies. Journal of Biological Chemistry 287, 14984-14993.

Starr, R.C., 1978. The culture collection of algae at the university of texas at austin Journal of phycology 14, 47-100.

Stebbins, G., Hill, G., 1980. Did multicellular plants invade the land? The American Naturalist 115, 342-353.

Steenstrup, J.J.S., 1845. On the alternation of generations; or the propagation and development of animals through alternate generations. Ray society.

Szövényi, P., Rensing, S.A., Lang, D., Wray, G.A., Shaw, A.J., 2010. Generation-biased gene expression in a bryophyte model system. Molecular Biology and Evolution 28, 803-812.

Szövényi, P., Ricca, M., Hock, Z., Shaw, J.A., Shimizu, K.K., Wagner, A., 2013. Selection is no more efficient in haploid than in diploid life stages of an angiosperm and a moss. Molecular biology and evolution 30, 1929-1939.

Tan, L., Showalter, A.M., Egelund, J., Hernandez-Sanchez, A., Doblin, M.S., Bacic, A.F., 2012. Arabinogalactan-proteins and the research challenges for these enigmatic plant cell surface proteoglycans. Frontiers in Plant Science 3, 140.

ten Hove, C.A., Heidstra, R., 2008. Who begets whom? Plant cell fate determination by asymmetric cell division. Current opinion in plant biology 11, 34-41.

Trivers, R.L., Hare, H., 1976. Haploidploidy and the evolution of the social insect. Science 191, 249-263.

Umen, J.G., 2014. Green algae and the origins of multicellularity in the plant kingdom. Cold Spring Harbor perspectives in biology 6, a016170.

Valero, M., Richerd, S., Perrot, V., Destombe, C., 1992. Evolution of alternation of haploid and diploid phases in life cycles. Trends in Ecology & Evolution 7, 25-29.

van Heeckeren, W.J., Dorris, D.R., Struhl, K., 1998. The mating-type proteins of fission yeast induce meiosis by directly activating mei3 transcription. Molecular and cellular biology 18, 7317-7326.

Van Hengel, A.J., Roberts, K., 2003. AtAGP30, an arabinogalactan ‐ protein in the cell walls of the primary root, plays a role in root regeneration and seed germination. The Plant Journal 36, 256-270.

van Hengel, A.J., Tadesse, Z., Immerzeel, P., Schols, H., Van Kammen, A., de Vries, S.C., 2001. N-acetylglucosamine and glucosamine-containing arabinogalactan proteins control somatic embryogenesis. Plant Physiology 125, 1880-1890.

Van Hengel, A.J., Van Kammen, A., De Vries, S.C., 2002. A relationship between seed development, arabinogalactan ‐ proteins (AGPs) and the AGP mediated promotion of somatic embryogenesis. Physiologia Plantarum 114, 637-644.

Verhaeghe, E.F., Fraysse, A., Guerquin-Kern, J.-L., Wu, T.-D., Devès, G., Mioskowski, C., Leblanc, C., Ortega, R., Ambroise, Y., Potin, P., 2008. Microchemical imaging of iodine distribution in the brown alga *Laminaria digitata* suggests a new mechanism for its accumulation. JBIC Journal of Biological Inorganic Chemistry 13, 257-269.

Wawra, S., Fesel, P., Widmer, H., Neumann, U., Lahrmann, U., Becker, S., Hehemann, J.H., Langen, G., Zuccaro, A., 2019. FGB1 and WSC3 are in planta-induced *beta*-glucan-binding fungal lectins with different functions. New Phytol 222, 1493-1506.

Willson, M.F., 1981. On the evolution of complex life cycles in plants: a review and an ecological perspective. Annals of the Missouri Botanical Garden, 275-300.

Woelkerling, W.J., 2004. Biologie et phylogénie des algues. Taylor & Francis.

Wu, H.-m., Wang, H., Cheung, A.Y., 1995. A pollen tube growth stimulatory glycoprotein is deglycosylated by pollen tubes and displays a glycosylation gradient in the flower. Cell 82, 395-403.

Wu, H.m., Wong, E., Ogdahl, J., Cheung, A.Y., 2000. A pollen tube growth ‐ promoting arabinogalactan protein from *Nicotiana alata* is similar to the tobacco TTS protein. The Plant Journal 22, 165-176.

Xu, J., Tan, L., Lamport, D.T., Showalter, A.M., Kieliszewski, M.J., 2008. The O-Hyp glycosylation code in *tobacco* and *Arabidopsis* and a proposed role of Hyp-glycans in secretion. Phytochemistry 69, 1631-1640.

Yadegari, R., Drews, G.N., 2004. Female gametophyte development. The Plant Cell 16, S133-S141.

Yang, J., Showalter, A.M., 2007. Expression and localization of AtAGP18, a lysine-rich arabinogalactan-protein in *Arabidopsis*. Planta 226, 169-179.

Yang, Z., Fu, Y., 2007. ROP/Rac GTPase signaling. Current opinion in plant biology 10, 490-494.

Yoon, H.S., Ciniglia, C., Wu, M., Comeron, J.M., Pinto, G., Pollio, A., Bhattacharya, D., 2006. Establishment of endolithic populations of extremophilic Cyanidiales (Rhodophyta). BMC Evolutionary Biology 6, 78.

Zeyl, C., Vanderford, T., Carter, M., 2003. An evolutionary advantage of haploidy in large yeast populations. Science 299, 555-558.

Zhong, W., Chia, W., 2008. Neurogenesis and asymmetric cell division. Current opinion in neurobiology 18, 4-11.

Zsebo, K.M., Wypych, J., McNiece, I.K., Lu, H.S., Smith, K.A., Karkare, S.B., Sachdev, R.K., Yuschenkoff, V.N., Birkett, N.C., Williams, L.R., Satyagal, V.N., Tung, W., Bosselman, R.A., Mendiaz, E.A., Langley, K.E., 1990. Identification, purification, and biological characterization of hematopoietic stem cell factor from buffalo rat liver-conditioned medium. Cell 63, 195-201.

# Annexe 1

# Development of a protocol for the purification of the sporophyte-inducing factor

The sporophyte-inducing factor is secreted into the culture medium by *Ectocarpus* sporophytes and has its effect on the cell fate of gametophyte initial cells, i.e. meio-spores. To characterise the factor and investigate the pathway it induces, it was important to establish an isolation and purification protocol for the sporophyte-inducing factor. This was the main task of my thesis work. Several approaches were tried to purify the diffusible factor. These experiments were not successful in the sense that they did not allow the isolation of a pure fraction of the diffusible factor. However, the methodology that was developed will be of interest for future attempts to isolate the factor. We have therefore described the protocols used in this section and discuss possible reasons why the experiments carried out were unsuccessful.

## Introduction

Many brown algae have been shown to produce sex attractants. These molecules are secreted by female gametes and attractant the male motile gametes. Several of these diffusible factors have been purified and characterised biochemically, including the sex pheromones of *Ectocarpus siliculosus*, *Cutleria multifida* and *Fucus serratus* (Müller, 1974; Müller et al., 1971; Müller and Jaenicke, 1973). These pheromones were isolated using gas chromatography combined with a bioassay for activity and identified by mass spectrometry and/or nuclear magnetic resonance (CMR). By analogy to these studies, our aim was to purify and characterise the diffusible factor that induces switching from the gametophyte to the sporophyte developmental program (Arun et al., 2013).

Several approaches were tested to purify the sporophyte-inducing factor, starting with large amounts of sporophyte condition medium (SCM). The approaches used were inspired by earlier work, such as that carried out on the hematopoietic stem cell factor from rat liver-condition medium (Zsebo et al., 1990). The first major step of all purification protocols was ultrafiltration, which was used to concentrate the factor and partially purify by size fractionation. This was followed by size exclusion or ion exchange chromatography, or a combination of these two approaches, depending on the experiment. The bioactivity of the sporophyte-inducing factor decreased after ultrafiltration and further loss of activity was observed following subsequent, column-based purification steps. These observations indicated loss of the factor during sequential purification steps and this was one of the factors that complicated the development of the purification procedure. In the following, we will describe the details of the procedures used to attempt to isolate the sporophyte-inducing factor and discuss possible reasons for their failure.

## Protocols

### Ultrafiltration of SCM

Before ultra-filtration, 40 L of SCM was filtered through a 0.22 µm filtration system (Stericup and Steritop, 500 ml Millipore Express PLUSE 0.22 µm PES). A large volume of SCM was

filtered in lots of 5 L, which was filtered in batches of 500 ml at room temperature and then returned to the cold room.

An ÄKTA$^{TM}$ flux (GE Healthcare BjÖrkgatan, Sweden) with a UFP-50-C-MM01A cartridge (for a 26 cm² membrane) was used to ultra-filtrate 40 L of SCM with a 50 kDa cut-off at room temperature (with SCM being kept on ice prior to filtering). To filter 10 L of SCM, the liquid was fed in aliquots from a reservoir into the starting reservoir so that there was a constant volume of about 300 ml in the latter, which was cycled through the filter resin, with <50kDa filtrate being collected during the cycling. When the first 10 L had been fed into the starting reservoir, the second batch of 10 L was added if necessary and the filtering continued. After all the SCM had been fed through the system and reduced to 200 ml, filtering was continued until the final volume of the retentate was reduced to 100 ml. This process took a considerable amount of time at room temperature (1-2L/days) and there was therefore potential problems with bacterial growth. The >50kDa molecules were concentrated in the retentate were designated uf-SCM for ultrafiltrated SCM (≡ 400x SCM).

**Size Exclusion Chromatography**

The following procedure was carried out three times using a total of 15ml uf-SCM ≡ 400x SCM: injected 5 ml of uf-SCM onto a Size Exclusion Chromatography (SEC) system consisting of a guard-column (26x120mm, Superdex 30 ® GE healthcare BjÖrkgatan, Sweden) and three columns of Superdex 30 (26x600mm, Superdex®30 GE healthcare BjÖrkgatan, Sweden) with a flow rate of 1ml.min-1 and eluted with 50 mM (pH 9.8) ammonium carbonate buffer (buffer run through 0.22 µm filter before use). Each run took 1200 min. The peak of concentration measured as IR was between 350- and 500-min. Fractions of 11 ml were collected between 300 and 1000 min of elution (about 62 fractions) and fractions 6 to 13 (which had the maximum IR signal) were pooled for further analysis. Fractions 6-13, pooled from all three runs, were then split into 3 batches: one for an SDS-PAGE (sodium dodecyl sulfate-polyacrylamide gel electrophoresis)/Yariv test (Zsebo et al., 1990), one for a bioassay and the third batch for IEX purification. Each of the 3 batches of pooled 6-13 fractions was freeze-dried (in lots of about 7 ml

in 15ml Falcon tubes and then the dry powder pooled for each of the three batches). The powder was not weighed, but the weight of 15ml 100x uf-SCM after SEC was about 0.1206g.

**Desalting of ultrafiltrated SCM for ion exchange chromatography**

Small volumes of uf-SCM were loaded onto PD-10 (8.3 ml of Sephadex™ G-25 Medium) desalting columns to remove the salt in the sample. For large volumes of SCM, desalting was carried out by dialysis. One hundred millilitres of uf-SCM (400x SCM) was dialysed in cellulose dialysis tubing membrane (12-14 kD, Spectra/Por® 2 dialysis membrane tubing, Repligen) in 5 L of MilliQ water at 4°C with rotation at 300 rpm for 36 hours and replacement of the MilliQ water every 6h. After dialysis, samples were separated into four 50 ml falcons and freeze-dried to allow the lyophilised sample to be resuspended in a chosen buffer. Ads-SCM named for ultrafiltrated medium after dialysis and dissolved in anion exchange start buffer.

**Ion Exchange purification**

The candidate protein Ec-20_004700.1 (Mannuronan C-5-epimerase 4, 886 AAs, 93 kDa protein) had a calculated pI of 3.88. Based on this, separation using cation exchange chromatography (Akta system, 1 ml S type column) was attempted to purify the factor, with a NaCl gradient and an elution buffer pH value around 1.48 (at least 1 unit lower than the protein pI).

**Cation exchange purification**

Cation exchange buffers: Start buffer: citrate buffer (20 mM, pH 1.49), Elution buffer: citrate buffer (20 mM, pH 1.49) +1M NaCl. Stock buffer A: 0.1 M solution of citric acid (2.10 g in 100 ml MilliQ H2O); stock buffer B: 0.1 M solution of sodium citrate (2.94 g in 100 ml MilliQ H2O). Citrate buffer is made by mixing 46.5 ml stock buffer A with 3.5ml stock buffer B and then adding MilliQ H2O up to 500 ml (20 mM, pH 1.49). Add 14.61 g NaCl to 250 ml citrate buffer to make the elution buffer.

The AKTA Purifier system includes a P 903 pump, which has a module A (A1 and A2 inlet tubing for start buffer) and a module B (B1 and B2 inlet tubing for elution buffer); normally only

use A1 and B1. An AM-925 mixer motor inside the housing spins a magnet at 600 rpm, causing the stirrer in the mixing chamber to rotate. An in-line filter (a 2 µm depth type filter) is fitted between the outlet of the Mixer M-925 and position 7 of the injection valve (an arrow on the in-line filter indicates the flow direction). Other components include an injection valve, a super loop, a UV-900 monitor, a pH/conductivity meter, a flow restrictor and a Frac-901 fraction collector.

General preparation: all solutions must be filtered through a 0.2 µm filter (unless they have already been through the SE column) and degassed. Check that there is no air in the inlet tubing and that the waste bottle is empty.

To start the system: after turning on the separation unit and logging on, the connection will be established automatically and will open 4 windows: the system Control, the result, etc. Immerse inlet tubing A1 and B1 in MilliQ H2O to clean the pump and column, because they are stored in 20% EtOH. Run the system from the computer as follows: System Control - Manual - Pump - Pumpwash purifier- A1 and B1 on – Inset; Alarm & Mon –Alarm pressure – High Alarm – 0.5 mPa – Inset – executer (use a syringe to take some water out of the pump, remove any air in the pump. Only do this once, every morning). Wash the column by setting the manual – pump –flow – 1 ml/min – inset – execute, wait about 5 min until the UV signal becomes stable. After changing the flow rate to low (0.3 ml/min), fit the HiTrapTm 1 ml CM-FF column (cation exchange column) onto the system without introducing bubbles. Let the system run for about 5 min at 1 ml/min until the UV is stable, wash the loop with 20 ml MilliQ H2O, set the flow rate to 0 ml/min and click end to stop this run. After immersing inlet tubing A1 and B1 in start buffer and elution buffer, respectively, start a new run to wash the pump and the column. First clean with start buffer (System Control - Manual – Pump – flow – 1 ml/min – inset, Alarm & Mon – Alarm pressure – High Alarm – 0.5 mPa – Inset – executer). When the UV signal is stable, set out zero UV and change to elution buffer wash (System Control - Manual – Pump – Gradient 100 B% (start buffer + 1 M NaCl) – Inset – Executer) for about 5 min then change back to start buffer and wash the loop with 6 ml of start buffer. Finally, stop the run, and start a new run to wash a second time if the pressure is very variable.

Sample application: loaded 2ml of desalted sample in cation buffer into the loop and started a new run of about 5 min to inject the sample to the column (Flow pash – Injection value – Inject – Inset - Execute). When the UV was stable, pumped cation start buffer onto the column for 10 min (collected flow-through in a bottle), then gradually diluted the cation start buffer with cation elution buffer (100% start buffer > 100% elution buffer gradient: Manual – Pump – Gradient – Gradient 100 B% –10 min, 1 ml/min – inset, Frac – Fraction 900 – Flacsize – 1 ml/min – inset – executer) over a period of 10 min, collected ten 1 ml fractions, then continued to pump elution buffer for 5 min (collected this final elution in the same bottle as the flow-through).

Cleaning the system after use: When the separation is finished, successively immerse A1 and B1 in MilliQ H2O and 20% EtOH, to clean the system and store in 20% EtOH.

### Anion exchange purification

Anion exchange buffers: Start buffer—Tris buffer (20 mM, pH 7.89), Elution buffer—Tris buffer (20 mM, pH 7.89) + 1 M NaCl. Stock buffer A (Tris buffer): 0.2 M solution of tris (hydroxymethyl) aminomethane (2.42 g in 100 ml MilliQ H2O); stock buffer B (Tris buffer): 0.2 M HCl (1.67 ml Hydrochloric acid fuming 37% in 100 ml MilliQ H2O). Tris buffer is made by mixing 12.5 ml stock buffer A with 11.05 ml stock buffer B and then adding MilliQ H2O up to 500 ml (20 mM, pH 7.89). Add 14.61 g NaCl to 250 ml Tris buffer to make the elution buffer.

General preparation and sample application were as for cation exchange (but replaced HiTrapTm 1 ml CM-FF with HiTrap$^{Tm}$ 1 ml Q-FF anion exchange column).

## Results of the diffusible factor purification experiments

### Experiment 1. Size exclusion chromatography

A first experiment was carried out to test the utility of size exclusion chromatography to fractionate the SCM. SCM was first subjected to ultrafiltration to increase the concentration of the sporophyte-inducing factor. When the SCM concentrated ultrafiltration retentate (designated uf-SCM) was diluted to a concentration equivalent to the initial SCM and bioassayed using meio-

spores, diffusible factor activity was detected but the activity was reduced compared to the original SCM (Fig. 1). This indicated that at least a proportion of the diffusible factor was still present after ultrafiltration. The uf-SCM was then subjected to size exclusion chromatography and a large molecular weight peak was detected between 330 and 450 min (Fig. 1A). The fractions corresponding to this peak (which were pooled and designated sec-SCM) contained the sporophyte-inducing diffusible factor activity (Fig. 1B). This experiment established a protocol for size exclusion chromatography of SCM and showed that active fractions could be recovered after chromatography. However, given the deduced size of the diffusible factor (based on ultrafiltration experiments, chapter Ⅱ) size exclusion chromatography is unlikely to allow isolation of the factor in a pure state unless coupled with another approach. We therefore carried out a second experiment to test the usefulness of ion exchange chromatography for purification of the factor.

**Experiment 2. Ion exchange chromatography**

A second experiment was carried out to determine whether ion exchange chromatography represented a useful method to fractionate the SCM. For this, SCM was pretreated by ultrafiltration, dialysis and freeze-drying before resuspending the sample in anion exchange start buffer for the separation step. During the anion exchange chromatography, the flow-through and a series of elution fractions were collected. Three peaks of UV signal were detected in the elution (Fig. 2). The fractions corresponding to these three peaks were designated ax2-SCM, ax3-SCM, and ax10-SCM. The starting SCM used for this experiment had a low level of diffusible factor activity and the meio-spore bioassays exhibited a high level of variance, making it difficult to follow the presence of the diffusible factor during the purification (Fig. 2). Therefore, whilst all the fractions tested exhibited higher activity than the PES control, only the SCM sample had significantly higher activity and no conclusions could be drawn from the analysis of the other fractions. In parallel, the various fractions were also analysed by SDS-PAGE but no proteins bands were detected after Commaisse blue staining (left panel, Fig. 3). Large molecular weight bands were detected in some fractions by silver staining (right panel, Fig. 3) but they were not in the expected size range.

In general, the difficulties encountered with the detection of the diffusible factor in these purification experiments may have been because the initial concentration of the factor was low or because the sporophyte-inducing factor was lost (adsorbed to surfaces during purification) or degraded during the experiments. Furthermore, if the factor consists of both large (>50 kDa) and small molecules (<50 kDa) some activity may have been lost during the ultrafiltration step. In conclusion, as a result of the difficulties with the bioassay, it was not possible to evaluate definitively whether the purification protocol had worked. One problem with both purification protocol is that the concentration step takes a long time to complete. Development of a method to efficiently concentrate the diffusible factor would facilitate detection of the factor in the meio-spore bioassay and should improve the detection of activity in anion exchange fractions.

Finally, we proposed that the sporophyte-inducing factor may be a glycoprotein or polysaccharide in the previous chapter (chapter II). If this hypothesis is correct, we may be able to apply lectin affinity chromatography (Gleeson et al., 1979) to isolate the diffusible factor. Indeed, any additional information about the nature of the diffusible factor would be helpful for developing a purification protocol. Future work should focus on developing large volume production of the diffusible factor, improving the bioassay and chemically characterising the diffusible factor.

## References

Gleeson, P.A., Jermyn, M.A., Clarke, A.E., 1979. Isolation of an arabinogalactan protein by lectin affinity chromatography on tridacnin-sepharose 4B. Analytical biochemistry 92, 41-45.

Müller, D., 1974. Sexual Reproduction and Isolation of a Sex Attractant in *Cutleria multijida* (Smith) Grey.(Phaeophyta). Biochemie und Physiologie der Pflanzen 165, 212-215.

Müller, D., Jaenicke, L., Donike, M., Akintobi, T., 1971. Sex attractant in a brown alga: chemical structure. Science 171, 1132-1132.

Müller, D.G., Jaenicke, L., 1973. Fucoserraten, the female sex attractant of *Fucus serratus* L.(Phaeophyta). FEBS letters 30, 137-139.

Zsebo, K.M., Wypych, J., McNiece, I.K., Lu, H.S., Smith, K.A., Karkare, S.B., Sachdev, R.K., Yuschenkoff, V.N., Birkett, N.C., Williams, L.R., 1990a. Identification, purification, and biological characterization of hematopoietic stem cell factor from buffalo rat liver-conditioned medium. Cell 63, 195-201.

Zsebo, K.M., Wypych, J., McNiece, I.K., Lu, H.S., Smith, K.A., Karkare, S.B., Sachdev, R.K., Yuschenkoff, V.N., Birkett, N.C., Williams, L.R., Satyagal, V.N., Tung, W., Bosselman, R.A., Mendiaz, E.A., Langley, K.E., 1990b. Identification, purification, and biological characterization of hematopoietic stem cell factor from buffalo rat liver-conditioned medium. Cell 63, 195-201.

## Figures

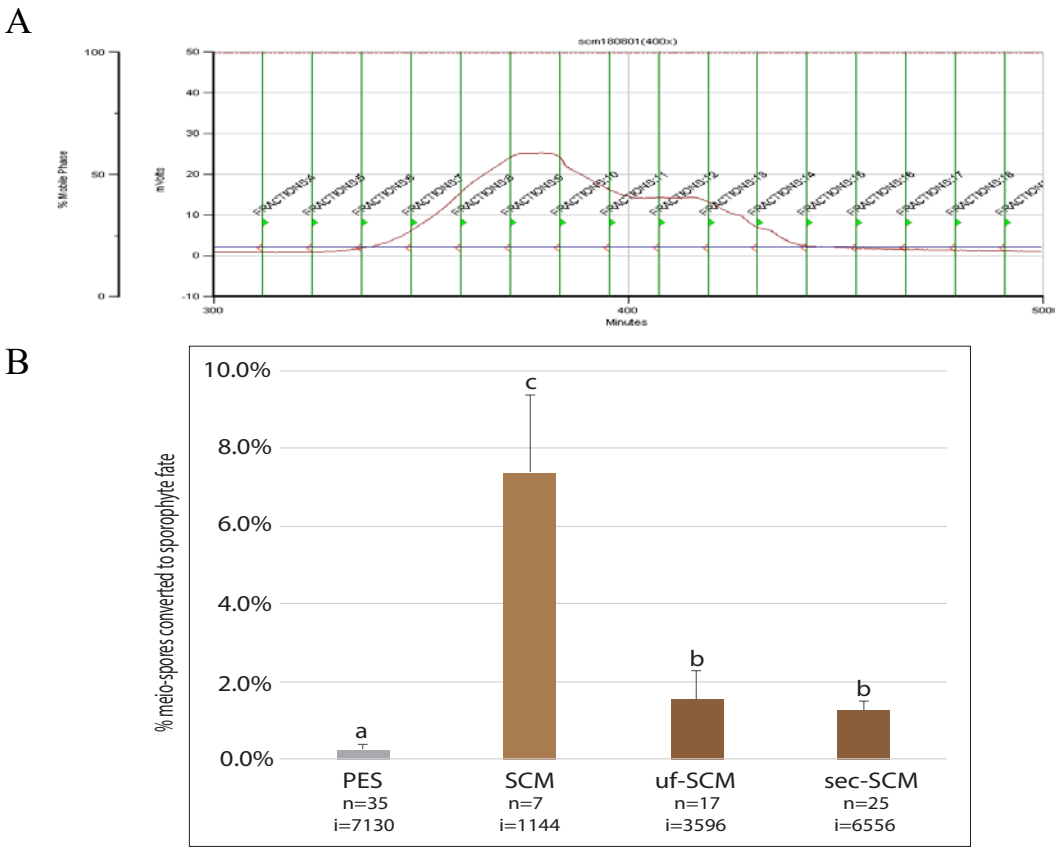


**Figure 1. Separation of ultrafiltrated SCM by size exclusion chromatography.** A. Detection of a high molecular weight peak in elution fractions. B. Bioassay of the pooled size exclusion chromatography fractions corresponding to the high molecular weight peak after diluting to a concentration equivalent to 1x SCM. Error bars indicated standard error of the mean, letters above bars indicated significant differences (p-value <0.05). PES, Provasoli-enriched natural seawater; SCM, sporophyte-condition medium; uf-SCM, ultrafiltrated sporophyte condition medium; sec-SCM, high molecular weight peak fractions of ultrafiltrated sporophyte condition medium after separation by size exclusion chromatography; n, number of replicates; i, number of individual germlings counted.

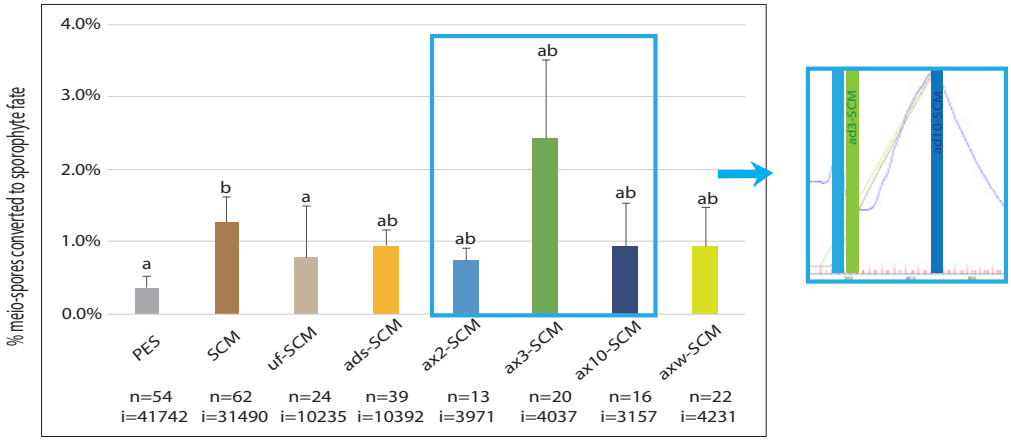


**Figure 2. Separation of SCM by anion exchange chromatography.** Fractions taken at each step of the purification protocol were tested using the meio-spores bioassay. All samples were diluted to a concentration equivalent to 1x SCM before carrying out the bioassays. Error bars indicated standard error of the mean, letters above bars indicated significant differences ($p$-value<0.05). PES, Provasoli-enriched natural seawater; SCM, sporophyte-condition medium; uf-SCM, ultrafiltrated sporophyte condition medium; ads-SCM, ultrafiltrated medium after dialysis, dissolved in anion exchange start buffer; ax2-SCM, second fraction eluted from anion exchange column; ax3-SCM, third fraction eluted from anion exchange column; ax10-SCM, tenth fraction eluted from anion exchange column; axw-SCM, flow through from the anion exchange column; n, number of replicates; i, number of individual germlings counted.

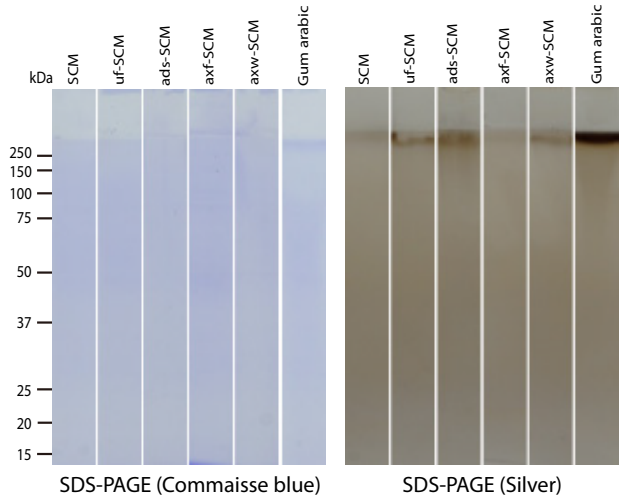


**Figure 3. Fractions collected during the anion exchange experiment run on SDS-PAGE.** Samples were separated by sodium dodecyl sulfate-polyacrylamide gel electrophoresis (SDS-PAGE) and stained with Commaisse blue or silver stain. SCM, sporophyte condition medium; uf-SCM, ultrafiltrated sporophyte condition medium; ads-SCM, ultrafiltrated medium after dialysis, dissolved in anion exchange start buffer; axf-SCM, pooled fractions eluted from the anion exchange column; axw-SCM, flow through from the anion exchange column.

# Annexe 2

## Résumé en français

La plupart des organismes eucaryotes se reproduisent sexuellement *via* deux processus importants: la méiose, qui produit des cellules haploïdes, et la syngamie, qui forme les zygotes par fusion de deux cellules haploïdes (gamètes). Selon la phase durant laquelle les divisions mitotiques se produisent, i.e., la phase haploïde, diploïde ou les deux phases du cycle de vie (Arun, 2012; Coelho et al., 2007; Perrot et al., 1991; Richerd et al., 1993; Valero et al., 1992), les cycles du vie ont été classés en trois types principaux: diploïdes (ou diplontiques), haploïdes (ou haplontiques) et haplo-diplontiques. Chez les organismes photosynthétiques au cycle de vie haplo-diplontique, deux générations multicellulaires distinctes s'alternent: le gamétophyte haploïde et le sporophyte diploïde.

Comme les générations de gamétophytes et de sporophytes sont construites à partir d'informations provenant d'un génome commun, il s'ensuit que les processus de régulation épigénétique doivent fonctionner à la fois pendant la méiose et pendant la syngamie, afin de déclencher le programme de développement approprié. L'expression différentielle des gènes au cours du cycle de vie produit un nombre important de gènes spécifiquement exprimés chez le gamétophyte ou chez le sporophyte (Dolan, 2009; Langdale, 2008; Mosquna et al., 2009; Okano et al., 2009). Par exemple, chez les espèces tels que *Ectocarpus* sp. et *Scytosiphon lomentaria*, les gènes spécifiquement exprimés chez le gamétophyte (20-23% du génome) sont plus nombreux que ceux exprimés spécifiquement chez le sporophyte (12-13% du génome), tandis que les gènes différentiellement exprimés chez le gamétophyte sont moins nombreux que ceux différentiellement exprimés chez le sporophyte chez les Laminariales (14-17% et 16-19% du génome, respectivement, de *Macrocystis pyrifera* et *Saccharina japonica*), *Funaria hygrometrica* (2.5% pour le gamétophyte et 5% pour le sporophyte) et *A. thaliana* (5% pour le gamétophyte et 25% pour le sporophyte) (Haerizadeh et al., 2009; Honys and Twell, 2003; Ma et al., 2008; Pina et al., 2005). L'expression différentielle des gènes au cours des cycles de vie haplo-diploïdes est souvent associée à des différences marquées dans la morphologie et les fonctions des générations de gamétophytes et de sporophytes. Le rôle des gènes à biais générationnel dans la médiation de ces différences morphologiques et fonctionnelles font l'objet d'études approfondies (Shaw et al., 2011; Szövényi et al., 2010).

Comme nous l'avons vu plus haut, chez de nombreux organismes, les générations de gamétophytes et de sporophytes sont morphologiquement et fonctionnellement différentes, de sorte que les changements de développement doivent être contrôlés avec précision pour éviter la production d'organismes chimériques. L'analyse génétique de l'alternance du cycle de vie chez ces organismes améliorera notre compréhension au niveau moléculaire de l'alternance des générations. Les premières preuves du contrôle génétique d'une transition entre générations d'un cycle de vie ont été rapportées pour un champignon unicellulaire, la levure *Saccharomyces cerevisiae*. Les gènes de type mating-type MATα2 et MATa1 produisent les protéines α2 et a1 qui se lient aux gènes spécifiques de l'haploïde et les répriment (Goutte and Johnson, 1988). α2 est homologue de protéines homéodomaines chez la *Drosophila* (Shepherd et al., 1984). Des systèmes similaires, impliquant également des régulateurs homéodomaine, ont été décrits dans d'autres champignons comme *Ustilago maydis* (Gillissen et al., 1992), *Coprinus cinereus* et le pathogène humain *Cryptococcus neoformans* (Kües et al., 1992). Le système d'accouplement de *Cryptococcus neoformans* a été particulièrement bien décrit. Chez les plantes à fleurs, *Arabidopsis* et la mousse *Physcomitrella patens* ont été utilisés pour étudier la régulation du cycle de vie, avec quelques limitations cependant. Le gamétophyte *d'Arabidopsis* est fortement dépendant de sa génération sporophytique, et aucun mutant affecté dans l'alternance des deux générations n'a encore été décrit chez *Physcomitrella patens*. Les algues marines font partie de la plupart des lignées de l'arbre phylogénétique eucaryotes et ont joué un rôle important dans l'évolution de la vie multicellulaire. Par conséquent, ces organismes offrent l'opportunité d'aborder diverses questions concernant l'origine et l'évolution des caractères eucaryotes généraux. La majorité des algues brunes ont un cycle de vie haplo-diploïde. Le génome d'une algue brune est devenu disponible ces dernières années (Cock et al., 2010). *Ectocarpus* a depuis émergé comme modèle biologique pour les algues brunes (Peters et al., 2004). De nombreux outils génétiques et génomiques sont disponibles pour *Ectocarpus*, y compris une annotation génomique de haute qualité (Cock et al., 2010; Cormier et al., 2017), des données transcriptomiques basées sur des puces à ADN (Dittami et al., 2009) et des technologies de séquençage des ARN (Ahmed et al., 2014; Luthringer et al., 2015; Macaisne et al., 2017), des cartes génétiques basées à la fois sur des marqueurs microsatellites (Heesch et al., 2010) et des marqueurs de séquençage de l'ADN associé à un site de restriction (Avia et al., 2017) et sur des

méthodes génétiques avancées (Godfroy et al., 2017). Ces caractéristiques ont fait *d'Ectocarpus* un bon choix en tant qu'organisme modèle fournissant un nouveau système pour étudier les processus de développement tels que les mécanismes de régulation qui contrôlent le cycle de vie au niveau moléculaire (Mignerot and Coelho, 2016; Peters et al., 2004a). Les travaux actuels ont montré que l'alternance des générations chez *Ectocarpus* est également contrôlée par deux facteurs de transcription à homéodomaine, ORO et SAM, qui régulent l'induction du programme de développement du sporophytique. Il est intéressant de noter que d'autres variations du cycle de vie de *Ectocarpus* ont été observées et soutiennent l'idée de génération et de ploïdie indépendantes du cycle de vie. Par exemple, des gamètes non-fécondés de souches de type sauvage peuvent se développer de façon autonome pour produire des parthéno-sporophytes haploïdes (Müller, 1967; Mignerot et al., 2019). Par conséquent, la génération sporophytique peut être haploïde dans certaines conditions. De même, il est possible de produire des gamétophytes diploïdes en croisant deux souches porteuses de la mutation oro (Coelho et al., 2011).

Cependant, l'alternance entre le gamétophyte et le sporophyte peut également être régulée par un facteur autonome, extracellulaire, sécrété dans le milieu de culture par les sporophytes. Ce facteur diffusible provoque une reprogrammation majeure du développement des cellules initiales (méio-spores) du gamétophyte. La reprogrammation du développement n'a pas été observée lorsque les méio-spores ont été traitées avec un milieu conditionné par des sporophytes (SCM), 48 heures après leur libération du sporange uniloculaire. Cela correspond au temps nécessaire aux méiospores pour synthétiser une paroi cellulaire, ce qui suggère que le facteur diffusible est incapable d'agir sur une cellule entourée par une paroi (bien qu'il soit également possible que d'autres événements cellulaires se produisent à ce stade pour rendre la méio-spore en développement insensible à ce facteur). Les cellules de tous les organismes photosynthétiques, multicellulaires et eucaryotes, y compris les plantes terrestres et les algues brunes, sont entourées par une paroi cellulaire dynamique, complexe et riche en glucides (Popper et al., 2011b). Dans l'arbre de vie, la complexité des organismes multicellulaires n'a évolué que dans un petit nombre de groupes eucaryotes dont notamment les plantes et les algues brunes. Il est intéressant de noter que chez les plantes et les algues brunes, ce processus a été associé à l'évolution des parois cellulaires complexes qui jouent un rôle important dans la reconnaissance, l'adhésion et la

communication entre les cellules. On pense que les parois cellulaires des algues brunes jouent un rle important dans l'immunité innée (Brownlee, 2002; Küpper et al., 2001), la résistance au stress mécanique et la protection contre les prédateurs (Popper et al., 2011a). Ils jouent également un rle crucial dans le contrle de la différenciation cellulaire, comme chez les plantes terrestres, et les processus de développement, tels que la croissance, la différenciation et la morphogenèse, sont intimement associés aux alternances du métabolisme de la paroi cellulaire (Quatrano and Stevens, 1976). Le lien entre la morphogenèse cellulaire et le dépt de la paroi cellulaire a été étudié dans les zygotes de Fucales, qui ont longtemps servi de modèles pour étudier la polarisation cellulaire et la division cellulaire asymétrique en rapport  la paroi cellulaire (Belanger and Quatrano, 2000; Deniaud-Bouët et al., 2014; Paciorek and Bergmann, 2010). Au cours de la germination, la croissance apicale s'amorce  un endroit prédéterminé  la surface du zygote et un rhizode émerge (Fowler and Quatrano, 1997; Kropf et al., 1988). La cellule apicale du rhizode s'allongera alors, tandis que la cellule du thalle proliférera par croissance diffuse (Bisgrove and Kropf, 2001). On pense que les composants de la paroi (e.g.,. les nouvelles protéines transmembranaires ayant des rles potentiels dans la communication cellule-cellule) contrlent la différenciation cellulaire pendant la génération sporophytique d'*E. siliculosus* (Le Bail et al., 2011). La fonction importante du principal constituant de la paroi cellulaire, l'alginate, se reflète dans les génomes d'algues brunes, qui codent un grand nombre d'enzymes mannuronan C5-épimérases MC5E (28 chez *E. siliculosus*) et de nombreuses protéines  domaine WSC (cell wall sensing components). Ces derniers peuvent tre impliqués dans les interactions entre l'alginate et les protéines. Ces deux grandes familles multigéniques, ainsi que les récepteurs kinases spécifiques de l'algue brune, et un large supplément de gènes liés  la paroi cellulaire, ont été décrits en détails dans le cadre de l'analyse du génome du modèle d'algue brune *E. siliculosus* (Cock et al., 2010; Michel et al., 2010; Richerd et al., 1993). Des preuves de génomiques structurelles ont montré que les gènes MC5E étaient associés aux domaines WSC (Oide et al., 2019; Wawra et al., 2019) et aux motifs centraux de protéines arabinogalactan (AGP) (Hervé et al., 2016).

Cependant, la nature biochimique de ce facteur diffusible n'a pas encore été décrite. L'objectif principal de cette étude est de caractériser le facteur diffusible sporophyte-inducteur. Les travaux

ont porté sur l'optimisation de la production, du stockage des essais biologiques du facteur sporophyte inducteur afin de fournir des informations sur sa nature biochimique. L'étude a également porté sur la relation entre le facteur sporophyte-inducteur et deux régulateurs génétiques, ORO et SAM, pour comprendre la voie de développement déclenchée par ce facteur. La caractérisation génétique (décrite au Chapitre IV) a révélé que ces deux facteurs de transcription à domaine homéodésique TALE régulent la transition du gamétophyte au sporophyte chez *Ectocarpus*. Fait intéressant, les travaux ont également montré que les protoplastes des gamétophytes oro ou sam (ces deux mutations transformant la génération sporophyte en un gamétophyte pleinement fonctionnel) sont insensibles au facteur diffusible induisant les sporophytes (Arun et al., 2019; Coelho et al., 2011) ce qui indiquent que que ORO et SAM peuvent faire partie du réseau de régulation déclenché par le facteur sporophytique (Arun et al., 2019). Nous avons déterminé les conditions optimales de production, de stockage et de détection de ce facteur et montré qu'il s'agit d'une molécule résistante à la chaleur et de poids moléculaire élevé (Chapitre II). Des avancées significatives dans la caractérisation du facteur diffusible ont été réalisées. Par exemple, plusieurs sources de données suggèrent que le facteur pourrait être une protéine arabinogalactane chimérique (AGP) et, de façon remarquable, l'incubation de spores de méio-spores avec des AGP végétales (gomme arabique) a imité l'effet du traitement par SCM, les incitant à passer au programme de développment du sporophyte. C'est intéressant parce que les AMP n'ont été caractérisés que récemment chez les algues brunes, et parce que ces analyses récentes ont également lié les AMP d'algues brunes aux processus de développement.  Dans le futur, il serait intéressant de traiter le facteur diffusible d'*Ectocarpus* avec de la déglycosylase pour éliminer les chaînes de sucre et ensuite doser séparément les fractions sucre et protéines. Cependant, la nature biochimique exacte du facteur diffusible doit encore être élucidée. Une procédure normalisée a été établie pour la production du facteur diffusible *d'Ectocarpus* et les essais biologiques (Chapitre III). Les conditions de production optimisées et les essais biologiques actuels nous ont permis de réaliser des travaux sur le facteur diffusible, mais une optimisation plus poussée faciliterait les expériences futures. En particulier, l'une des principales contrainte du système est qu'un grand nombre de tests sont nécessaires pour obtenir des résultats statistiquement significatifs. Toute amélioration future qui permettrait de

mesurer de façon robuste l'activité des facteurs diffusibles avec moins de tests faciliterait grandement l'exploration des fonctions sur ce facteur.

Dans cette thèse, nous avons finalement caractérisé le gène *BASELESS* (*BAS*) (Ec-21_001770) qui résulte en des phénotypes très similaires à ceux observés chez les mutants '*distag*' (Godfroy et al., 2017) aux niveaux cellulaire et morphologique, incluant des défauts cytosquelettiques lors de la division cellulaire initiale et la perte complète des systèmes basaux durant les deux générations du cycle de vie. Le clonage par séquençage a révélé que *BAS* code une sous-unité régulatrice de type B" de la protéine phosphatase 2A. Le niveau élevé de similarité des phénotypes des mutants *dis* et *bas* suggère que le TBCCd1 et le PP2A sont deux composants essentiels de la machinerie cellulaire qui régule la division de la cellule initiale et intervient dans l'établissement du devenir des cellules basales dans le thalle en développement. Il serait particulièrement intéressant à l'avenir d'étudier la fonction de Ec-21_001770 dans *Ectocarpus* et de comprendre la relation entre BAS (c'est-à-dire PP2A) et DIS (TBCCd1).